Title
Xenobiotic oxidation by hemoglobin and myoglobin

Author
Catalano, Carlos Enrique

Publication Date
1987

Peer reviewed|Thesis/dissertation

XENOBIOTIC OXIDATION BY HEMOGLOBIN AND MYOGLOBIN: A Mechanistic Study

by

CARLOS ENRIQUE CATALANO

DISSERTATION

Submitted in partial satisfaction of the requirements for the degree of

DOCTOR OF PHILOSOPHY

in

PHARMACEUTICAL CHEMISTRY

in the

GRADUATE DIVISION

of the

UNIVERSITY OF CALIFORNIA

San Francisco

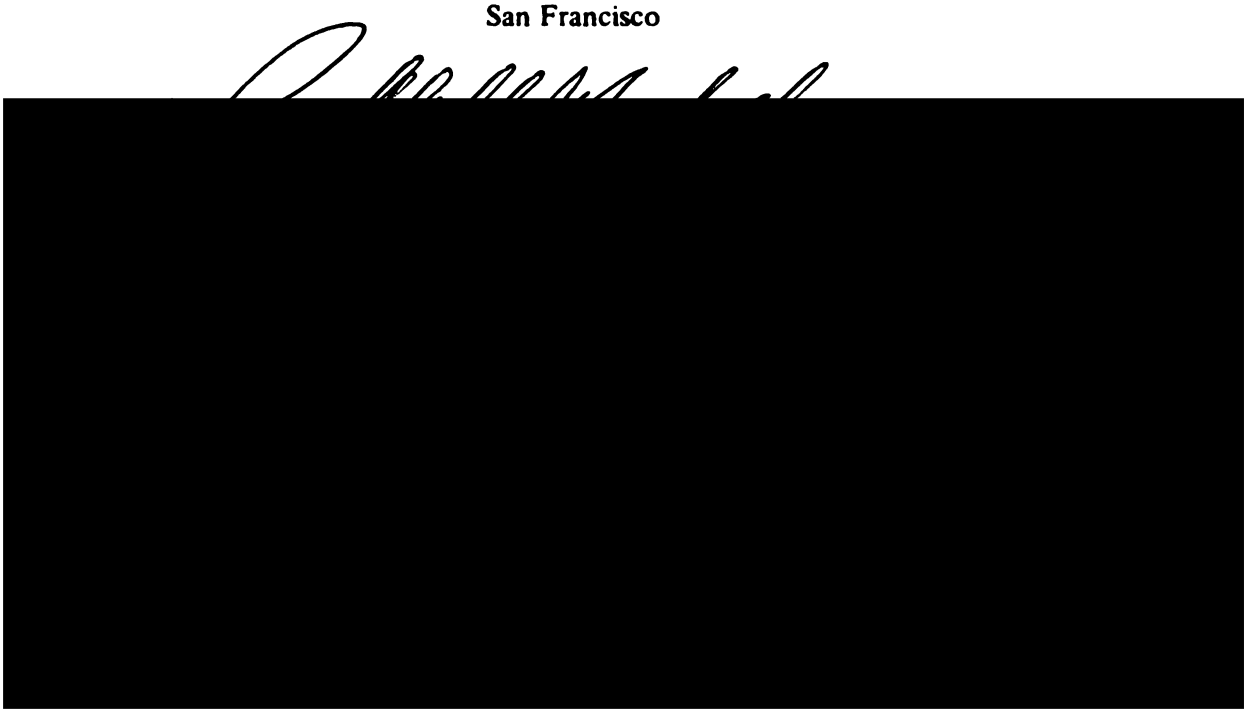

Dedication

For Christina,

who stayed with me even when i didn't deserve it

with Love

Acknowledgments

It is with mixed feelings that I leave the laboratory of Dr. Paul R. Ortiz de Montellano. The support and encouragement given to me by my comrads and co-workers has always made the hard times go just a little bit easier. I can never thank them enough for this. I especially wish to thank Dr. Ortiz de Montellano for teaching me science. He has always been available to discuss problems as well as triumphs and treated mistakes as education rather than tragedy. Con respetar y admiracion, gracias Patron.

I wish to also thank Dr. Neal Castagnoli and Dr. Martin Shetlar for their willingness to take the time to talk, for their help, and for their advice over the past several years. Thanks must go to Drs. George Kenyon and C. C. Wang for all the letters that they have written on my behalf. A particular note of thanks to Dr. Bill Abrth and Pat Bethel for their assistance in obtaining mass spectra for all my "peculiar" peptide samples.

A special thank you to Professor Frederick and Harriet Thon for their encouragement and support over the past many years. You have made me feel what I do is important and this has carried me through the times when I was weak. Thank you.

Xenobiotic Oxidation by Hemoglobin and Myoglobin: A Mechanistic Study

by Carlos Enrique Catalano

Abstract

Hemoglobin and Myoglobin effect the peroxide dependent oxidation of styrene to styrene oxide. This oxidation proceeds without stereochemical selectivity, results in the partial loss of stereochemistry with trans-[^{2}H]-styrene utilized as the substrate, incorporates molecular oxygen and is inhibited by radical trapping agents. These data have been rationalized with a protein-bound peroxy radical oxidizing species. Peroxide oxygen is also incorporated into part of the oxide product and is best explained with a monooxygenase-type mechanism involving direct oxygen transfer from the ferryl-oxo hemoprotein to the olefin.

Hemoglobin and myoglobin also oxidize 7,8-dihydroxy-7,8-dihydrobenzo(a)pyrene to the 7,8,9,10-tetrahydroxy derivative with incorporation of both peroxide and solvent oxygen, but NOT molecular oxygen. Trans- and cis-stilbene are oxidized to the corresponding epoxides with quantitative incorporation of the peroxide oxygen. Cis-stilbene is also oxidized to trans-stilbene oxide with at least 32% of the oxygen deriving from molecular oxygen but less than 7%

coming from the peroxide. Again, the remainder of the epoxide oxygen is assumed to derive from the medium.

Three distinct mechanisms for the hemoglobin- and myoglobin-dependent oxidations are proposed which are consistent with the data: 1) a monooxygenase-type mechanism similar to that of Cytochrome P450 oxidations, 2) a peroxidase-type mechanism similar to that of peroxidase oxidations, and 3) a novel cooxidation mechanism involving a protein-bound peroxy radical species. The factors which influence flux through each of these oxidative pathways are discussed.

The interaction of myoglobin with peroxide results in the loss of half of the tyrosine content in the protein. Tyrosine 103 in the horse myoglobin sequence has been identified as the modified residue by amino acid, mass spectral, and N-terminal sequence analyses of the peptides resulting from trypsin and staphylococcal V8 protease digestion of the peroxide-treated hemoprotein.

The prosthetic heme becomes covalently attached to the apoprotein in approximately 10% of peroxide-treated myoglobin. The heme-containing peptide isolated from proteolytic digestion of peroxide-treated horse myoglobin was examined. Amino acid and mass spectral analysis of the "heme-peptide" strongly suggest, but do not prove, that the heme is covalently linked to tyrosine 103 of the horse myoglobin sequence. A mechanism for this attachment is

proposed which is a logical extension of the peroxy radical mechanism for substrate oxidation discussed above.

Table of Contents

Chapter One: Introduction

Introduction 1

Hemoprotein Structure

The Globins 4

The Cytochromes P450 7

The Peroxidases 10

Interaction of Hemoproteins with Peroxides

The Peroxidases 12

The Cytochromes P450 14

The Globins 16

Xenobiotic Oxidation by Hemoglobin and Myoglobin 23

Proposal for Thesis 25

Chapter Two: Xenobiotic Oxidation by Hemoglobin and Myoglobin

Styrene Oxidation

Products Formed by Hemoglobin and H_2O_2 27

Dependence on Incubation Parameters 33

Origin of Oxygen in Styrene Oxide 40

Stereochemical Fidelity 43

Stereoselectivity 45

Benzo(a)pyrene-7,8-Diol Oxidation

Products Formed by Hemoglobin and H_2O_2 49

Origin of Oxygen in BAPT 56

Stilbene Oxidation

Products Formed From trans-Stilbene by Hemoglobin and H_2O_2 61

Products Formed From cis-Stilbene by Hemoglobin and H_2O_2 61

Origin of Oxygen in the Stilbene Oxides 64

Linoleic Acid Oxidation

Oxygen Consumption During Linoleate Oxidation 69

Products Formed by Hemoglobin and H_2O_2 72

Miscellaneous Substrate Oxidations 79

Chapter Three: Myoglobin Oxidative Damage

Peroxide Oxidation of Kangaroo Myoglobin 84

Peroxide Oxidation of Horse Myoglobin

Oxidation with H_2O_2 88

Amino Acid Composition of Oxidized Myoglobin 88

Trypsin Digestion of H_2O_2 Horse Myoglobin

Horse Myoglobin Peptide Maps 94

Characterization of Peptide A 99

Characterization of the Tryptic Heme-Peptide 102

Mass Spectrum of Microperoxidase 107

Mass Spectrum of the Horse Myoglobin Tryptic Heme-Peptide 110

Staphyloccocal V8 Protease Digestion of Horse Myoglobin

Horse Myoglobin Peptide Maps 115

Characterization of V8 Protease Peptides 125

Nature of Modified Amino Acids and Heme in the H_2O_2 Treated Myoglobin

Acid Hydrolysis of Horse Myoglobin 128

Pronase Digestion of Horse Myoglobin 130

Peroxide Oxidation of Meso-Heme Reconstituted Horse Myoglobin 133

Chapter Four: Discussion of Results

Substrate Oxidation by Hemoglobin and Myoglobin

Styrene Oxidation 136

Benzo(a)pyrene-7,8-Diol Oxidation 154

Stilbene Oxidation 157

Linoleic Acid Oxidation 161

Miscellaneous Substrate Oxidations 163

Summary of Substrate Oxidation 166

Horse Myoglobin Peroxide Induced Protein Damage 180

The Big Picture 184

Chapter Five: Experimental Details

Materials and Methods 190

Experimental Details for Chapter Two

Styrene Oxidation 192

Benzo(a)pyrene-7,8-Diol Oxidation 201

Stilbene Oxidation 204

Linoleic Acid Oxidation 207

Miscellaneous Substrate Oxidations 209

Experimental Details for Chapter Three

Protein Assay Methods 210

Preparation and Analysis of Peroxide Damaged Myoglobin 212

Proteolytic and Acidic Protein Digestion 215

Analytical Methods 217

Preparation and Characterization of Proto- and Meso-Reconstituted Horse Myoglobins 219

Kangaroo Myoglobin 228

ESR Studies 237

References 239

List of Tables

Table 1.1	Comparison of Selected Heme Containing Proteins	22
Table 2.1	Factors Affecting Product Yield	37
Table 2.2	Formation of Benzandehyde and Styrene Oxide by Different Hemoptoteins	42
Table 2.3	Source of the Oxygen in Styrene Oxide	42
Table 2.4	Formation of BAPT by Different Hemoproteins	59
Table 2.5	Oxygen Dependence of BAPT Yield	59
Table 2.6	Source of Oxygen in the Tetrol Product	60
Table 2.7	Stilbene Oxide Yield	66
Table 2.8	Incorporation of ^{18}O from $H_2{}^{18}O_2$ into Stilbene Oxide	66
Table 2.9	Incorporation of ^{18}O from $^{18}O_2$ into cis-Stilbene Oxide	68
Table 2.10	Source of Oxygen in Stilbene Oxide: Summary	68
Table 2.11	Oxygen Consumption During the Oxidation of Linoleic Acid by Hb and H_2O_2	71
Table 2.12	Oxygen Consumption During the Oxidation of Linoleic Acid by Mb and H_2O_2	71
Table 2.13	Oxidation of Miscellaneous Compounds by Hemoglobin and H_2O_2	83
Table 3.1	Non-Extractable Heme Content of Peroxide-Treated Horse Myoglobin	92
Table 3.2	Horse Myoglobin Amino Acid Analysis	93
Table 3.3	Theoretical Peptides Derived from Trypsin Digestion of Horse Myoglobin	98
Table 3.4	Amino Acid Composition of Horse Myoglobin Tryptic Peptide A	101
Table 3.5	Amino Acid Composition of Horse Myoglobin Tryptic Peptide A ($-H_2O_2$)	104
Table 3.6	Amino Acid Composition of Horse Myoglobin Tryptic Heme Peptide	105

Table 3.7	Summary of the Amino Acid Compositions of Horse Myoglobin Tryptic Peptide A and the Heme-Peptide	106
Table 3.8	Theoretical Peptides Derived from Staphylococcal V8 Digestion of Horse Myoglobin	118
Table 3.9	Amino Acid Composition of the Staphylococcal V8 Protease Heme-Peptide	126
Table 3.10	Amino Acid Composition of the Staphylococcal V8 Protease Peptides B and C	127
Table 4.1	Epoxide Yields from Methemoglobin and Horse Metmyoglobin Oxidation of Olefins	166
Table 4.2	Source of Oxygen in Hemoprotein Dependent Oxidations	168
Table 4.3	Significance of Each Mechanistic Pathway in the Oxidation of Olefins by Hemoglobin	174
Table 4.4	Significance of Each Mechanistic Pathway in the Oxidation of Olefins by Myoglobin	174
Table 4.5	Hansch Octanol/Water Partition Coefficients for Compounds Used in this Stydy	176
Table 4.6	Oxidation Potentials for Compounds Used in this Study	179
Table 5.1	Horse Myoglobin Milimolar Extinction Coefficients	212
Table 5.2	Hemoprotein Concentration from Spectral Data	221
Table 5.3	Hemoprotein Concentration from Pyridine Hemochromogen Data	224
Table 5.4	Hemoprotein Concentration from the Biorad Protein Assay	225
Table 5.5	Protein Concentration from the Lowry Assay	226
Table 5.6	Summary of Calculated Hemoprotein Concentrations (uncorrected)	227
Table 5.7	Summary of Calculated Hemoprotein Concentrations (corrected)	227
Table 5.8	Low Temperature ESR Spectral Parameters	238

List of Figures and Schemes

Figure 1.1 The Structure of Iron Protoporphyrin IX 2

Figure 1.2 The Crystal Structure of Sperm Whale Myoglobin 5

Figure 1.3 The Crystal Structure of Cytochrome $P450_{cam}$ 9

Figure 1.4 The Crystal Structure of Yeast Cytochrome C Peroxidase 11

Figure 1.5 The Catalytic Cycle of Cytochrome P450 15

Figure 1.6 Interaction of Hemoglobin with H_2O_2 21

Figure 2.1 Hemoglobin Soret Loss with Time 28

Figure 2.2 Products Formed in the Oxidation of Styrene by Hemoglobin and H_2O_2 29

Figure 2.3 Mass Spectra of the Products Isolated in the Oxidation of Styrene by Hb and H_2O_2 31

Figure 2.4 HPLC Chromatogram of the Products Isolated from the Oxidation of Styrene by Hemoglobin and H_2O_2 32

Figure 2.5 Time Course for Product Formation and Heme Soret Loss 34

Figure 2.6 Dependence of Product Formation on Hydrogen Peroxide Concentration 35

Figure 2.7 Dependence of Product Formation on Styrene Concentration 36

Figure 2.8 Oxygen Evolution in the Interacton of Hemoglobin with Hydrogen Peroxide 39

Figure 2.9 Mass Spectra of Styrene Oxide Derived from Hb Oxidation of Styrene either in an $^{18}O_2$ Environment or by $H_2{}^{18}O_2$ 41

Figure 2.10 NMR Spectrum of Styrene Oxide Derived from Hb Oxidation of [^{2}H]-Styrene 44

Figure 2.11 Mass Spectrum of Styrene Oxide Derived from Hb Oxidation of [^{2}H]-Styrene 46

Figure 2.12 NMR Chemical Shift of Styrene Oxide Protons vs. Eu(hfc)III Added 47

Figure 2.13 NMR Spectrum of Enantiomeric trans-Protons of Styren Oxide Derived from Hb Oxidation of Styrene 48

Figure 2.14 HPLC Chromatogram of the Products Formed from the Oxidation of BAPD by Hb and H_2O_2 50

Figure 2.15 The Electronic Absorption Spectra of the Products Formed from the Oxidation of BAPD 51

Figure 2.16 Chemical Structures and Nomenclature of the Benzo(a)pyrene Derivatives 52

Figure 2.17 HPLC Chromatogram of Acetylated BAPT Formed from the Oxidation of BAPD by Hb and H_2O_2 53

Figure 2.18 Mass Spectrum of the Acetylated BAPT Formed from the Oxidation of BAPD by Hb and H_2O_2 54

Figure 2.19 HPLC Chromatograms of the Products Formed from the Oxidation of BAPD by Hb, SMB and HMb 57

Figure 2.20 Mass Spectra of Acetylated BAPT Formed from From the Oxidation of BAPD by Hemoglobin Either in an $^{18}O_2$ Environment or by H_2O_2 58

Figure 2.21 GC Chromatogram of the Products Formed from the Oxidation of trans-Stilbene by Hemoglobin and H_2O_2 62

Figure 2.22 GC Chromatogram of the Products Formed from the Oxidation of cis-Stilbene by Hemoglobin and H_2O_2 63

Figure 2.23 Mass Spectra of the Stilbene Oxides Formed from the Oxidation of trans- and cis-Stilbenes by Hemoglobin Either in an $^{18}O_2$ Environment or by H_2O_2 65

Figure 2.24 Oxygen Evolution by Hb and H_2O_2 in the Presence and Absence of Linoleic Acid 70

Figure 2.25 Oxygen Evolution by Mb and H_2O_2 in the Presence and Absence of Linoleic Acid 73

Figure 2.26 Chemical Structures and Nomenclature of the Linoleic Acid Derivatives 75

Figure 2.27 CG Analysis of the Products Formed from the Oxidation of Linoleic Acid by Hemoglobin and H_2O_2 at 37°C 76

Figure 2.27 CG Analysis of the Products Formed from the Oxidation of Linoleic Acid by Hemoglobin and H_2O_2 at 0°C 77

Figure 2.29 Mass Spectrum of 13-TODA Formed from the Oxidation of Linoleic Acid by Hb and H_2O_2 78

Figure 2.30 Miscellaneous Substrate Oxidations Examined 80

Figure 2.31 CG Analysis of the Products Formed from the Oxidation of Aniline by Hb and H_2O_2 81

Figure 2.32 CG Analysis of the Products Formed from the Oxidation of N-Methylaniline by Hemoglobin and H_2O_2 82

Figure 3.1 SDS-PAGE Gel of Peroxide-Treated Myoglobins From Sperm Whale and Red Kangaroo 85

Figure 3.2 The ESR Spectra of Sperm Whale Myoglobin Before and After Peroxide-Treatment 86

Figure 3.3 The ESR Spectra of Peroxide-Treated Myoglobins from Whale, Horse and Kangaroo 87

Figure 3.4 The Electronic Absorption Spectra of Peroxide-Treated and Control Myoglobin 89

Figure 3.5 The Electronic Absorption Spectra of the Hemes Extracted from Peroxide-Treated and Control Myoglobin 90

Figure 3.6 The Electronic Absorption Spectra of the Apoproteins from Peroxide-Treated and Control Myoglobin after Heme Extraction 91

Figure 3.7 HPLC Chromatogram of the Myoglobin Tryptic Peptides: Modified Gradient 95

Figure 3.8 HPLC Chromatogram of the Myoglobin Tryptic Peptides: Standard Gradient 96

Figure 3.9 Expanded Region of the HPLC Chromatogram of the Myoglobin Tryptic Peptides: Standard Gradient 97

Figure 3.10 The Chemical Structure of Horse Myoglobin Tryptic Peptide #17 100

Figure 3.11 The L-SIMS Mass Spectrum of Peptide A 103

Figure 3.12 The Chemical Structure of Microperoxidase 108

Figure 3.13 The L-SIMS Mass Spectrum (positive mode) of Microperoxidase (MS-50) 109

Figure 3.14 The L-SIMS Mass Spectrum (negative mode) of Microperoxidase (MS-50) 111

Figure 3.15 The L-SIMS Mass Spectrum (negative mode) of Microperoxidase (WEIN-MS) 111

Figure 3.16 Isolation of the Heme-Peptide From a Preparative Incubation: HPLC Chromatogram 112

Figure 3.17 The Electronic Absorption Spectra of Fractions Isolated From the Preparative Isolation of the Heme-Peptide 113

Figure 3.18 The L-SIMS Mass Spectrum (negative mode) of the Heme-Peptide 114

Figure 3.19 HPLC Chromatogram of the Myoglobin V8 Protease Peptides 116

Figure 3.20 The Electronic Absorption Spectrum of the V8 Protease Heme-Peptide 117

Figure 3.21 The Expanded Region of the HPLC Chromatogram of the V8 Protease Peptides 120

Figure 3.22 The Electronic Absorption Spectrum of the V8 Protease Peptides B and D 121

Figure 3.23 The Expanded Region of the HPLC Chromatogram of the V8 Protease Peptides: Fluorescence Detection 122

Figure 3.24 Resolution of V8 Protease Peptides B and C: HPLC Chromatogram 123

Figure 3.25 Resolution of V8 Protease Peptides B and C: HPLC Chromatogram, Fluorescence Detection 123

Figure 3.26 HPLC Chromatogram of Acid Hydrolyzed Horse Myoglobin: Gradient #1 129

Figure 3.27 HPLC Chromatogram of Acid Hydrolyzed Horse Myoglobin: Gradient #2 131

Figure 3.28 HPLC Chromatogram of Pronase Digested HorseMyoglobin: Gradient #1 132

Figure 3.29 The Electronic Absorption Spectra of Peroxide-Treated Meso- and Proto-Heme Reconstituted Horse Myoglobins 134

Figure 3.30 The Electronic Absorption Spectra of the Apoproteins Resulting From Heme Extraction From Meso- and Proto-Heme Reconstituted Horse Myoglobins 135

Scheme 4.1 Oxidation of Styrene by Hemoglobin and H_2O_2: Monooxygenase Mechanism 138

Figure 4.1 Relationship of Tyrosine and the Prosthetic Heme in Hemoglobin and Myoglobin 140

Figure 4.2 Mechanism for the Oxidative Coupling of Phenols 142

Scheme 4.2 Oxidation of Styrene by Hemoglobin and H_2O_2: Cooxidation Mechanism 143

Figure 4.3 Reaction of Phenyl Radical with Substrates and Oxygen 145

Figure 4.4 Oxidation of Styrene by a Tyrosine Peroxy Radical Species 147

Scheme 4.4 Formation of Benzaldehyde by Hemoglobin and H_2O_2: Racidal Cation Pathway 149

Scheme 4.5 Formation of Benzaldehyde by Hemoglobin and H_2O_2: Peroxy Radical Pathway 151

Scheme 4.6 Formation of Benzaldehyde by Hemoglobin and H_2O_2: Singlet Oxygen Pathway 153

Scheme 4.7 Oxidation of BAPD by Hemoglobin and H_2O_2 156

Scheme 4.8 Oxidation of Stilbene by Hb and H_2O_2 158

Figure 4.4 Approach of Stilbene to Model Porphyrins 160

Figure 4.5 Approach of Stilbene to Hemoglobin 162

Scheme 4.9 Oxidation of Linoleic Acid by Hb and H_2O_2 164

Scheme 4.10 Summary of the Mechanisms of Olefin Oxidation by Hb and H_2O_2 170

Figure 4.6 Alternate Mechanisms for Direct Ferryl-oxo Oxygen Transfer from a High-Valent Protein Intermediate to an Olefin 172

Figure 4.7 Steric Bulk of the Olefins Used in this Study 178

Scheme 4.11 Mechanism for the Peroxide-Dependent Covalent Attachment of Heme to Globin 183

Figure 4.8 Proposed Mechanism of Peroxide Decomposition by Cytochrome C Peroxidase 186

Figure 4.9 The Electronic "Push" Provided by the Cysteine Thiolate in P450 187

Figure 5.1 The Mechanism of H_2O_2-Mediated Oxidation of Menadione 196

Figure 5.2 The Electronic Absorption Spectrum of Proto-Heme Reconstituted Horse Myoglobin 221

Figure 5.3 The Electronic Absorption Spectrum of Meso-Heme Reconstituted Horse Myoglobin 223

Figure 5.4 Sephadex G-100 Chromatographic Separation of Kangaroo Myoglobin Components 230

Figure 5.5 Electronic Absorption Spectra of Kangaroo Myoglobin Peaks I and II Eluted from the Sephadex G-100 Column 231

Figure 5.6 DEAE-Sephadex Chromatographic Separation of Kangaroo Myoglobin Components 232

Figure 5.7 Electronic Absorption Spectra of Kangaroo Myoglobin Peaks I and II Eluted from the DEAE-Sephadex Column 234

Figure 5.8 SDS-PAGE Gel of Kangaroo Myoglobin Isolation at the Various Stages of Purification 235

Figure 5.9 SDS-PAGE Gel of Purified Kangaroo Myoglobins 236

Abbreviations

BAPD, 7,8-dihydroxy-7,8-dihydrobenzo(a)pyrene; **BAPT**, 7,8,9,10-tetrahydroxy-7,8,9,10-tetrahydrobenzo(a)pyrene; **BAP diol-epoxide**, 7,8-dihydroxy-9,10-oxo-benzo(a)pyrene; **BHT**, butylated hydroxytoluene; **BSTFA**, Bis(trimethylsilyl)-trifluoroacetamide; **DABCO**, 1,4-Diazabicyclo[2.2.2]octane; **EIMS**, electron impact mass spectrometry; **ESR**, electron spin resonance; **Eu(hfc)III**, tris-[3-(heptafluoropropylhydroxy-methylene)-d-camphorato]europium III; **GC**, gas-liquid chromatography; **Hb**, bovine hemoglobin; **Heme**, iron protoporphyrin IX; **HMb**, horse muscle myoglobin; **13-HODA**, 13-Hydroperoxy-$^{\Delta 9,11,trans}$-octadecanoic acid; **HPLC**, high performance liquid chromatography; **LSIMS**, liquid matrix secondary ion mass spectrometry; **m-CPBA**, meta-chloroperbenzoic acid; **methoxy-BAPT**, 10-methoxy-7,8,9-trihydroxy-7,8,9,10-tetrahydrobenzo(a)pyrene; **NMR**, nuclear magnetic resonance; **P450**, cytochrome P450; **P^{O}-Fe^{IV}**, a ferryl-oxo, porphyrin radical species; **POBN**, α-(4-pyridyl-1-oxide)-N-tert-butylnitrone; **R^{O}-Fe^{IV}**, a ferryl-oxo, protein radical species; **SDS-PAGE**, Sodium dioctylsulfonate-Polyacrylamide gel electrophoresis; **SMb**, sperm whale myoglobin; **SOD**, Superoxide dismutase; **TFA**, trifluoroacetic acid; **13-TODA**, 13-O-Trimethylsilyl-$^{\Delta 9,11,trans}$-octadecanoic acid; **TPCK**, L-1-tosylamide-2-phenylethylchloromethyl ketone.

Chapter 1 Introduction

The heme[1] containing proteins comprise a diverse group of proteins performing a wide variety of biological functions. These functions include electron transport (cytochromes b, c_1, c, a, a_3), oxygen transport (myoglobin, hemoglobin), protection from chemical (catalase) and biological (lactoperoxidase, myeloperoxidase) insult, hormone biosynthesis (horseradish peroxidase, thyroid peroxidase), structural biosynthesis (ovoperoxidase, locust peroxidase) and metabolism of endogenous and exogenous compounds (cytochromes P450) (Salemme, 1977; Dickerson and Geis, 1983; Dunford, 1982; Marnett, et al., 1986; Coles, 1966; White and Coon, 1980; Jefcoate, 1986). All of these hemoproteins have iron protoporphyrin IX (Figure 1.1) in common as their prosthetic group except myeloperoxidase which contains a closely related chlorin (Ikeda-Saito et al., 1984). The means by which each of these proteins modulates the chemical reactivity of the same prosthetic group remains a matter of intensive research.

A priori, one can envision two general methods for the modulation of chemical reactivity. The first is insulation of the reactive center with steric barriers. The prosthetic heme in the high potential cytochromes of the respiratory

---

[1]Abbreviations, see page xviii.

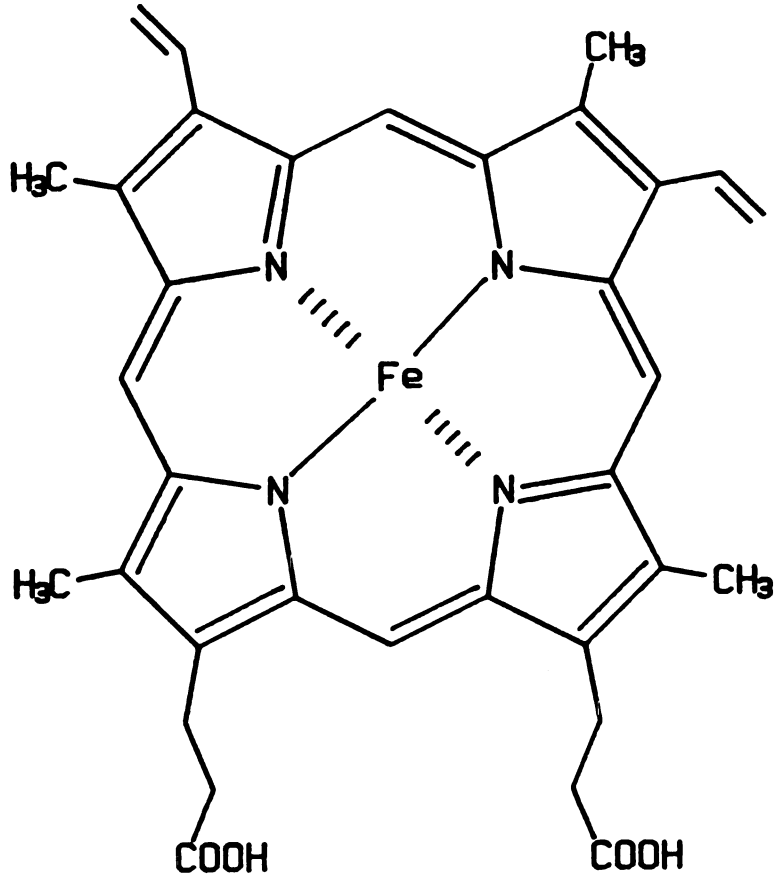

Figure 1.1. The Structure of Iron Protoporphyrin IX.

chain is buried in a hydrophobic pocket with only an edge exposed to the solvent. The heme iron forms axial coordinate bonds with two strong field ligands, histidine and methionine (Salemme, 1977). This effectively blocks the binding of exogenous ligands to the heme iron and preserves the integrity of the one electron redox cycle that is required for electron transfer. The peroxidases bind peroxides at the sixth iron coordination site and form an iron-oxo species that effects the one electron oxidation of substrates without directly involving the iron-bound oxygen (Dunford, 1982; Marnett et al., 1986). As with the cytochromes, the porphyrin ring in these hemoproteins is buried within the protein structure such that only an edge is exposed for electron transfer (Ortiz de Montellano, 1987; Ator and Ortiz de Montellano, 1987).

A second method to modulate chemical reactivity is through electronic control of the intermediates. The globins (hemoglobin and myoglobin) are maintained in the ferrous state in vivo and reversibly bind molecular oxygen (Dickerson and Geis, 1983). Ferrous cytochrome P450 will similarly bind molecular oxygen but the outcome is oxygen activation and transfer to a substrate (Ortiz de Montellano, 1986). This difference in reactivity has been attributed to an electronic "push" towards oxygen activation provided by the P450's (White and Coon, 1980; Poulos, 1986). Both the globins and the P450's provide an amino acid residue that binds to one of the available iron coordination sites (the

proximal ligand). This ligand is a histidine in the case of the globins and a cysteine thiolate in the P450's. It is commonly accepted that the driving force towards oxygen activation in the P450's is provided, at least in part, by an increase in electron density at the proximal ligand. Ligation to the heme iron cannot be the sole determinant of reactivity, however, since both the globins (oxygen transport proteins) and the peroxidases (peroxide metabolizing enzymes) provide a histidine residue as the proximal ligand to the heme prosthetic group. It is becoming increasingly evident that other protein factors affect the reactivity of the heme-iron.

Hemoprotein Structure

The Globins

Myoglobin consists of a single polypeptide chain of 152 to 153 amino acids depending on the species. The protein is composed of eight right handed α-helices, labeled A through H, that fold to form the pocket in which the sole prosthetic heme group is bound (Figure 1.2). The amino acid sequences of several myoglobins are known and show that strong interspecies structural homology exists. There are five invariant residues in the sequence, including HIS 87 which is the proximal ligand to the heme iron. Hydrophylic amino acid residues cover the surface of the protein while the area surrounding the heme binding pocket is composed of

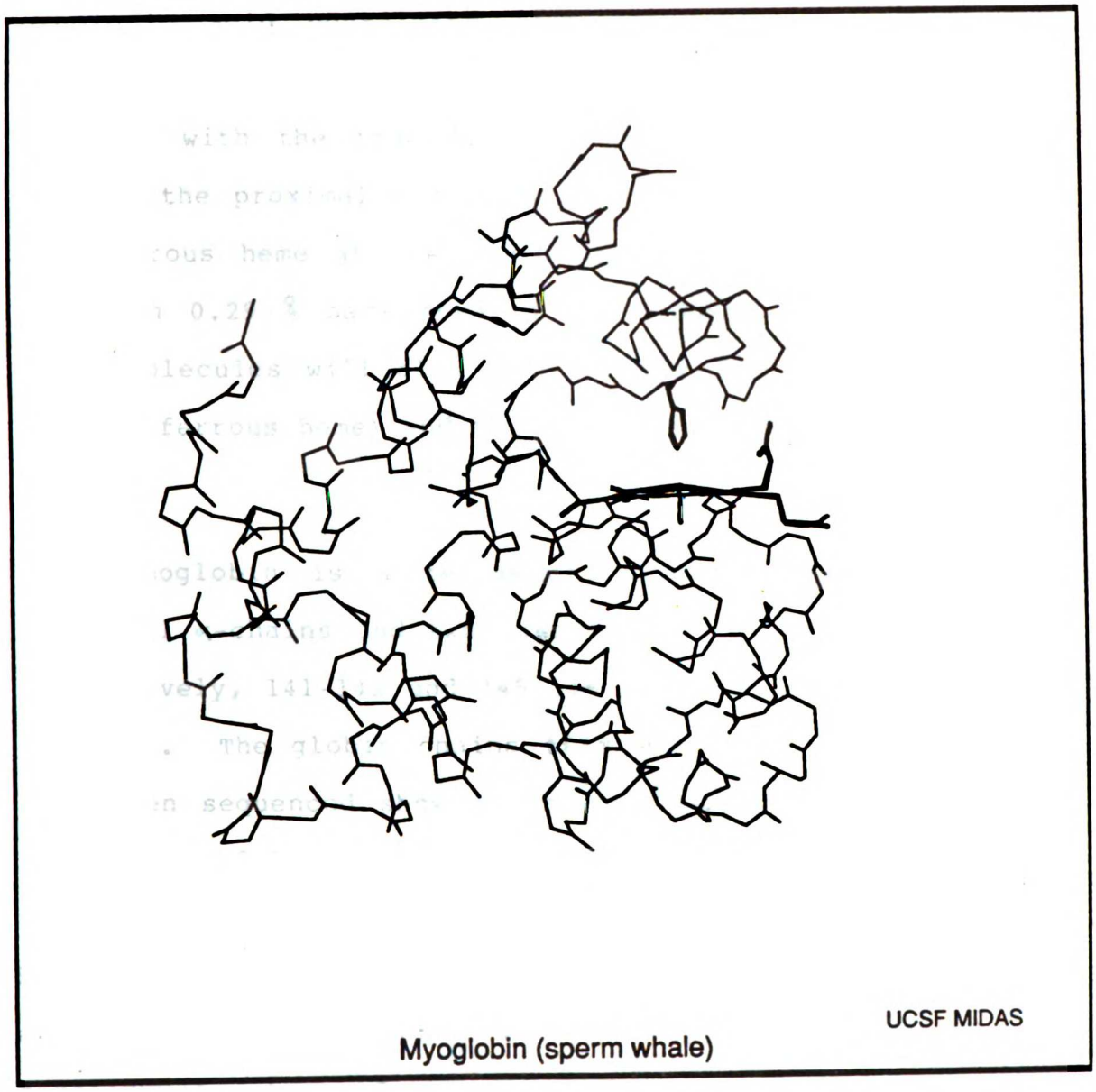

Figure 1.2. The Crystal Structure of Sperm Whale Myoglobin

strongly hydrophobic amino acids. The porphyrin macrocycle is buried within the protein structure except for the propionic acid containing edge which is exposed to the solvent. The heme prosthetic group in deoxymyoglobin is puckered with the iron 0.55 Å out of the porphyrin plane towards the proximal histidine. Oxygen binds reversibly to the ferrous heme at the sixth coordination site and draws the iron 0.29 Å back towards the porphyrin plane. Other small molecules will also bind to the heme iron, including CO, NO (ferrous heme) and NO_2^-, OH^-, F^-, CN^- and N_3^- (ferric heme).

Hemoglobin is a tetrameric protein composed of two identical α-chains and two identical β-chains that contain, respectively, 141-142 and 145-146 amino acids (depending on species). The globin chains from the various species that have been sequenced show strong homology to each other and to the myoglobins discussed above. The five invariant residues found in the myoglobins, including the proximal histidine (HIS 87 in the α-chains, HIS 92 in the β-chains), are also found in both of the hemoglobin chains. The tertiary structure of these chains is quite similar to that of the myoglobins, with one iron protoporphyrin IX prosthetic group contained within each folded globin chain. As with myoglobin, the region surrounding the heme binding pocket is composed of highly hydrophobic amino acid residues. The surface of the tetramer, which exhibits 222 symmetry, is covered with hydrophylic amino acids. The

hemes are buried within the protein superstructure, except that, as with myoglobin, the propionic acid-containing heme edge is exposed to the surrounding medium.

The tetramer is under allosteric control, with 2,3-diphosphoglycerate, chloride ions and protons acting as allosteric inhibitors of oxygen binding. Conversely, the binding of oxygen to one of the subunits cooperatively enhances the binding of oxygen to the remaining unoccupied sites. The heme iron moves into the porphyrin plane upon oxygen binding, as it does with myoglobin (vide supra), and this is believed to be the initiating event in cooperativity. Both cooperativity and allosteric inhibition involve a conformational change between a high (R) and low (T) oxygen affinity state.

The Cytochromes P450

The P450's comprise a group of enzymes that function in the oxidative metabolism of both xenobiotics and endogenous substrates. These enzymes are found in several mammalian, fish and bacterial species and have been described in detail by Black and Coon (1986). The proteins are generally highly hydrophobic, membrane-bound, and have molecular weights ranging from 56,373 to 60,053 daltons. All of these proteins contain a single ferric heme as the prosthetic group and it is generally accepted that they all possess a cysteine thiolate as the proximal heme ligand. The recent determination of the crystal structure for a cytosolic

bacterial P450 ($P450_{cam}$: Poulos, 1986) has made possible scrutiny of the physical structure of these enzymes.

Like the globins, $P450_{cam}$ is dominated by α-helical structure (Figure 1.3). Twelve helical segments (A to L) are arranged in three layers with the prosthetic heme sequestered between two of them. Proximal coordination to the heme iron is provided by CYS 357 with no electron density indicative of a sixth ligand available in the substrate (camphor) bound structure. The heme is totally insulated from the surrounding medium by a tight, highly hydrophobic, binding pocket. Camphor is similarly sequestered from the surrounding medium by hydrophobic protein residues with no clear route for substrate entry or product release. This obviously does occur, however, and this fact, combined with the ability of molecules of considerable size to form iron-bound complexes with $P450_{cam}$, intimates a high degree of flexibility in the protein structure.

Structural homology (Black and Coon, 1986) and a propensity to bind lipophilic substrates (Bakes et al., 1982; Al-Gailany et al., 1978; Lewis et al., 1986) suggest that the active sites of the hydrophobic membrane-bound P450's are similar to that of cytosolic $P450_{cam}$. Further support for this notion is provided by a series of experiments utilizing suicide substrates that alkylate the heme prosthetic group. The regiochemistry of these

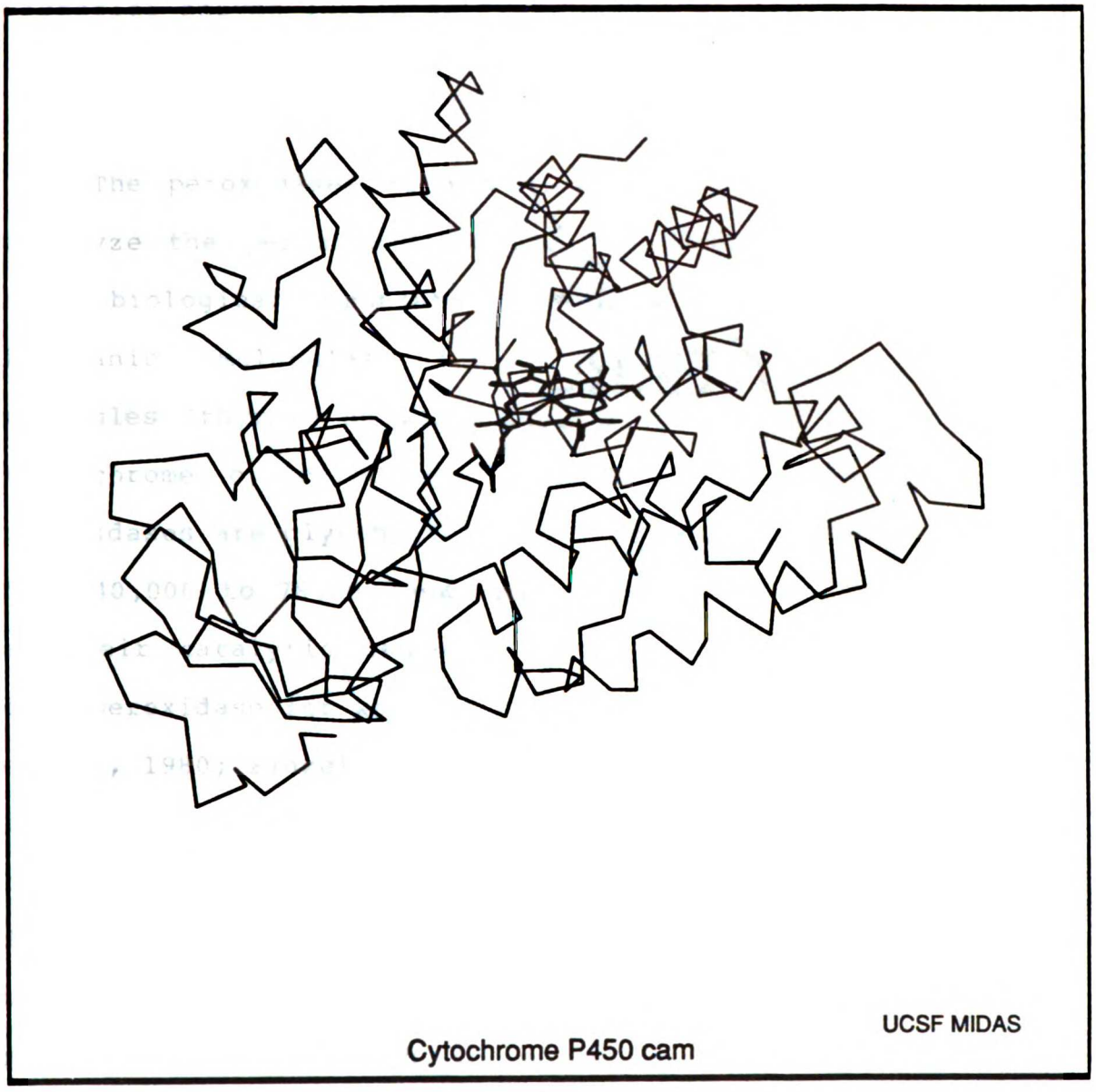

Figure 1.3. The Crystal Structure of Cytochrome $P450_{cam}$.

alkylations provides a topological map of the active site that is similar to that seen in the crystal structure of the bacterial enzyme (Ortiz de Montellano, 1987).

The Peroxidases

The peroxidases form a diverse group of enzymes that catalyze the peroxide-dependent, one-electron oxidation of their biological substrates. These substrates may be small inorganic molecules (Cl^-, myeloperoxidase), organic molecules (thyroid hormone, thyroid peroxidase) or proteins (cytochrome c, cytochrome c peroxidase). Many of the peroxidases are glycoproteins with molecular weights ranging from 40,000 to 78,000 and most have iron protoporphyrin IX as their catalytic center. Cytochrome c peroxidase, the only peroxidase for which a crystal structure exists (Poulos et al., 1980; Finzel et al., 1984), is a typical hemoprotein in that it is composed mainly of α-helical structure (Figure 1.4). Ten helices labeled A through J are folded into two distinct domains with a channel 5 Å wide and 10 Å deep between them. This provides a binding site for the prosthetic heme, which is sandwiched between helices B (domain I) and F (domain II) such that only an edge (pyrrole rings A and D) is exposed to solvent. Proximal ligation is provided by HIS 175, which is hydrogen bonded to a buried aspartic acid residue (ASP 235). The major difference between the peroxidases and the hemoproteins discussed above is the presence of hydrophilic amino acids and water on the

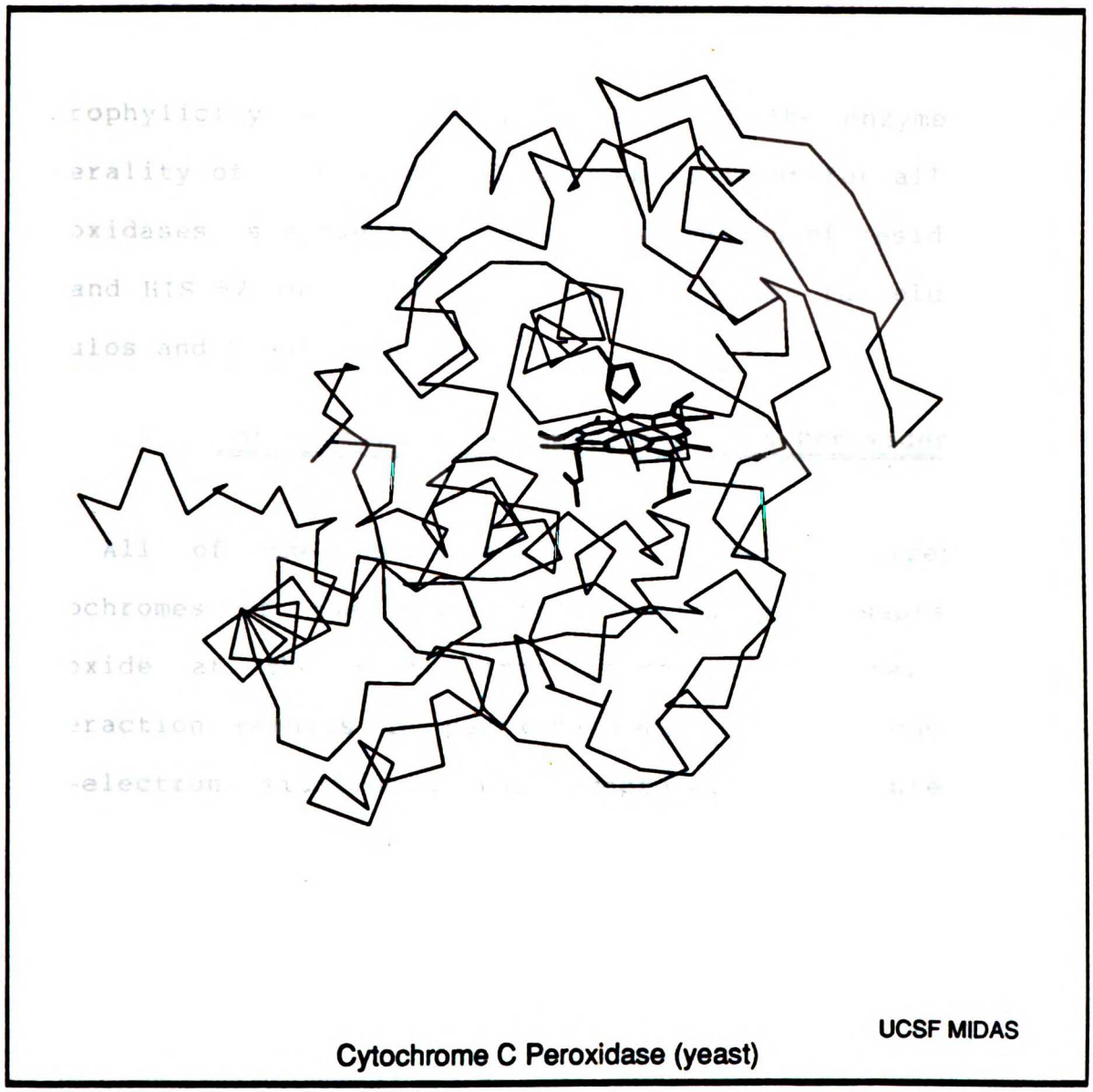

Figure 1.4. The Crystal Structure of Yeast Cytochrome C Peroxidase.

distal (peroxide binding) side of the active site. Arginine 48, histidine 52 and three highly ordered waters form a tight hydrogen bonding network that adds substantial hydrophylicity to the catalytic site of the enzyme. The generality of a polar distal heme environment for all of the peroxidases is suggested by the conservation of residues ARG 48 and HIS 52 in the peroxidase sequences so far elucidated (Poulos and Kraut, 1980).

Interaction of Hemoproteins with Peroxides

All of the heme containing proteins (except the cytochromes of the respiratory chain, vide supra) bind peroxide at the sixth iron coordination site. This interaction results in peroxide reduction and concomitant two-electron oxidation of the hemoprotein. The interaction of horseradish peroxidase with hydrogen peroxide has been thoroughly studied and the oxidized intermediates (compounds I and II) serve as prototypes for other peroxide-oxidized hemoproteins.

The Peroxidases

The reaction of horseradish peroxidase with hydrogen peroxide initially yields a two electron oxidized intermediate (compound I, equation 1) which has been characterized as a ferryl (iron-oxo), porphyrin radical species ($P^{O}Fe^{IV}$) by ENDOR (Roberts et al., 1981), Mossbauer (Schulz et al., 1984), EPR (ibid), resonance Raman (Oertling

and Babcock, 1985) and UV (Dolphin, 1981) spectroscopy. Horseradish peroxidase compound I effects the one electron oxidation of organic substrates (AH_2), yielding

1) HRP + H_2O_2 --> Compound I + H_2O

2) Compound I + AH_2 --> Compound II + AH^o

3) Compound II + AH_2 --> HRP + AH^o

a free radical species and a second intermediate termed compound II (equation 2). Compound II has similarly been characterized as a ferryl iron-oxo species one oxidation equivalent above the resting state (Terner et al., 1985; Schulz et al., 1984; Hanson et al., 1981). Further reduction of the hemoprotein by a second substrate yields another free radical and the protein in the ferric resting state (equation 3).

Most other peroxidases react quite similarly with peroxide to give (if only transiently) an intermediate two oxidation equivalents above the resting state. The first oxidation equivalent is invariantly taken from the heme iron. The second can be taken from either the porphyrin (chloroperoxidase, Rutter et al., 1984) or an amino acid residue near the oxidized heme (cytochrome c peroxidase, Yonetani, T., 1976; Coulson, 1971). In some proteins a transient porphyrin radical cation is observed that quickly decomposes to a stable protein radical (R^oFe^{IV}) with the

protein still two oxidizing equivalents above the resting state (lactoperoxidase, Courtin, 1982; thyroid peroxidase, Virion et al., 1985).

Catalase is related to the peroxidases and also binds and reduces peroxide to give an intermediate two equivalents above the resting state (compound I, equation 4). The usual cycle then involves a two electron oxidation of a second peroxide molecule to give water and molecular oxygen

4) Catalase + H_2O_2 --> Compound I + H_2O

5) Compound I + H_2O_2 --> Catalase + O_2 + H_2O

(equation 5), although compound I is capable of one electron oxidation reactions similar to those of the peroxidases (Schonbaum and Chance, 1976).

The Cytochromes P450

The normal catalytic route for xenobiotic oxidation by P450 is shown in Figure 1.5. This cycle and the details of oxygen activation have been described in detail in several recent reviews (White and Coon, 1980; Sligar et al., 1984; Ortiz de Montellano, 1986) and will not be expanded upon here. It is sufficient to say that activation of molecular oxygen by P450 and its accessory proteins and cofactors ultimately yields an intermediate formally at the Fe^V oxidation state. This intermediate is a transient, highly

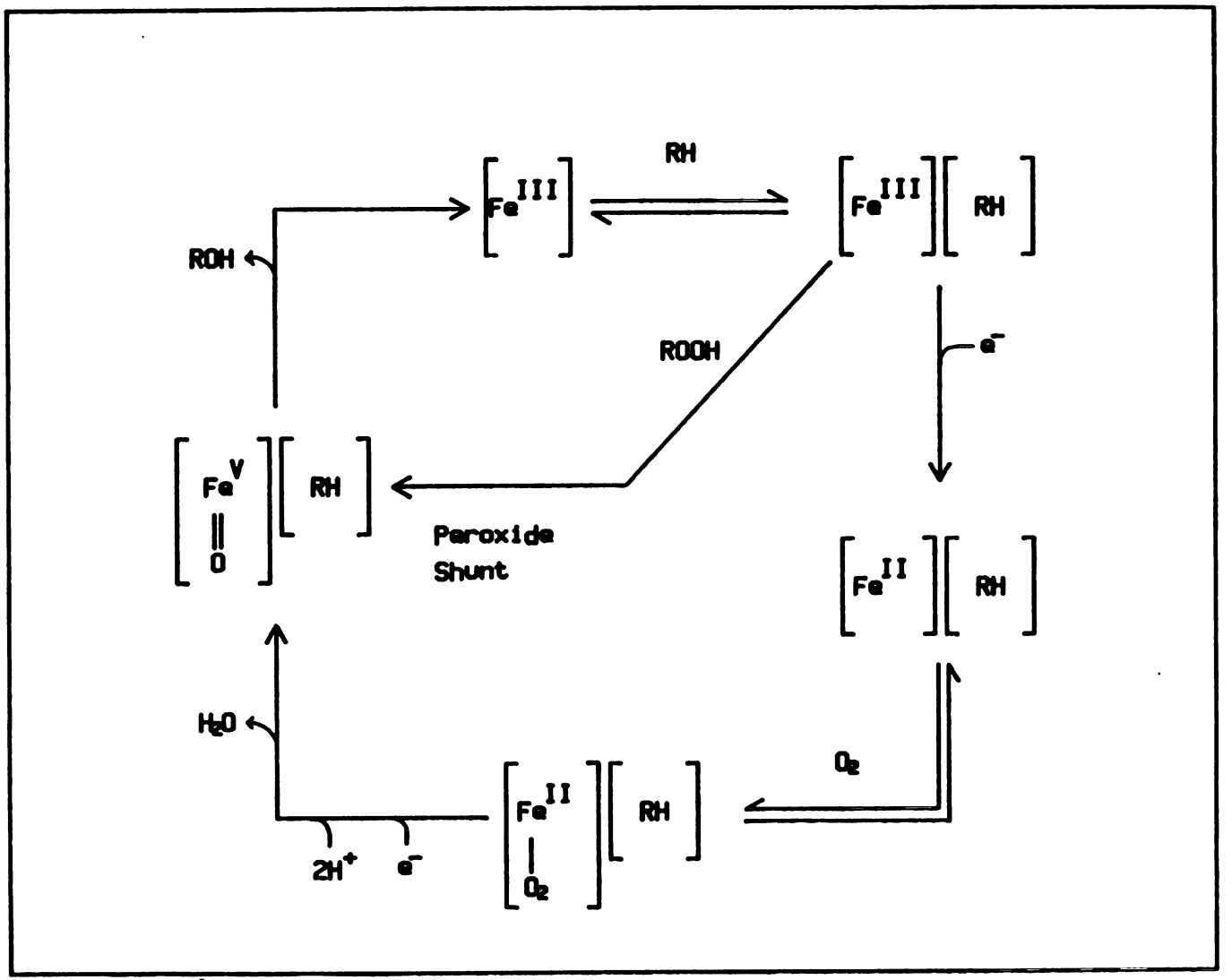

Figure 1.5. The Catalytic Cycle of Cytochrome P450.

reactive species which has frustrated attempts at its characterization. For this reason, the nature of the oxidized iron-oxo intermediate ($P^{\cdot}Fe^{IV}$, $R^{\cdot}Fe^{IV}$, etc) remains speculative.

Addition of peroxide to the ferric resting enzyme yields an intermediate capable of oxidizing substrates without the help of the accessory proteins or cofactors (the peroxide shunt). As in the normal catalytic cycle, the actual oxidant is highly reactive and exists only transiently. The interaction of peroxide with the ferric hemoprotein presumably yields the same iron-oxo species as is generated in the normal catalytic cycle. However, the high valent state of P450 is not limited to the peroxidative reactions catalyzed by the peroxidases. O-dealkylation of alkyl ethers, hydroxylation of aromatic substrates, and hydroxylation of unactivated hydrocarbons (a hallmark of P450 reactions) have been described in hydroperoxide-dependent P450 oxidations (Ortiz de Montellano, 1986).

The Globins

In 1935 Keilin and Hartree reported the formation of a red complex in the interaction of methemoglobin with hydrogen peroxide. This complex, the formation of which required one equivalent of peroxide per mole of heme, was converted back to the original globin upon addition of reducing agents. Early studies of H_2O_2-oxidized metmyoglobin suggested that the oxidized hemoprotein was one

electron above resting state (George and Irvine, 1952). Further investigation, however, revealed that a transient, two electron oxidized protein was the initial product of this reaction (vide infra). The intermediate has been characterized as a ferryl-oxo species by UV spectroscopy and magnetic succeptibility studies (ibid). This complex is quite stable but does return to the ferric ground state within 48 hours. Ferryl-myoglobin is quickly reduced to the ferric state by ascorbic acid, guiacol, iodide ion and ferrocyanide with concomitant oxidation of these compounds. The reduction of ferryl-myoglobin to metmyoglobin, both in the presence and absence of reducing agents, occurs faster at acidic pH.

An initial burst of luminescence is observed when H_2O_2 is added to metmyoglobin in the presence of luminol. The combination of a singly oxidized hemoprotein (vide supra) and luminescence was taken as evidence for the formation of a hydroxy radical by myoglobin and H_2O_2 via equation 6. This is basically Fenton chemistry with the iron one

6) $$Fe^{III} + H_2O_2 \dashrightarrow Fe^{IV} + HO^- + {}^{\circ}OH$$

oxidation equivalent higher at all points in the reaction. Later studies, however, revealed that the energetics of this mechanism are inconsistent with those observed experimentally (George and Irvine, 1956). An alternate

proposal for the nature of the oxidized intermediate was presented and is shown in equations 7 and 8. An initial two electron oxidation of the hemoprotein yields a transient

7) $Fe^{III} + H_2O_2 \longrightarrow Fe^{V}$

8) $Fe^{V} + RH \longrightarrow Fe^{IV} + R^{o}$

perferryl iron species in the rate determining step. This intermediate is then "quickly reduced to the ferryl state by reducing matter present, e.g., groups on the protein" (RH).

The concept that an oxidation equivalent is centered on a protein residue is supported by the detection of a free radical signal in peroxide-treated myoglobin (Gibson et al., 1958). This signal, which is dependent on the presence of both myoglobin and H_2O_2, increases with increasing myoglobin concentration. Addition of catalase AFTER formation of the complex has no effect on the signal but reducing agents eliminate it. The lifetime of the ESR signal is on the order of minutes and is dependent on pH (decrease with decreasing pH) and peroxide concentration (decrease with increasing $[H_2O_2]$). The spectral characteristics of the ESR signal have been investigated and compared to those for oxidized amino acids and dipeptides (King et al., 1964; King et al., 1967). The hemoprotein signal compares well in location (g=2.0036), line width (11 gauss) and saturation

characteristics to the ESR signals observed for phenylalanine, tyrosine, and DOPA radicals.

Addition of chloroiridate (a one electron oxidant) to horse myoglobin results in its oxidation to a ferryl-species accompanied by rapid precipitation of the protein. No free radical signal is detected in chloroiridate-oxidized horse myoglobin. Similar treatment of sperm whale myoglobin does not result in any change in the electronic spectrum of the protein but the oxidant is consumed and a weak ESR signal is observed. This has been interpreted as oxidation of an amino acid residue on the protein in preference to the heme iron in sperm whale myoglobin. (King and Winfield, 1966; King et al., 1967).

Oxygen evolution is observed in the reaction of peroxide with myoglobin (King et al., 1963). The amount of oxygen evolved, however, is 40% less than expected from catalytic decomposition of H_2O_2 and it has been suggested that oxygen resorption occurs secondary to the oxidation of protein amino acid residues (ibid). Examination of the aromatic amino acid region of the electronic spectrum suggests that oxidation of either a phenylalanine (-> tyrosine) or tyrosine (-> DOPA) residue occurs during the interaction of peroxide with myoglobin (King et al., 1967).

Treatment of hemoglobin and most myoglobins with hydrogen peroxide results in the formation of dimers and polymers (Rice et al., 1983). This polymerization is

prevented by the addition of cyanide, catalase or ascorbic acid to the incubation medium. Amino acid analysis of peroxide treated sperm whale myoglobin revealed the loss of 1.4 tyrosine residues in the monomeric and 1.8 tyrosine residues in the dimerized protein. Horse myoglobin, which does not dimerize under these conditions, shows the loss of 0.6 tyrosine residues per protein. It has been suggested that dimerization is the result of cross-linking of protein-bound tyrosine radicals (ibid). Small losses of histidine and lysine were also noted in both H_2O_2 treated hemoproteins.

All of these data are consistent with a ferryl iron, aromatic amino acid radical formulation for the hydrogen peroxide-oxidized states of hemoglobin and myoglobin. The properties of the ESR signal, the spectral changes observed, and the nature of protein modification strongly suggest that a tyrosine is the site of radical formation in the interaction of peroxide with globins (Figure 1.6).

A summary of the peroxide oxidized intermediates for all the hemoproteins discussed is shown in Table 1.1.

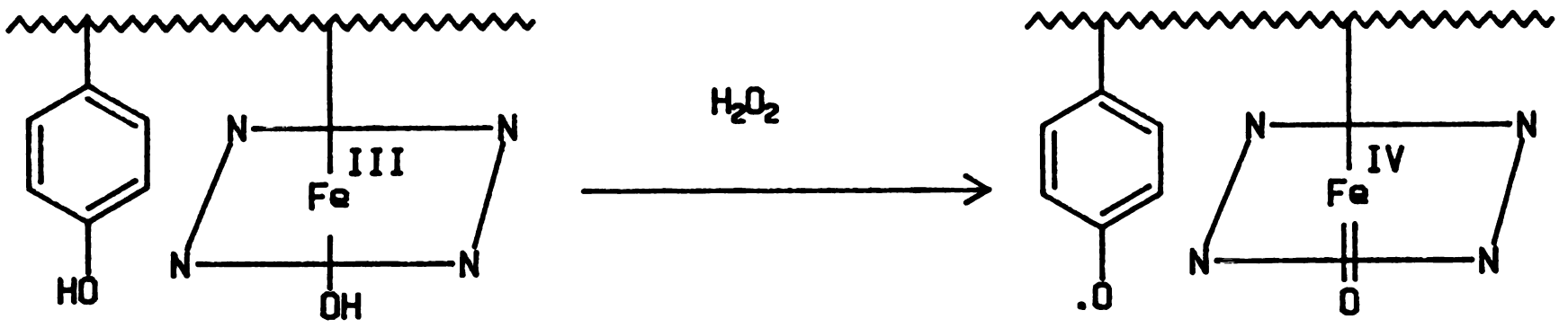

Figure 1.6. Interaction of Hemoglobin and Myoglobin with Hydrogen Peroxide: Formation of a Ferryl-Oxo, Tyrosine Radical Species.

Table 1.1. Comparison of Selected Heme Containing Proteins

Protein	Subunit M.W.	Quatern. Structure	Heme Ligand	H_2O_2 Form
Myoglobin[a]	17,000	monomer	His	R^{o}-Fe^{IV}
Hemoglobin[a]	15,500	tetramer	His	R^{o}-Fe^{IV}
Cytochrome P450[b]	56,000	monomer	Cys	? $[Fe]^{V}$
Horseradish peroxidase[c]	40,000	monomer	His	P^{o}-Fe^{IV}
Chloroperoxidase[c]	42,000	monomer	Cys	P^{o}-Fe^{IV}
Lactoperoxidase[c]	77,000	monomer	His[d]	P^{o}-Fe^{IV} ->R^{o}-Fe^{IV}
Thyroid Peroxidase[c]	62,000	-	-	R^{o}-Fe^{IV}
Cytochrome C peroxidase[c]	34,000	monomer	His	R^{o}-Fe^{IV}
Catalase[c]	60,000	tetramer	Tyr	P^{o}-Fe^{IV}

[a]Dickerson and Geis, 1983; [b]Black and Coon, 1986; [c]Marnett et al., 1986; [d]Manthey et al., 1986; R^{o}-Fe^{IV}, a ferryl-protein radical intermediate. P^{o}-Fe^{IV}, a ferryl-porphyrin radical intermediate

Xenobiotic Oxidation by Hemoglobin

Intact erythrocytes catalyze the oxidation of O-aminophenol (Tomoda et al., 1986), the epoxidation of styrene (Belvedere and Tursi, 1981; Tursi et al., 1983) and the hydroxylation of aniline and 4-chloroaniline (Blisard and Mieyal, 1979; Lenk and Sterzl, 1984). The formation of methemoglobin occurs concomitantly with these oxidations and is often followed by red cell lysis. Oxy-hemoglobin has been suggested as the oxidant in these reactions as well as in the decarboxylation of DOPA by erythrocyte hydrolysates (Tate et al., 1972; Yamabe and Lovenberg, 1972).

The oxidation of organic molecules by erythrocytes and oxyhemoglobin has led to the suggestion that this hemoprotein might be useful as a model for cytochrome P450 oxidations. In this vein, complex systems containing hemoglobin, cytochrome P450 reductase (or another electron carrier such as FAD, FMN or methylene blue) and NADPH have been examined for their ability to effect the oxidation of xenobiotics. Aromatic ring hydroxylation, N-dealkylation and O-dealkylation reactions have been demonstrated in such model systems (Golly and Hlavica, 1983; Starke et al., 1984; Cambou et al., 1984; Esclade et al., 1986). The results must be interpreted carefully, however, since catalase inhibits these reactions which, as true P450 model systems, should show no dependence on hydrogen peroxide.

Cooxidation of epinephrine to adrenochrome has been observed during the autooxidation of oxyhemoglobin to methemoglobin (Misra and Fridovich, 1972). This cooxidation is inhibited by catalase and superoxide desmutase and is consistent with the fact that both superoxide and hydrogen peroxide are formed in the autooxidation process (Sannes and Hultquist, 1978; Wallace et al., 1982). The binding of oxygen to ferrous hemoglobin polarizes an electron from the heme iron towards the oxygen ligand. The hydrophobic nature of the heme binding pocket favors return of this electron to the iron upon dissociation of the ligand (Carrell et al., 1977; Chiu et al., 1982). Nevertheless, autooxidation of oxyhemoglobin occurs under normal circumstances such that approximately 3% of the hemoprotein present in vivo is in the met form. In the red cell, the oxidized globin is continually reduced back to the ferrous form by a flavoprotein (NADH:cytochrome b_5 oxidoreductase)-cytochrome b_5 reducing system. Autooxidation and peroxide formation are enhanced by protons and anions (Wallace et al., 1982). Aromatic compounds containing amine, nitro or hydroxy substituents similarly accelerate the oxidation of oxyhemoglobin and are themselves oxidized, presumably reducing oxygen in the process. Both inner sphere (Doyle et al., 1984) and outer sphere (Kawanishi and Caughey, 1985) oxidation mechanisms have been proposed.

The oxidation of oxyhemoglobin to methemoglobin and the generation H_2O_2 during catalysis by this hemoprotein

create a situation favorable to ferryl-hemoglobin formation. Hydrogen peroxide dependent oxidation of nitroxide radicals (Yamaguchi et al., 1984), N-demethylation of aminopyrene (Zbaida et al., 1984), and epoxidation of styrene (Cantoni et al., 1982) by methemoglobin have been reported. The detection of phenoxy radicals by ESR spectroscopy during the oxidation of phenols by methemoglobin and hydrogen peroxide (Shiga and Imaizumi, 1973) attests to the peroxidase activity of this system. Furthermore, both methemoglobin and metmyoglobin effect membranal lipid peroxidation in a peroxide dependent manner (Kanner and Harel, 1985; Harel and Kanner, 1985).

The oxidation of hemoglobin to the ferric state, the ability of complicated reducing systems to evolve hydrogen peroxide (Kuthan et al., 1978; Grover and Piette, 1981) and the inhibition of substrate oxidation by catalase suggest that the substrate oxidations by the P450 model systems discussed above are actually mediated by methemoglobin and hydrogen peroxide.

Proposal for Thesis

Hemoglobin and myoglobin react with peroxide to generate an oxidized intermediate very similar to that observed with the peroxidases. Unlike the peroxidases, however, this interaction bleaches the heme chromophore and modifies amino acid residues of the protein. This is not

surprising if one considers that the hemoprotein was "designed" for oxygen transport, not peroxide reduction. The nature of the globin modification caused by peroxide is unknown and is to be examined in this study.

The "reactive" center in the globins is iron protoporphyrin IX, the same prosthetic group contained in several peroxide and xenobiotic metabolizing enzymes. Each of these hemoproteins modulates the reactivity of the heme iron towards a specific catalytic purpose but this specificity can be altered by appropriate manipulation of the incubation parameters. In this vein, the activation of hemoglobin (or myoglobin) by hydrogen peroxide to a species capable of oxidative metabolism might be utilized as a model for cytochrome P450 oxidations. A detailed investigation of hydrogen peroxide activated hemoglobin is therefore proposed to evaluate the validity of such a comparison.

The hemoproteins are notable in that they all contain the same prosthetic heme group and yet function in widely different capacities. This provides an opportunity to explore the manner in which protein structure modulates chemical reactivity. The interaction of peroxide with the oxygen transport hemoproteins is admittedly an artificial situation; However, the mechanism of xenobiotic oxidation and the nature of the resultant globin modification may yield insight into the more general methods whereby proteins control reactive intermediates.

Chapter 2 Xenobiotic Oxidation by Hemoglobin

Styrene Oxidation

Products Formed in the Oxidation of Styrene by Hemoglogin and Hydrogen Peroxide. Addition of hydrogen peroxide to hemoglobin results in immediate hypochromic red shift of the Soret band of the ferric hemoprotein from 408 nm to 412 nm (characteristic of a ferryl (Fe^{IV}=O) hemoprotein) followed by irreversible, time dependent loss of the heme chromophore (Figure 2.1). The remaining Soret band eventually returns to 408 nm and the hemoprotein retains the ability to react in a similar manner with H_2O_2 (Figure 2.1). The extent of chromophore loss is temperature dependent with greater effects observed at 37°C (80% loss) than at 0°C (40% loss). Myoglobins from sperm whale, horse and red kangaroo exhibit similar spectral changes and Soret losses upon reaction with H_2O_2. All incubations were performed at 0°C, unless otherwise stated, to preserve the hemoprotein as much as possible during the incubation period.

Incubation of styrene with hemoglobin and H_2O_2 results in the formation of two products that are detectable by GC analysis (Figure 2.2). These were unambiguously identified as benzaldehyde and styrene oxide by coelution of the products with the authentic standards and comparison of the

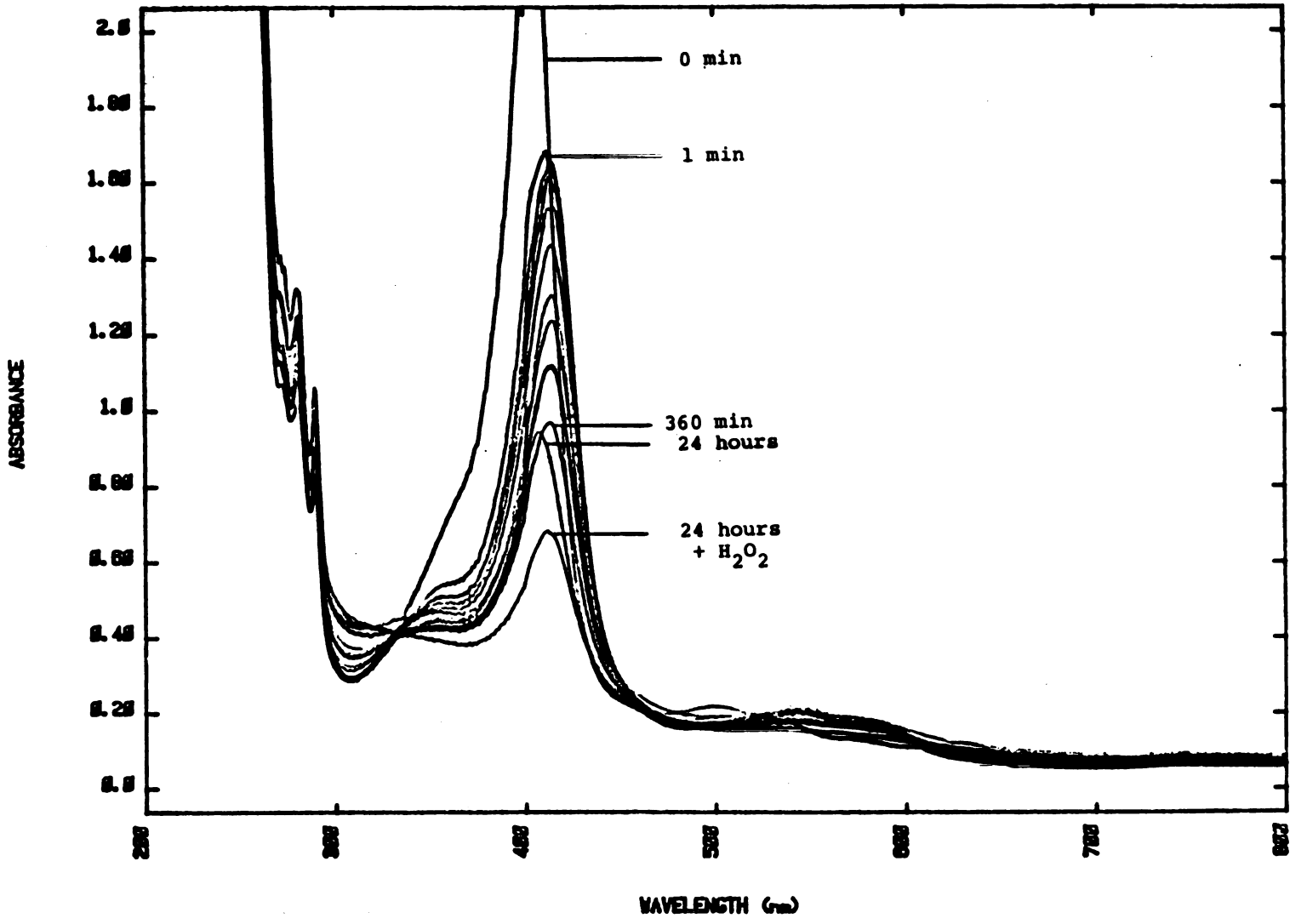

Figure 2.1. Hemoglobin Soret Loss with Time.

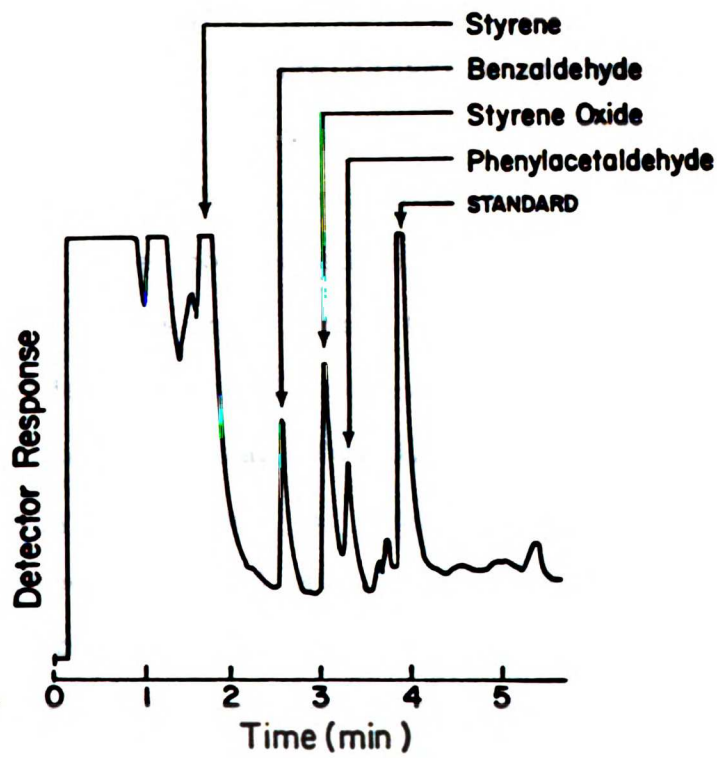

Figure 2.2. Products Formed in the Oxidation of Styrene by Hemoglobin and Hydrogen Peroxide.

mass spectra of the products with those of authentic samples of benzaldehyde and styrene oxide (Figure 2.3). GC analysis also showed the presence of phenylacetaldehyde (identified using the same methods) but it was shown NOT to be a product of the reaction by the following procedure. Reverse Phase-HPLC analysis, after removal of residual styrene by low pressure chromatography, showed the presence of two products (Figure 2.4, peaks 1 and 2) with retention times identical to those of autentic benzaldehyde/phenylacetaldehyde and styrene oxide, respectively. Both of the aldehydes have the same retention time under the conditions that were employed. Peaks 1 and 2 were collected and analyzed by gas-liquid chromatography. This confirmed the identity of the latter as styrene oxide and the former as benzaldehyde. No trace of phenylacetaldehyde was found. These data show that phenylacetaldehyde is not a product of the oxidation of styrene by hemoglobin and H_2O_2. Thermal rearrangement of styrene oxide, presumably catalyzed by some component of the incubation extract, is probably responsible for the artifactual formation of phenylacetaldehyde during the GC analysis. The amount of phenylacetaldehyde formed depends on the condition of the GC column and can be minimized by heating a freshly packed column heated overnight at 200°C. The styrene oxide:phenylacetaldehyde ratio was variable, however, so the styrene oxide yields reported below include the phenylacetaldehyde formed during the GC analysis.

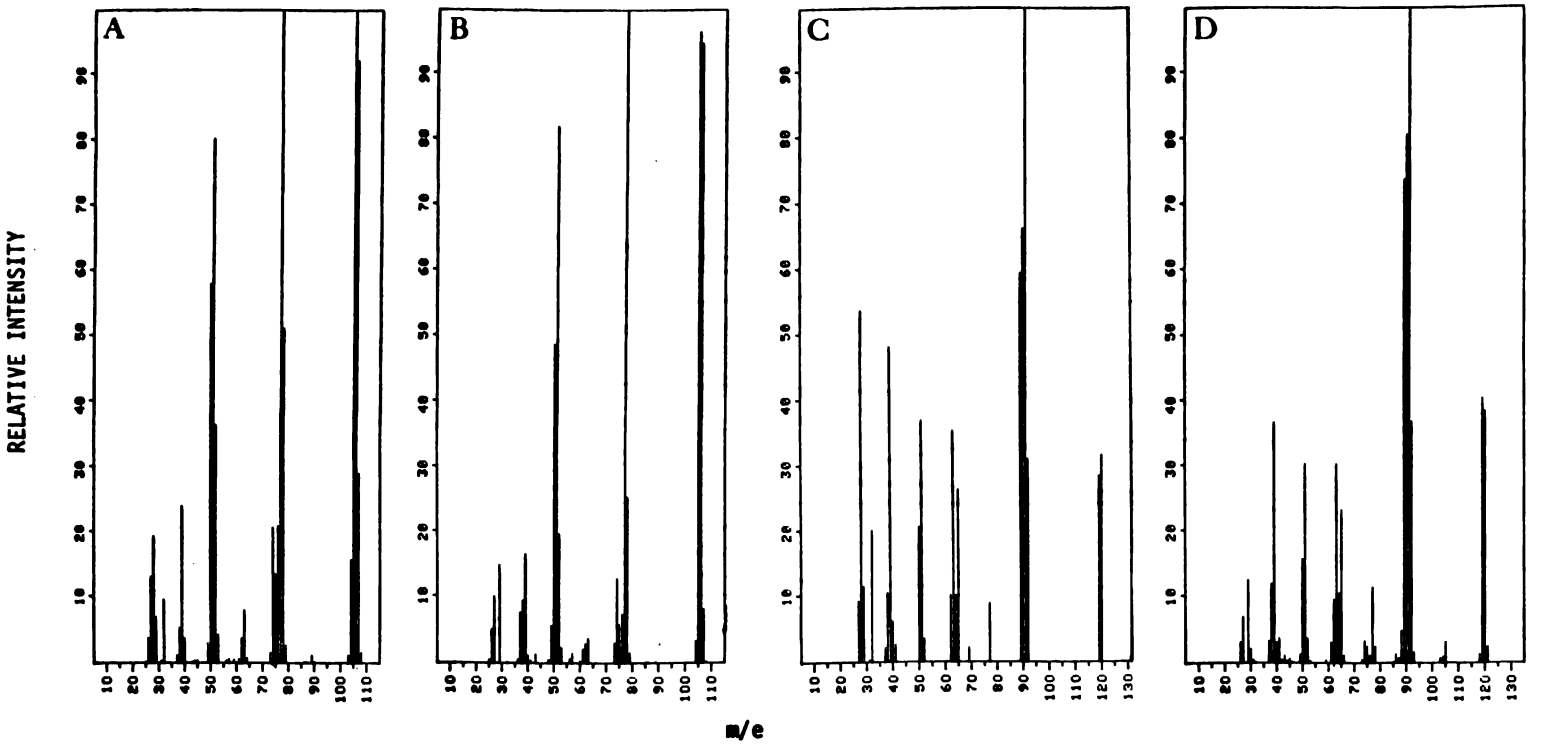

Figure 2.3. Mass Spectra of the Products Isolated in the Oxidation of Styrene by Hemoglobin and Hydrogen Peroxide. A) Authentic Benzaldehyde, B) Benzaldehyde Metabolite, C) Authentic Styrene Oxide and D) Styrene Oxide Metabolite.

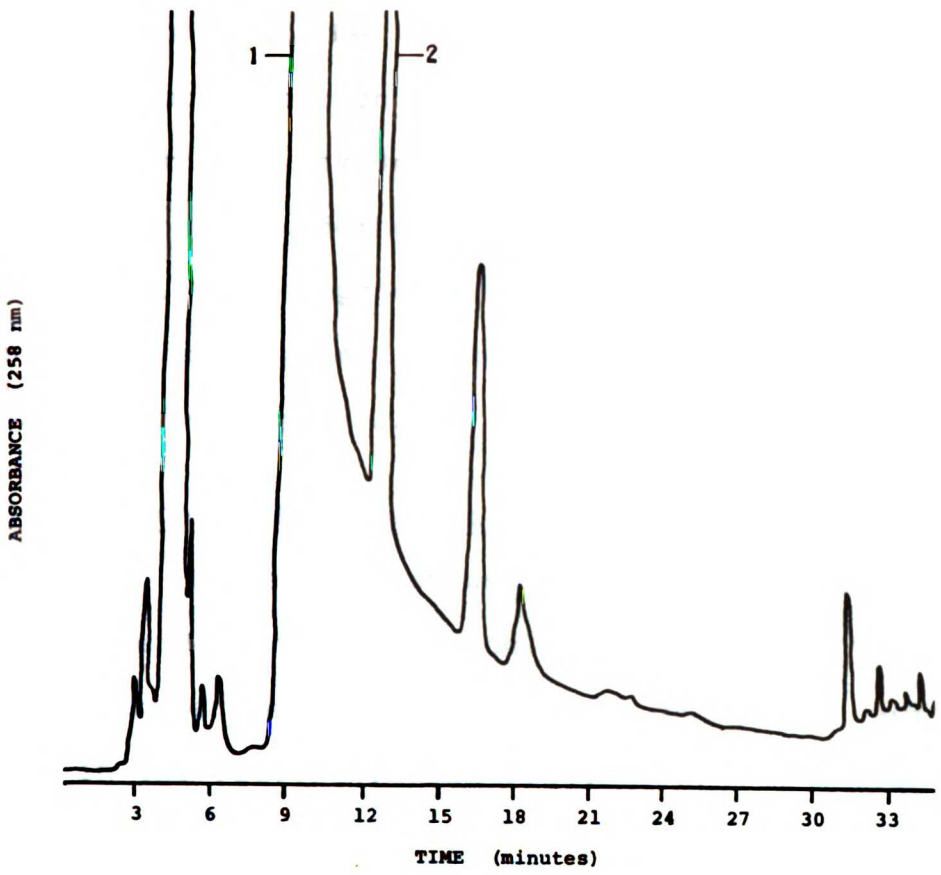

Figure 2.4. HPLC Chromatogram of the Products Isolated from the Oxidation of Styrene by Hemoglobin and Hydrogen Peroxide. 1) Benzaldehyde and 2) Styrene Oxide.

Product formation and loss of the heme chromophore level off after approximately 90-120 minutes (Figure 2.5). The electronic spectrum when product formation levels off is that of a ferryl hemoprotein. GC analysis shows, furthermore, that substantial amounts of styrene are still present. This precludes substrate exhaustion as the factor responsible for cessation of the reaction. Product yield is related to the peroxide concentration, with a maximum reached at a peroxide:heme ratio of approximately 15-20 (Figure 2.6). The product yield also depended on the concentration of styrene, with the maximum corresponding to 5-10 mM styrene (Figure 2.7).

Dependence of Product Formation on Incubation Parameters. Table 2.1 shows that product formation is strictly dependent on both hemoglobin and H_2O_2. The role of H_2O_2 is further evidenced by the inhibitory action of catalase in the reaction. The requirement for a ferric, but not ferrous, prosthetic heme is demonstrated by the substantial decrease in product formation observed in the presence of KCN compared to the slight decrease observed in the presence of CO. Superoxide and hydroxyl radical can be discounted as the reactive oxidizing species by the inability of superoxide dismutase and mannitol, respectively, to inhibit the reaction. Both ascorbic acid and BHT attenuate product yield but the mechanism of this inhibition is difficult to interpret. Both of these compounds can intercept free radicals but can also reduce

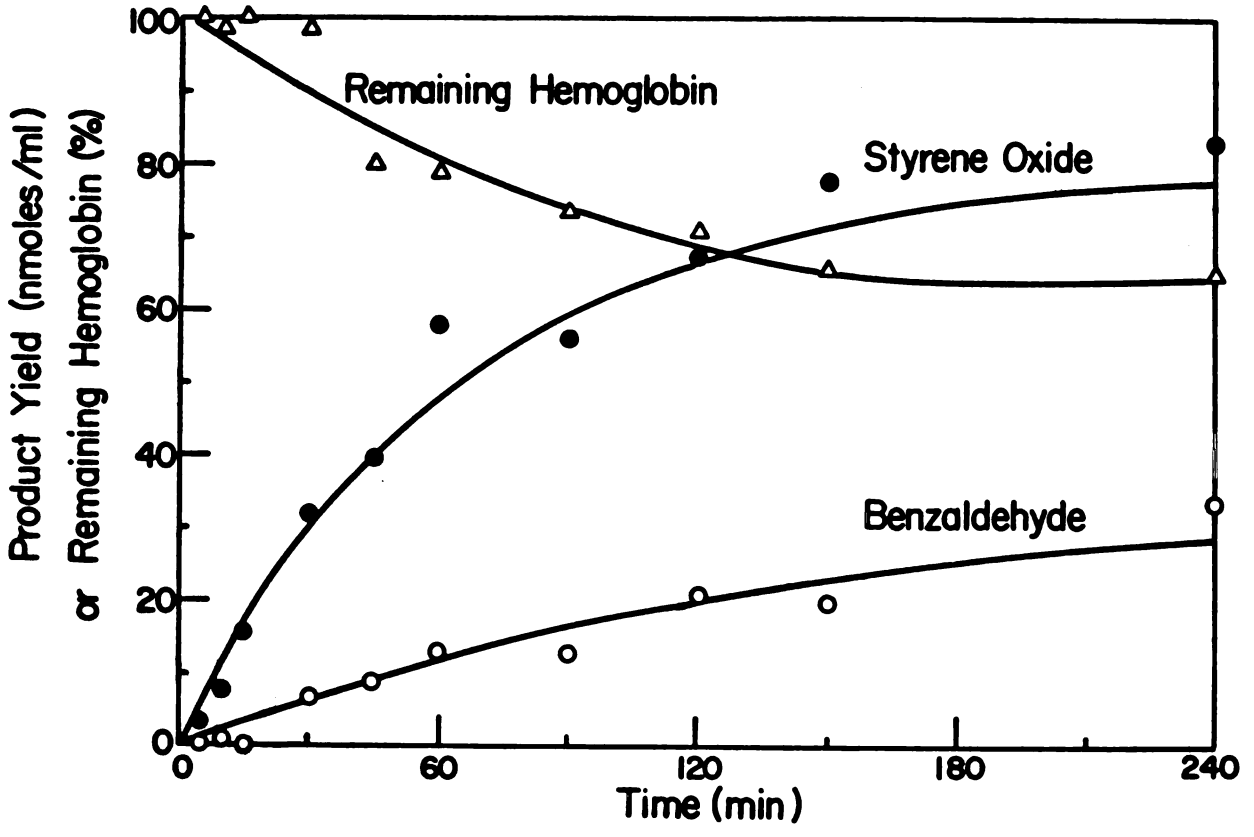

Figure 2.5. Time Course for Product Formation and Heme Soret Loss.

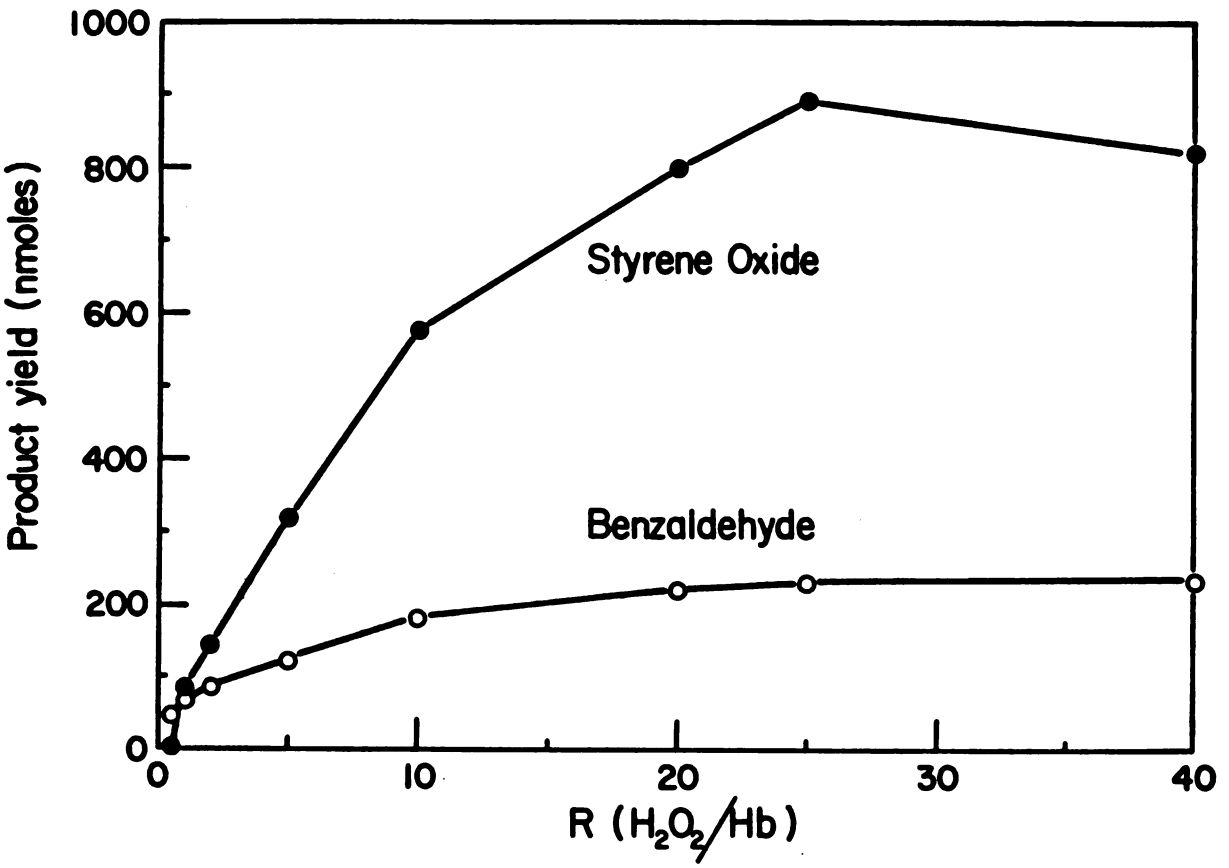

Figure 2.6. Dependence of Product Formation on Hydrogen Peroxide Concentration.

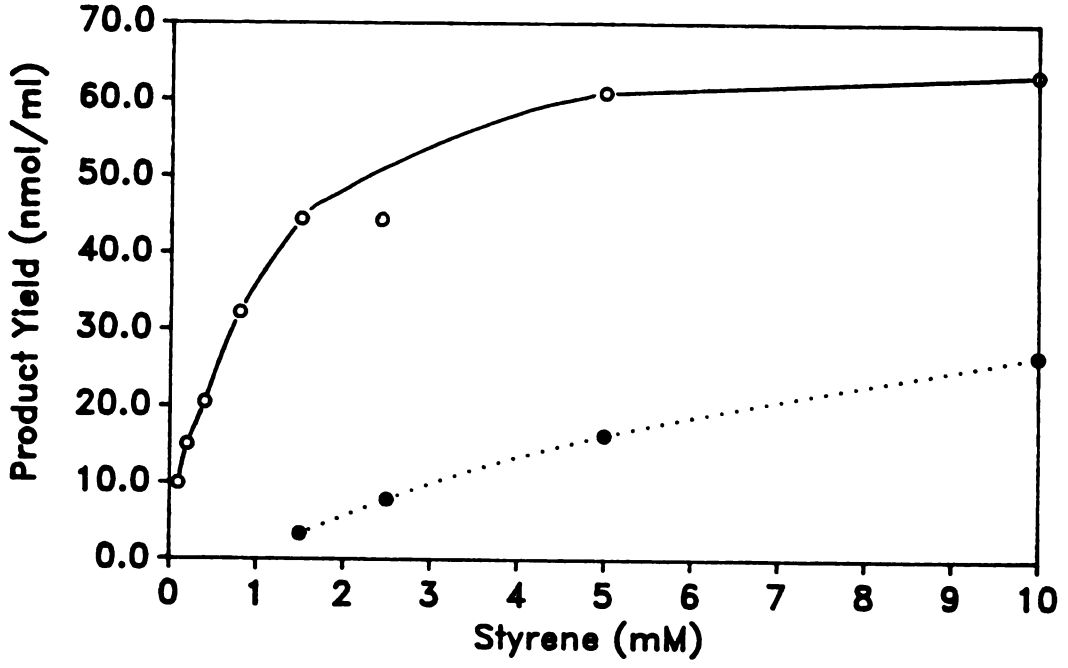

Figure 2.7. Dependence of Product Formation on Styrene Concentration.

Table 2.1. Factors Affecting Product Yield

Incubation Modification	Relative %	
	Benzaldehyde	Styrene Oxide
Normal Incubation[a]	100	100
-Hemoglobin	5	1
-H_2O_2	6	8
+Catalase (60 u/ml)	16	ND.[b]
+KCN (50 mM)	14	15
+CO (1:1 with O_2)	85	95
+SOD (60 u/ml)	100	107
+Mannitol (50 mM)	114	104
+BHT (50 mM)	70	74
+POBN (50 mM)	101	57
+DABCO (50 mM)	60	125
+Ascorbic Acid (50 mM)	28	3
-O_2 (Argon atmosphere)		
Non-chelexed buffer	82	88
Chelexed buffer	69	63
-Styrene, +Styrene oxide (1 ug/ml)	ND	-

[a]10 μM hemoglobin, 600 μM H_2O_2 and 10 mM styrene (duplicate 10 ml incubations) kept at 0°C for 90 minutes. Unless stated, the buffers were NOT treated with chelex before use. Product yield in the controls was 54 nmol/ml styrene oxide and 29 nmol/ml benzaldehyde. [b]ND, not detectable.

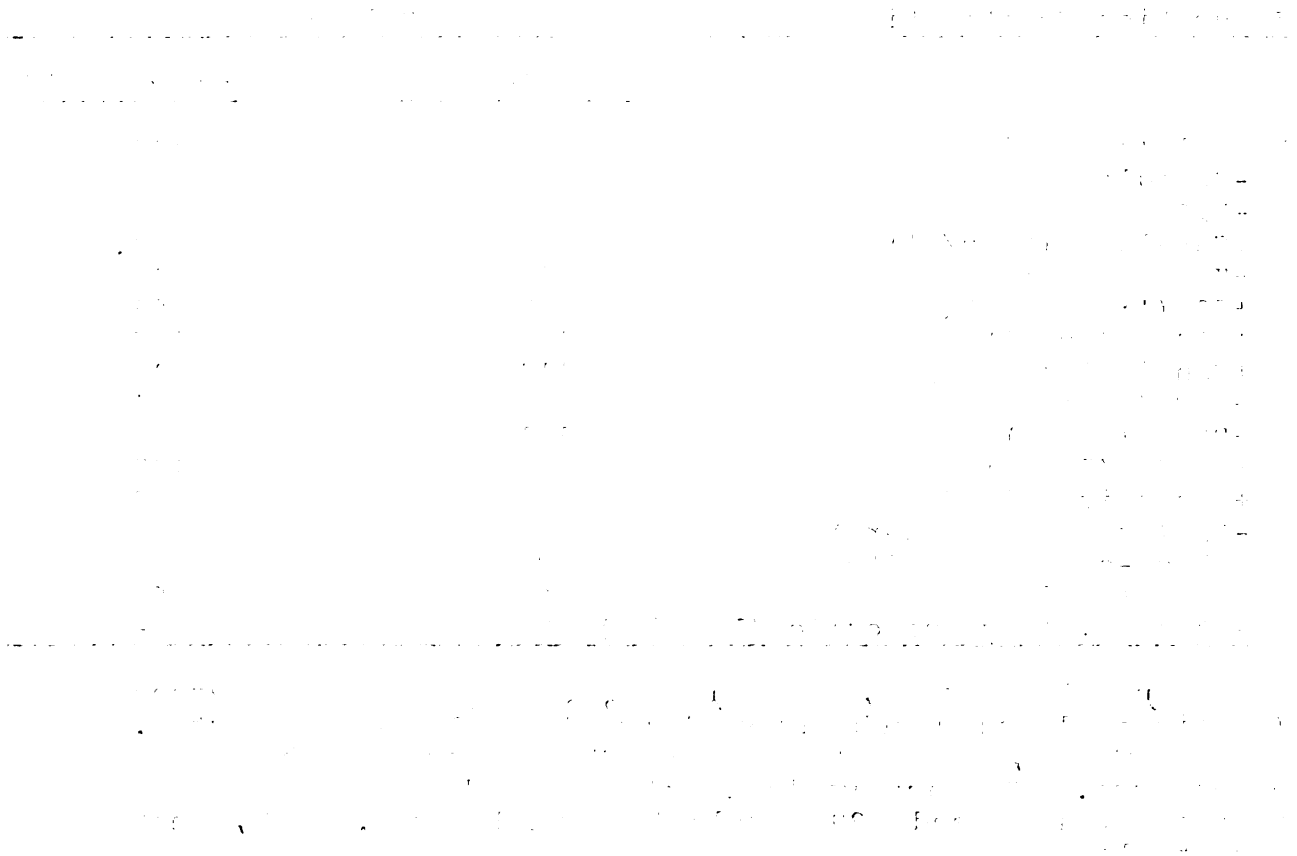

the high valent hemoprotein. POBN, a free radical trap, inhibits styrene oxide formation but has little effect on the yield of benzaldehyde. This suggests a difference in the oxidative pathway leading to the two products. The existence of such a difference is further supported by the fact that DABCO, a singlet oxygen trap, inhibits benzaldehyde production but has little effect on the yield of styrene oxide.

The attenuated product yield in the absence of O_2 (Table 2.1, argon atmosphere) suggests molecular oxygen is involved in the oxidation process. The extent of this involvement cannot be determined since oxygen is evolved in the reaction of hemoglobin with hydrogen peroxide. Figure 2.8 (inset) shows the time course of oxygen evolution by hemoglobin and H_2O_2. The figure shows, furthermore, that the amount of oxygen evolved per mole of heme increases with increasing concentration of the hemoprotein at a constant H_2O_2:heme ratio. Subsequent experiments showed that addition of H_2O_2 to buffer alone also resulted in oxygen evolution. Chelex treatment of the buffers to remove trace metals, attenuates, but does not eliminate, oxygen evolution and decreases the product yield under anaerobic conditions (Table 2.1).

Myoglobins from sperm whale, horse, and red kangaroo similarly oxidize styrene in the presence of H_2O_2. Table 2.2 shows that the efficiency of this oxidation decreases in

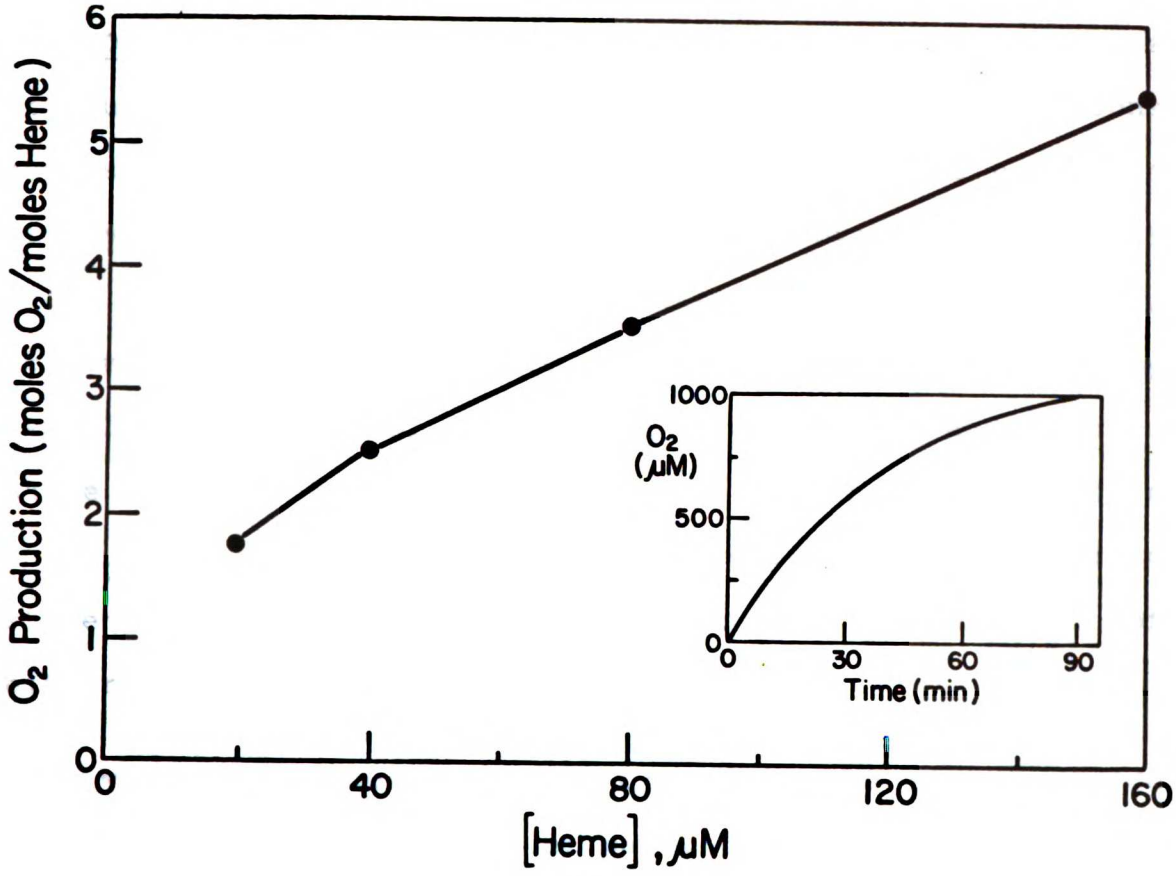

Figure 2.8. Oxygen Evolution in the Interaction of Hemoglobin with Hydrogen Peroxide.

the order of hemoglobin > whale myoglobin > horse myoglobin > kangaroo myoglobin. The ratio of benzaldehyde to styrene oxide, however, is similar with each of the hemoproteins.

Origin of Oxygen in the Styrene Oxide Product. The attenuation of product yield under anaerobic conditions suggests that molecular oxygen is utilized in the oxidation of styrene by hemoglobin and hydrogen peroxide. Figure 2.9 shows the mass spectra of authentic styrene oxide (^{16}O), styrene oxide isolated from the oxidation of styrene by hemoglobin and $H_2{}^{16}O_2$ in an $^{18}O_2$ environment, and styrene oxide isolated from the oxidation of styrene by hemoglobin and $H_2{}^{18}O_2$. Table 2.3 lists the incorporation of ^{18}O into styrene oxide by various hemoproteins in the presence of either $H_2{}^{18}O_2$ or $^{18}O_2$.

The table shows that the oxygen in the styrene oxide product derives, at least in part, from molecular oxygen. The less than complete ^{18}O-incorporation by hemoglobin utilizing $^{18}O_2$ was reproducible (two separate experiments on two separate days), so the low incorporation of label is not due to inefficient deoxygenation of the incubation mixture. This is confirmed by ^{18}O-incorporation studies utilizing $H_2{}^{18}O_2$. Treatment of the incubation buffer with chelex substantially reduces the amount of labeled oxygen incorporated into styrene oxide from $H_2{}^{18}O_2$ (Table 2.3), presumably by decreasing the evolution of $^{18}O_2$ from the peroxide.

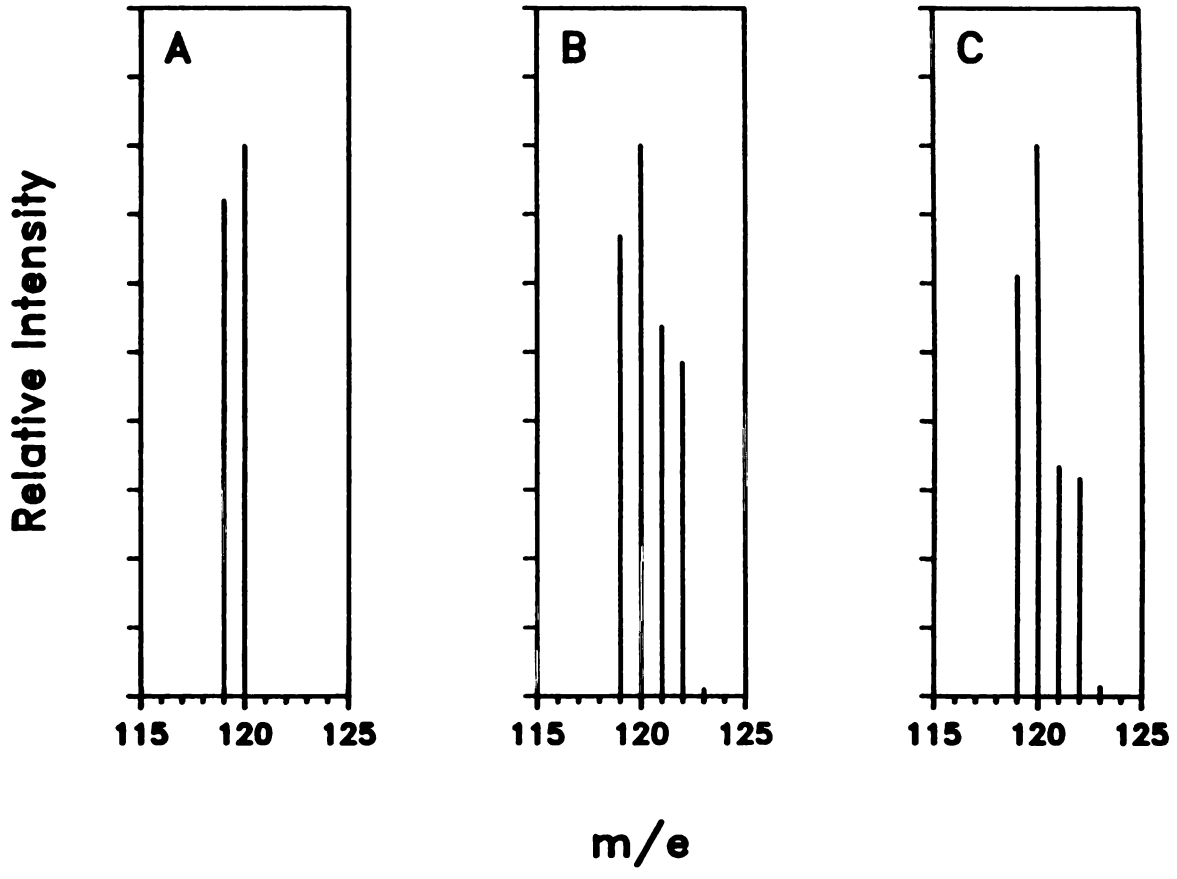

Figure 2.9. Molecular Ion Region of the Mass Spectrum of A) ^{16}O-Styrene Oxide Standard, B) Styrene Oxide Isolated from the Oxidation of Styrene by Hemoglobin and $H_2{}^{16}O_2$ in an $^{18}O_2$ Environment and Styrene Oxide Isolated from the Oxidation of Styrene by Hemoglobin and $H_2{}^{18}O_2$.

Table 2.2. Formation of Benzaldehyde and Styrene Oxide by Different Hemoproteins

Hemoprotein[a]	Relative %	
	Benzaldehyde	Styrene Oxide
Hemoglobin (bovine)	100	100
Myoglobin (sperm whale)	43	62
Myoglobin (horse heart muscle)	23	34
Myoglobin (horse skeletal muscle)	25	34
Myoglobin (red kangaroo)	ND[b]	10

[a]40 μM heme, 600 μM H_2O_2 and 10 mM styrene (duplicate 10 ml incubations) kept at 0°C for 90 minutes. Buffers were NOT treated with chelex before use. [b]ND, not detectable.

Table 2.3. Source of the Oxygen in Styrene Oxide

Hemoprotein[a]	Chelex Treatment	^{18}O-incorporation	
		$H_2{}^{18}O_2$	$^{18}O_2$
		Percent	
Hemoglobin (bovine)	no	70	38
Myoglobin (whale)	no	55	67
Myoglobin (horse)	no	35	78
Hemoglobin (bovine)	yes	47	NE[b]
Myoglobin (horse)	yes	16	NE

[a]40 μM heme, 600 μM H_2O_2 and 10 mM styrene kept at 0°C for 90 minutes. [b]NE, not examined.

Stereochemical Fidelity: Oxidation of trans-[1-^{2}H]-Styrene Oxide. The products of a 500 ml preparative incubation containing hemoglobin, H_2O_2 and trans-[1-^{2}H]-styrene were isolated using low pressure chromatography. The NMR spectrum (240 mHz) of the deuterated oxide product is shown in Figure 2.10 along with that for chemically oxidized (m-CPBA) trans-[1-^{2}H]-styrene and authentic undeuterated styrene oxide. Each of the epoxide protons appears as a doublet of doublets in the undeuterated oxide due to spin coupling (AB spin system) with the other two protons (J_{CT}=5.6Hz, J_{BC}=2.5Hz, J_{BT}=4.1Hz). The full splitting pattern is not observed in the deuterated compound due to the fact that the ^{2}H-^{1}H coupling constant is only 20% of the ^{1}H-^{1}H coupling constant. This decreases the J_{BC} splitting beneath the resolution of the instrument (<1 Hz) and the epoxide protons in the deuterated compound therefore appear as doublets. The chemically generated oxide exhibits a very weak signal at 3.15 ppm consistent with the presence of a trace of unlabeled styrene in the starting material. Note that the signal appears as a doublet of doublets, as expected for the nondeuterated compound and not from loss of the deuterium stereochemistry. The styrene oxide derived from incubation of labeled styrene with hemoglobin and H_2O_2 shows a strong signal at 3.15 ppm integrating to 33% of the total area for the cis and trans protons. This signal, which appears as a doublet, indicates a true loss of stereochemistry and not loss of deuterium label. This is

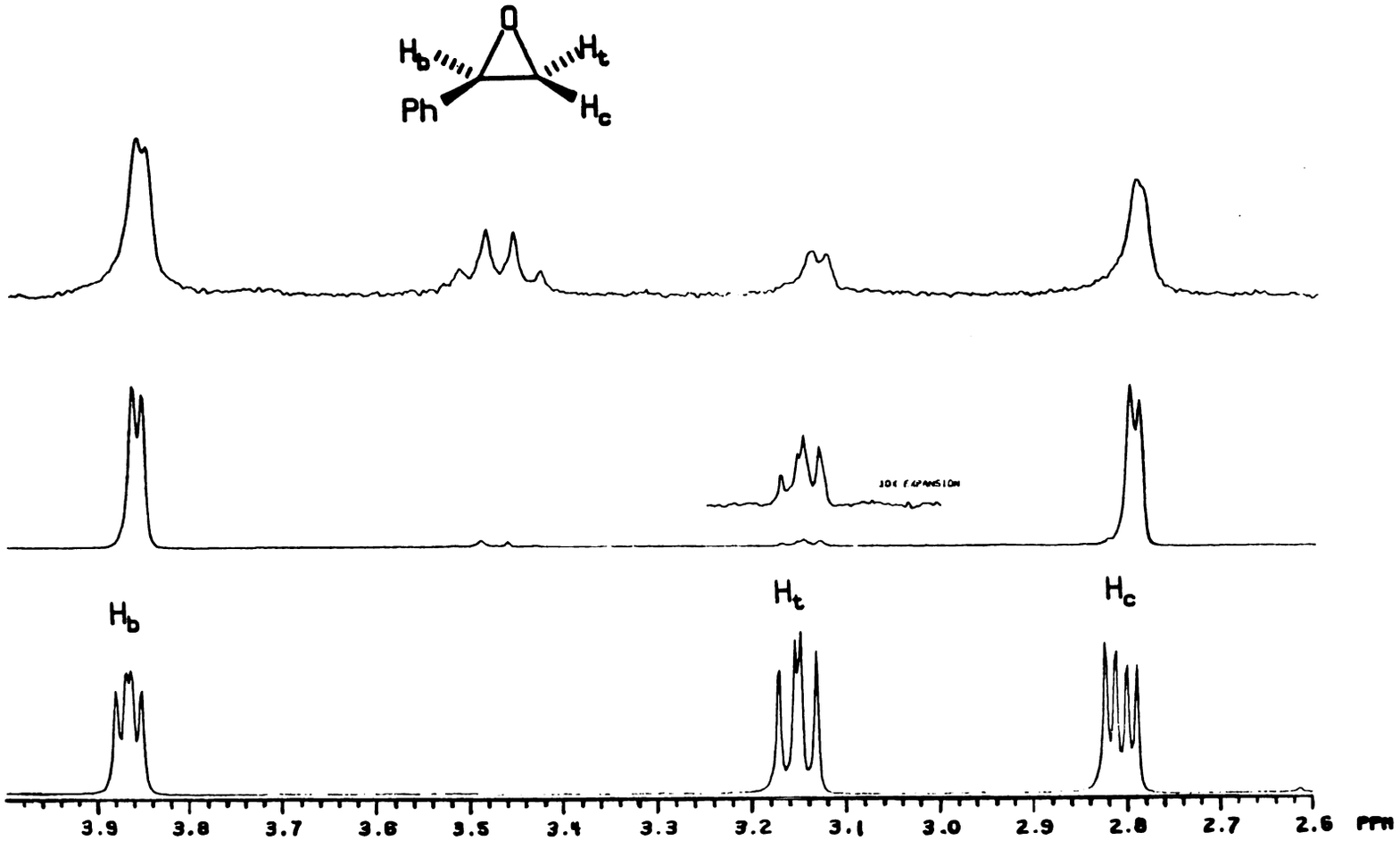

Figure 2.10. NMR Spectra of [^{1}H]-Styrene Oxide Standard (lower trace), Styrene Oxide Isolated from the Oxidation of trans-[^{2}H]-Styrene by m-CPBA (middle trace), and Styrene Oxide Isolated from the Oxidation of trans-[^{2}H]-Styrene by Hemoglobin and Hydrogen Peroxide.

confirmed by the mass spectrum of the oxide product, which is identical to that of chemically generated trans-[1-^{2}H]-styrene oxide (Figure 2.11). These data clearly demonstrate that the deuterium stereochemistry is inverted in approximately one-third of the styrene oxide product.

Stereoselectivity: Absolute Stereochemistry of Styrene Epoxidation. Incremental addition of tris-[3-(heptafluoropropylhydroxymethylene)-d-camphorato] Europium III (Eu(hfc) III) to authentic racemic styrene oxide results in a progressive increase in the NMR chemical shifts of the epoxide protons as well as a broadening of their signals. Figure 2.12 shows a plot of chemical shift vs. Eu(hfc)III added. Note that the enantiomeric trans-protons begin to resolve at approximately 3.5 ppm and can be completely resolved using this method. Similar addition of Eu(hfc)III to styrene oxide generated from incubation of styrene with hemoglobin and H_2O_2 results in the NMR spectrum shown in Figure 2.13. The signals appear as triplets rather than as doublets of doublets due to peak broadening by the paramagnetic shift reagent. Integration of the enantiomeric trans-proton signals for both of the oxides yields, within experimental error, a value of 1:1 for the ratio of the peaks. This demonstrates the absence of any stereoselectivity in the epoxidation reaction.

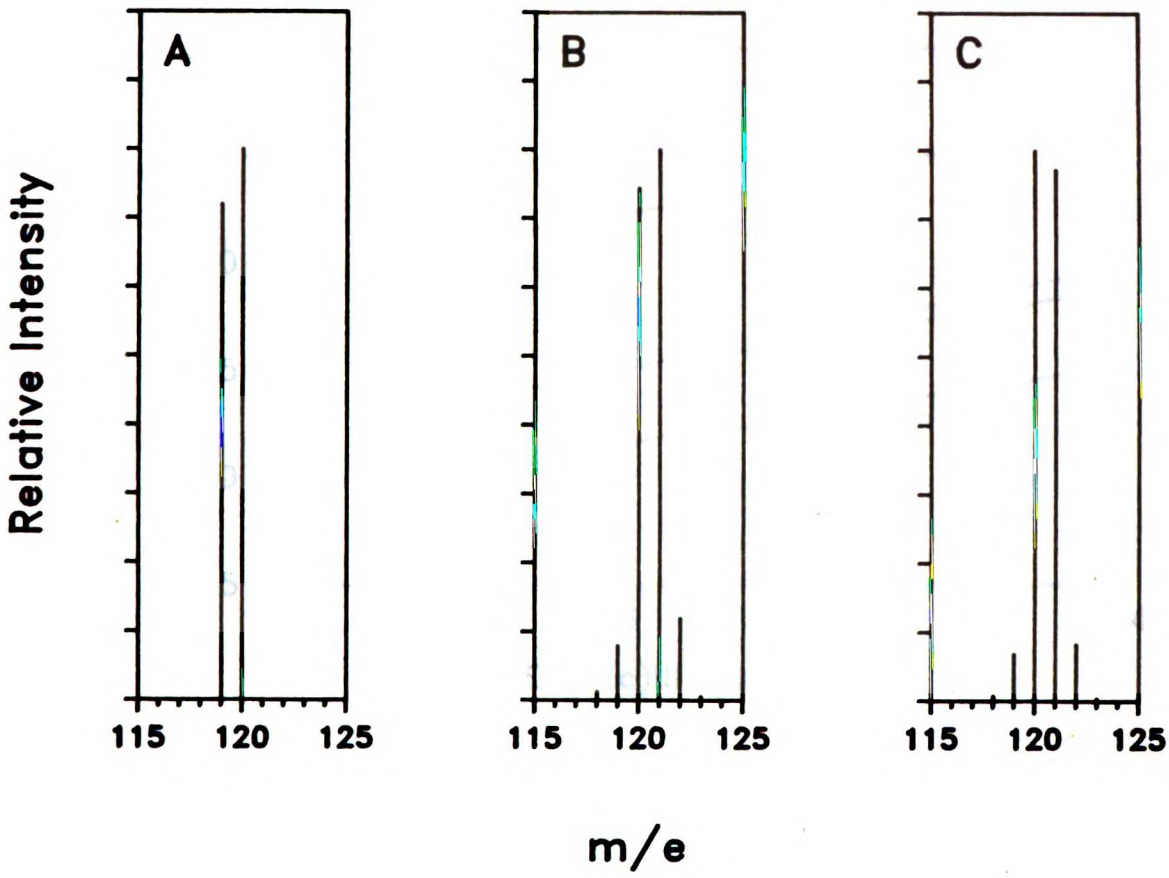

Figure 2.11. Molecular Ion Region of the Mass Spectra of A) [^{1}H]-Styrene Oxide Standard, B) Styrene Oxide Isolated from the Oxidation of trans-[^{2}H]-Styrene by m-CPBA and C) Styrene Oxide Isolated from the Oxidation of trans-[^{2}H]-Styrene by Hemoglobin and Hydrogen Peroxide.

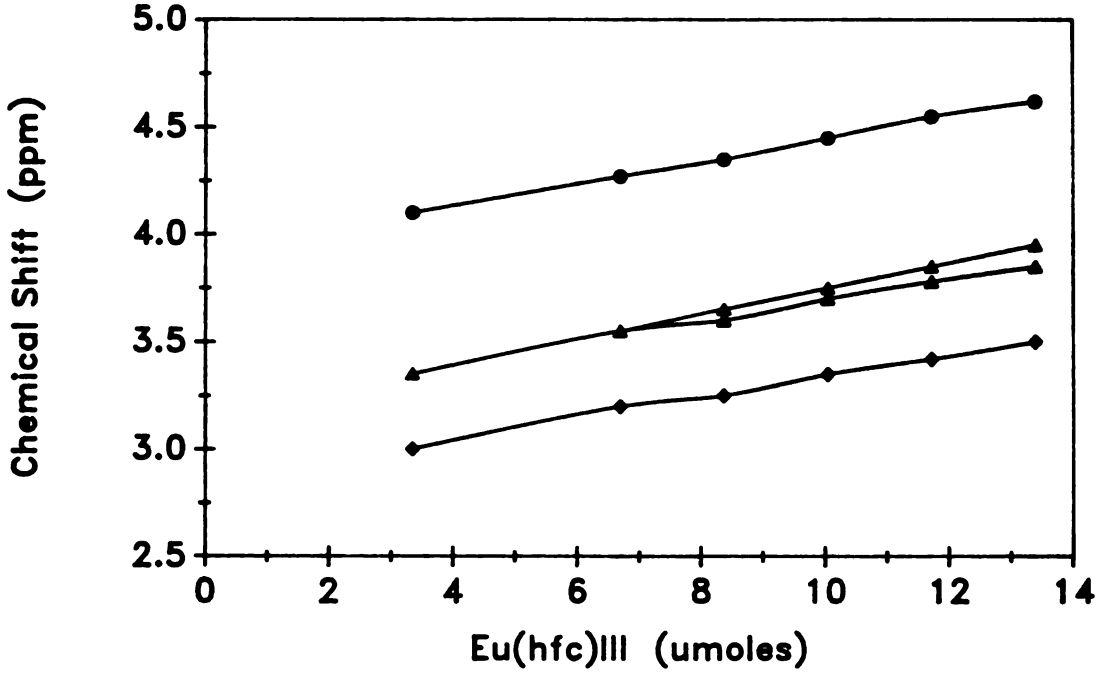

Figure 2.12. NMR Chemical Shift of Styrene Olefinic Protons vs. Eu(hfc)III Added. Upper Trace, Benzylic Proton; Middle Trace, Trans Proton; Lower Trace, Cis Proton.

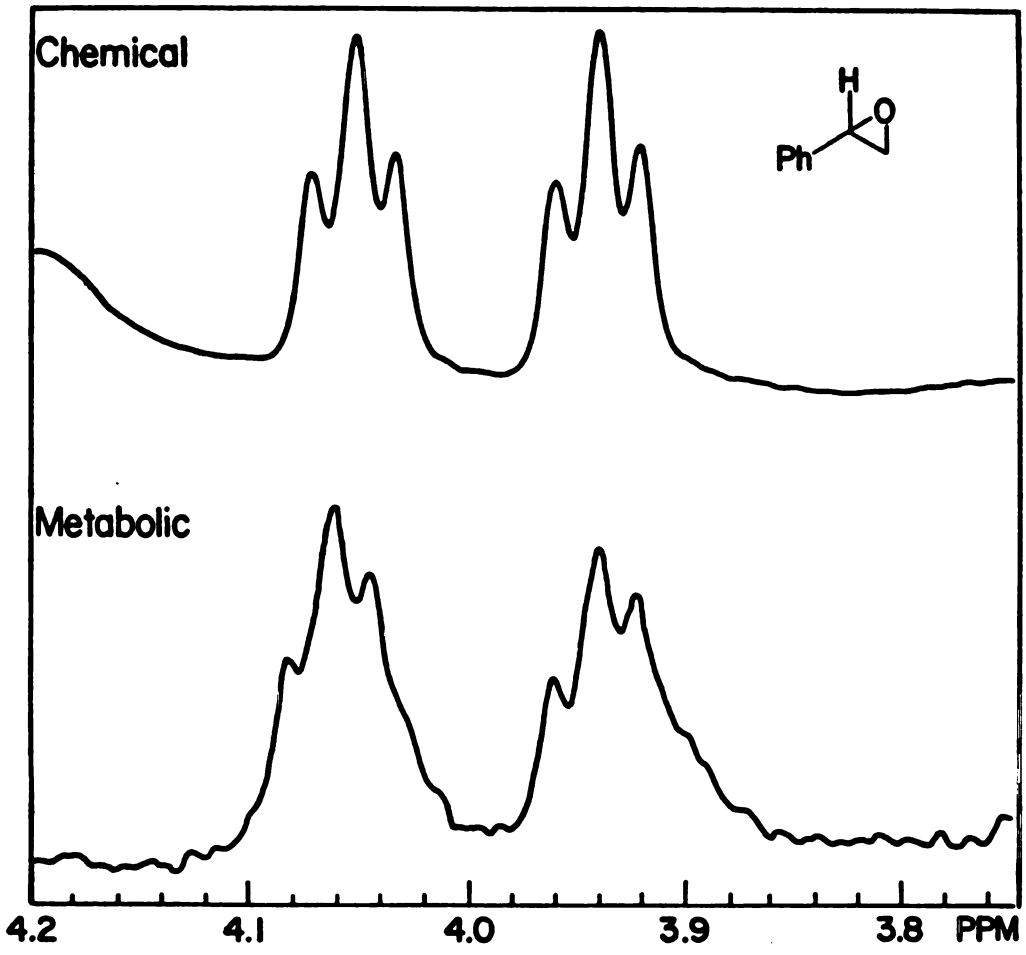

Figure 2.13. The Trans Proton Region of the NMR Spectra of Styrene Oxide Isolated from the Oxidation of Styrene by m-CPBA (upper trace) and Hemoglobin/H_2O_2 (lower trace). Resolution of the Enantiomeric Trans Protons was Accomplished with the Addition of Eu(hfc)III as Described in Chapter 5.

trans-7,8-Dihydroxy-7,8-dihydrobenzo(a)pyrene Oxidation

Products Formed in the Oxidation of trans-7,8-Dihydroxy-7,8-dihydrobenzo(a)pyrene by Hemoglobin and Hydrogen Peroxide. Incubation of trans-7,8-dihydroxy-7,8-dihydrobenzo(a)pyrene (BAPD) with hemoglobin and H_2O_2 results in the formation of two HPLC detectable products (Figure 2.14, peaks a and d). The formation of these products depends on the presence of both hemoglobin and H_2O_2. As shown in Figure 2.15, the electronic spectra of the two products are identical to that of authentic 7,8,9,10-tetrahydroxy-7,8,9,10-tetrahydrobenzo(a)pyrene (BAPT) (λ_{max}= 247, 267, 278, 313, 327, 344 nm). The nomenclature for the benzo(a)pyrene stereoisomers is shown in Figure 2.16. The early eluting peak (a), whose retention time is identical to that for the anti-trans isomer of BAPT, was collected and peracetylated. The HPLC retention time (Figure 2.17) and electronic spectrum of this derivative are identical to those of authentic anti-trans-7,8,9,10-tetraaceto-7,8,9,10-tetrahydrobenzo(a)pyrene. The mass spectra of the acetylated product and the authentic standard, shown in Figure 2.18, are identical to a published spectrum of the peracetylated tetrol (Dix et al., 1985: m/e 488 (M^+), 284 (M^+-2HOAc-2ketene, base peak), 428 (M^+-HOAc), 368 (M^+-2HOAc), 326 (368-2HOAc). These data unambiguously identify the first oxidation product as the anti-trans isomer of 7,8,9,10-tetrahydroxy-7,8,9,10-tetrahydrobenzo(a)

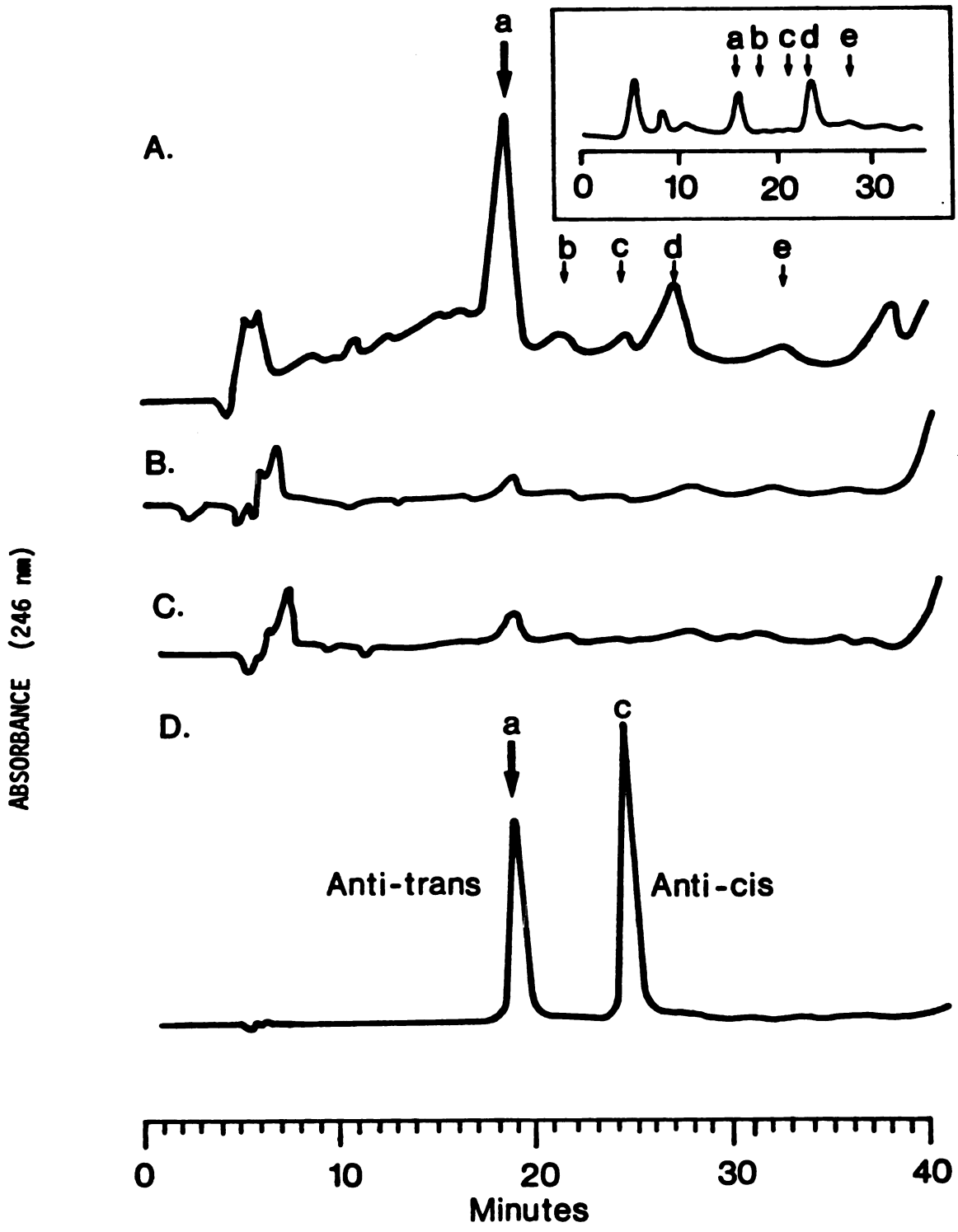

Figure 2.14. HPLC Chromatograms of the Products Formed from the Oxidation of 7,8-Dihydroxy-7,8-dihydrobenzo(a)pyrene by Hemoglobin and Hydrogen Peroxide. Trace A, Complete Incubation Mixture (10 uM Hemoglobin, 35 uM BAPD, 600 uM H_2O_2, 100 uM Tween 20); Trace B, Incubation Lacking Hemoglobin; Trace C, Incubation Lacking H_2O_2; Trace D, 7,8,9,10-Tetrahydroxy-7,8,9,10-tetrahydrobenzo(a)pyrene Standards.

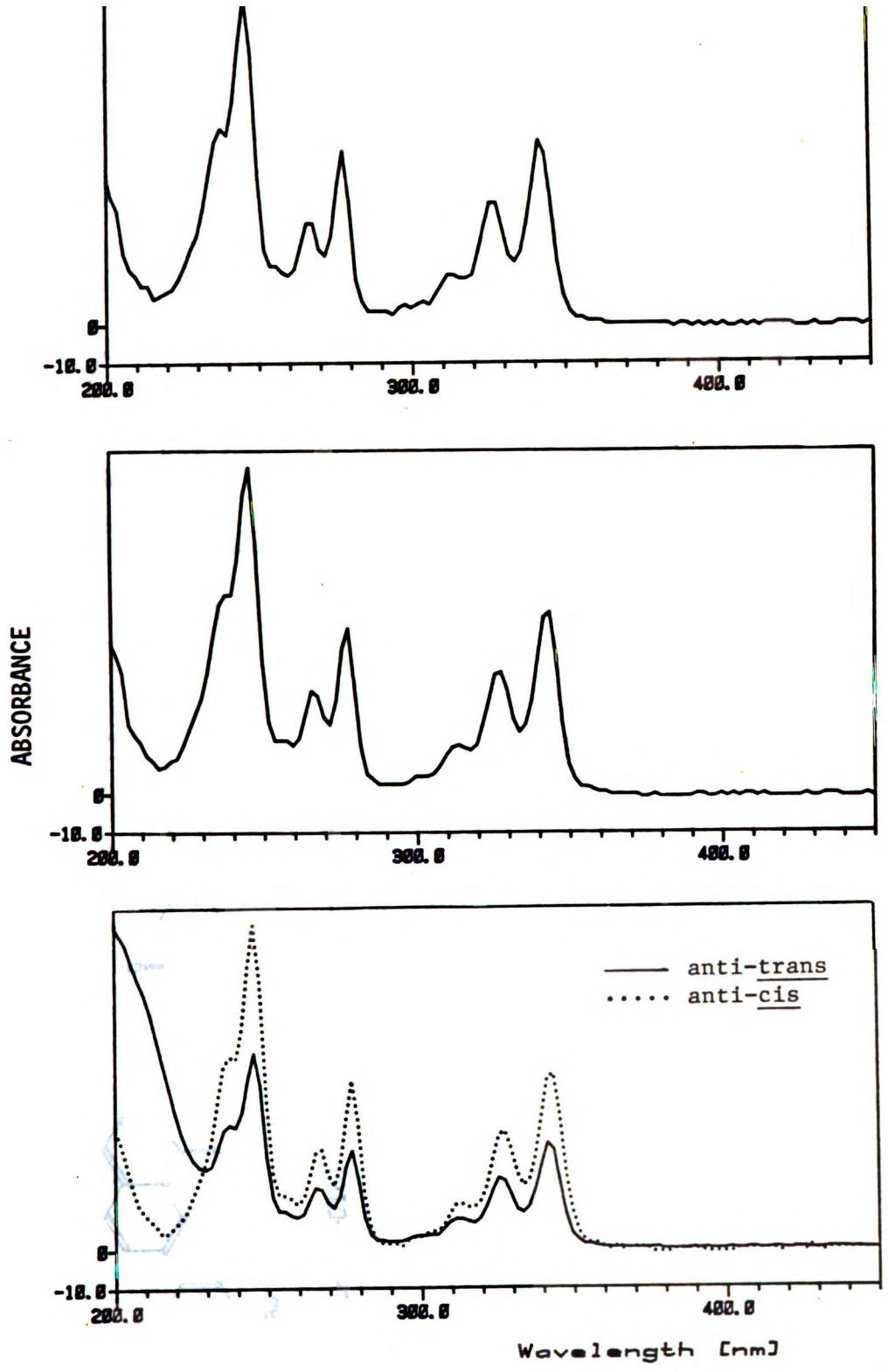

Figure 2.15. The Electronic Absorption Spectra of the Products Formed from the Oxidation of BAPD by Hemoglobin and H_2O_2. Spectra for Peak a (upper trace), peak d (middle trace) and the BAPD Standards (lower trace) were Obtained as They Eluted from the HPLC Column (Figure 2.14).

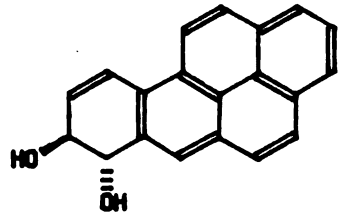

trans-Diol

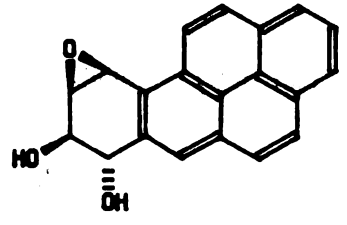

anti-Diol-Epoxide

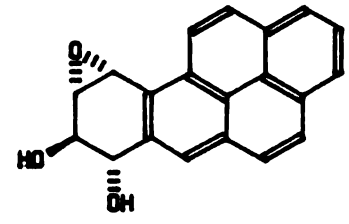

syn-Diol-Epoxide

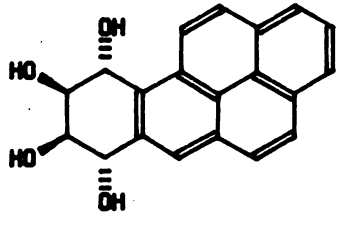

anti-trans-Tetrol

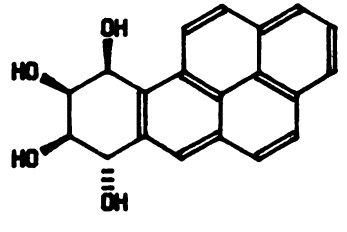

anti-cis-Tetrol

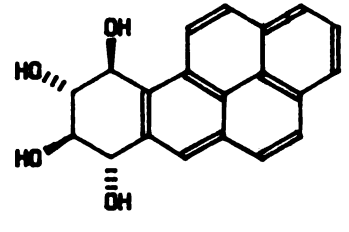

syn-trans-Tetrol

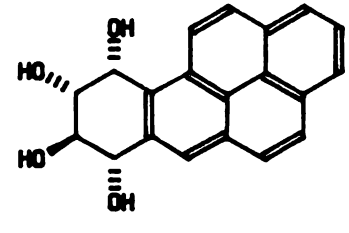

syn-cis-Tetrol

Figure 2.16 Chemical Structures and Nomenclature of the Benzo(a)pyrene Derivatives.

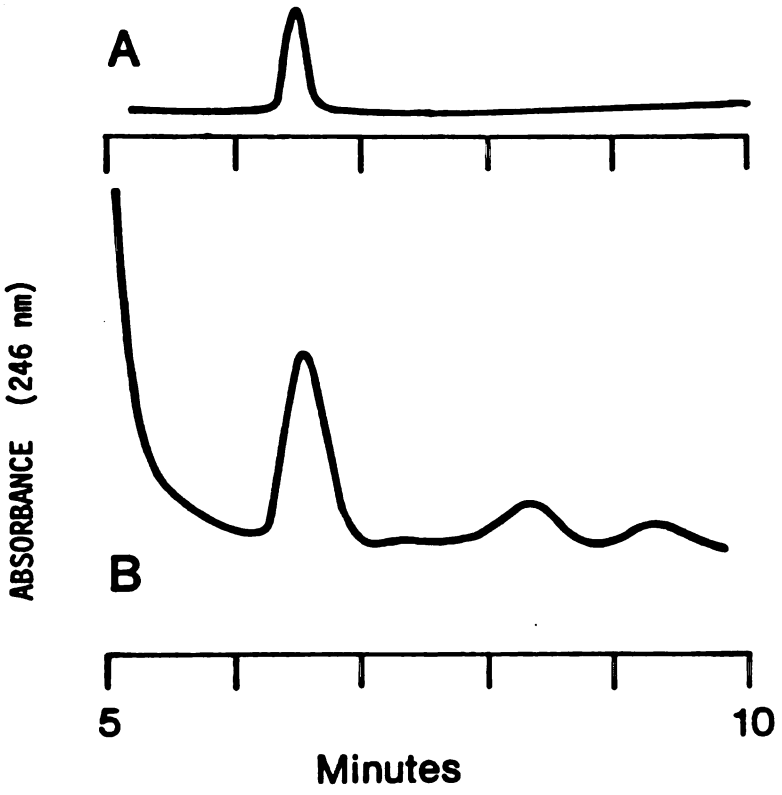

Figure 2.17. HPLC Chromatograms of (A) Acetylated 7,8,9,10-Tetrahydroxy-7,8,9,10-tetrahydrobenzo(a)pyrene Standard and Acetylated Peak a (Figure 2.14).

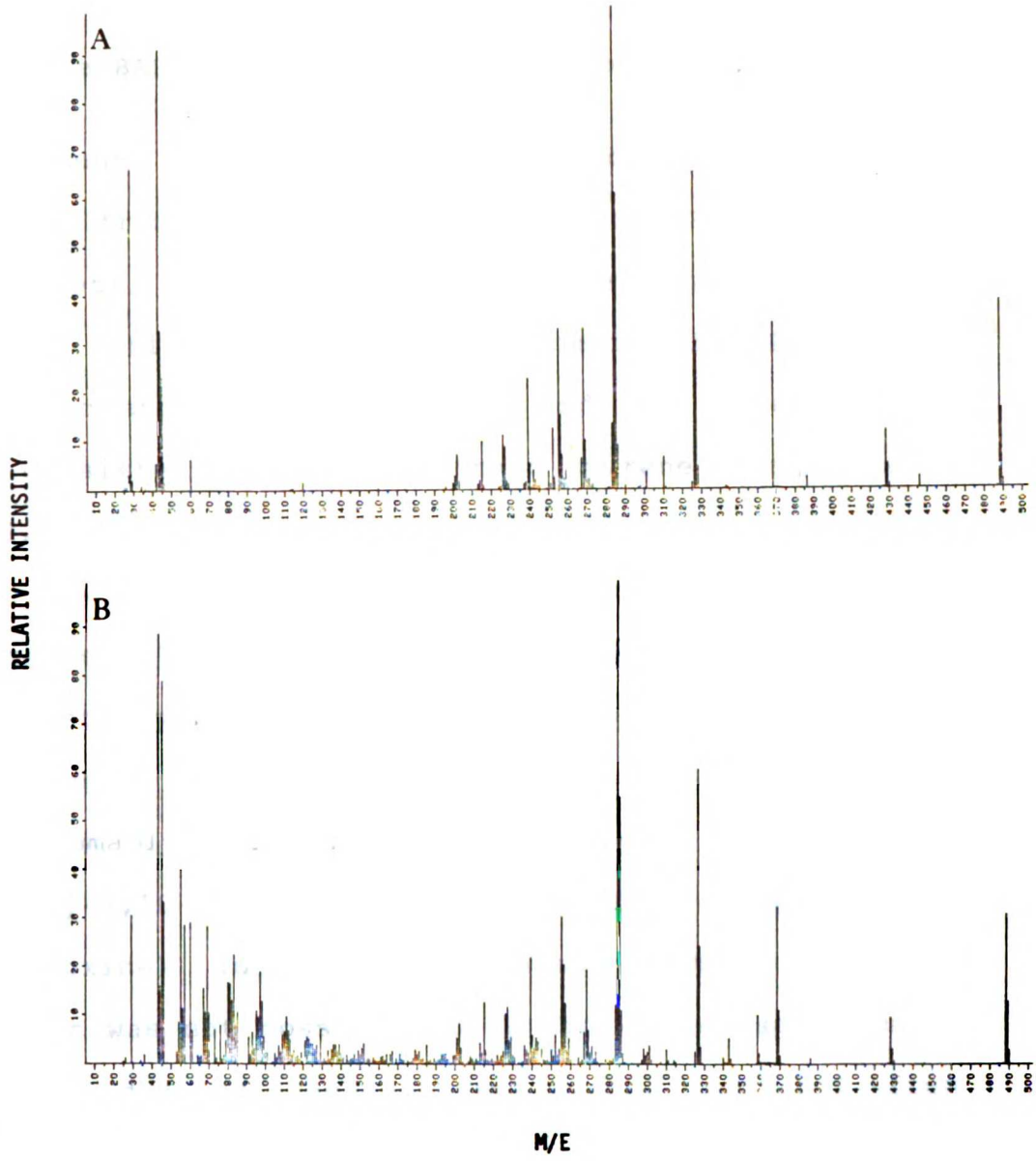

Figure 2.18. Mass Spectra of (A) Acetylated 7,8,9,10-Tetrahydroxy-7,8,9,10-tetrahydrobenzo(a)pyrene Standard and (B) Acetylated Peak a (Figure 2.14).

pyrene. The yield of this product, determined spectroscopically (ε_{246}= 80,100 $M^{-1}cm^{-1}$), was found to be approximately 0.05-0.1 nmol/ml/30 min. None of the other three possible BAPT isomers are detected by HPLC.

The amount of the second oxidation product varies substantially from incubation to incubation (Peak d, Figure 2.14 and inset). It elutes with a retention time between that for the anti-cis and syn-cis isomers of BAPT (Figure 2.14, peaks c and e, respectively) and has an electronic spectrum consistent with an intact pyrene ring system (Figure 2.15). The relative order of elution and the electronic spectrum of this product identify it as anti-trans-10-methoxy-7,8,9-trihydroxy-7,8,9,10-tetrahydrobenzo (a)pyrene (methoxy-BAPT). The formation of the methoxy-BAPT derivative, which has been reported under similar conditions (ibid), presumably results from methanolysis of the anti-7,8-dihydroxy-9,10-oxo-7,8,9,10-tetrahydrobenzo(a)pyrene (BAP-diol-epoxide) intermediate during workup and HPLC analysis. It was not possible to obtain a mass spectrum of this product due to the limited amount isolated from preparative incubations.

The compounds isolated from the incubation mixture represent the expected hydrolysis and methanolysis products of anti-BAP-diol-epoxide. The data thus strongly suggests that the anti-diol epoxide is the sole product derived from the oxidation of BAPD by hemoglobin and H_2O_2.

Incubation of BAPD with whale or horse myoglobin and H_2O_2 similarly results in the formation of anti-trans-BAPT (peak a) and variable amounts of the 10-methyl ether (not shown) as the sole oxidation products (Figure 2.19). As observed for the oxidation of styrene, the product yield decreases in moving from hemoglobin to whale myoglobin to horse myoglobin (Table 2.4). Although the absolute yield of BAPT (0.05 to 0.1 nmol/ml/30 min for Hb) is substantially less than that of styrene oxide (30 nmol/ml/min for Hb), the relative yield as one traverses the hemoprotein series remains similar for the two substrates (compare Tables 2.2 and 2.4).

Origin of the Oxygen in the Benzo(a)pyrene Tetrol Product. Unlike the oxidation of styrene, the relative BAPT yield increased (hemoglobin) or only slightly decreased (myoglobin) in an anaerobic environment (Table 2.5). The relative lack of oxygen sensitivity in BAPD oxidation was further explored by examining the incorporation of ^{18}O into the tetrol by hemoglobin in the presence of either $^{18}O_2$ or $H_2{}^{18}O_2$. Figure 2.20 displays the molecular ion region of the mass spectrum of authentic [^{16}O]-7,8,9,10-tetraaceto-7,8,9,10-tetrahydrobenzo(a)pyrene (a) along with the products isolated from incubations utilizing either $^{18}O_2$ (b) or $H_2{}^{18}O_2$ (c). It is clear from the figure that little molecular oxygen is incorporated into the product while a substantial fraction of the oxygen derives from the peroxide. The same result is obtained when horse myoglobin

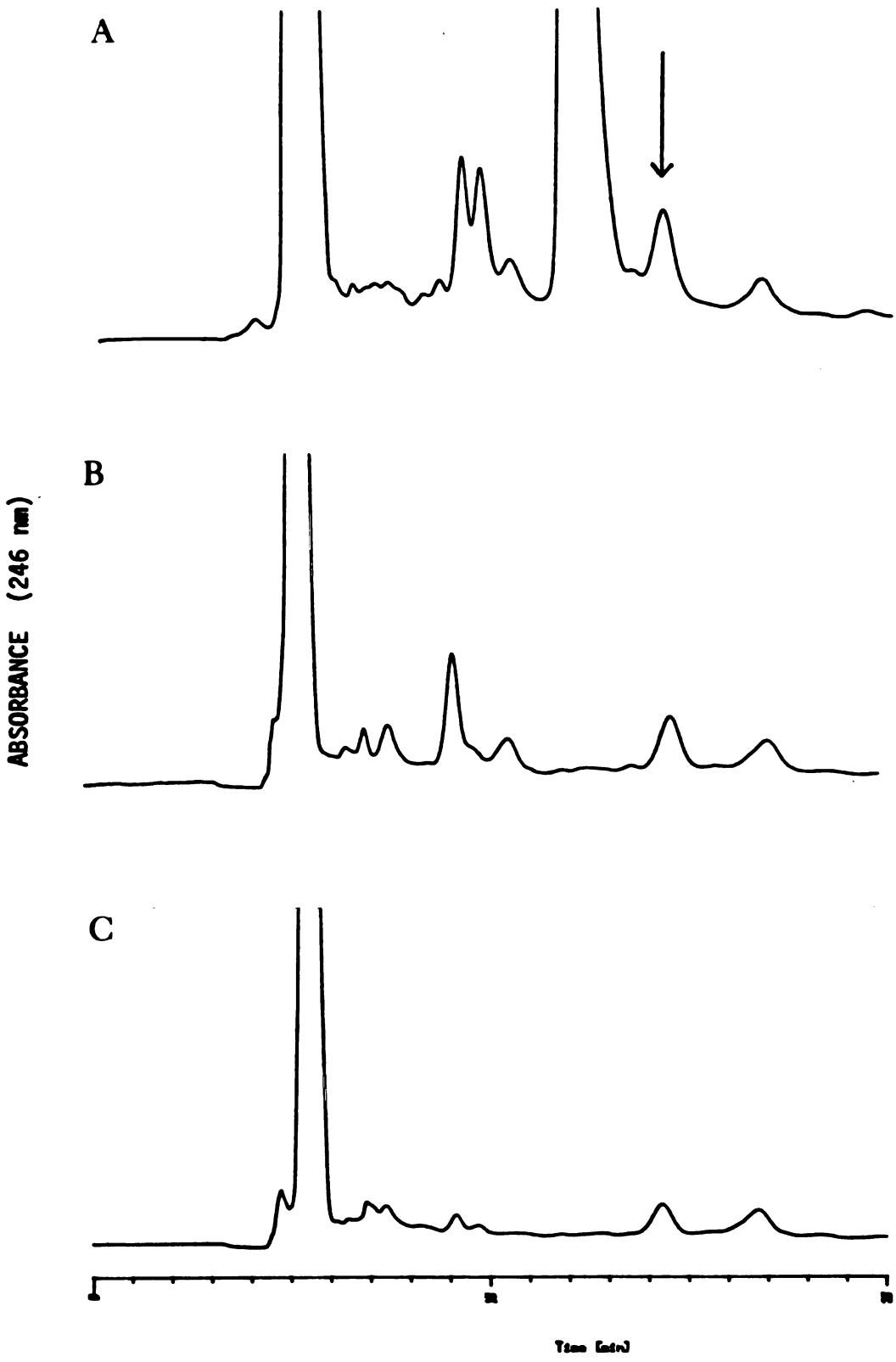

Figure 2.19. HPLC Chromatograms of the Products Isolated From the Peroxide-Dependent Oxidation of 7,8-Dihydroxy-7,8-dihydrobenzo(a)-pyrene by (A) Hemoglobin, (B) Sperm Whale Myoglobin and (C) Horse Myoglobin. The Arrow Indicates the Retention Time of Authentic 7,8,9,10-Tetrahydroxy-7,8,9,10-tetrahydrobenzo(a)pyrene.

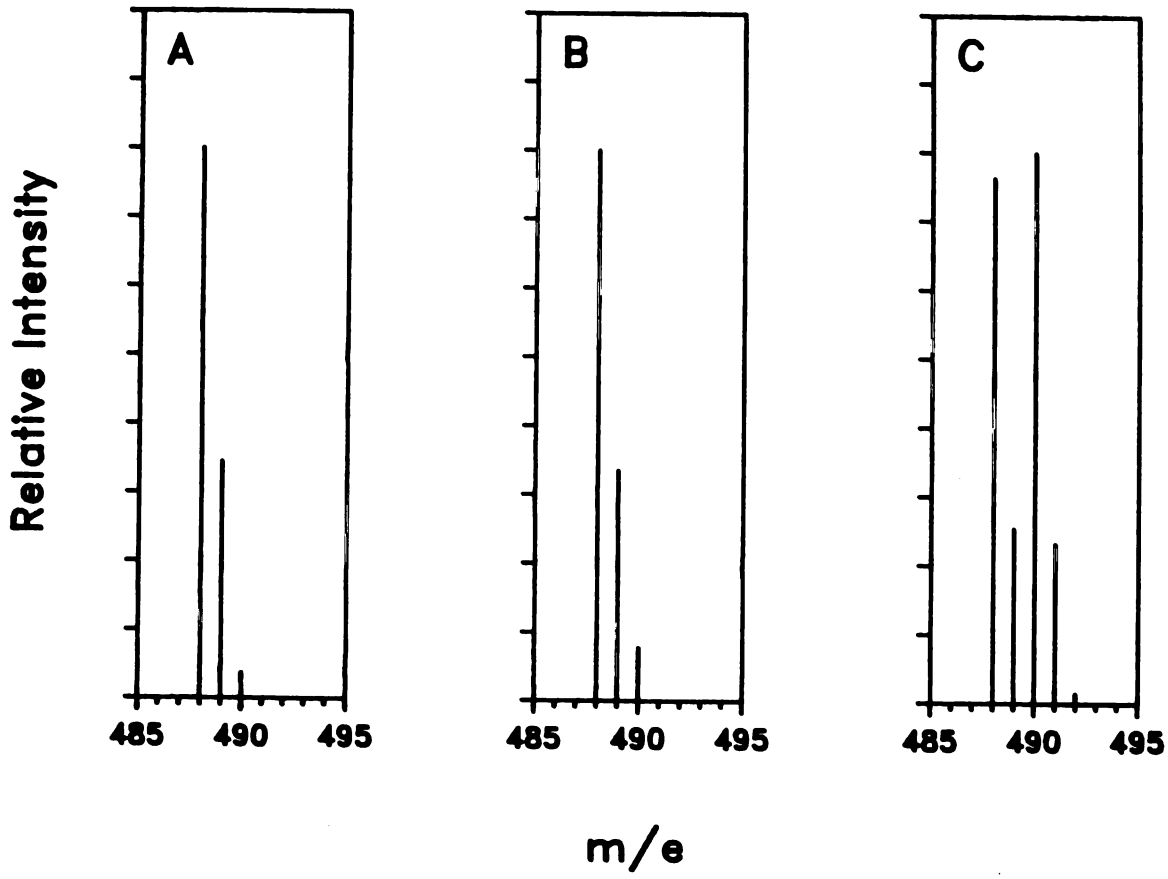

Figure 2.20. Molecular Ion Region of the Mass Spectra of (A) Acetylated BAPT Standard (^{16}O), (B) Acetylated BAPT Isolated From the Oxidation of BAPD by Hemoglobin in an $^{18}O_2$ Environment and (C) Acetylated BAPT Isolated From the Oxidation of BAPD by Hemoglobin by $H_2{}^{18}O_2$.

Table 2.4. Formation of BAPT by Different Hemoproteins

Hemoprotein[a]	Relative Yield
Hemoglobin (bovine)	100
Myoglobin (sperm whale)	56
Myoglobin (horse)	26

[a]40 μM heme, 600 μM H_2O_2 and 35 μM BAPD kept at 0°C for 30 minutes.

Table 2.5. Oxygen Dependence of BAPT Yield

Hemoprotein[a]	Oxygen	Tetrol Yield relative %
Hemoglobin (bovine)	+	100
	-	165
Myoglobin (horse)	+	100
	-	88

[a]40 μM heme, 600 μM H_2O_2 and 35 μM BAPD kept at 0°C for 30 minutes.

is used in place of hemoglobin. The results for both hemoproteins, tabulated in Table 2.6, clearly demonstrate that the oxygen in the tetrol product does NOT derive from molecular oxygen but does derive, to a substantial extent, from the peroxide.

Table 2.6. Source of Oxygen in the Tetrol Product

Hemoprotein[a]	^{18}O-incorcoration	
	$H_2{}^{18}O_2$	$^{18}O_2$
	Percent	
Hemoglobin (bovine)	66	<1
Myoglobin (horse)	50	<1

[a] 40 μM heme, 600 μM H_2O_2 and 35 μM BAPD kept at 0°C for 30 minutes.

Stilbene Oxidation

Products Formed in the Oxidation of trans-Stilbene by Hemoglogin and Hydrogen Peroxide. Incubation of trans-stilbene with hemoglobin and H_2O_2 results in the formation of a single major product detectable by GC analysis (Figure 2.21). This product is identified as trans-stilbene oxide by coelution of the product and the authentic oxide as a single peak when injected onto the gas chromatograph simultaneously. The presence of this product is strictly dependent on the presence of both hemoglobin and hydrogen peroxide. A second minor product that elutes at approximately 12 minutes (Figure 2.21) whose presence exhibited a similar globin and peroxide dependence is also observed. The identity of this product has not been established.

Products Formed in the Oxidation of cis-Stilbene by Hemoglobin and Hydrogen Peroxide. Incubation of cis-stilbene with H_2O_2 results in the formation of two major products detectable by GC analysis (Figure 2.22). These products were identified as above and found to be cis-stilbene oxide (retention time=11.4 min) and trans-stilbene oxide (rt=15.7 min). The presence of both of these products is strictly dependent on the presence of both hemoglobin and hydrogen peroxide. As with the oxidation of trans-stilbene, a minor unidentified product that elutes at approximately 12.1 minutes is observed in the oxidation of cis-stilbene.

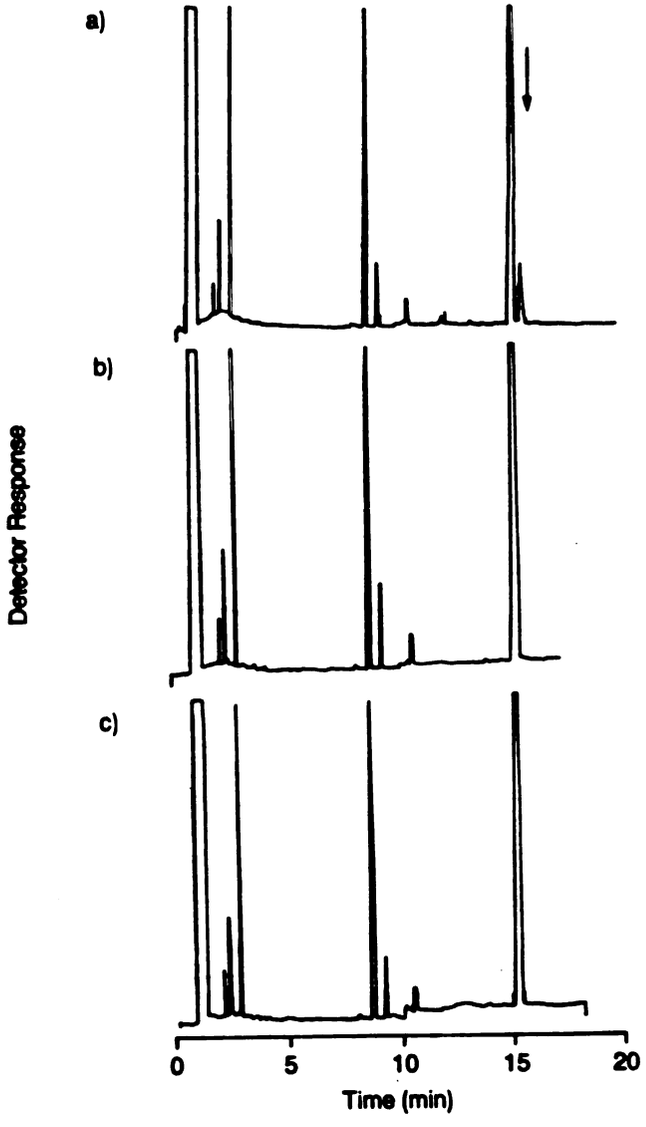

Figure 2.21. Gas Chromatographic Analysis of the Products Formed From the Oxidation of trans-Stilbene by Hemoglobin and H_2O_2. Trace A, Complete Incubation Mixture; Trace B, Incubation Lacking Hemoglobin and Trace C, Incubation Lacking H_2O_2. The Arrow Indicates the Retention Time of Authentic trans-Stilbene Oxide.

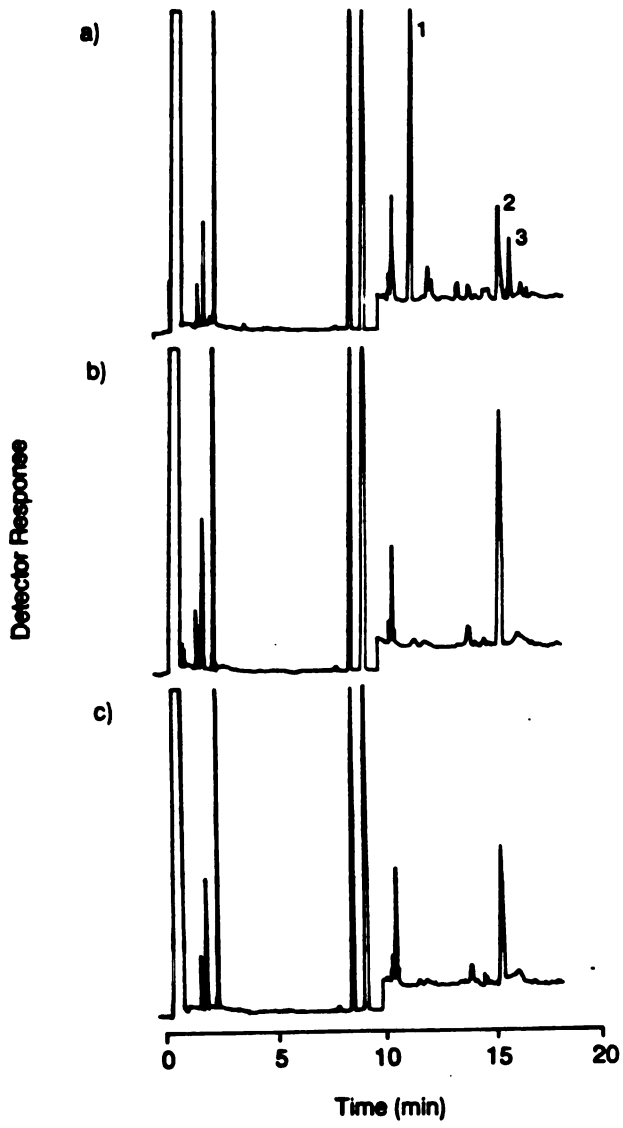

Figure 2.22. Gas Chromatographic Analysis of the Products Formed From the Oxidation of cis-Stilbene by Hemoglobin and H_2O_2. Trace A, Complete Incubation Mixture; Trace B, Incubation Lacking Hemoglobin and Trace C, Incubation Lacking H_2O_2. The Retention Times of Authentic cis-Stilbene Oxide, trans-Stilbene and trans-Stilbene Oxide are Indicated by Peaks 1, 2, and 3, Respectively.

The cis-stilbene starting material was contaminated with a small amount of trans-stilbene (<0.5%) that was not removed by low pressure chromatography. The trace of trans-stilbene in the incubation extracts is not, however, increased by the presence of hemoglobin and H_2O_2.

Horse myoglobin similarly oxidizes trans-stilbene to trans-stilbene oxide and cis-stilbene to both the cis and trans oxide isomers, but the product yields are much lower than in the corresponding hemoglobin incubations. Table 2.7 shows the product yields for all of the reactions.

Origin of the Oxygen in the Stilbene Oxide Products. GC mass spectrometric analysis unambiguously identifies trans-stilbene oxide as the product of the hemoglobin catalyzed oxidation of trans-stilbene. The mass spectrum of the oxide product, shown in Figure 2.23 (trace c), clearly shows substantial incorporation of ^{18}O from the peroxide. Table 2.8 reveals that both hemoglobin and myoglobin exclusively utilize the peroxide oxygen in this oxidation.

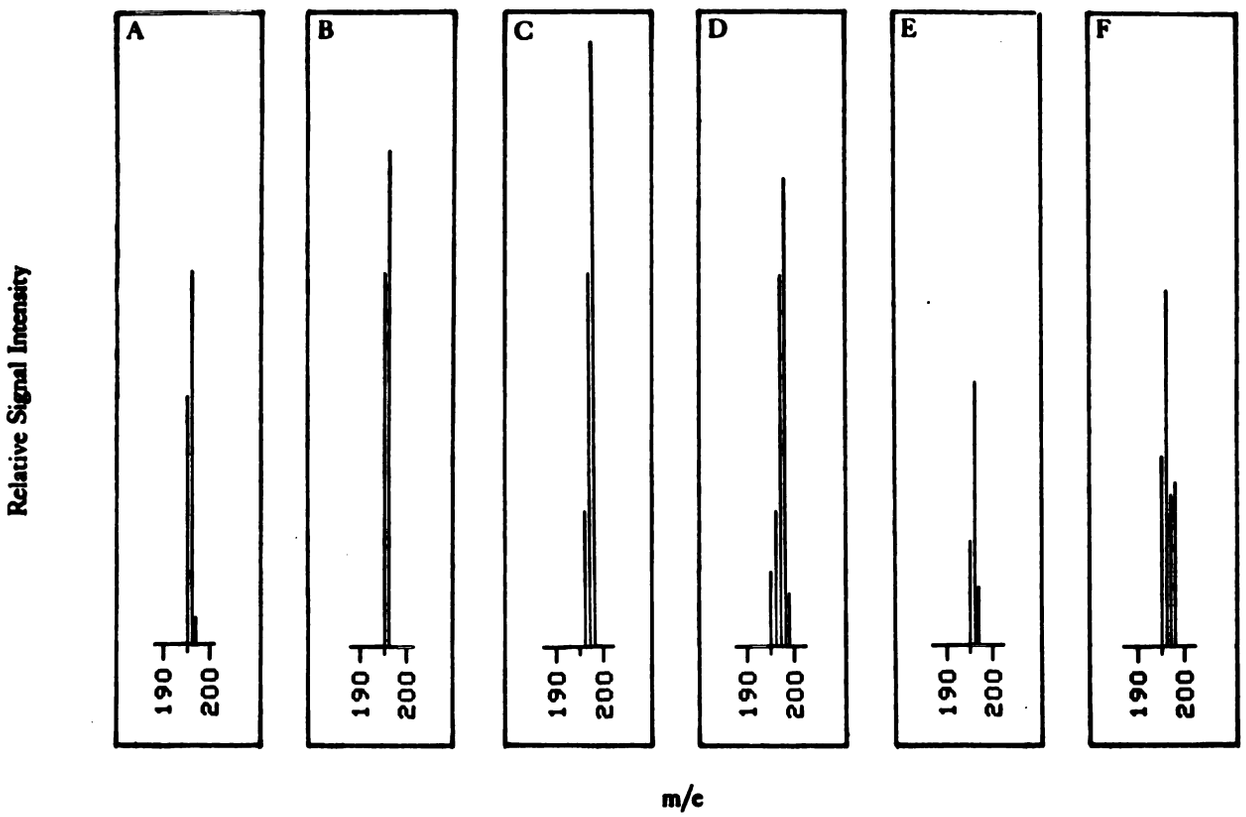

Figure 2.23. Molecular Ion Region of the Mass Spectra of (A) trans-Stilbene Oxide Standard, (B) cis-Stilbene Oxide Standard, (C) trans-Stilbene Oxide Formed From the Oxidation of trans-Stilbene by Hemoglobin and $H_2{}^{18}O_2$, (D) cis-Stilbene Oxide Formed From the Oxidation of cis-Stilbene by Hemoglobin and $H_2{}^{18}O_2$, (E) trans-Stilbene Oxide Formed From the Oxidation of cis-Stilbene and $H_2{}^{18}O_2$ and trans-Stilbene Oxide Formed From the Oxidation of cis-Stilbene in an $^{18}O_2$ Enviroment.

Table 2.7. Stilbene Oxide Yield

Hemoprotein[a]	Olefin	Oxide	Yield[b]
Hemoglobin	trans	trans	1.0
(bovine)	cis	cis	0.7
		trans	0.14
Myoglobin	trans	trans	0.13
(equine)	cis	cis	0.27
		trans	0.05

[a]40 μM hemoprotein, 600 μm H_2O_2 and 50 μM substrate kept at 0°C for 30 minutes. [b]nmol/ml/30 min.

Table 2.8. Incorporation of ^{18}O from $H_2{}^{18}O_2$ into Stilbene Oxide

			Total Ions			
Hemoprotein[a]	Olefin	Oxide	196	198	%198	$\%^{18}O$[b]
Hemoglobin	trans	trans	1006	4496	82	105
(bovine)	cis	cis	22568	78372	78	101
		trans	3667	ND[c]	<5	<7[d]
Myoglobin	trans	trans	ND	2420	-	100
(equine)	cis	cis	5299	23748	82	107
		trans	ND	ND	-	-

[a]40 μM heme, 600 μM H_2O_2 and 50 μM stilbene kept at 0°C for 90 minutes. [b]Based on an ^{18}O content of 76.7% in the $H_2{}^{18}O_2$. [c]ND, not detectable. [d]This value represents an upper limit based on the total number of ions reported for the smallest peak in the spectrum (200 ions).

GC mass spectrometric analysis unambiguously identifies cis-stilbene oxide as a product of the hemoglobin catalyzed oxidation of cis-stilbene. The mass spectrum of cis-stilbene oxide isolated from an incubation utilizing $H_2{}^{18}O_2$, also shown in Figure 2.23 (trace d), clearly demonstrates substantial incorporation of peroxide oxygen. Table 2.8 reveals that both hemoglobin and horse myoglobin exclusively utilize the peroxide oxygen in this oxidation.

GC mass spectrometric analysis of the same incubation extract also unambiguously identifies trans-stilbene oxide as a product of the hemoglobin catalyzed oxidation of cis-stilbene. The mass spectrum of the trans isomer, shown in Figure 2.23 (trace e), has no mass peaks indicative of oxygen incorporation from the labeled peroxide.

The mass spectrum of trans-stilbene oxide isolated from the hemoglobin catalyzed oxidation of cis-stilbene under an $^{18}O_2$ environment, shown in Figure 2.23 (trace f), indicates molecular oxygen is incorporated into the trans isomer. The results on the source of the oxygen in the trans-stilbene oxide derived from cis-stilbene are given in Tables 2.8 and 2.9. The low yield of the trans isomer made accurate quantitation of the labeled oxygen difficult due to the sensitivity limits of the mass spectrometer. This was particularly true for the myoglobin catalyzed incubations.

Table 2.10 summarizes the results of the oxidation of stilbene by hemoglobin and myoglobin utilizing both $H_2{}^{18}O_2$

Table 2.9. Incorporation of ^{18}O from $^{18}O_2$ into cis-Stilbene Oxide

		Total Ions			
Hemoprotein[a]	Oxide	196	198	%198	$\%^{18}O$[b]
Hemoglobin	cis	107219	1456	1.3	1.4[b]
(bovine)	trans	8941	4083	31.3	32.0
Myoglobin	cis	28345	ND[c]	<1	<1[d]
(equine)	trans	5155	ND	<1	<1[e]

[a] 40 μM heme, 600 μM H_2O_2 and 50 μM cis-stilbene kept at 0°C for 90 minutes. [b] Based on an ^{18}O content of 98% in the $^{18}O_2$. [c] ND, not detectable. [d] Based on the number of ions in the smallest peak in the spectrum (200 ions). [e] Based on the number of ions in the smallest peak in the spectrum (23 ions).

Table 2.10. Source of Oxygen in Stilbene Oxide: Summary

		Cis-Oxide		Trans-Oxide	
Hemoprotein[a]	Olefin	H_2O_2	O_2	H_2O_2	O_2
Hemoglobin	trans	-	-	105	-
	cis	101	1.4	<7	32
Myoglobin	trans	-	-	100	-
	cis	107	<1	-	<1

and $^{18}O_2$. Oxidation of trans-stilbene by both hemoproteins results in 100% incorporation of peroxide oxygen into the oxide product. Oxidation of the cis-olefin to the cis-oxide similarly results in 100% incorporation of the peroxide oxygen. In contrast, trans-stilbene oxide derived from the hemoglobin catalyzed oxidation of cis-stilbene results in less than 7% incorporation of peroxide oxygen. Molecular oxygen is incorporated into 32% of the product with the remaining oxygen presumably being derived from the solvent. Quantitation of labeled oxygen incorporation into the products derived from the horse myoglobin catalyzed oxidations are less accurate due to the low product yields, but similar trends were observed.

Linoleic Acid Oxidation

Oxygen Consumption During the Oxidation of Linoleic Acid by Hemoglobin and Hydrogen Peroxide. As stated earlier, addition of H_2O_2 to hemoglobin results in oxygen evolution (see styrene oxidation). Figure 2.24 A, shows a typical oxygen tension curve at 37°C in the absence of linoleic acid. Oxygen evolution decreases with decreasing hemoglobin concentrations to the point that below 80 μM (heme), net oxygen consumption is observed (Table 2.11). The figure reveals that oxygen evolution is attenuated by linoleic acid. This is true for all hemoglobin concentrations as shown in Table 2.11. This table readily demonstrates that linoleic acid causes net

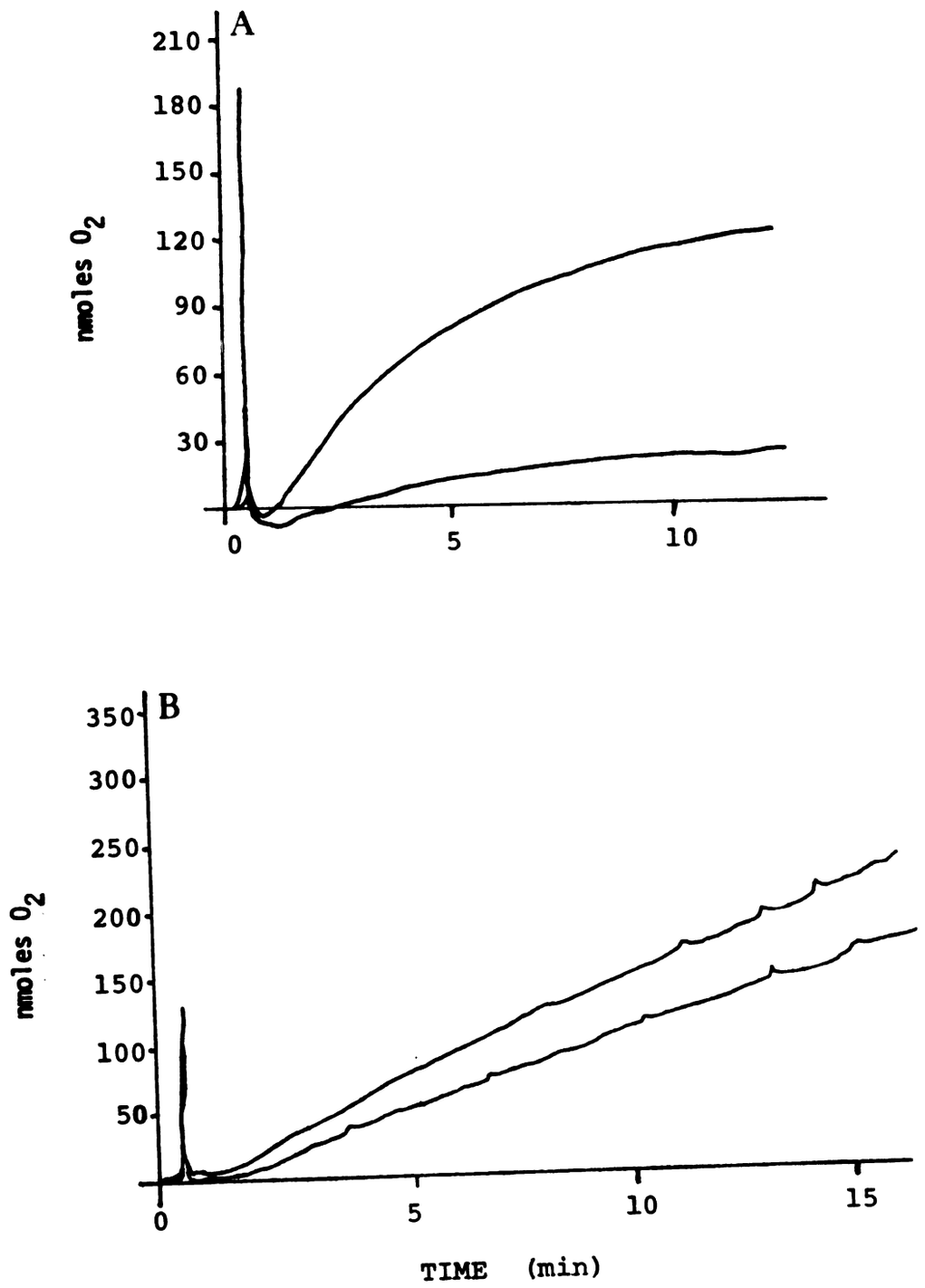

Figure 2.24. Oxygen Evolution by Hemoglobin (20 μM) and H_2O_2 (1.2 mM) at 37°C (A) and 0°C (B) in the Absence (upper trace) and Presence (lower trace) of Linoleic Acid (400 μM). The Buffer (0.2 M PBS (pH 7.4) containing 100 μM Tween 20) was Treated with Chelex Before Use.

Table 2.11. Oxygen Consumption During the Oxidation of Linoleic Acid By Hemoglobin and Hydrogen Peroxide

Hemoglobin[a]	[Heme]	-Linoleate	+Linoleate	Oxygen Consumed[b]
40 nmoles	160 μM	+142	+63	79
20 nmoles	80 μM	+10	-29	39
10 nmoles	40 μM	-25	-54	29
5 nmoles	20 μM	-19	-28	9

[a]Peroxide:heme ratio was 15 in every incubation (2 ml). These values represent the mean of 2 to 3 incubations.
[b]Total change in oxygen tension reported after 10 minutes at 37°C.

Table 2.12. Oxygen Consumption During the Oxidation of Linoleic Acid by Horse Myoglobin and Hydrogen Peroxide

Myoglobin[a]	[Heme]	-Linoleate	+Linoleate	Oxygen Consumed[b]
160 nmoles	160 μM	+248	+189	59
80 nmoles	80 μM	+94	+41	53
40 nmoles	40 μM	+30	+2	28
20 nmoles	20 μM	+12	-6	6

[a]Peroxide:heme ratio was 15 in every incubation (2 ml).
[b]Total change in oxygen tension reported after 15 minutes at 37°C.

oxygen consumption at all concentrations of the hemoprotein that were tested. It is of interest that, in most cases, approximately two moles of oxygen are consumed per mole of hemoglobin (4 moles of heme). Similar results are observed at $0^{o}C$ (Figure 2.24 B). Note, however, that oxygen evolution continues to rise beyond 15 minutes at $0^{o}C$ whereas it leveled off by 10 minutes at $37^{o}C$ (See also, Figure 2.8).

Figure 2.25 shows the results of similiar experiments ($37^{o}C$) utilizing horse myoglobin in place of hemoglobin. Again, oxygen evolution is observed that decreases with decreasing hemoprotein concentration (Table 2.12). As with hemoglobin, addition of linoleic acid to the incubation mixture results in attenuated oxygen evolution at all myoglobin concentrations. Unlike the hemoglobin incubations conducted at $37^{o}C$, the oxygen tension in the myoglobin incubations continues to rise at a shallow rate beyond 15 minutes. Non-reproducible instrument drift over extended periods combined with the slow change in oxygen tension after 15 minutes make accurate determination of oxygen "consumption" during the oxidation of linoleic acid impossible.

Products Formed in the Oxidation of Linoleic Acid by Hemoglobin and Hydrogen Peroxide. Three products were expected from the oxidation of linoleic acid by hemoglobin and H_2O_2. The first was 13-hydroperoxy-$^{\Delta 9,11}$,trans-

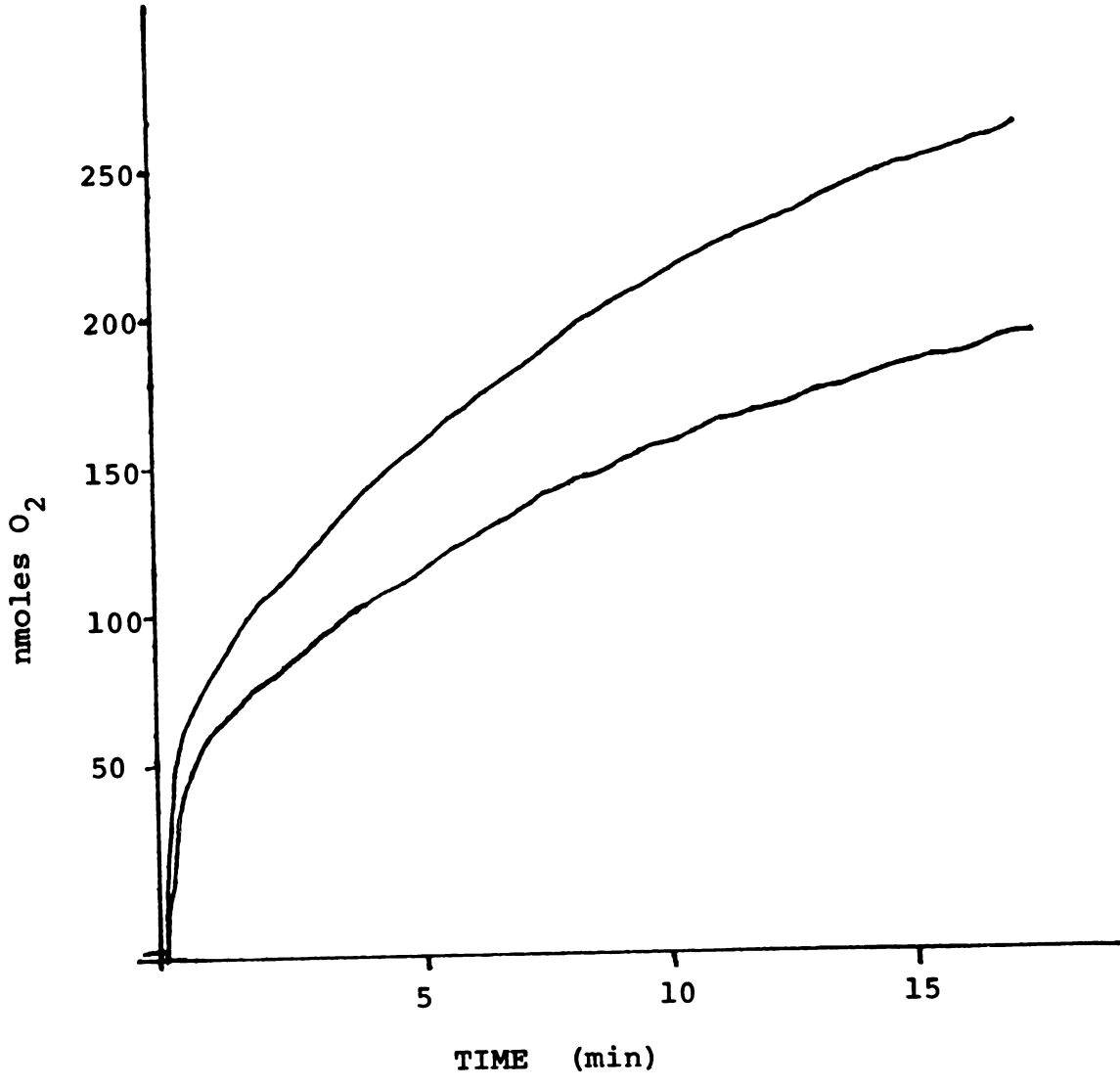

Figure 2.25. Oxygen Evolution by Horse Myoglobin (80 μM) and H_2O_2 at 37°C in the Absence (upper trace) and Presence (lower trace) of Linoleic Acid (400 μM). The Buffer (0.2 M PBS (pH 7.4) containing 100 μM Tween 20) was Treated with Chelex Before Use.

octadecanoic acid (13-HODA), which would appear as 13-O-trimethylsilyl-$^{\Delta 9,11,trans}$-octadecanoic acid methyl ester (13-TODA) after derivatization. The second two were the 9,10- and 12,13-epoxy-linoleic acid methyl esters. The structures for all of the linoleic acid derivatives are shown in Figure 2.26.

Incubation of linoleic acid with hemoglobin and H_2O_2 at 37°C results in the formation of a single GC detectable product (Figure 2.27, peak 3). The formation of this product depends on both hemoglobin and H_2O_2. Its retention time is longer than that of either authentic 13-TODA (1) or either of the isomeric linoleic epoxides (2). The product may therefore be the silylated methyl ester of 9-hydroxy-12,13-epoxy-octadecenoic acid, a known product of the decomposition of 13-HODA by hemoglobin (Hamberg, 1974). There was not enough material for GC mass spectrometric analysis and the actual identity of this oxidative product remains speculative.

Incubation of linoleic acid with hemoglobin and hydrogen peroxide at 0°C results, again, in the formation of a single major GC detectable product (Figure 2.28, peak 1). This peak, which now has the same retention time as that for 13-TODA, is only formed in the presence of both hemoglobin and H_2O_2. GC mass spectrometric analysis shows that the product has a chromatographic retention time and a mass spectrum (Figure 2.29) identical to those of 13-TODA. These

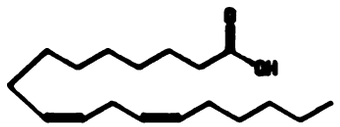

Linoleic Acid

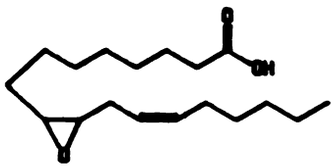

9, 10-Epoxy-Linoleic Acid

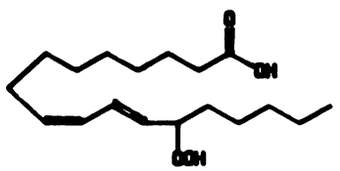

13-HODA

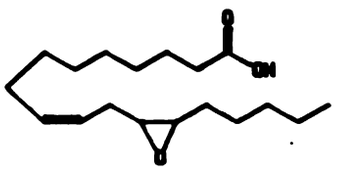

12, 13-Epoxy-Linoleic Acid

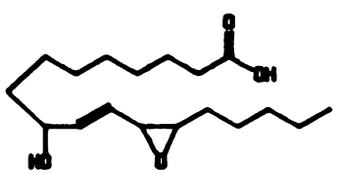

9-Hydroxy-12, 13-Epoxy-
Octadecanoic Acid

Figure 2.26. Chemical Structures and Nomenclature of the Linoleic Acid Derivatives.

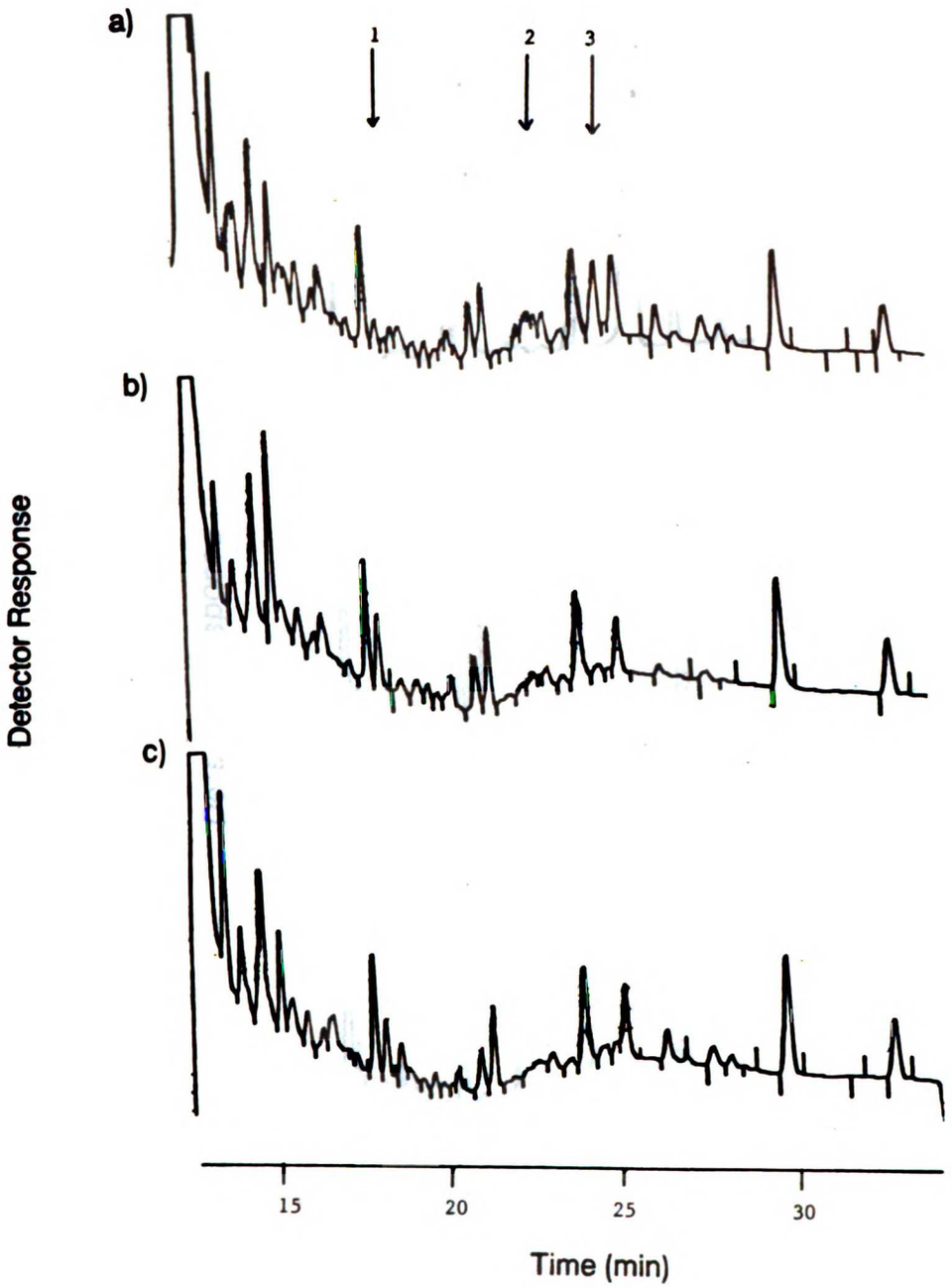

Figure 2.27. Gas Chromatographic Analysis of the Products Formed From the Oxidation of Linoleic Acid by Hemoglobin and H_2O_2 at 37°C. Trace a, Complete Incubation Mixture (see Chapter 5); Trace b, Incubation Lacking Hemoglobin; Trace c, Incubation Lacking H_2O_2. The Retention Times of 13-TODA and the Epoxy-linoleic Acids are Indicated by Arrows 1 and 2, Respectively.

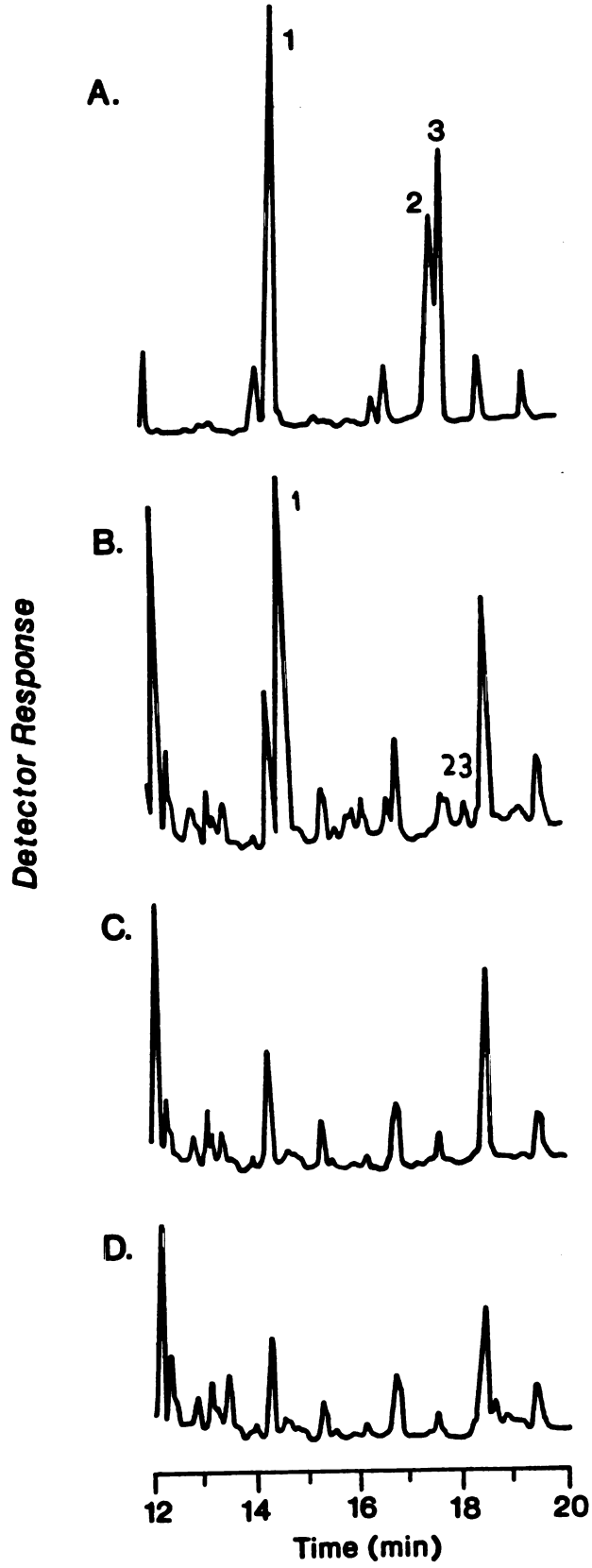

Figure 2.28. Gas Chromatographic Analysis of the Products Formed From the Oxidation of Linoleic Acid by Hemoglobin and H_2O_2 at 0°C. Trace A, Linoleic Acid Standards; Trace B, Complete Incubation Mixture (see Chapter 5); Trace C, Incubation Lacking Hemoglobin; Trace D, Incubation Lacking H_2O_2. Peak 1, 13-TODA; Peaks 2 and 3, Epoxy-Linoleic Acids.

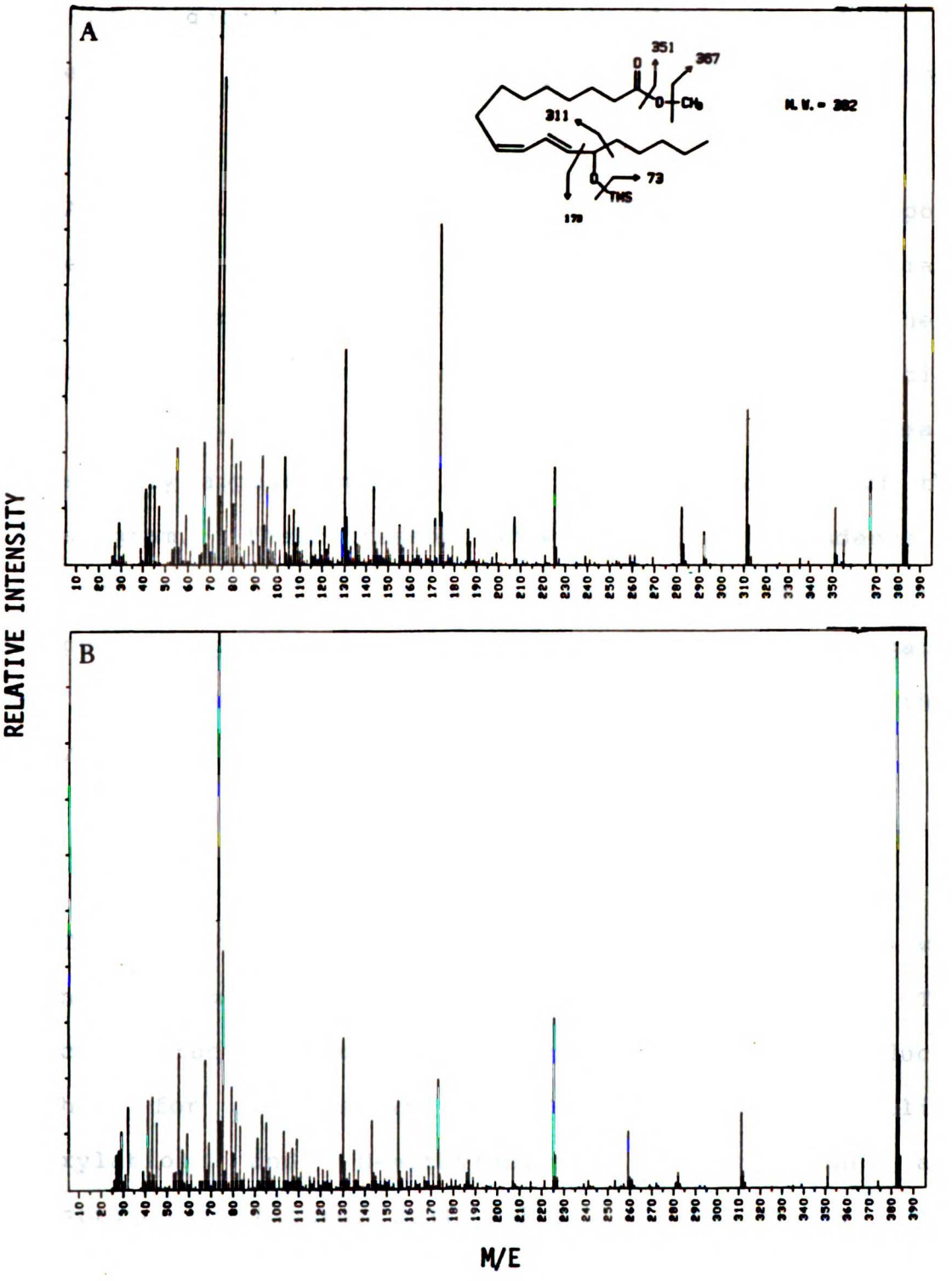

Figure 2.29. Mass Spectrum of (A) Authentic 13-TODA and (B) 13-TODA Isolated From the Oxidation of Linoleic Acid by Hemoglobin and H_2O_2 at 0°C.

data unambiguously identify the oxidation product of linoleic acid as 13-hydroperoxy-$^{\Delta 9,11,trans}$-octadecanoic acid.

A specific search for the 9,10- and 12-13-epoxy linoleic acids reveals very small peaks with the appropriate retention times (Figure 2.28, peaks 2 and 3); however, there was not enough of these materials to unambiguously identify them by GC/MS. Additionally, several other small peaks consistently appear in the 14 to 18 minute region of the chromatogram. Their presence shows a similar dependence on hemoglobin and H_2O_2. These peaks may be due to the decomposition products of 13-HODA by hemoglobin, but again, there was not enough material to unambiguously identify them by GC/MS.

Miscellaneous Substrate Oxidations

The oxidative range of the hemoglobin/H_2O_2 system was examined utilizing the compounds listed in Table 2.13. The chemical structures of the substrates and the products searched for are shown in Figure 2.30. Aniline hydroxylation and N-methylaniline dealkylation are demonstrated in Figures 2.31 and 2.32, respectively. The other reaction products listed in the table were not detected; however, in every case (except cyclohexane) there was a substantial hemoglobin and peroxide dependent increase in the color of the incubation mixture. This color was

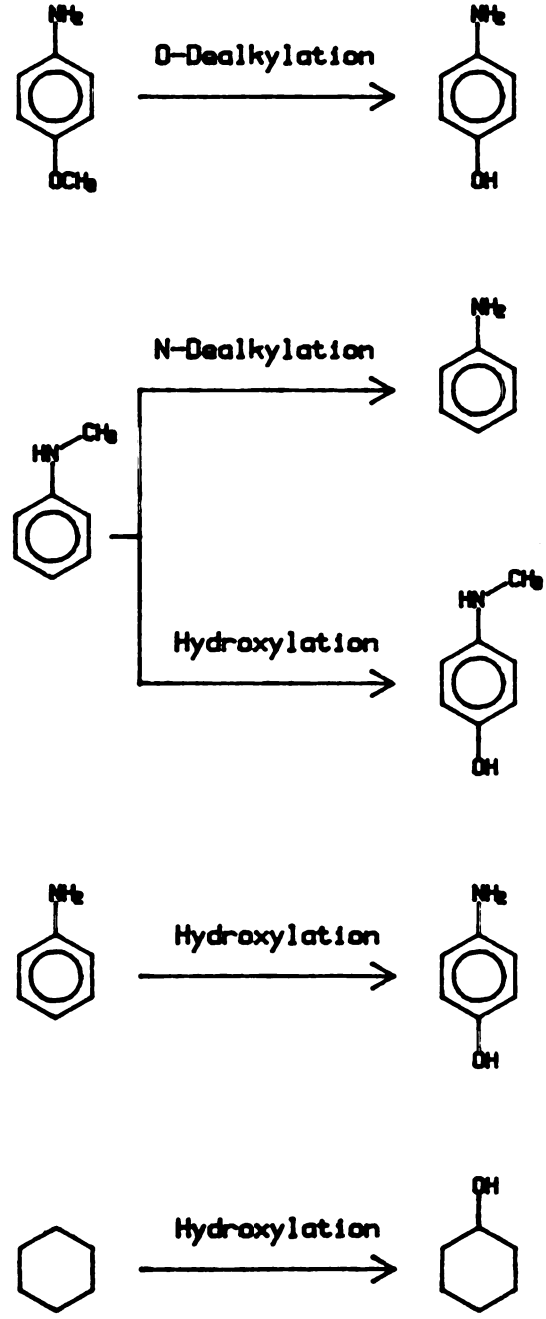

Figure 2.30. Miscellaneous Substrate Oxidations Examined.

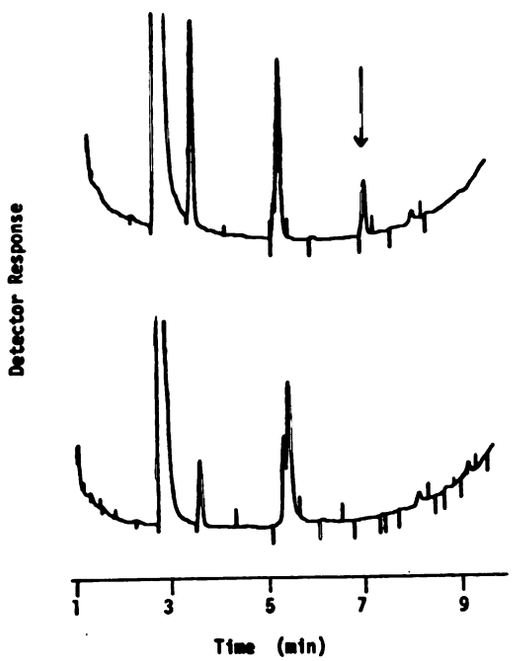

Figure 2.31. Gas Chromatographic Analalysis of the Products Formed From the Oxidation of Aniline by Hemoglobin and H_2O_2. The Chromatograms for a Complete Incubation Mixture (upper trace) and an Incubation Lacking H_2O_2 are Shown. The Arrow Indicates the Retention Time of Authentic p-Aminophenol.

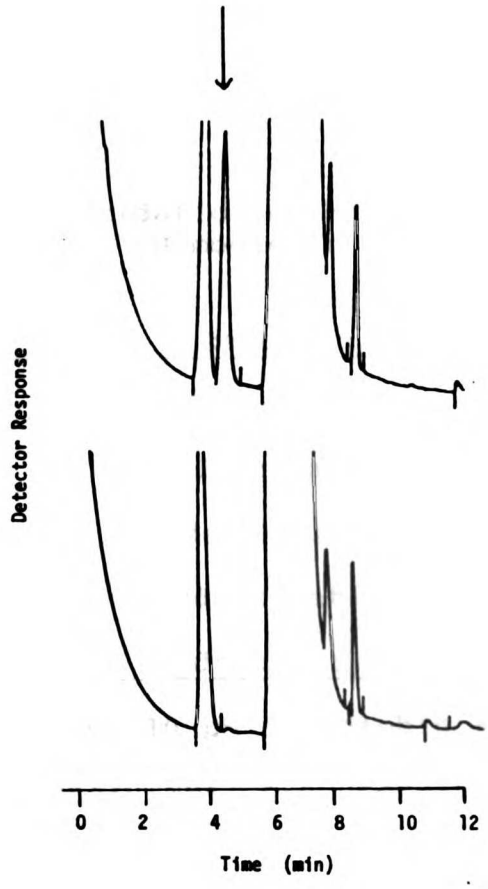

Figure 2.32. Gas Chromatographic Analysis of the Products Formed From the Oxidation of N-Methylanaline by Hemoglobin and H_2O_2. The Chromatograms for a Complete Incubation Mixture (upper trace) and an Incubation Lacking H_2O_2 are Shown. The Arrow Indicates the Retention Time of Authentic Aniline.

ether extractable and may represent polymeric compounds resulting from the one electron oxidation of the parent substrates (Saunders et al., 1964).

Table 2.13. Oxidation of Miscellaneous Compounds by Hemoglobin and H_2O_2

Substrate[a]	Reaction	Product	Present[b]
p-anisidine	O-dealkylation	p-aminophenol	No
aniline	hydroxylation	p-aminophenol	Yes
N-methylaniline	N-dealkylation	aniline	Yes
	hydroxylation	p-hydroxy-NMA[c]	No
cyclohexane	hydroxylation	cyclohexanol	No

[a]10 mM substrate, 10 μM hemoglobin and 600 μM H_2O_2 kept at 0°C for 30 minutes. [b]Detectable by gas chromatographic analysis. [c]p-hydroxy-NMA, p-hydroxy-N-methylaniline.

Chapter 3 Myoglobin Oxidative Damage

Peroxide Oxidation of Red Kangaroo Myoglobin

A 12% SDS-PAGE gel of hydrogen peroxide treated myoglobins from red kangaroo and sperm whale is shown in Figure 3.1. This clearly demonstrates the dimerization of whale myoglobin upon peroxide treatment as reported by Rice (1983). Similar treatment of myoglobin from the red kangaroo shows no evidence of dimer (or polymer) formation.

The ESR spectrum of sperm whale aquo-metmyoglobin consists of a single peak centered at approximately g=6, typical of a high-spin ferric hemoprotein (Dickinson and Symons, 1983). The spectra of aquo-metmyoglobins from horse and red kangaroo are virtually identical to that of the whale protein. Addition of H_2O_2 to whale myoglobin results in the disappearance of the g=6 signal with the concomitant appearance of a new signal at g=2.004 (King, et al., 1967; Figure 3.2). Horse and kangaroo myoglobins react similarly except that both exhibit an additional low field signal at g=2.027 (Figure 3.3). It is of interest that the TYR 151 in whale myoglobin is replaced with phenylalanine in both of these hemoproteins. Furthermore, neither the horse nor the kangaroo myoglobin forms intermolecular cross-links upon treatment with hydrogen peroxide.

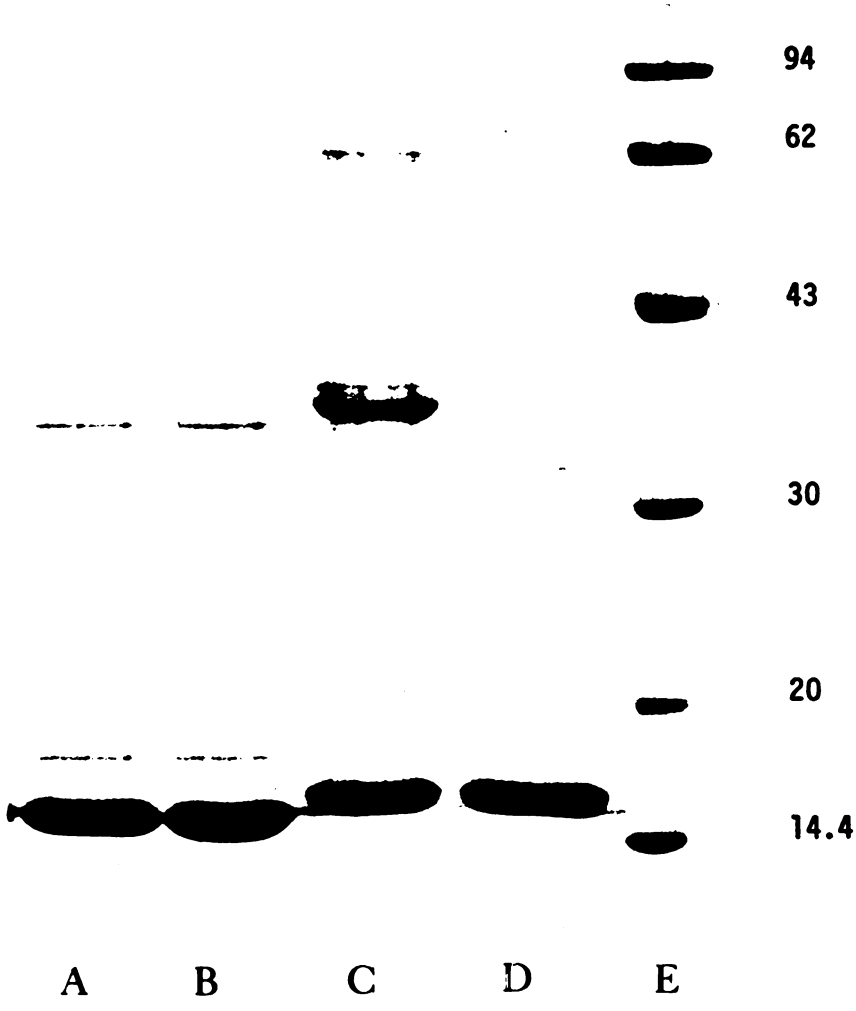

Figure 3.1. SDS-PAGE Gel of (A) H_2O_2-Treated Kangaroo Myoglobin, (B) Non-Treated Control Kangaroo Myoglobin, (C) H_2O_2-Treated Sperm Whale Myoglobin, (D) Non-Treated Control Sperm Whale Myoglobin and (E) Molecular Weight Standards. The Molecular Weights of the Standards (in thousands) are Indicated to the Right of The Figure.

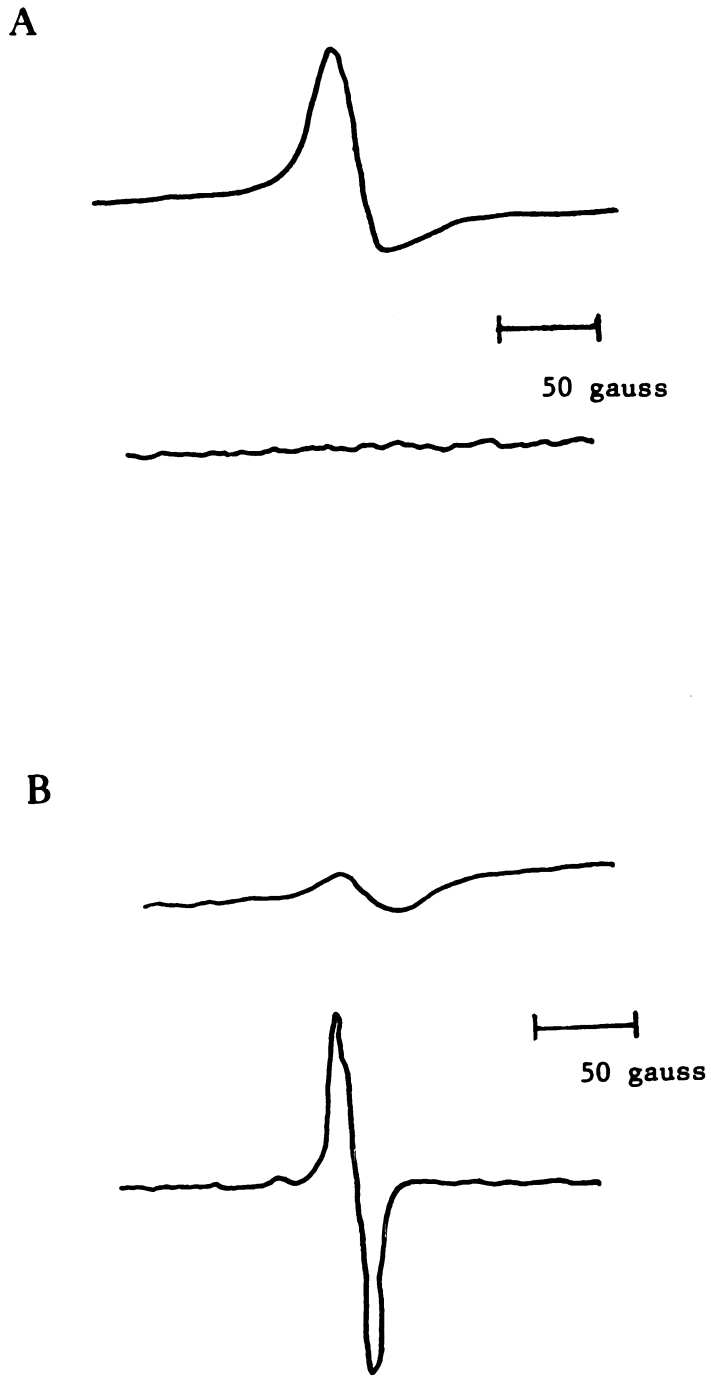

Figure 3.2. The ESR Spectra of Sperm Whale Myoglobin Before (A: upper trace, g=6 region; lower trace, g=2 region) and After (B: upper trace, g=6 region; lower trace, g=2 region) the Addition of Hydrogen Peroxide. Spectra were Recorded as Described in Chapter 5.

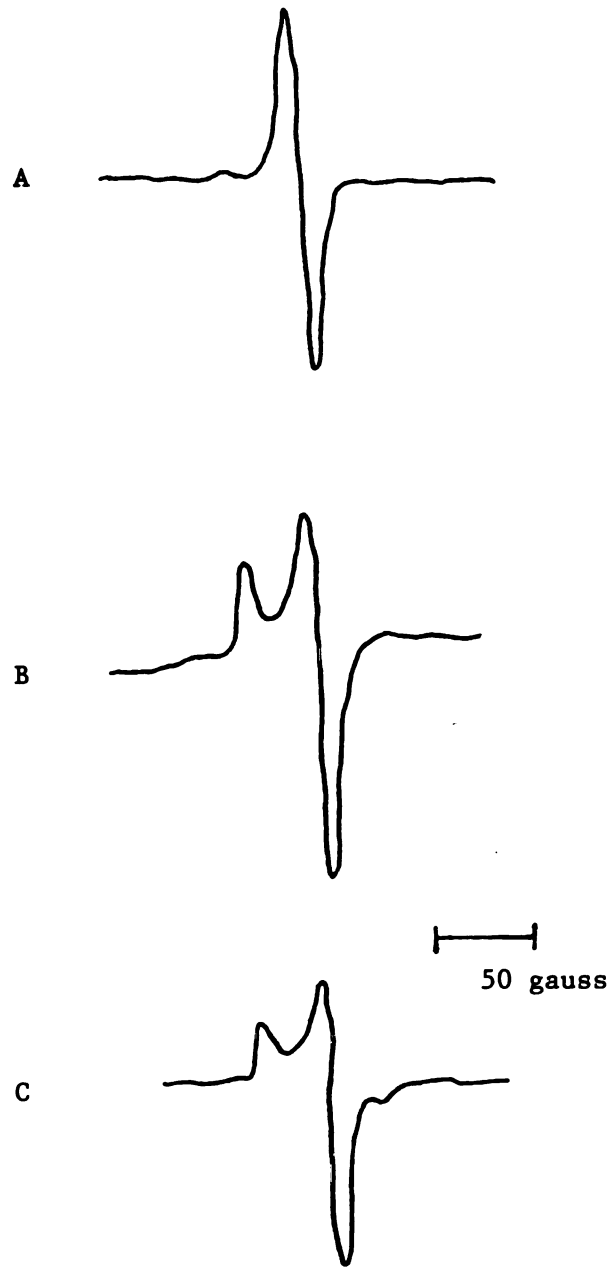

Figure 3.3. The ESR Spectra of H_2O_2-Treated Sperm Whale Myoglobin (A), Horse Myoglobin (B) and Kangaroo Myoglobin (C). g = 2 Region is Displayed for All Spectra. Spectra were Recorded as Described in Chapter 5.

Peroxide Oxidation of Horse Myoglobin

Oxidation of Horse Myoglobin with Hydrogen Peroxide. Incubation of horse myoglobin, styrene and H_2O_2 for 30 minutes at $0^{\circ}C$ results in a 10% decrease in the heme Soret absorbance relative to the Soret absorbance of a control incubation lacking H_2O_2 (Figure 3.4). The electronic spectrum of the peroxide treated hemoprotein is otherwise identical to that of the non-treated control. Figure 3.5 shows that the heme prosthetic groups of both proteins, after extraction with acidic acetone, are also identical. The heme prosthetic group is completely extracted from the non-treated control, however, whereas approximately 10% of the heme remains attached to the peroxide treated hemoprotein (Figure 3.6). As shown in Table 3.1, approximately the same amount of heme remains bound to the apoprotein in the presence or absence of styrene and under anaerobic as well as aerobic conditions.

Amino Acid Composition of Peroxide Treated Horse Myoglobin. The experimental amino acid compositions of peroxide treated horse myoglobin and non-treated control myoglobin are shown in Table 3.2. The only clear difference between the two sets of data is the loss of approximately 50% of the tyrosine content with peroxide treatment.

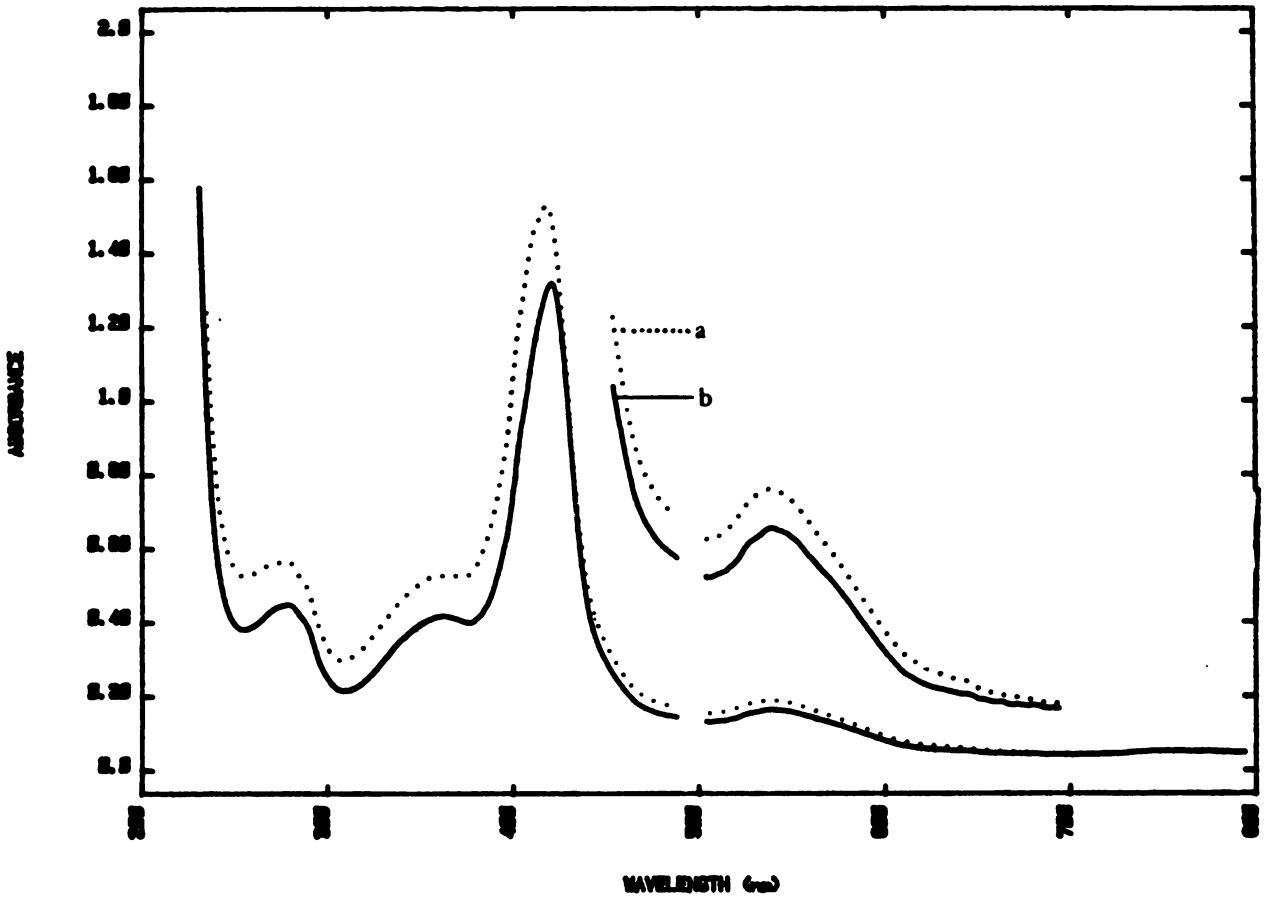

Figure 3.4. The Electronic Absorption Spectra of H_2O_2-Treated Horse Myoglobin (a) and Non-Treated Control (b). Loss of Soret Intensity was Determined as Described in Chapter 5.

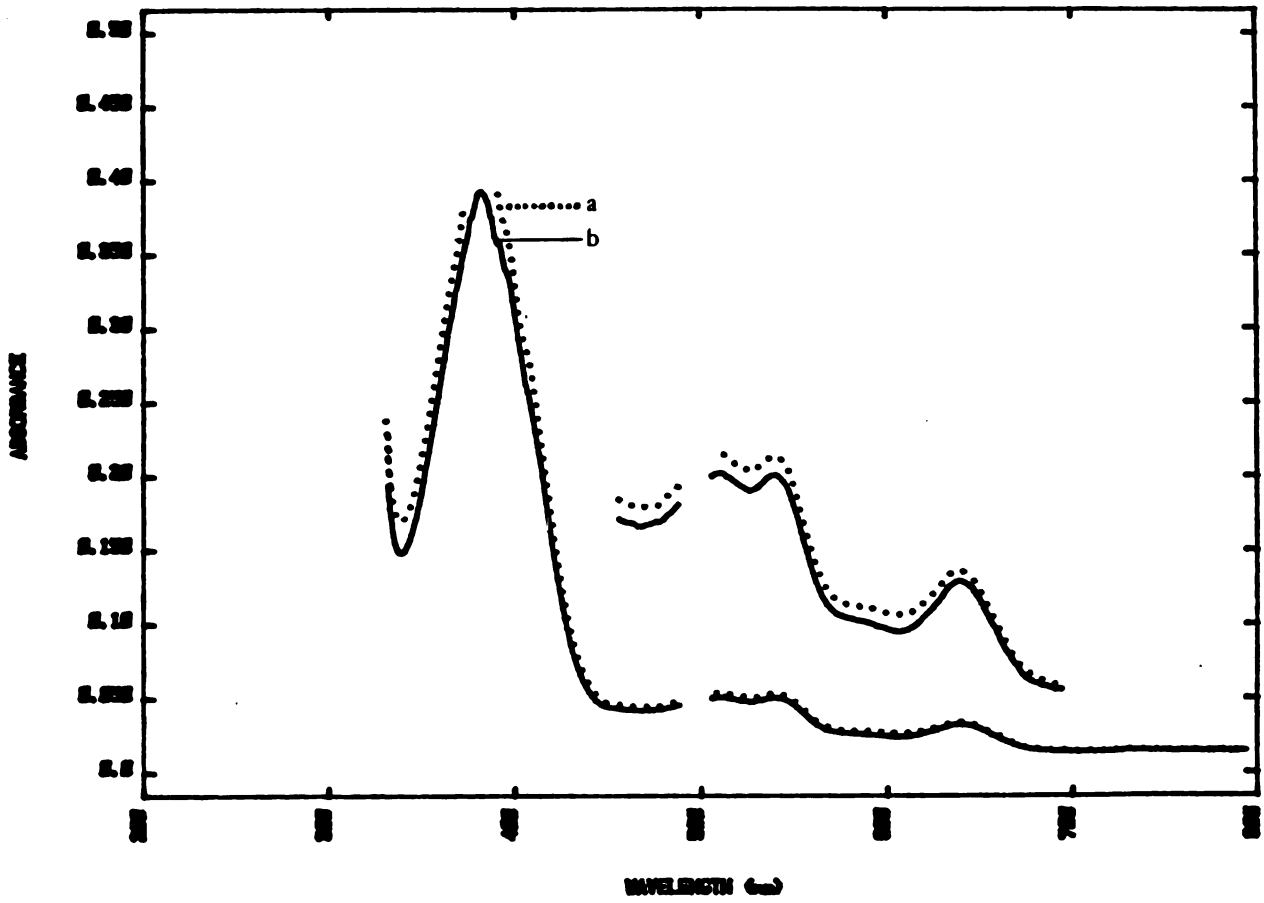

Figure 3.5. The Electronic Absorption Spectra of the Hemes Extracted From H_2O_2-Treated Horse Myoglobin (a) and Non-Treated Control (b). The Hemes Were Extracted by the Acidic-Acetone Method as Described in Chapter 5.

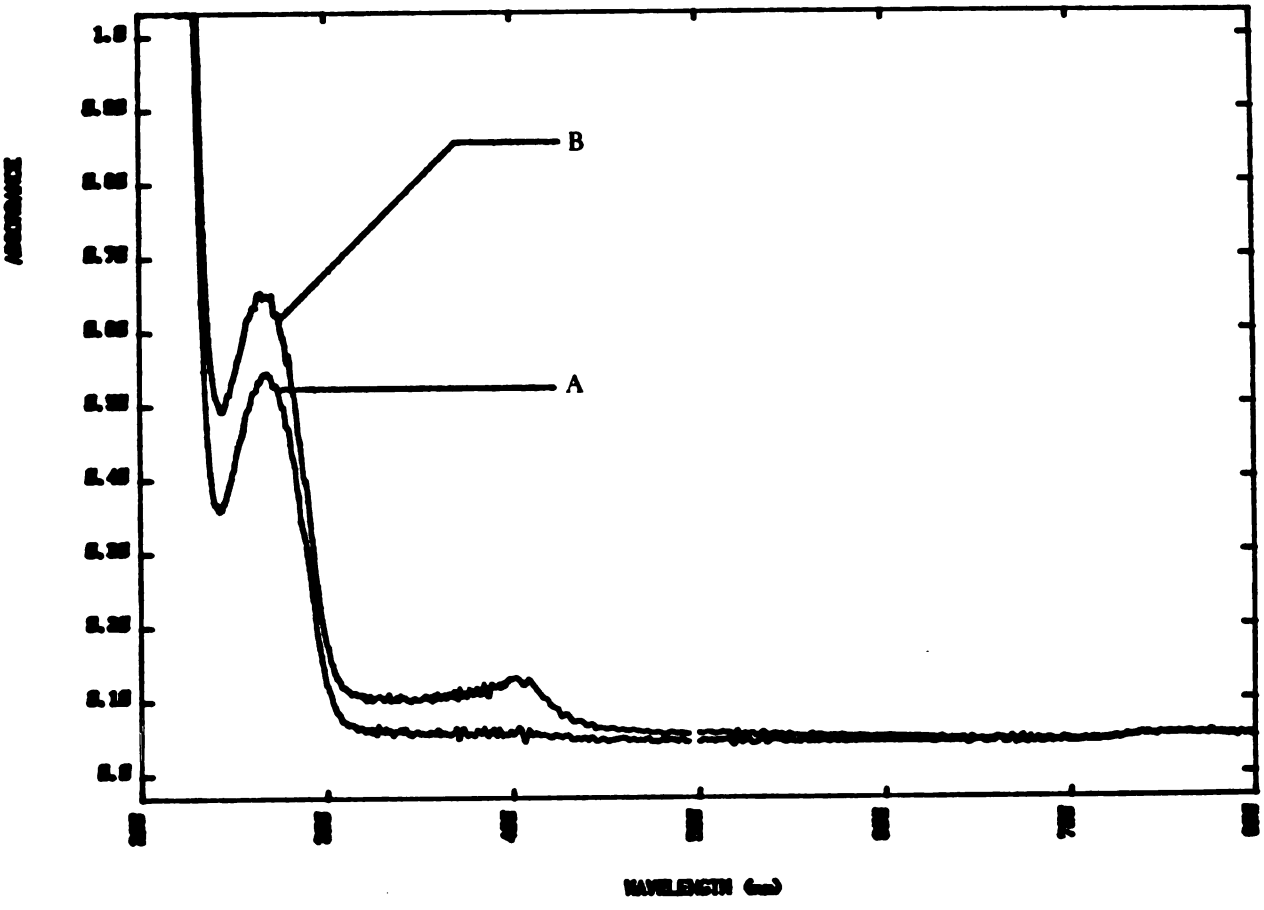

Figure 3.6. The Electronic Absorption Spectra of the Apoproteins After Heme Extraction From H_2O_2-Treated Horse Myoglobin (b) and Non-Treated Control (a). The Amount of Heme Remaining After Extraction with Acidic-Acetone was Determined as Described in Chapter 5.

Table 3.1. Non-Extractable Heme Content of Peroxide Treated Horse Myoglobin

Protein	Styrene	Oxygen	Soret:280nm*	Heme Bound relative %
Holoprotein	Yes	Yes	2.28	100.0
Apoprotein	Yes	Yes	0.225	9.9
Apoprotein	No	Yes	0.286	12.5
Apoprotein	No	No	0.236	10.4

*Ratio of Soret band to 280 nm (aromatic amino acid) band of the electronic spectrum.

Table 3.2. Horse Myoglobin Amino Acid Analysis

Amino Acid*	$-H_2O_2$	$+H_2O_2$	Theory
Asx#	10.0	10.0	10
Glx	18.7	18.5	19
Ser	3.5	3.4	5
Gly	11.8	11.3	15
His	9.8	9.9	11
Arg	2.2	2.1	2
Thr	6.0	5.9	7
Ala	13.8	13.6	15
Pro	2.9	2.7	4
Tyr	1.0	0.5	2
Val	10.0	9.7	7
Met	1.4	1.4	2
Ile	10.2	10.2	9
Leu	15.9	15.6	17
Phe	7.2	7.1	7
Lys	19.8	19.6	19

*HCl hydrolysis for 72 hours. #Set to 10.

Trypsin Digestion of Myoglobin

Horse Myoglobin Peptide Maps. The peptides theoreticaly expected from complete trypsin digestion of horse myoglobin are listed in Table 3.3. Typical HPLC chromatograms of the horse myoglobin peptides obtained from tryptic digestion are shown in Figure 3.7. Three chromatograms are displayed for each protein: The upper trace represents the absorbance at 220 nm (peptide backbone), the middle trace that at 280 nm (aromatic amino acids) and the lower that at 400 nm (heme Soret). The majority of the peptides elute with an acetonitrile concentration of between 0 and 40% (0 and 90 minutes) as is true of most peptides (Allen, 1981). Although some variation is observed in these chromatograms, HPLC analyses of several digests show there is no consistent difference between the peroxide treated and non-peroxide treated control myoglobin peptide fragments in the 0 to 90 minute region.

Under the analytical conditions employed, the holoprotein elutes at approximately 90 minutes and free heme at approximately 115 minutes. There is a substantial increase in the 400 nm absorbance in the 90 to 120 minute region of the chromatogram after peroxide treatment. The standard peptide elution gradient (see methods) shows this absorbance is associated with several peaks (Figure 3.8).

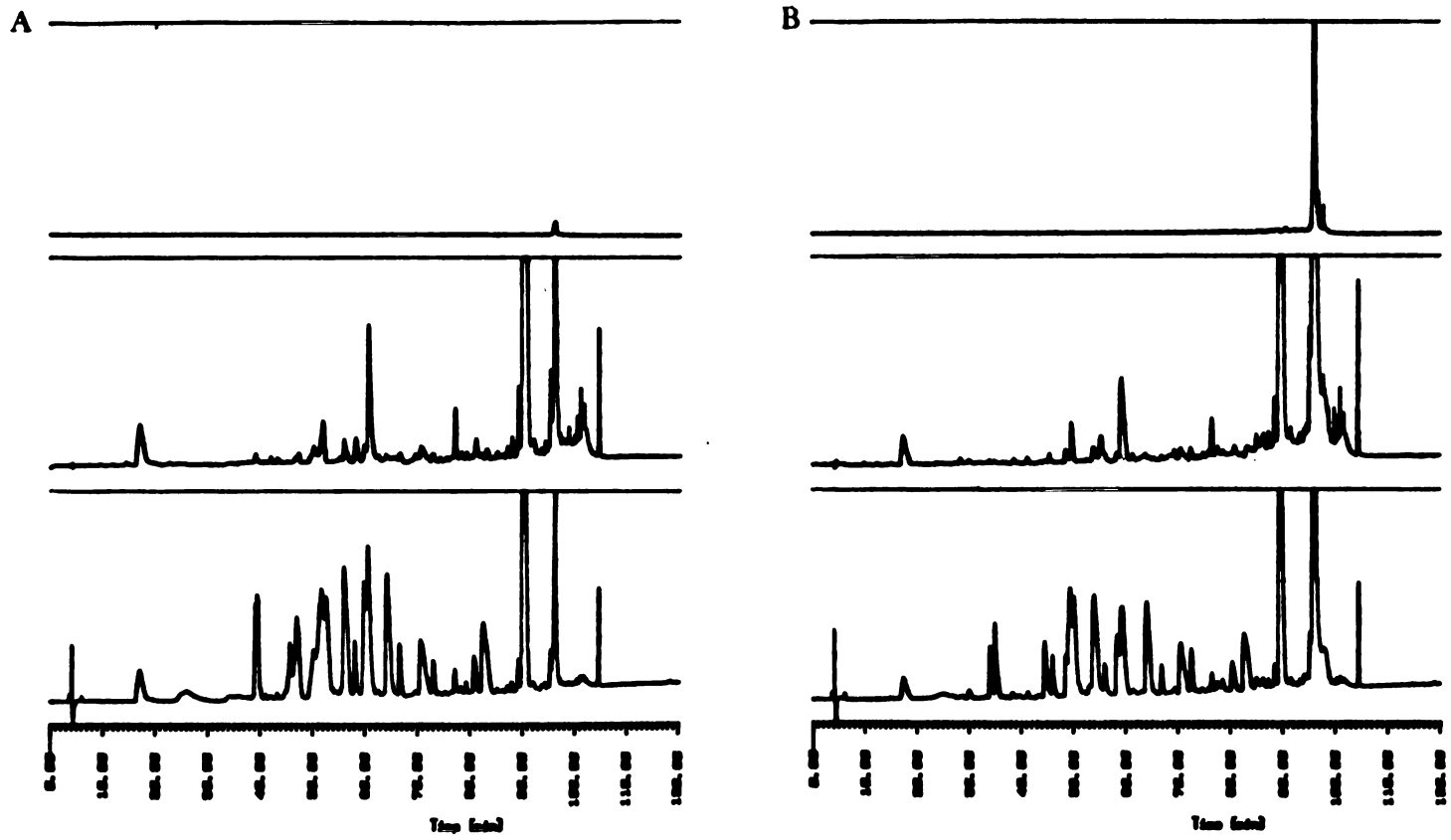

Figure 3.7. HPLC Chromatograms of the Peptides Resulting from Trypsin Digestion of H_2O_2-Treated Horse Myoglobin (B) and Non-Treated Control (A).[2] Absorbance was Simultaneously Monitored at 398 nm (upper trace), 280 nm (middle trace) and 220 nm (lower trace). The Elution Gradient Differed Slightly from That Described in Chapter 5: 0 to 40% B over 90 minutes followed by 40 to 100% B over 5 minutes.

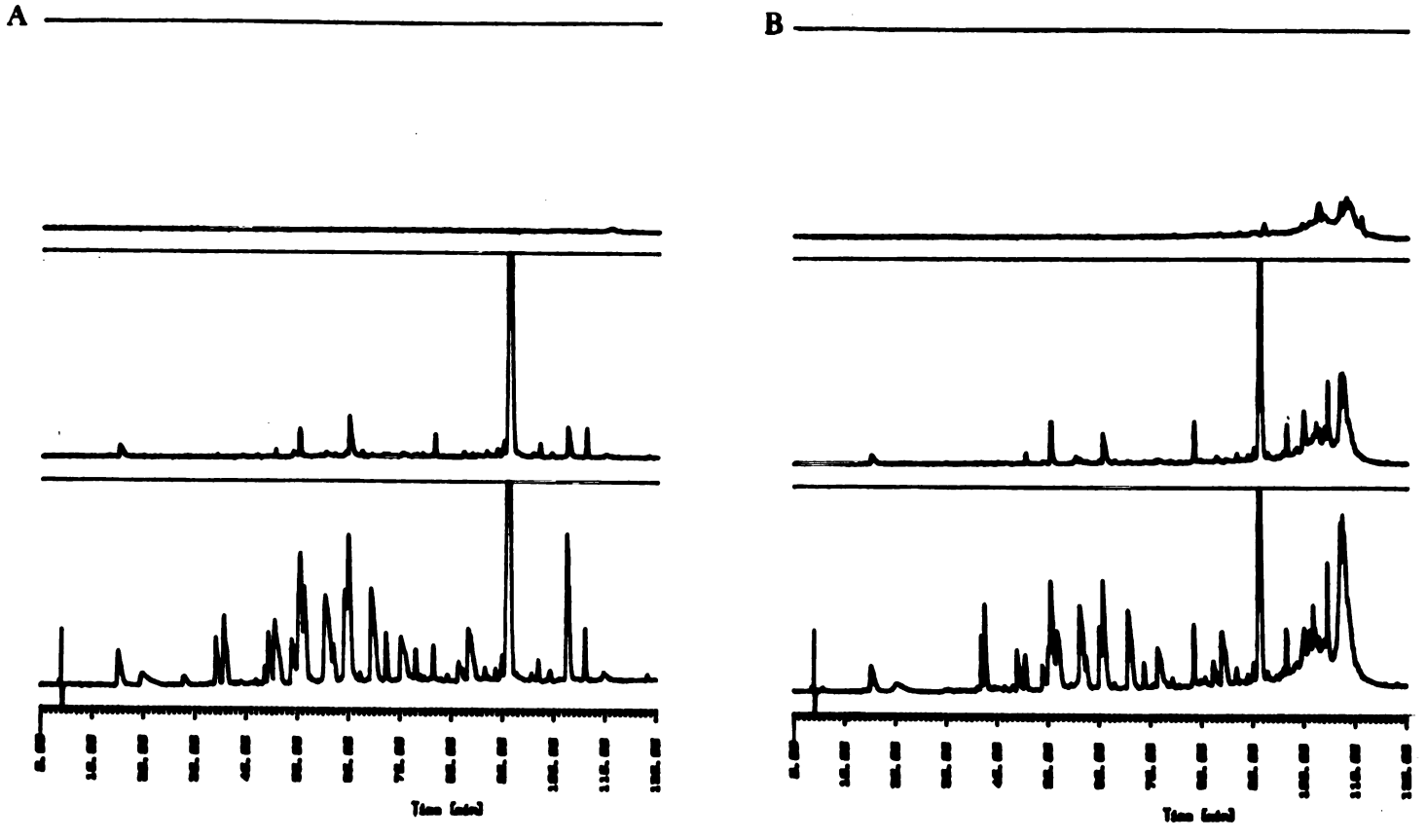

Figure 3.8. HPLC Chromatograms of the Peptides Resulting from Trypsin Digestion of H_2O_2-Treated Horse Myoglobin (B) and Non-Treated Control (A). Absorbance was Simultaneously Monitored at 398 nm (upper trace), 280 nm (middle trace) and 220 nm (lower trace). HPLC Conditions are Described in Chapter 5.

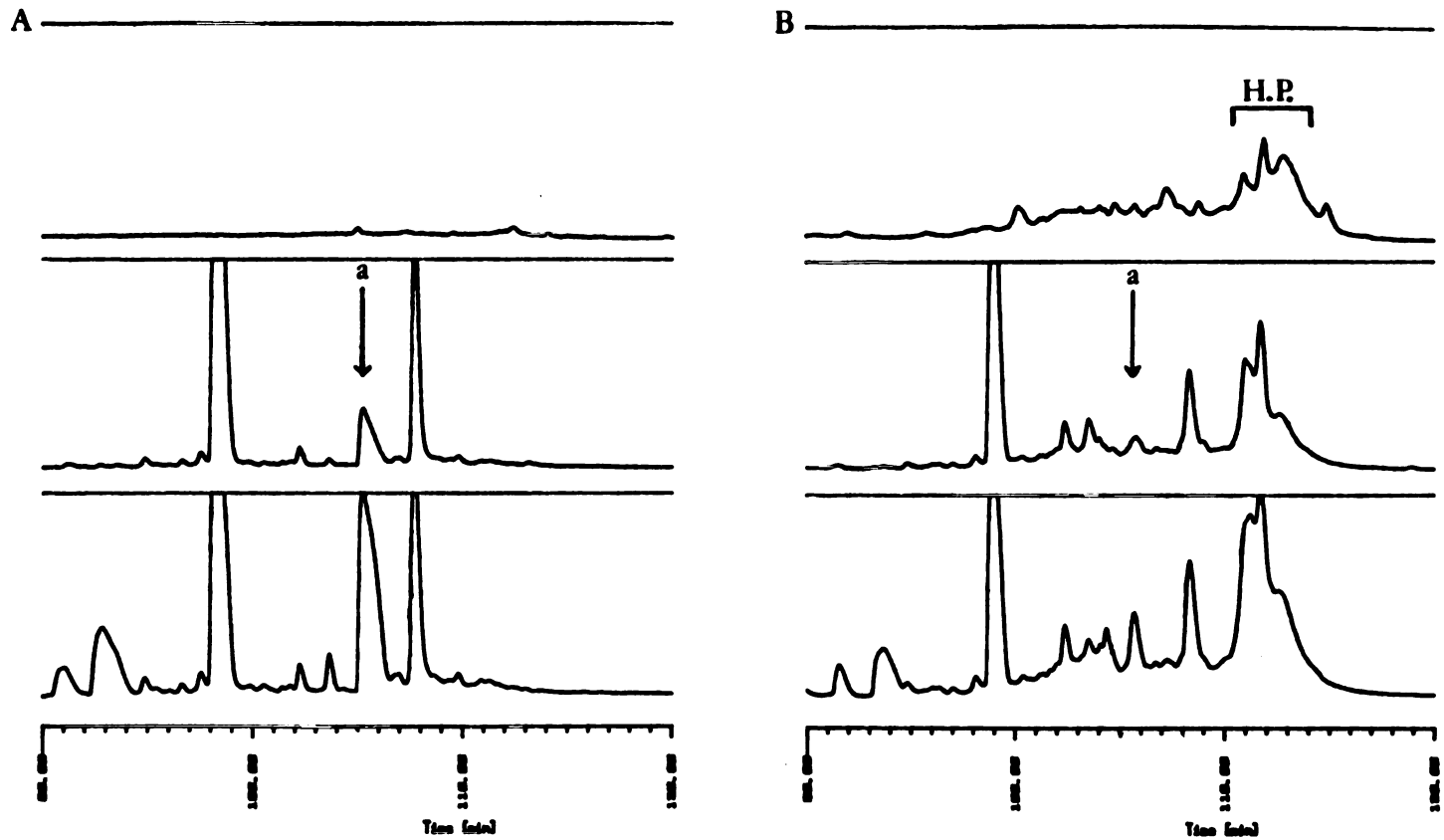

Figure 3.9. Expanded Region of the HPLC Chromatograms of the Peptides Resulting from Trypsin Digestion of H_2O_2-Treated Horse Myoglobin (B) and Non-Treated Control (A). Absorbance was Simultaneously Monitored at 398 nm (upper trace), 280 nm (middle trace) and 220 nm (lower trace). a, Peptide A; H.P., the "Heme-Peptide".

Table 3.3. Theoretical Peptides Derived from Trypsin Digestion of Horse Myoglobin

Peptide #	Sequence	Mass
1	G-L-S-D-G-E-W-Q-Q-V-L-N-V-W-G-K	1815
2	V-E-A-D-I-A-G-H-G-Q-E-V-L-I-R	1606
3	L-F-T-G-H-P-E-T-L-E-K	1271
4	F-D-K	408
5	F-K	293
6	H-L-K	396
7	T-E-A-E-M-K	707
8	A-S-E-D-L-K	661
9	K	146
10	H-G-T-V-V-L-T-A-L-G-G-I-L-K	1378
11	K	146
12	K	146
13	G-H-H-E-A-E-L-K	920
14	P-L-A-Q-S-H-A-T-K	952
15	H-K	283
16	I-P-I-K	469
17	Y-L-E-F-I-S-D-A-I-I-H-V-L-H-S-K	1884
18	H-P-G-N-F-G-A-D-A-Q-G-A-M-T-K	1501
19	A-L-E-L-F-R	747
20	N-D-I-A-A-K	630
21	Y-K	309
22	E-L-G-F-Q-G	649

However, as shown in Figure 3.9, the majority of the 400 nm absorbance is associated with a set of 3 very closely spaced peptides that elute between 110 and 114 minutes and are not present in non-peroxide-treated control incubations. Several HPLC columns and a variety of HPLC conditions were examined without success in attempts to better separate these peptides. They were, therefore, collected and analyzed as a single fraction and are referred to as the "heme-peptide". Concomitant with the appearance of the heme-peptide, a peak eluting at approximately 105 minutes (Figure 3.9, peptide A) is attenuated.

Characterization of Tryptic Peptide A. Peptide A (Figure 3.9) isolated from digests of both control and peroxide treated myoglobin was submitted for amino acid compositional analysis. Table 3.4 shows that the amino acid composition of both peptides is quite similar, which suggests that the two peptides are the same. Comparison of the amino acid composition of peptide A with that for the peptides theoretically generated by tryptic digestion of horse myoglobin strongly suggests that it is peptide #17 (Table 3.3), which includes amino acids 103 to 118 of the horse myoglobin sequence. The sequence of this peptide is shown in Figure 3.10 and its theoretical amino acid composition is listed in Table 3.4.

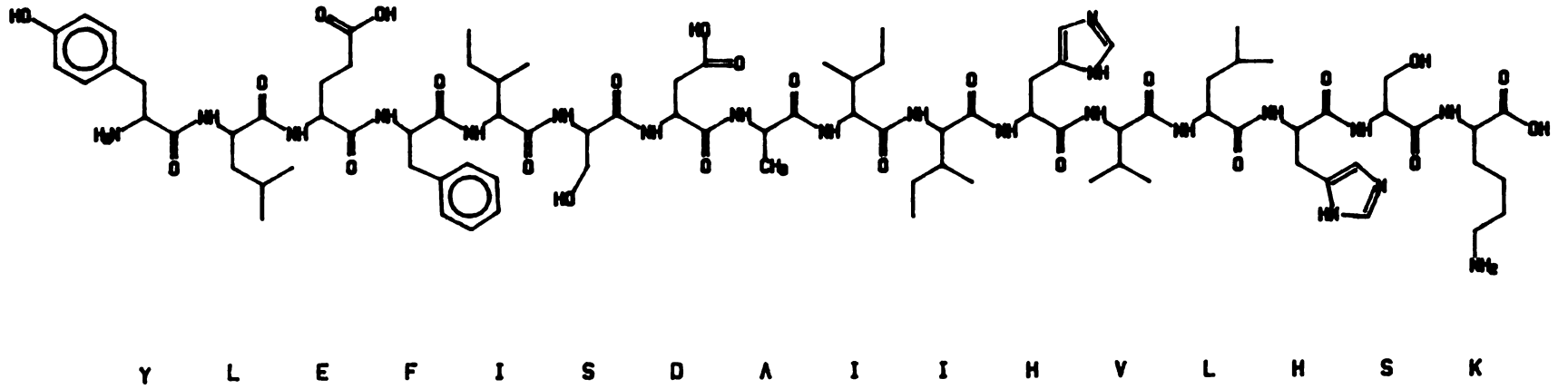

Figure 3.10. The Chemical Structure of Horse Myoglobin Tryptic Peptide #17 (Table 3.3). The One-Letter Code for Each Amino Acid is Also Displayed.

Table 3.4. Amino Acid Composition of Horse Myoglobin Tryptic Peptide A

Amino Acid*	$-H_2O_2$	$+H_2O_2$	Theory@
Asx#	1.0	1.0	1
Glx	0.9	1.3	1
Ser	2.3	1.7	2
His	2.2	1.9	2
Ala	1.3	0.9	1
Tyr	1.1	0.5	1
Val	1.1	0.8	1
Ile	2.0	2.0	3
Leu	2.2	2.1	2
Phe	1.0	1.2	1
Lys	1.0	1.4	1
Gly	0.1	0.5	0
Pro	0.1	0.5	0

*24 hour HCl hydrolysis. #Set to 1.0. @Peptide #17, amino acid residues 102-118 in the horse myoglobin sequence (see Table 3.3, Figure 3.10).

The theoretical nominal mass of peptide #17 is 1884. If allowance is made for the natural abundance of ^{13}C and for protonation of the peptide in the mass spectrometer (L-SIMS in the positive mode), a mass of 1886 is expected for this peptide. The mass spectra (MS-50) of the peptides A

obtained from peroxide-treated and non-treated horse myoglobin are shown in Figures 3.11 a and b, respectively. Both spectra exhibit a molecular ion at m/e 1886.

Sequencing of the three N-terminal amino acid residues of peptide A isolated from the non-peroxide treated myoglobin yielded the sequence Tyr-Leu-Glu. Peptide #17 is the only peptide derived by tryptic digestion of horse myoglobin that has this N-terminal sequence (Table 3.3).

Characterization of the Tryptic Heme-Peptide. Peptide A from non-peroxide treated myoglobin and the heme-peptide from the peroxide-treated hemoprotein were isolated from several different tryptic digests and were submitted for amino acid compositional analysis. The results of these analyses are shown in Tables 3.5 and 3.6. Comparison of the two tables reveals that the amino acid compositions of both peptides are identical, within experimental error, with two exceptions: the serine content is attenuated and tyrosine is virtually absent in the heme-peptide. The theoretical composition of peptide #17 is listed in Table 3.7 along with a summary of the data for peptide A from untreated myoglobin and the heme-peptide from the peroxide treated hemoprotein.

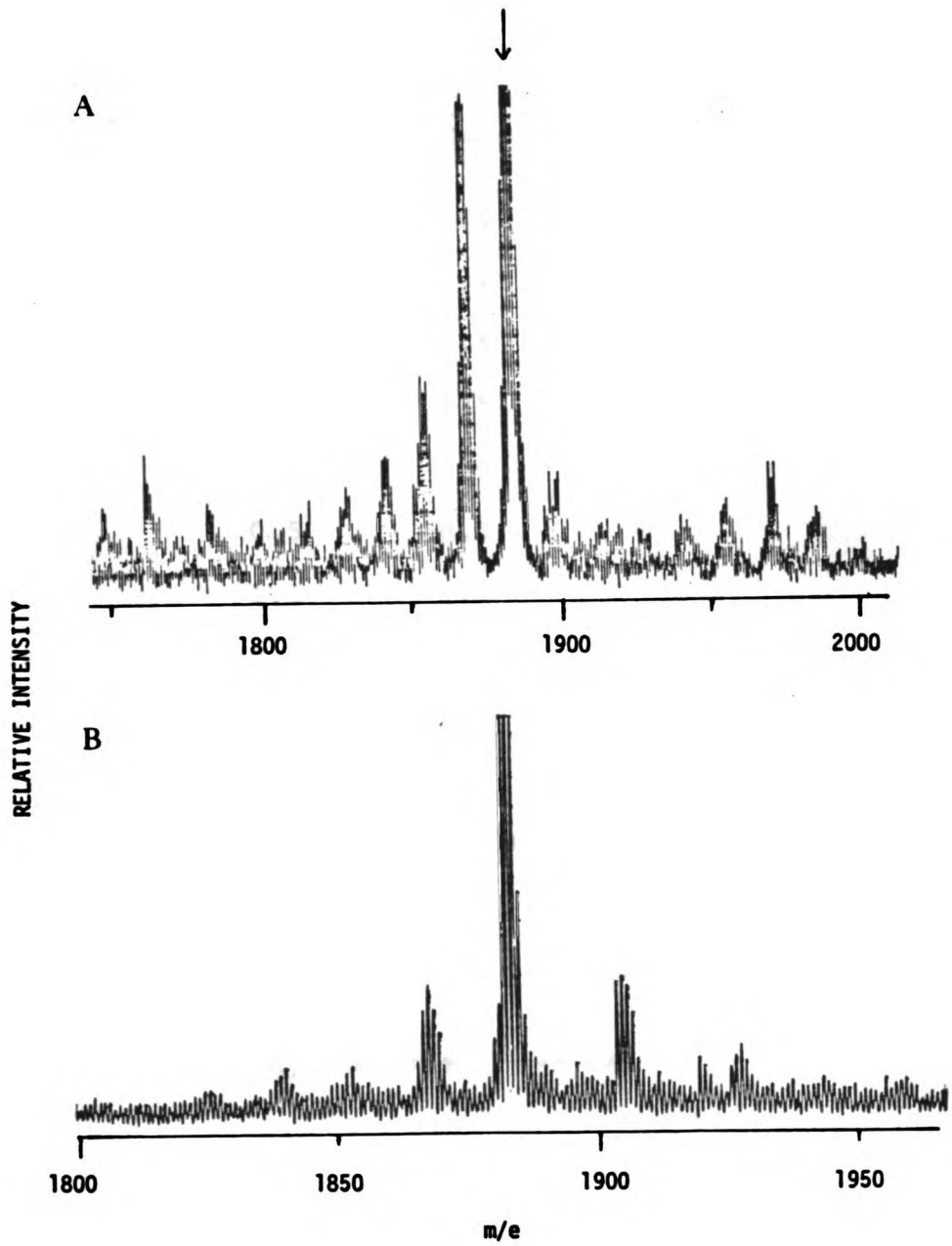

Figure 3.11. The LSIMS (positive mode) Mass Spectra of Peptides A Isolated from Tryptic Digestion of H_2O_2-Treated Horse Myoglobin (B) and Non-Treated Control (A). The Arrow Indicates an m/e of 1886 mass units. The Spectra were Recorded on the MS-50 Mass Spectrometer.

Table 3.5. Amino Acid Composition of Horse Myoglobin Tryptic Peptide A ($-H_2O_2$)

Amino Acid*	1	2	3	4	Average
Asx#	1.0	1.0	-	1.0	1.0
Glx	1.4	1.2	-	0.9	1.2
Ser	0.9	1.6	-	2.3	1.6
His	0.7	1.5	-	2.2	1.5
Ala	0.5	1.0	-	1.3	0.9
Tyr	0.5	0.7	-	1.1	0.8
Val	1.1	0.8	-	1.1	1.0
Ile	0.8	1.1	-	2.0	1.3
Leu	1.5	1.6	-	2.2	1.8
Phe	0.5	0.7	-	1.0	0.7
Lys	1.3	1.2	-	1.0	1.2
Gly	1.1	0.6	-	0.1	0.6
Thr	0.1	0.3	-	0.1	0.1

*24 hour HCl hydrolysis. #Set to 1.0.

Table 3.6. Amino Acid Composition of the Horse Myoglobin Tryptic Heme Peptide

Amino Acid*	1	2	3	4	Average
Asx#	1.0	1.0	1.0	1.0	1.0
Glx	1.6	1.7	1.8	1.8	1.7
Ser	0.8	0.8	0.8	0.6	0.8
His	1.2	1.3	1.1	1.6	1.3
Ala	1.1	1.2	1.3	1.5	1.3
Tyr	0.1	0.1	0.1	N.D+	0.1
Val	0.8	0.7	0.6	0.7	0.7
Ile	1.5	1.1	0.9	0.9	1.1
Leu	1.7	1.7	1.5	1.7	1.7
Phe	1.1	0.8	0.6	0.7	0.8
Lys	3.0	N.D+	1.4	1.3	1.9
Gly	1.0	1.1	1.4	1.6	1.3
Thr	0.5	0.6	0.6	0.8	0.6

*24 hour HCl hydrosysis. #Set to 1.0. +ND, not detectable.

Table 3.7. Summary of the Amino Acid Compositions of Horse Myoglobin Tryptic Peptide A and the Heme-Peptide

Amino Acid*	Peptide A ($-H_2O_2$)	Heme-Peptide	Theory@
Asx#	1.0	1.0	1
Glx	1.2	1.7	1
Ser	1.6	0.8	2
His	1.5	1.3	2
Ala	0.9	1.3	1
Tyr	0.8	0.1	1
Val	1.0	0.7	1
Ile	1.3	1.1	3
Leu	1.8	1.7	2
Phe	0.7	0.8	1
Lys	1.2	1.9	1
Gly	0.6	1.3	0
Thr	0.1	0.6	0

*24 hour HCl hydrolysis. #Set to 1.0. @Peptide #17, Table 3.3, Figure 3.10.

Low serine and histidine values are typical in analyses of amino acid compositions due to oxidation of these residues during the hydrolysis step (Allen, 1981). Adjacent isoleucine residues (see Figure 3.10), in addition, are not readily hydrolyzed after only 24 hours hydrolysis time (ibid).

A mass spectrum has not yet been obtained for the heme-peptide on the MS-50. A very strong ion current is present but no mass peaks appear in scans up to a mass range of 4000. The limited material available led to the use of microperoxidase as a model compound with which to optimize the mass spectrometric conditions for heme-bound peptides.

Mass Spectrum of Microperoxidase. Microperoxidase is a heme-bound undecapeptide derived from pepsin hydrolysis of cytochrome C. The structure of microperoxidase is shown in Figure 3.12. The theoretical mass for microperoxidase is nominally 1862. A positive mode L-SIMS mass spectrum (MS-50) for microperoxidase (Figure 3.13, trace a) shows molecular ion peaks centered at 1862 mass units. The mass peaks 22 units higher correspond to the monosodium salt. A very strong ion current was detected in the mass spectrometer and yet the molecular ion peaks were quite weak. Subsequent work showed that very strong mass peaks are present that are centered at 618 mass units (Figure 3.13, trace b). These peaks undoubtedly represent free

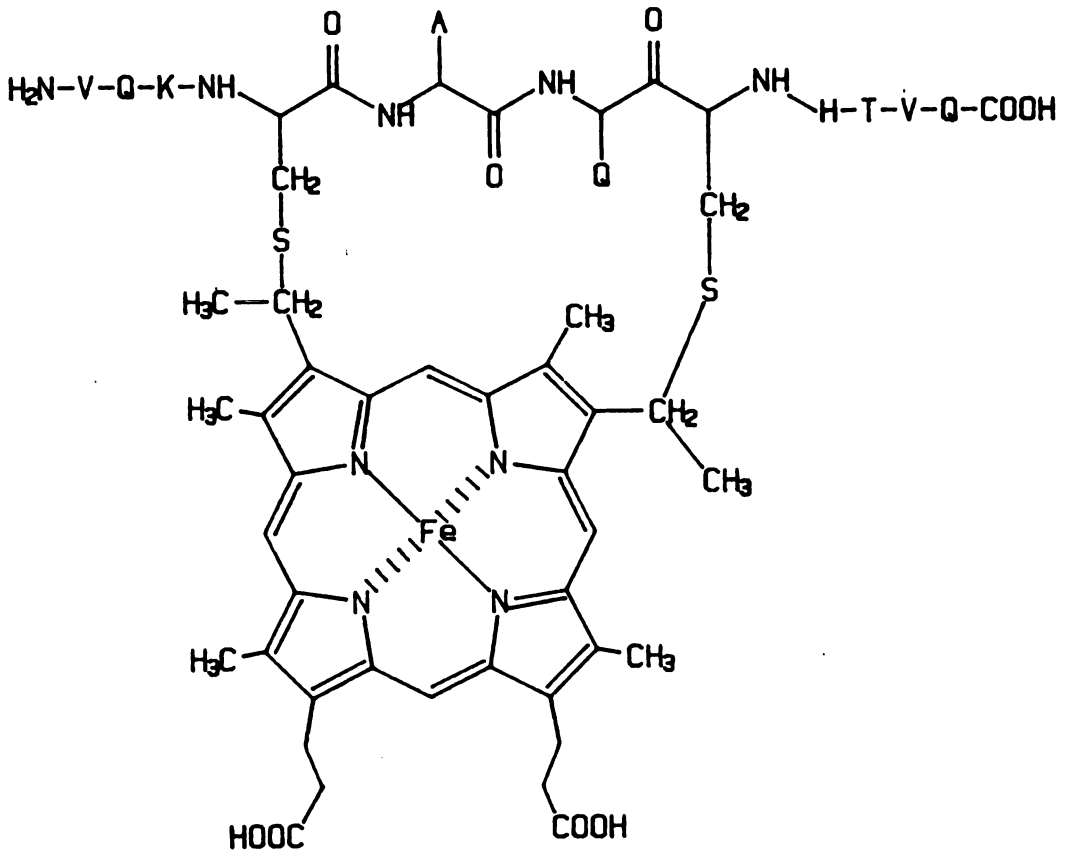

Figure 3.12. The Chemical Structure of Microperoxidase. The One-Letter Code for Several of the Amino Acids are Displayed in the Figure.

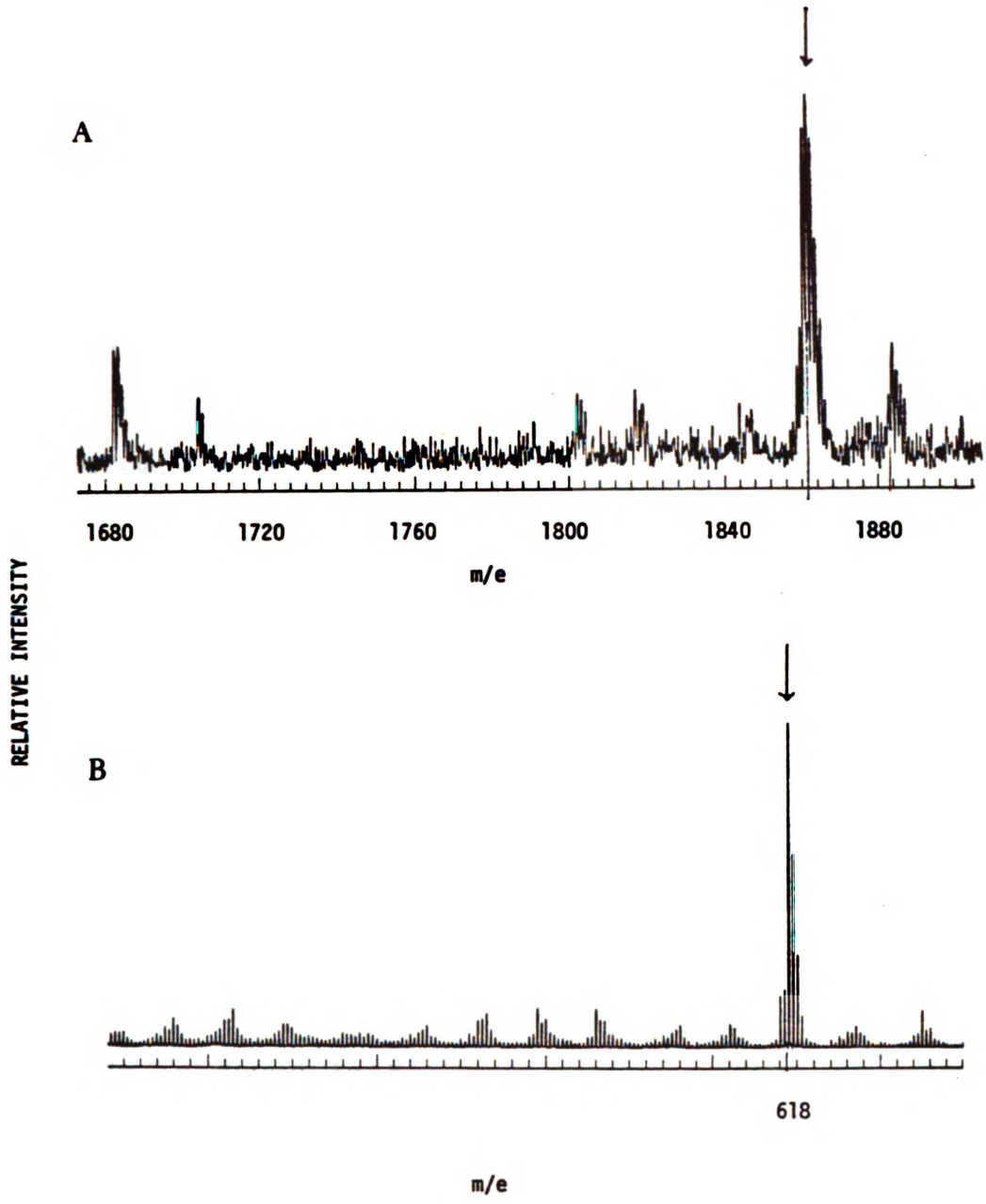

Figure 3.13. The LSIMS (positive mode) Mass Spectrum of Microperoxidase. A) Scan of the High Molecular Weight Region with an Arrow at 1862 mass units. B) Scan of the Low Molecular Weight Region with an Arrow at 618 mass units. The Spectrum was Recorded on the MS-50 Mass Spectrometer.

heme. No peaks were observed at 1250 mass units, the mass of the heme-free peptide.

A negative mode L-SIMS mass spectrum obtained for microperoxidase (MS-50, Figure 3.14) shows mass peaks centered at 1859 mass units. There are also peaks centered at 1988 that are probably due to the thioglycerol (mw=108) adduct of the mono-sodium salt (mw=22) of microperoxidase. Unlike the L-SIMS spectrum in the positive mode, no mass peaks are observed at 616 mass units in the negative mode spectrum.

An L-SIMS mass spectrum (negative mode) of microperoxidase obtained using the WEIN mass spectrometer is shown in Figure 3.15. This spectrum shows a molecular ion peak at 1861 mass units.

Mass Spectrum of the Horse Myoglobin Heme-Peptide. A preparative tryptic digest was performed on peroxide treated horse myoglobin and the heme-peptide was isolated by HPLC. A typical chromatogram for the preparative isolation of this peptide is shown in Figure 3.16. Fractions were collected as indicated in the expanded chromatogram and the electronic spectra for pooled fractions I, II and III are shown in Figure 3.17 a, b and c, respectively.

The expected nominal mass of peptide #17 covalently linked to heme is 2500 mass units. A negative mode L-SIMS mass spectrum of the heme-peptide was obtained using the

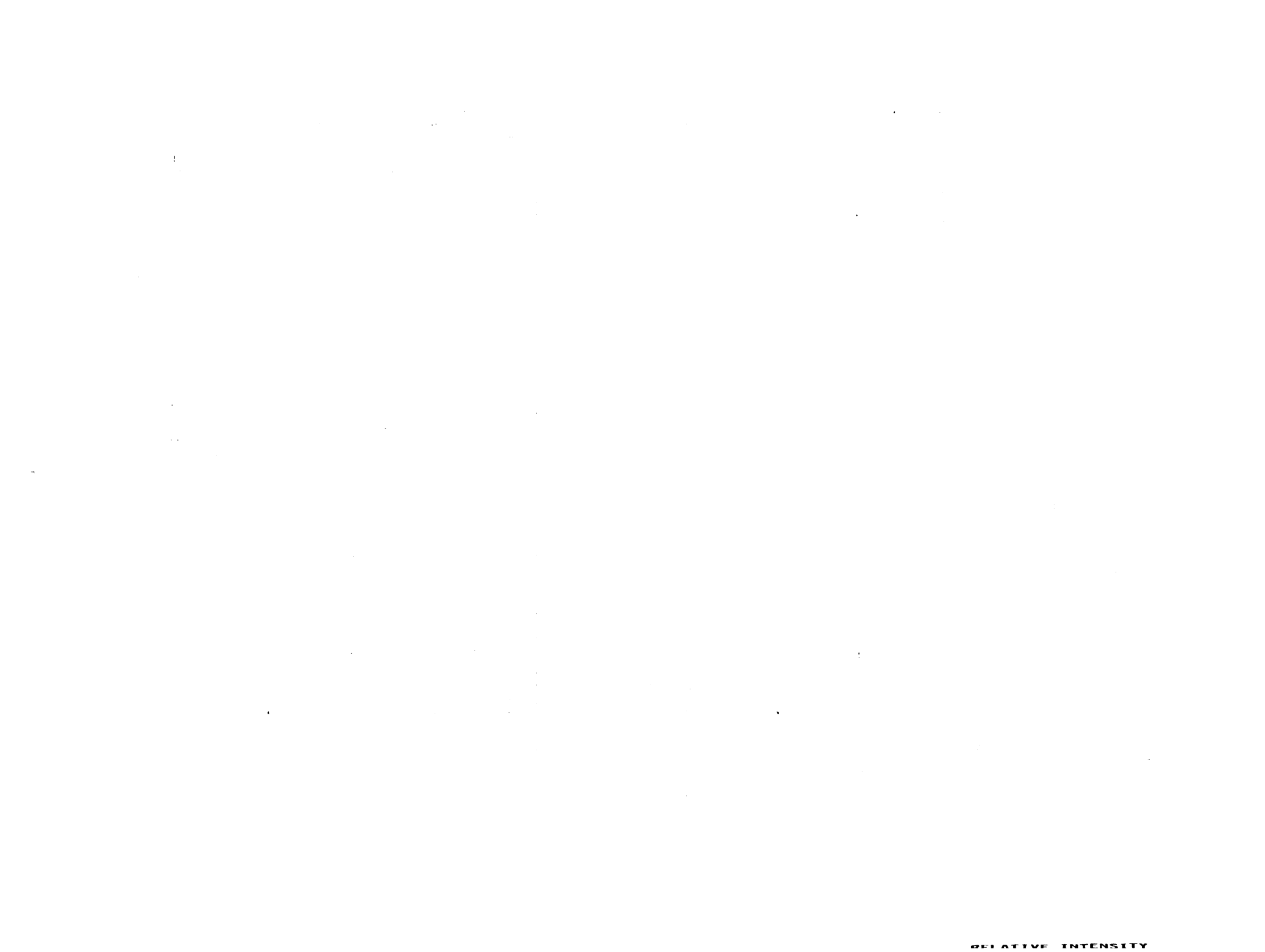
RELATIVE INTENSITY

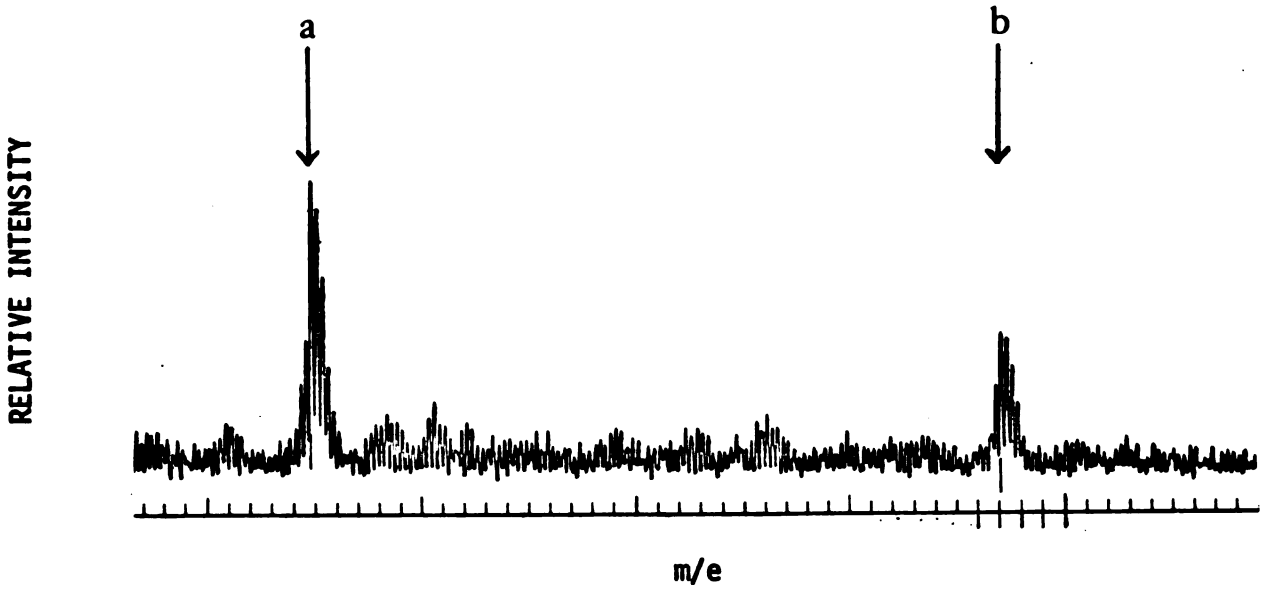

Figure 3.14. The LSIMS (negative mode) Mass Spectrum of Microperoxidase. The Arrows Indicate an m/e of 1859 (a) and 1988 (b) mass units. The Spectra was Recorded on the MS-50 Mass Spectrometer.

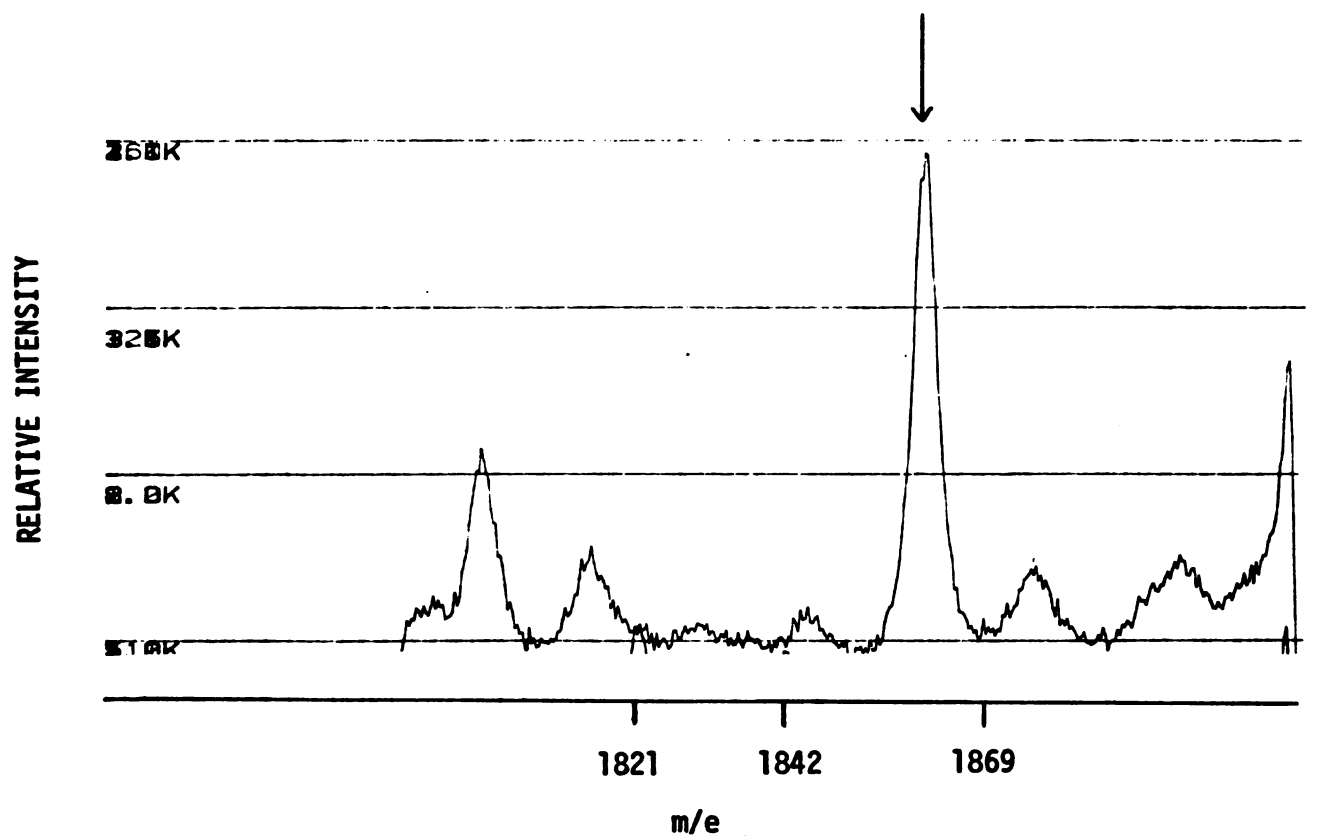

Figure 3.15. The LSIMS (negative mode) Mass Spectrum of Microperoxidase Obtained on the WEIN Mass Spectrometer. Molecular Weight Standards: $(RbI)_8I^-$, 1821; $(CsF)_{12}F^-$, 1842; $(Rb_7CsI_8)I^-$, 1869 mass units. The Arrow Indicates an m/e of 1860 mass units.

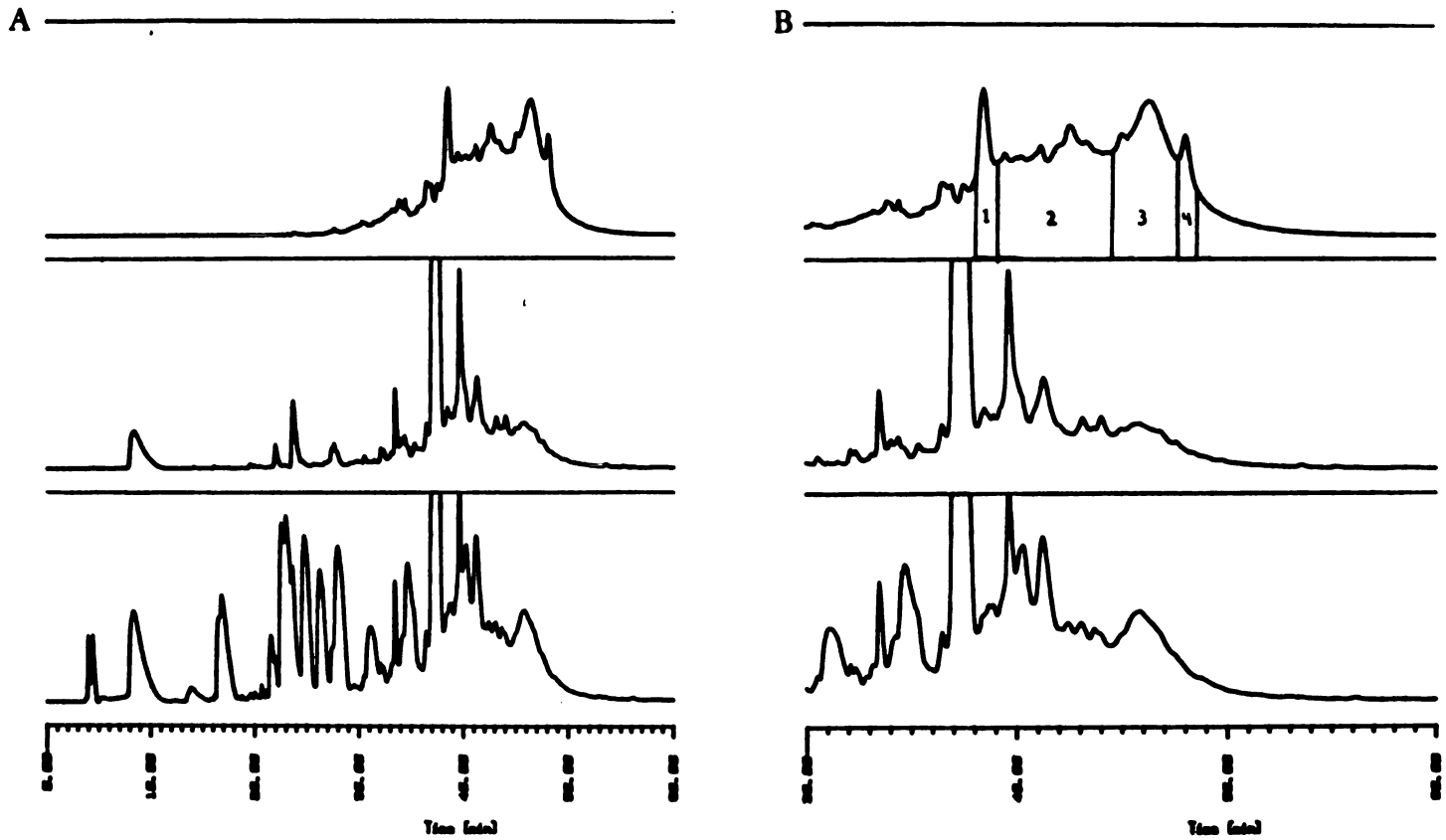

Figure 3.16. Isolation of the Heme-Peptide (fraction 3) From the Preparative Trypsin Digestion of Peroxide-Treated Horse Myoglobin. The Full Chromatogram (A) and an Expanded Region (B) Indicating the Fractions Collected (1-4). Absorbance was Simultaneously Monitored at 398 nm (upper trace), 280 nm (middle trace) and 220 nm (lower trace). HPLC Conditions are Described in Chapter 5.

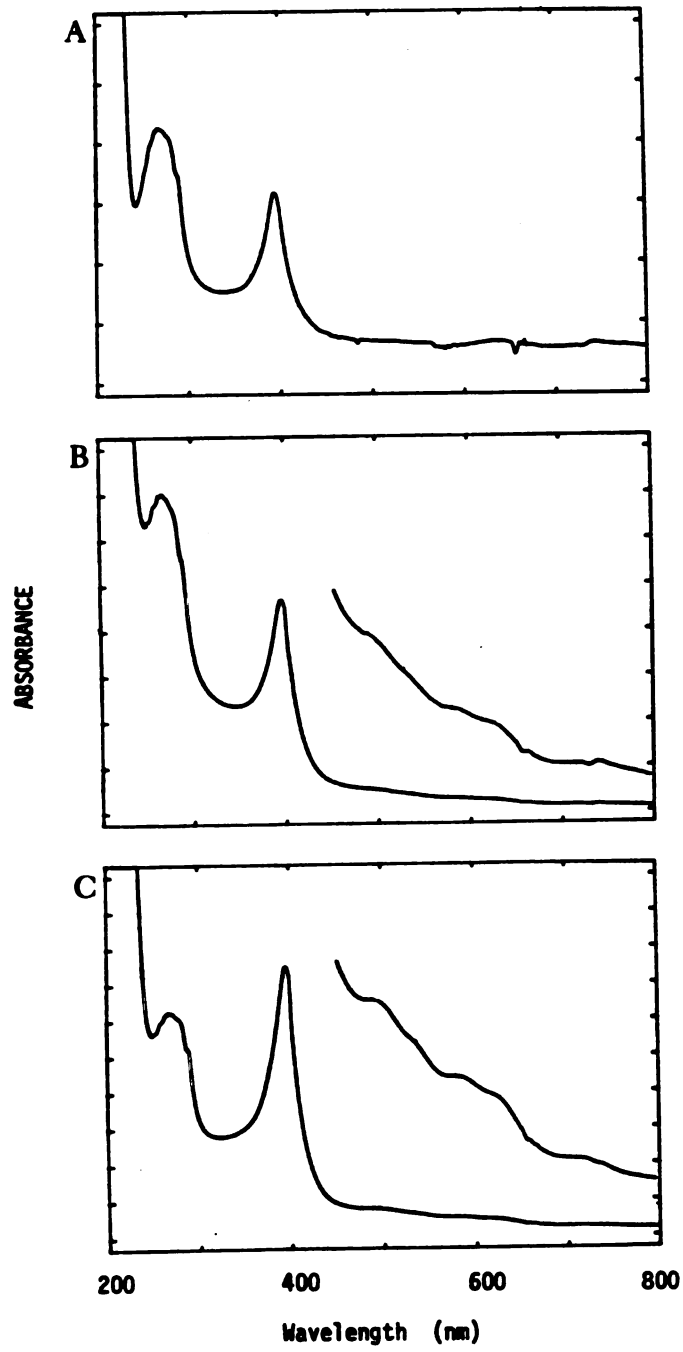

Figure 3.17. The Electronic Absorption Spectra of Fractions 1 to 3 Isolated From the Preparative Tryptic Digestion of Peroxide-Treated Horse Myoglobin (see Figure 3.16).

WEIN-MS and is shown in Figure 3.18. Mass peaks are observed centered at 2504 mass units which is consistent with peptide #17 covalently linked to heme.

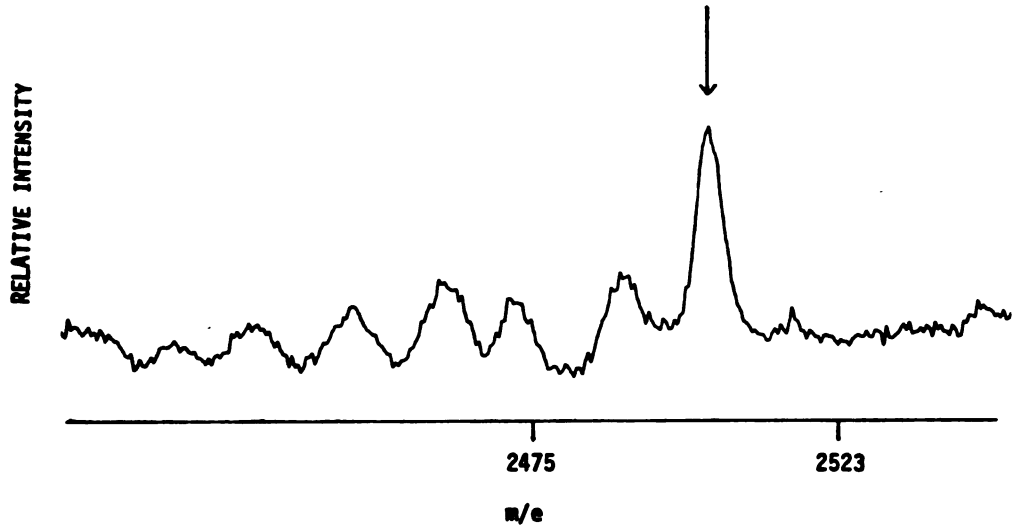

Figure 3.18. The LSIMS (negative mode) Mass Spectrum of the "Heme-Peptide" Obtained on the WEIN Mass Spectrometer. The Arrow Indicates an m/e of 2504 mass units.

Staphylococcal V8 Protease Digestion of Myoglobin

Horse Myoglobin V8 Protease Peptide Maps. Table 3.8 lists the peptides theoretically expected from complete digestion of horse myoglobin with Staphylococcal V8 protease. Figure 3.19 shows a typical HPLC chromatogram of the peptides resulting from V8 protease digestion of horse apomyoglobin. As with the trypsin digests discussed above, there is an increase in the 400 nm absorbance associated with the peptides after peroxide treatment. Again, this increase is associated with closely spaced peptides that elute as a broad band (the "heme-peptide") late in the gradient program at approximately 103 minutes.

The electronic spectra of this heme-peptide, recorded during elution from the HPLC column using the Hewlett Packard diode array detector, is shown in Figure 3.20. This spectrum exhibits distinct absorption bands at 270 nm and 398 nm and is consistent with a heme attached to a peptide containing at least one aromatic acid residue.

A second difference between the hydrogen peroxide-treated and non-treated myoglobin peptides is evident by careful examination of Figure 3.19. A peptide eluting at approximately 57.5 (Peptide B) appears to be at least partially modified with peroxide treatment and migrates with a slightly longer (1 minute) retention time (Peptide C). Most of the 280 nm absorbance of the original peak appears

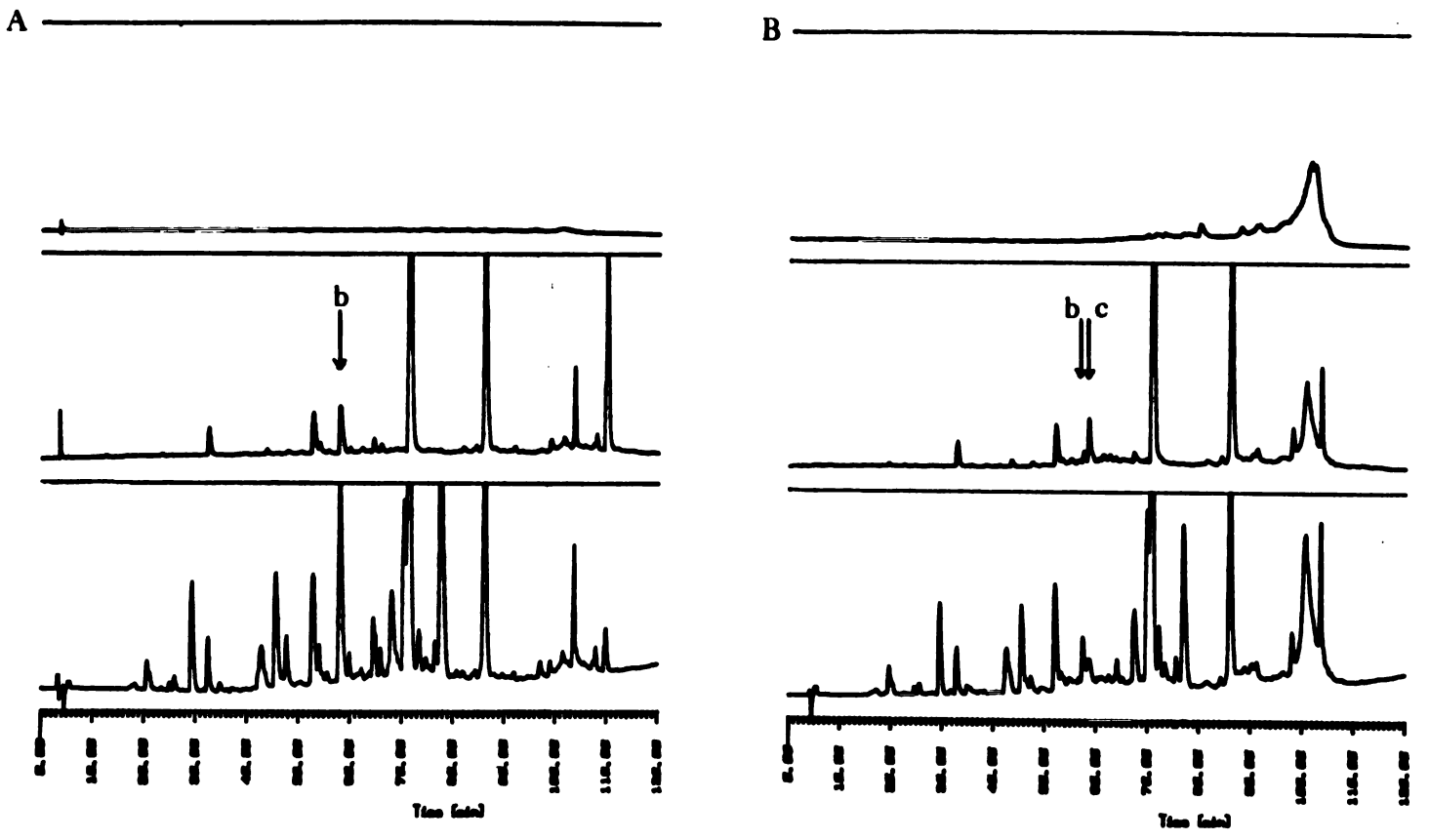

Figure 3.19 HPLC Chromatograms of the Peptides Resulting from Staphylococcal V8 Protease Digestion of H_2O_2-Treated Horse Myoglobin (B) and Non-Treated Control (A). Absorbance was Simultaneously Monitored at 398 nm (upper trace), 280 nm (middle trace) and 220 nm (lower trace). Peptides B and C are indicated by Arrows b and c, Respectively. HPLC Conditions are Described in Chapter 5.

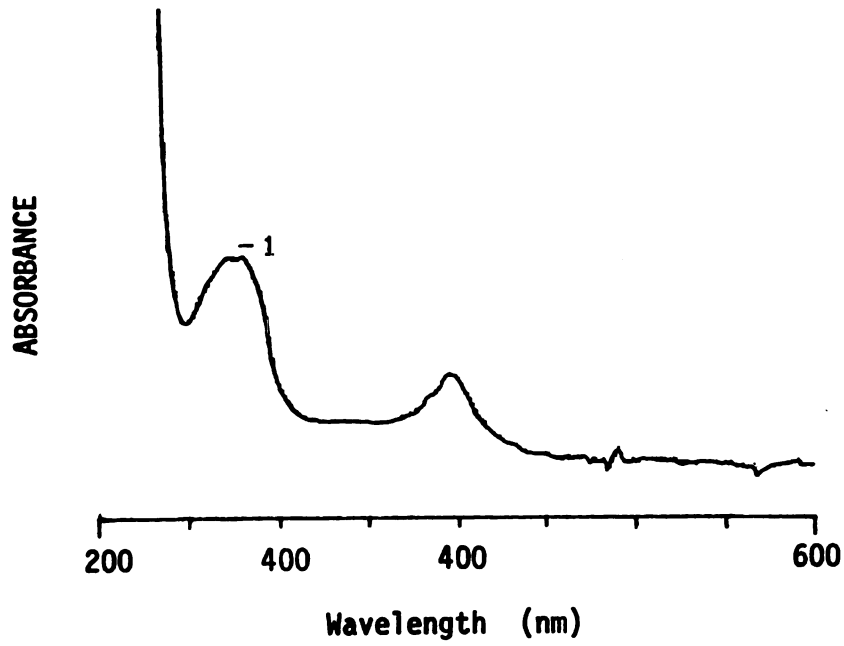

Figure 3.20. The Electronic Absorption Spectrum of the Staphylococcal V8 Protease "Heme-Peptide". The Spectrum was Recorded During Elution From the HPLC Column (see Figure 3.19).

Table 3.8. Theoretical Peptides Derived from Staphylococcal V8 Digestion of Horse Myoglobin

Peptide #	Sequence	Mass
1	G-L-S-D-G-E	576
2	W-Q-Q-V-L-N-V-W-G-K-V-E	1485
3	A-D-I-A-G-H-G-Q-E	896
4	V-L-I-R-L-F-T-G-H-P-E	1281
5	T-L-E	361
6	K-F-D-K-F-K-H-L-K-T-E	1420
7	A-E	218
8	M-K-A-S-E	564
9	D-L-K-K-H-G-T-V-V-L-T-A-L-G-G-I-L -K-K-K-G-H-H-E	2579
10	A-E	218
11	L-K-P-L-A-Q-S-H-A-T-K-H-K-I-P-I-K -Y-L-E	2314
12	F-I-S-D-A-I-I-H-V-L-H-S-K-H-P-G-N -F-G-A-D-A-Q-G-A-M-T-K-A-L-E	3275
13	L-F-R-N-D-J-A-A-K-Y-K-E	1467
14	L-G-F-Q-G	520

to be associated with the modified peptide. This difference is clearly shown in the expanded chromatogram shown in Figure 3.21.

The electronic spectra of these peptides were taken during elution from the HPLC column utilizing the Hewlett Packard diode array detector (Figure 3.22). Peptide B in the non-peroxide treated control (trace a) exhibits a tyrosine-like spectrum with a maximum at approximately 280 nm. The electronic spectrum of the residual Peptide B in the peroxide-treated hemoprotein also shows very weak absorption at 280 nm. The peroxide-modified peptide (Peptide c), however, exhibits a maximum at 270 nm (trace c).

The HPLC chromatogram utilizing fluoresence detection is shown in Figure 3.23. It is notable that most of the fluorescence associated with Peptide B is lost with peroxide treatment and no new fluorscesent peptides appear in the chromatogram.

The peptides eluting between 57 and 60 minutes (see Figure 3.19) were collected and rechromatographed using a shallow elution gradient (see methods). The chromatograms for the two samples clearly show a change with peroxide treatment (Figure 3.24). Fluorescence detection similarly shows a decrease in the fluorescence intensity in the peroxide treated peptides (Figure 3.25). Again, no new fluorescent peptides are observed after peroxide treatment.

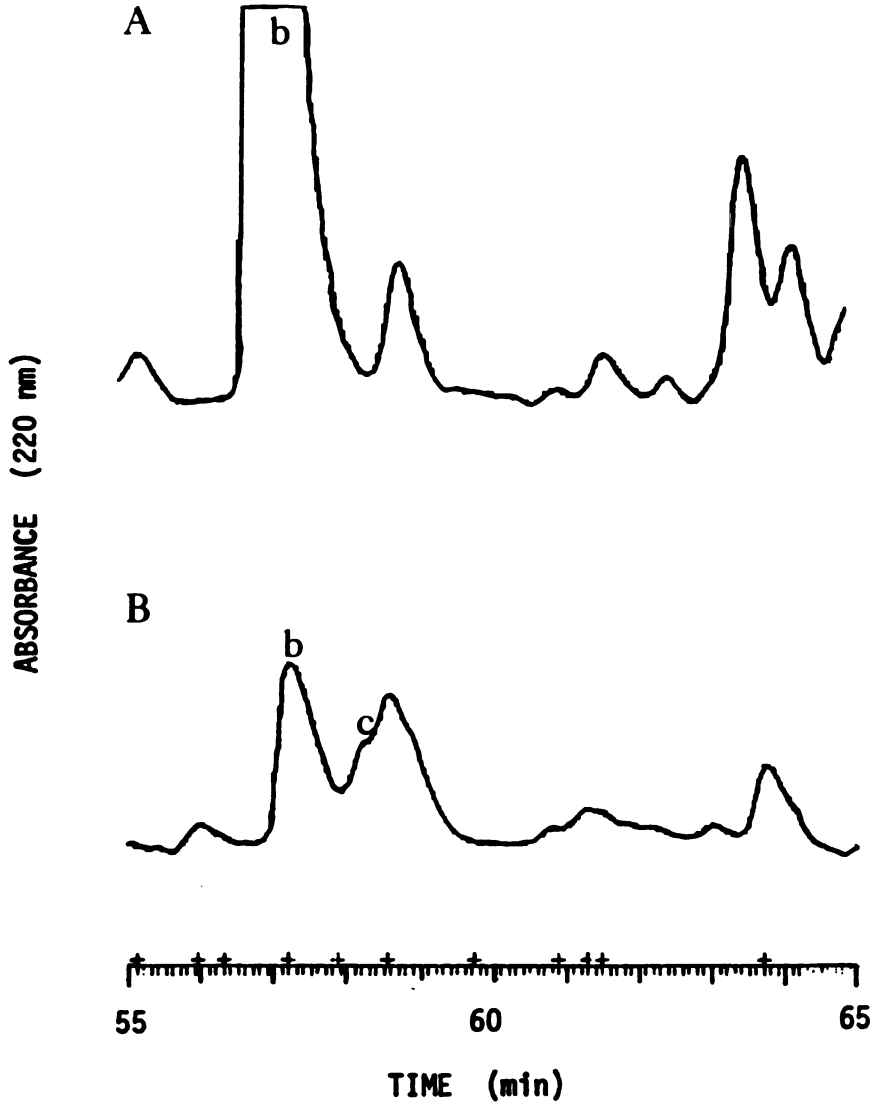

Figure 3.21. The Expanded Region of the HPLC Chromatograms of the Peptides Resulting from Staphylococcal V8 Protease Digestion of H_2O_2-Treated Horse Myoglobin (B) and Non-Treated Control (A). Peptides B and C are indicated by b and c, Respectively. HPLC Conditions are Described in Chapter 5.

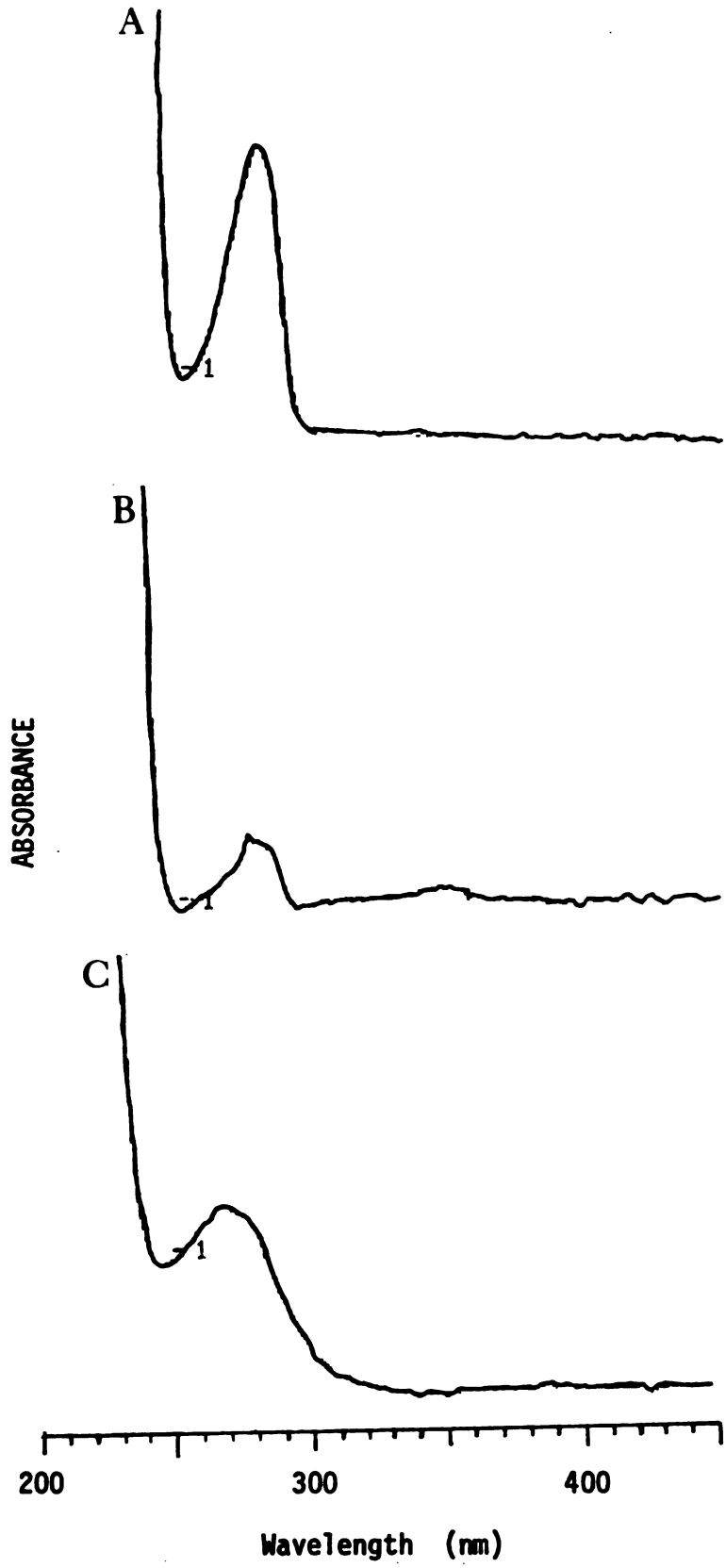

Figure 3.22. Electronic Absorption Spectra of Peptide B From the Control Incubation (A), Peptide B From H_2O_2-Treated Horse Myoglobin (B) and Peptide C From H_2O_2-Treated Horse Myoglobin (C). The Spectra were Recorded During Elution From the HPLC Column (see Figure 3.21).

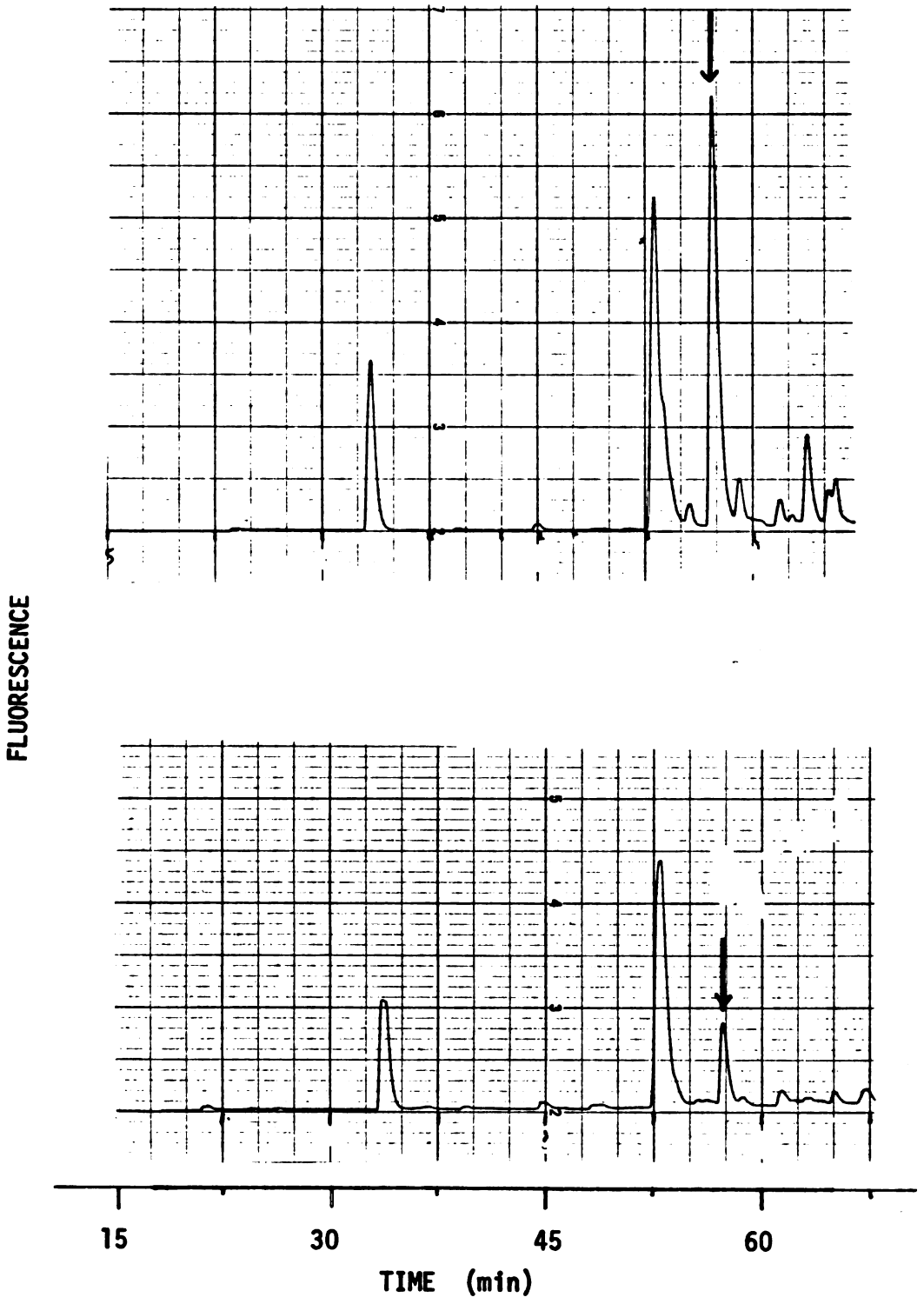

Figure 3.23. The HPLC Chromatograms of the Peptides Resulting from Staphylococcal V8 Protease Digestion of H_2O_2-Treated Horse Myoglobin (lower trace) and Non-Treated Control (upper trace). Fluorescence Detection: Excitation at 280nm, Emission Monitored at 320 nm.

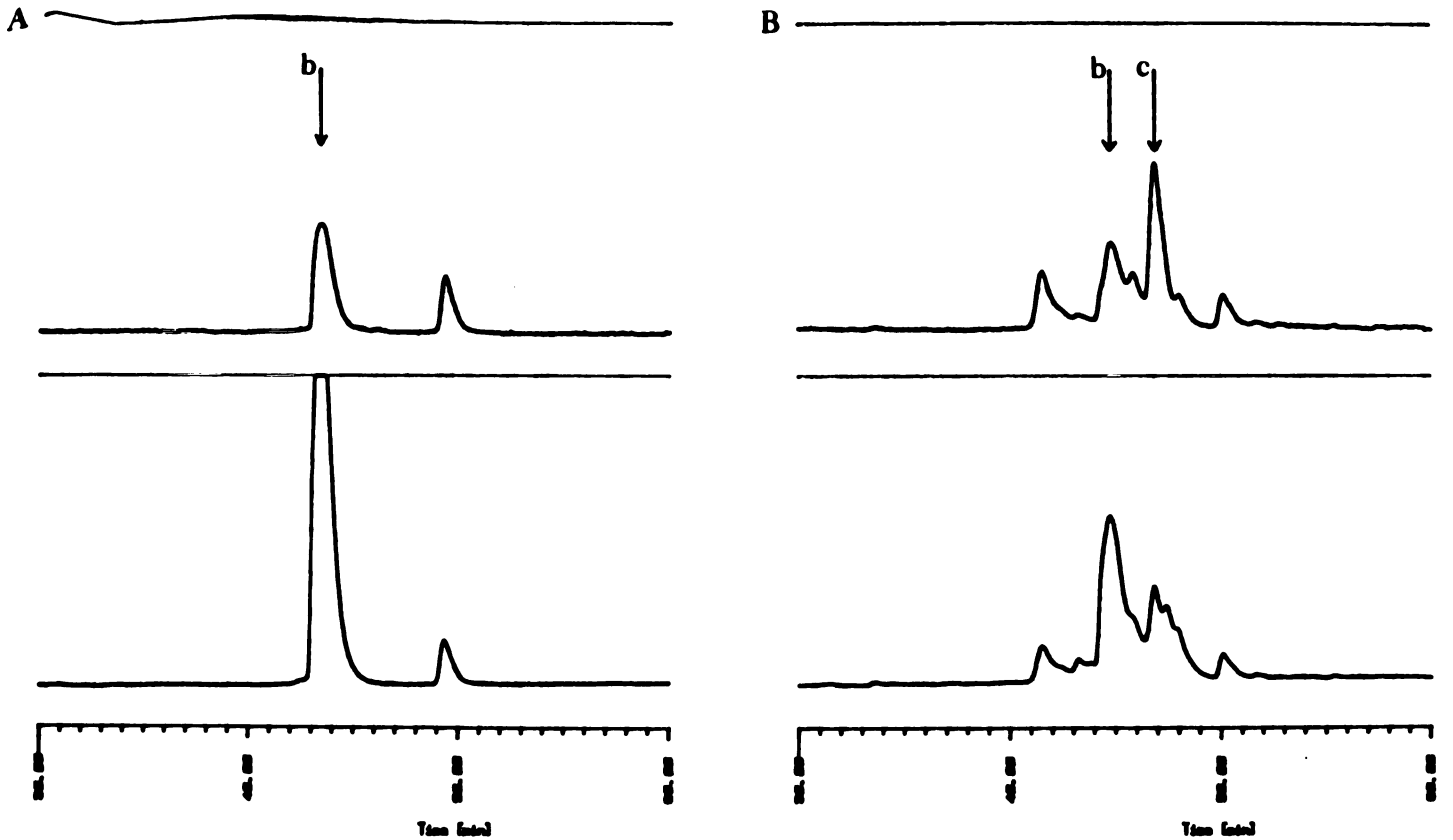

Figure 3.24. Resolution of the V8 Protease Horse Myoglobin Peptides Eluting Between 57 and 60 minutes in the Standard HPLC Gradient (see Figure 3.21). (A) Control Incubation and (B) H_2O_2-Treated Myoglobin. Absorbance was Simultaneously Monitored at 280 nm (upper trace) and 220 nm (lower trace). Peptides B and C are indicated by Arrows b and c, Respectively. The Revised HPLC Gradient is Described in Chapter 5.

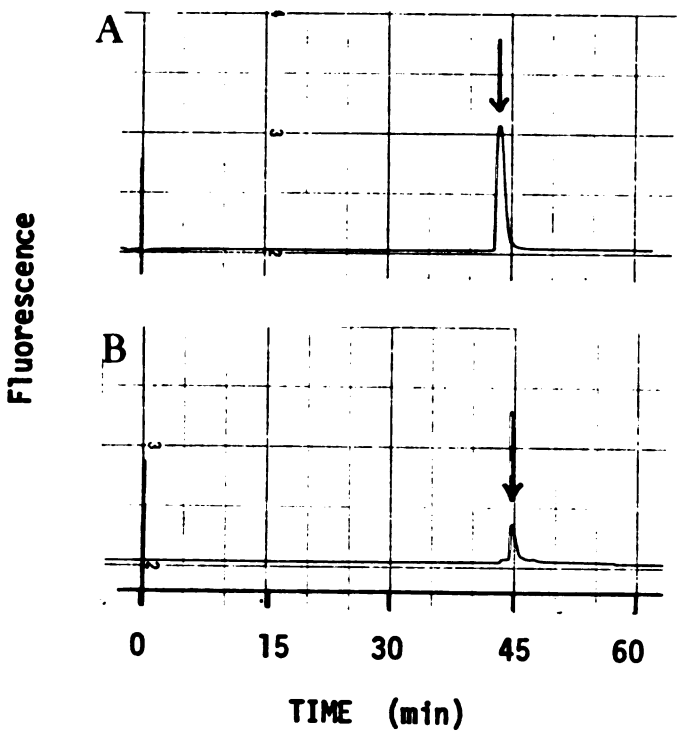

Figure 3.25. Resolution of the V8 Protease Horse Myoglobin Peptides Eluting Between 57 and 60 minutes in the Standard HPLC Gradient (see Figure 3.21). (A) Control Incubation and (B) H_2O_2-Treated Myoglobin. Fluorescence Detection: Excitation at 280nm, Emission Monitored at 320 nm. The Revised HPLC Gradient is Described in Chapter 5.

Characterization of the Staphylococcal V8 Protease Peptides. Amino acid analysis of the heme-peptide is shown in Table 3.9. Comparison of the amino acid composition of the theoretical peptides listed in Table 3.8 with that for the heme-peptide reveals closest similarity to peptide #11. The theoretical composition of this peptide is also listed in Table 3.9.

Peptides B and C from peroxide-treated myoglobin (Figure 3.24) were collected and submitted for amino acid compositional analysis. Table 3.10 shows that the composition of both peptides are quite similar, which suggests that the two peptides are the same. Comparison of the amino acid composition of these peptides with the peptides theoretically generated from V8 protease digestion of horse myoglobin suggests that it is composed of peptide #10 plus peptide #11 (Table 3.8). It is of interest that the tyrosine content of Peptide C is only 40% that of Peptide B suggesting tyrosine 103 is lost with peroxide treatment.

Table 3.9. Amino Acid Composition of the Staphylococcal V8 Protease Heme-Peptide

Amino Acid*	Amount	Theory@
Leu	2.5	3
Lys	2.5	4
Pro	0.9	2
Ala#	2.0	2
Glx	3.3	2
Ser	1.1	1
His	1.6	2
Thr	1.1	1
Ile	1.1	2
Tyr	<0.1	1
Val	1.5	0
Asx	1.8	0
Phe	0.9	0
Gly	2.4	0

*24 hour HCl hydrolysis. #Set to 2.0. @Peptide #11, Table 3.8.

Table 3.10. Amino Acid Composition of the Staphylococcal V8 Protease Peptides B and C

Amino Acid*	Peptide B	Peptide C	Theory@
Leu	3.3	3.6	3
Lys	3.0	4.1	4
Pro	2.3	2.3	2
Ala#	3.0	3.0	3
Glx	2.6	2.6	3
Ser	1.1	1.4	1
His	2.1	2.4	2
Thr	1.2	1.8	1
Ile	1.8	2.3	2
Tyr	0.8	0.3	1
Val	0.2	0.3	0
Asx	0.6	0.6	0
Phe	0.5	1.1	0
Gly	0.9	0.9	0

*24 hour HCl hydrolysis. #Set to 3.0. @Peptide #10 plus #11, Table 3.8.

Nature of the Modified Amino Acid and Heme in the H_2O_2 Treated Myoglobin

Acid Hydrolysis of H_2O_2-Treated Myoglobin. Acid hydrolysis of peroxide treated horse apomyoglobin followed by HPLC analysis yielded the chromatogram shown in Figure 3.26 (trace b). Also shown in the figure is the chromatogram for the hydrolysate of the non-peroxide treated control (trace a). Under these chromatographic conditions, L-dopa elutes at approximately 7 minutes, tyrosine at approximately 10 minutes and heme at approximately 62 minutes. Retention times were quite variable, however, due to a leaky HPLC pump. The chromatograms of the two hydrolyzed proteins are very similar between 0 and 50 minutes. No peaks were observed that eluted in the region of L-dopa. L-Dopa has been detected in acid hydrolysates of tyrosinase-treated proteins when thioglycolic acid was added to prevent oxidation and polymerization of the catechol (Ito et al., 1984). Acid hydrolysis of the proteins in the presence of thioglycolic acid, however, also yielded no detectable L-dopa.

An increase in absorbance in the 398 nm tracing in the region where the heme standard elutes is observed after peroxide treatment of horse myoglobin (Figure 3.26). The peak is quite broad, however, and is superimposed on several sharp components.

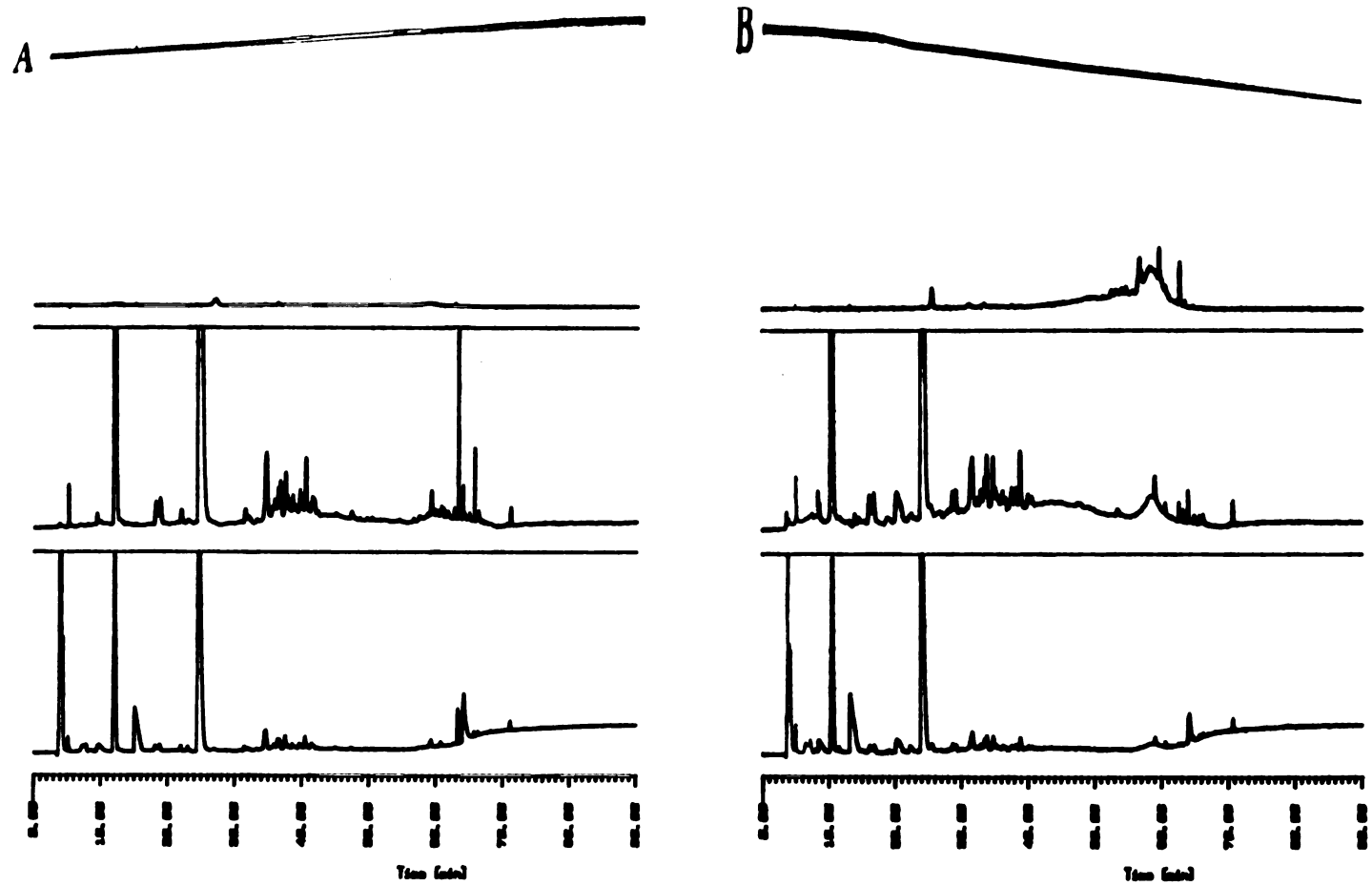

Figure 3.26. The HPLC Chromatograms of Acid Hydrolyzed Horse Myoglobin: Peroxide-Treated (B) and Non-Treated Control (A). Absorbance was Simultaneously Monitored at 398 nm (upper trace), 280 nm (middle trace) and 220 nm (lower trace). The Acetonitrile/Water Gradient System Described in Chapter 5 was Used.

A second HPLC method specifically designed to isolate modified hemes was utilized in an attempt to isolate the heme adduct from peroxide treated myoglobin. The resulting chromatograms are shown in Figure 3.27. Heme standard elutes at 9 minutes under these conditions. A very weak peak elutes at 22 minutes in the peroxide treated sample which is absent in the non-peroxide treated control.

Attempts to carry out the hydrolysis on a preparative scale (100 ml) in order to obtain sufficient material for identification of the modified heme were frustrated by an inability to maintain an anaerobic environment during the 24 hour hydrolysis period. The heme chromophore was invariably lost during this proceedure.

Pronase Digestion of H_2O_2-Treated Myoglobin. Pronase digestion of peroxide-treated horse apomyoglobin followed by HPLC analysis yields the chromatogram shown in Figure 3.28. The chromatogram for the non-peroxide treated myoglobin is also shown in the figure. The chromatogram for the peroxide-treated protein is virtually identical to that for the non-treated control and is qualitatively similar to that for the acid hydrolyzed samples (see Figure 3.26). Again, there is a weak increase in 398 nm asorbance in the peroxide treated protein but it elutes as a very broad peak.

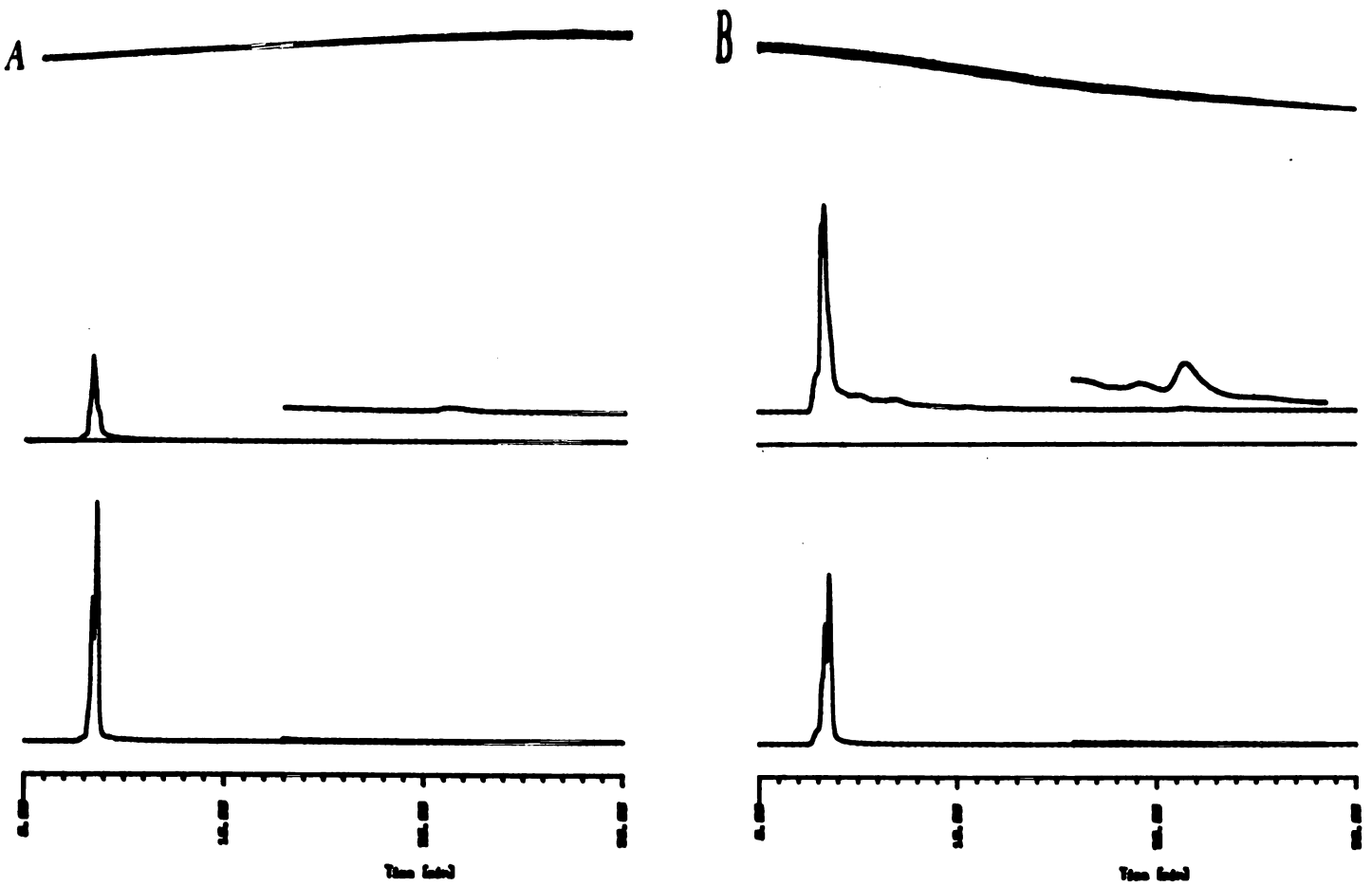

Figure 3.27. The HPLC Chromatograms of Acid Hydrolyzed Horse Myoglobin: Peroxide-Treated (B) and Non-Treated Control (A). Absorbance was Simultaneously Monitored at 398 nm (upper trace) and 280 nm (lower trace). The Methanol/Water/Acetic Acid Gradient System Described in Chapter 5 was Used.

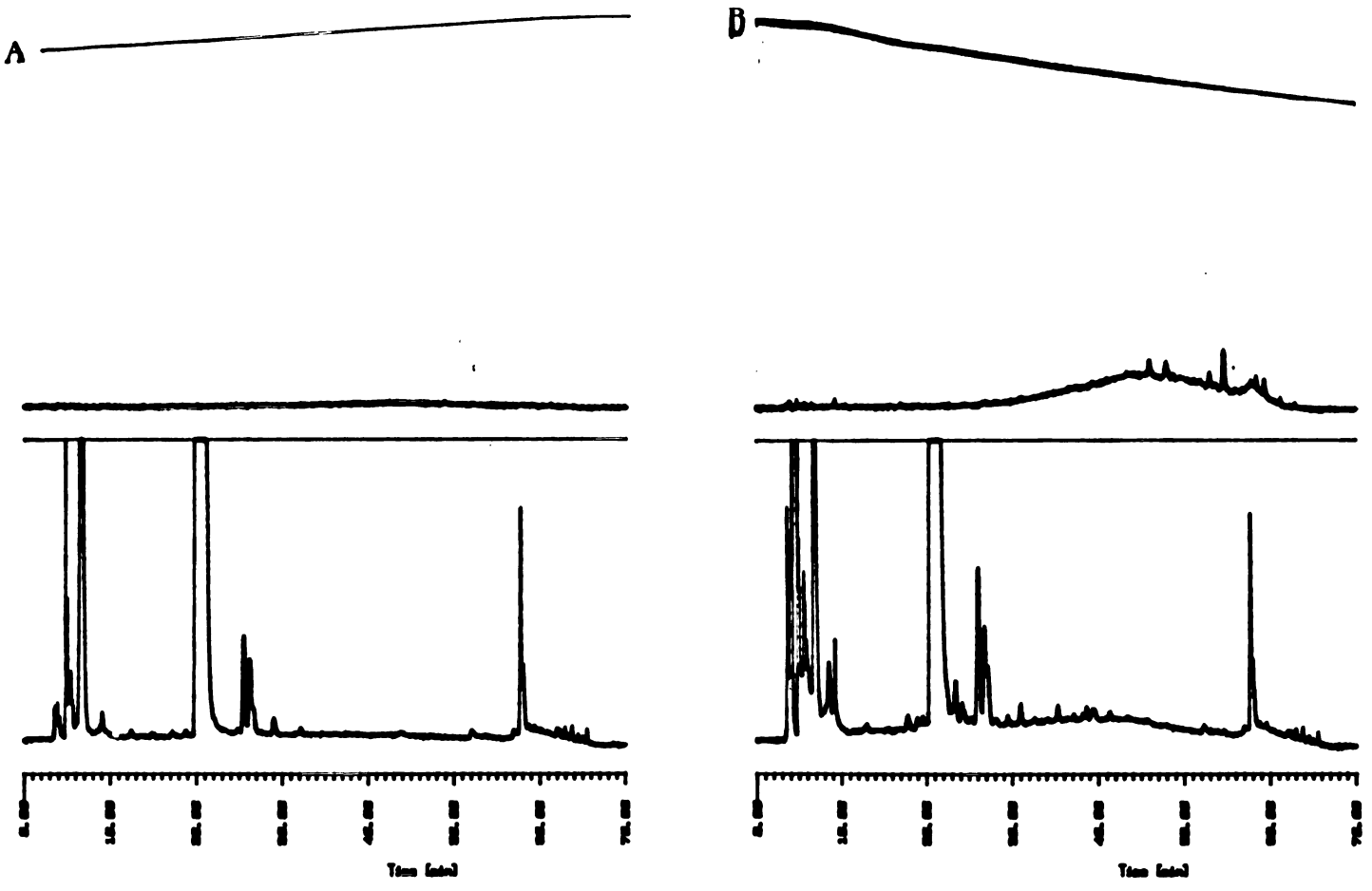

Figure 3.28. The HPLC Chromatograms of Pronase Digested Horse Myoglobin: Peroxide-Treated (B) and Non-Treated Control (A). Absorbance was Simultaneously Monitored at 398 nm (upper trace) and 280 nm (lower trace). The Acetonitrile/Water Gradient System Described in Chapter 5 was Used.

Hydrogen Peroxide Oxidation of Meso-Heme Reconstituted Horse Myoglobin. Addition of hydrogen peroxide to horse myoglobin reconstituted with meso-heme results in spectral changes (Figure 3.29, trace a) similar to those observed with proto-myoglobin (trace b) except all the maxima are slightly blue-shifted. The hypochromic red shift of the Soret band and changes in the visible region of the spectrum again suggest the presence of a ferryl heme prosthetic group (Fe^{IV}=O). The electronic absorption spectrum of the apoprotein obtained after removal of meso-heme is given in Figure 3.30, trace A. The ratio of the Soret band to the 280 nm absorbance for the peroxide treated meso-myoglobin apoprotein is within experimental error of that for the non-peroxide treated control, indicating that peroxide dependent cross-linking of meso-heme to the protein does not occur. Approximately 8% residual heme is observed in the peroxide-treated proto-myoglobin apoprotein, in agreement with previous results (see Table 3.1). Unfortunately, there was a similar amount of residual heme in the non-peroxide treated proto-myoglobin apoprotein control (Figure 3.30, trace b).

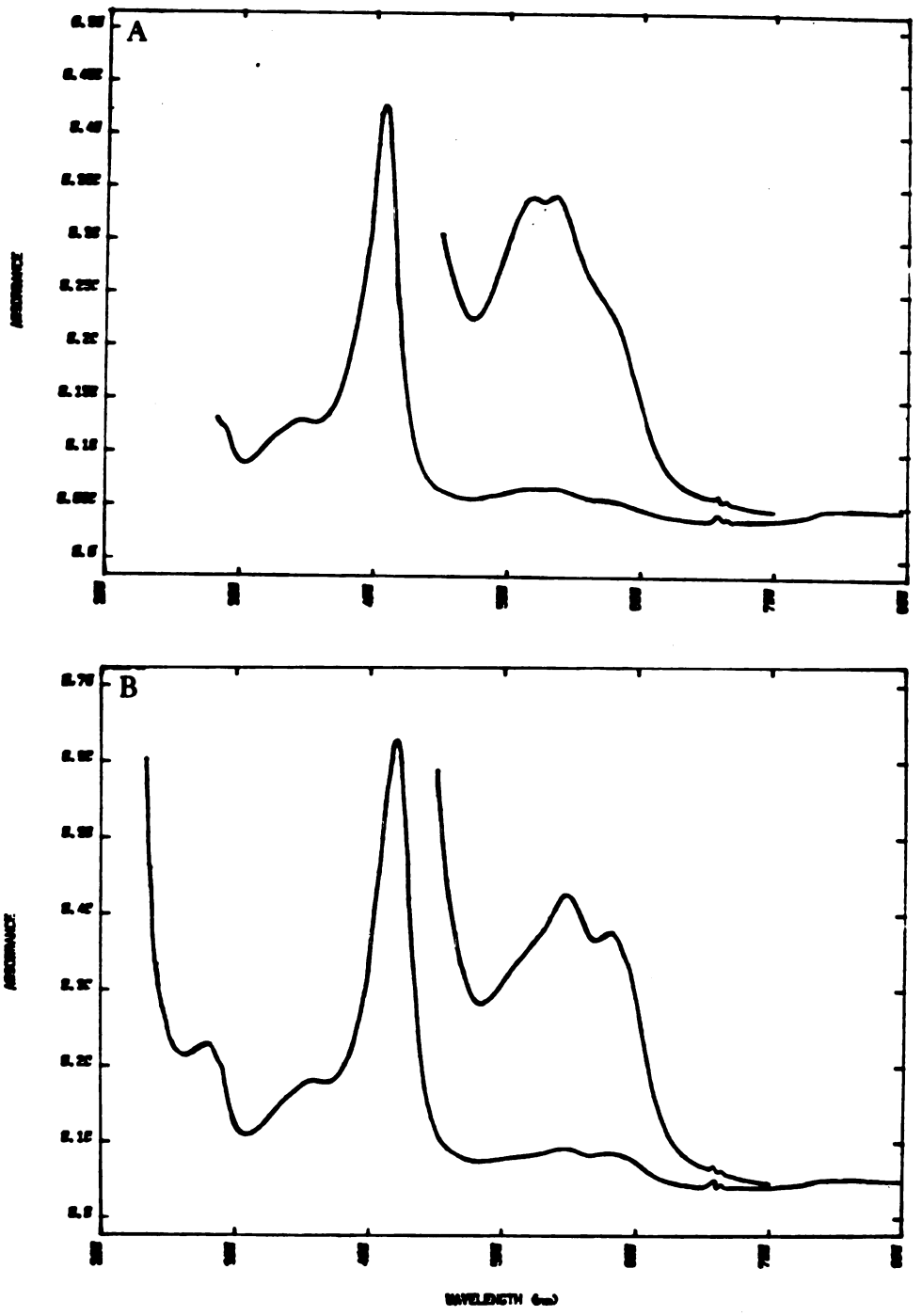

Figure 3.29. The Electronic Absorption Spectra of Hydrogen Peroxide Treated Meso-Heme Reconstituted (A) and Proto-Heme Reconstituted (B) Horse Myoglobins.

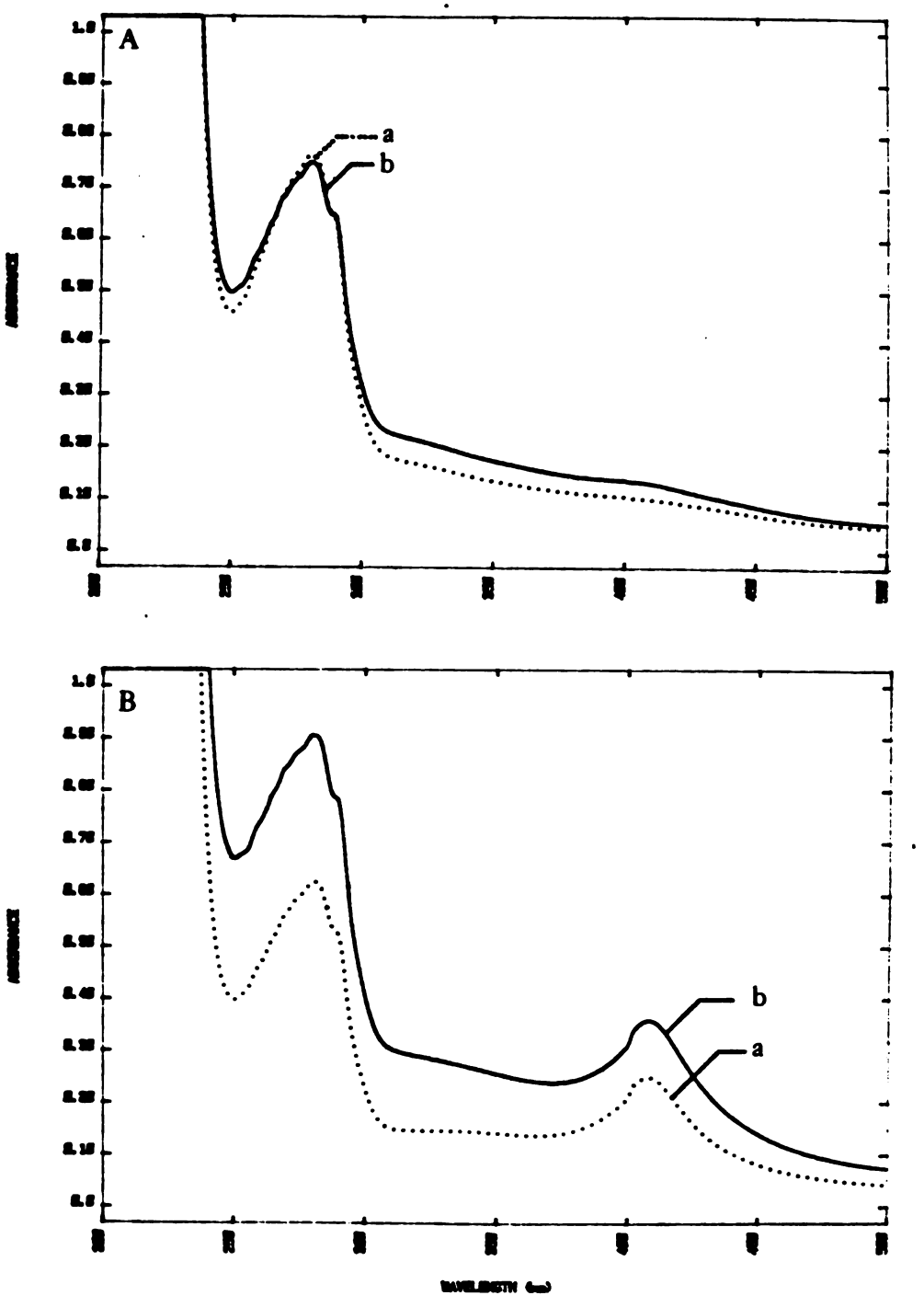

Figure 3.30. The Electronic Absorption Spectra of the Apoproteins Resulting From Heme Extraction of Meso-Heme Reconstituted (A) and Proto-Heme Reconstituted (B) Horse Myoglobins. Trace b, Peroxide Treated and Trace a, Non-Treated Control.

Chapter 4 Discussion of Results

Substrate Oxidation by Hemoglobin and Myoglobin

Styrene Oxidation

The products of the oxidation of styrene by hemoglobin and hydrogen peroxide are styrene oxide and benzaldehyde (Figures 2.2 and 2.3). The interaction of hemoglobin with H_2O_2 results in bleaching of the heme chromophore (Figure 2.1) and the time course for this spectral loss parallels that for product formation (Figure 2.5). These data, combined with the strict requirement for both peroxide and hemoglobin in the oxidation process (Table 2.1), provide strong support for a hemoprotein mediated reaction.

The inhibitory effect of KCN and the inability of CO to inhibit the oxidative event (Table 2.1) suggest that iron in the ferric but not ferrous oxidation state is required at some point in the reaction pathway. The lack of stereoselectivity in the oxidation of styrene (Figure 2.13) demonstrates free access to both the re and si faces of the olefinic bond and implies an unconstrained reaction environment. Superoxide and hydroxy radicals can be discounted as freely diffusible oxidizing agents by the inability of superoxide dismutase and mannitol,

respectively, to inhibit the epoxidation reaction (Table 2.1).

A mechanism for the oxidation of styrene to styrene oxide by hemoglobin and hydrogen peroxide consistent with the above data and analogous to that for cytochrome P450 mediated oxidations is presented in Scheme 4.1. In this scheme, interaction of hemoglobin with peroxide results in the removal of two oxidizing equivalents from the hemoprotein, one from the heme iron (Fe^{III} -> Fe^{IV}=O) and the second from an amino acid residue on the protein (R -> R^{o}). Attack of the ferryl oxygen on the olefinic bond yields an intermediate, the structure of which is still ambiguous, which collapses to the oxide product and the resting ferric hemoprotein. The requirement for a ferric hemoprotein and H_2O_2, and the inhibition by cyanide, are all accounted for by this scheme. The predicted incorporation of peroxide oxygen into the oxide product is also consistent with the experimental data. The inhibitory effects of ascorbic acid and BHT (Table 2.1) can be accounted for by reduction of the ferryl iron-oxo species to the unreactive ferric state (George and Irvine, 1952; Shiga and Imaizumi, 1973) but could also be due to interception of the radical intermediate.

The interaction of hemoglobin and myoglobin with hydrogen peroxide has been discussed in detail in chapter 1. Spectroscopic evidence (electronic, resonance Raman, nmr,

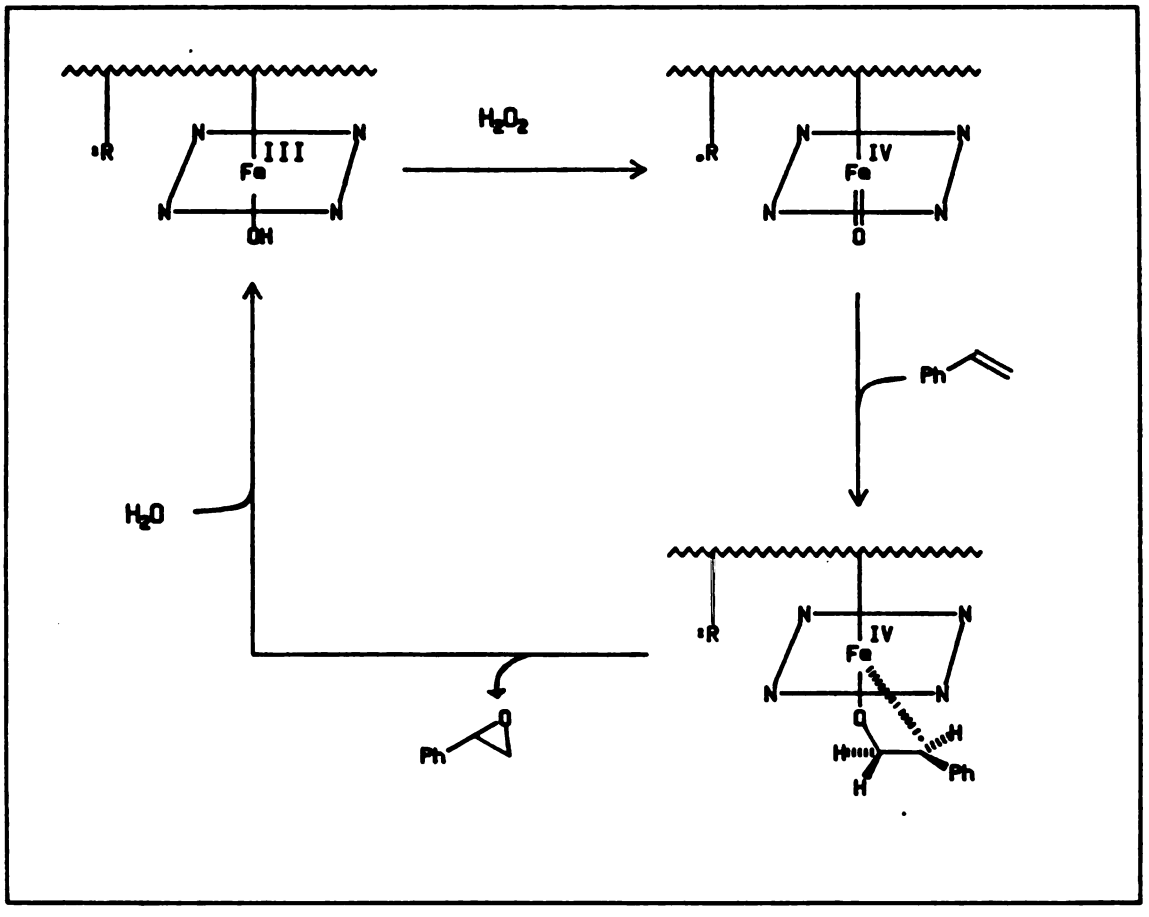

Scheme 4.1. Oxidation of Styrene by Hemoglobin and Hydrogen Peroxide: Direct Ferryl-oxygen Transfer Mechanism.

ESR, Mossbauer, etc.) supports the formation of a ferryl iron and an amino acid radical in the oxidized hemoprotein. The ESR studies done by King (1967) specifically suggest a tyrosine residue as the site of the protein radical.

Figure 4.1 shows the crystal structure coordinates for the heme prosthetic group and tyrosines 42 and 103 of equine methemoglobin and sperm whale metmyoglobin, respectively. With few exceptions (shark, platypus and red kangaroo myoglobins), there is an analogous tyrosine residue in the amino acid sequences of all the hemoglobins (chains) and myoglobins examined to date (Dayhoff, 1976; Dickerson and Geis, 1983). A phenylalanine residue invariably replaces the tyrosine in all of the hemoglobin chains and the myoglobin exceptions listed above. The distance between the heme prosthetic group and the tyrosine residue is shown by the crystal structures to be less than 4 Å (closest contact distances). It therefore seems likely that these are the tyrosine residues involved in radical formation.

A plethora of information exists in the literature on the one electron oxidation of phenols and the reactions of the resultant phenoxy radicals (see Taylor and Battersby, 1967). Carbon-carbon bond formation to yield ortho-ortho and ortho-para coupling products is typical of phenoxy radicals. Carbon-oxygen bond formation to give dimeric ethers does not occur under normal conditions. The

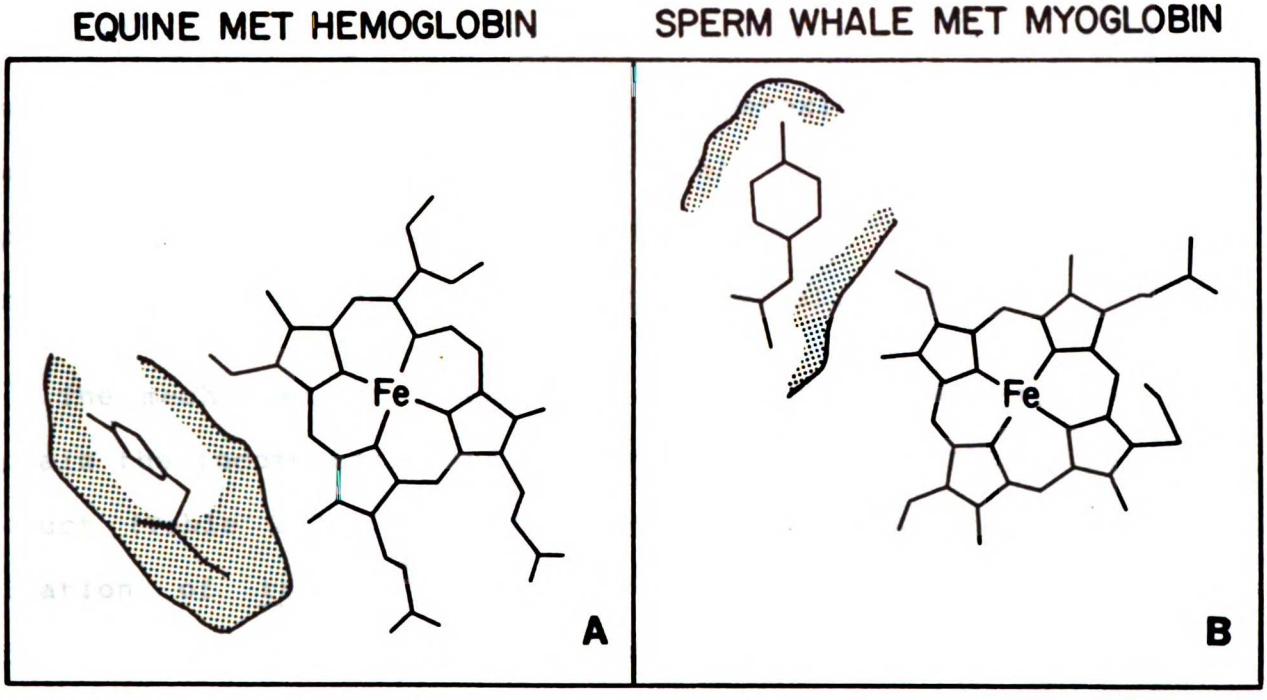

Figure 4.1. Relationship of Tyrosine 42 ∝ in the Crystal Structure of Equine Methemoglobin and Tyrosine 103 in the Crystal Structure of Sperm Whale Metmyoglobin to the Prosthetic Heme and the Protein Exterior.

mechanism for coupling of the phenoxy radicals is shown in Figure 4.2. With strong oxidizing agents, further oxidation of the dimeric phenols to diphenoquinones and higher polymeric products takes place. Phenoxy radicals have been detected by ESR spectroscopy in incubations containing phenols, methemoglobin and hydrogen peroxide (Shiga and Imaizumi, 1973), and dityrosine (3,3'-bis tyrosine) has been reported as a product of the oxidation of tyrosine by horseradish peroxidase and H_2O_2 (Yoshio et al., 1984).

The mechanism in Scheme 4.1 does little, however, to explain the incorporation of molecular oxygen into the oxide product (Table 2.3). The loss of stereochemistry in the oxidation of trans-[^{2}H]-styrene (Figure 2.10) is also difficult to reconcile both with the retention of stereochemistry observed with P450 epoxidations and with the congested nature of the heme binding pocket (chapter 1). Scheme 4.2 depicts a second mechanism for the epoxidation of styrene by hemoglobin consistent with the latter set of data. The interaction of hemoglobin with hydrogen peroxide yields the ferryl-oxo, amino acid radical species depicted in Scheme 4.1. Addition of molecular oxygen to the amino acid radical yields a peroxy radical that is capable of adding to the styrene olefinic bond. Radical ring closure yields the epoxide and, after electron transfer from the protein to the iron, a modified hemoprotein at the ferric oxidation state.

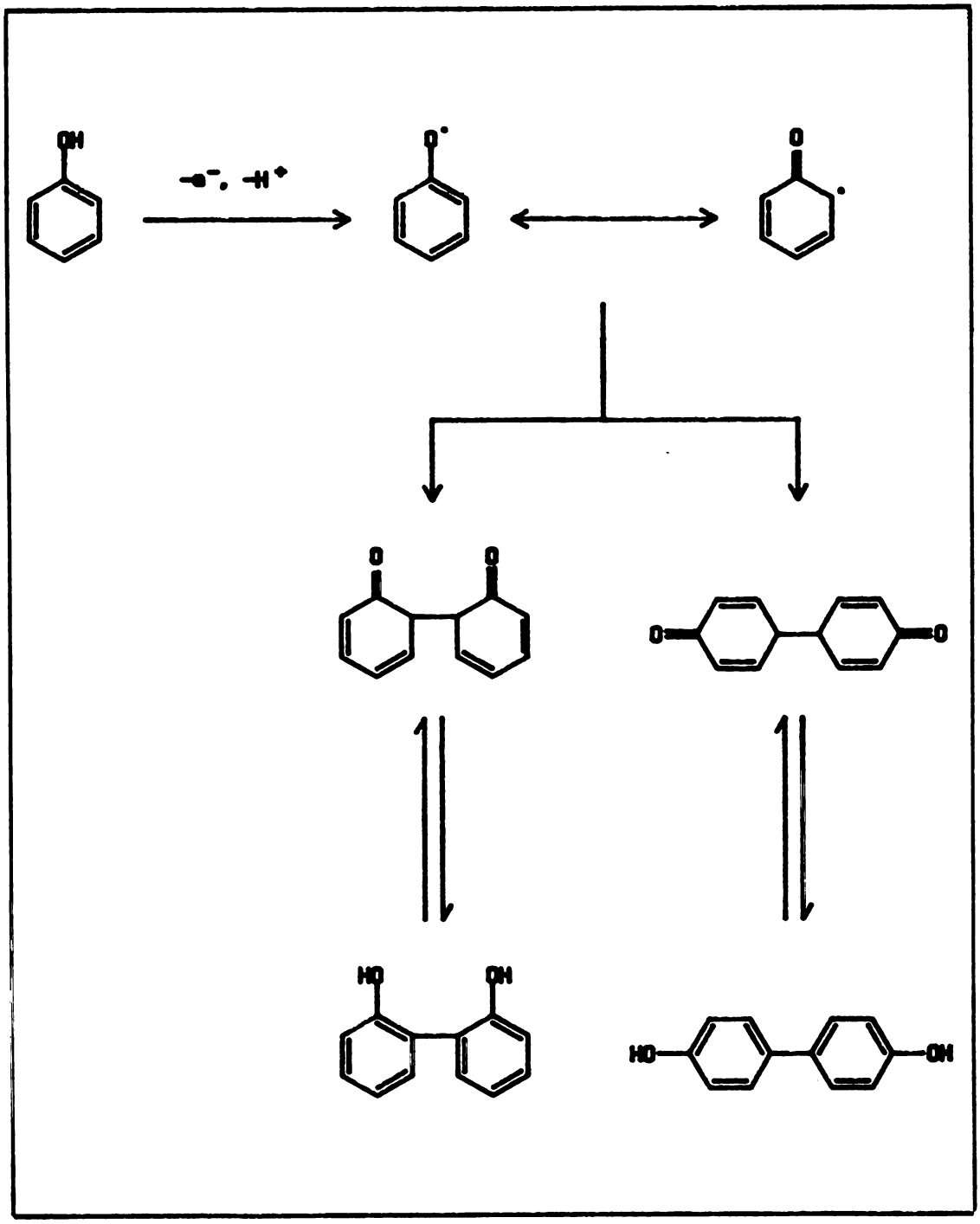

Figure 4.2. Mechanism for the Oxidative Coupling of Phenols.

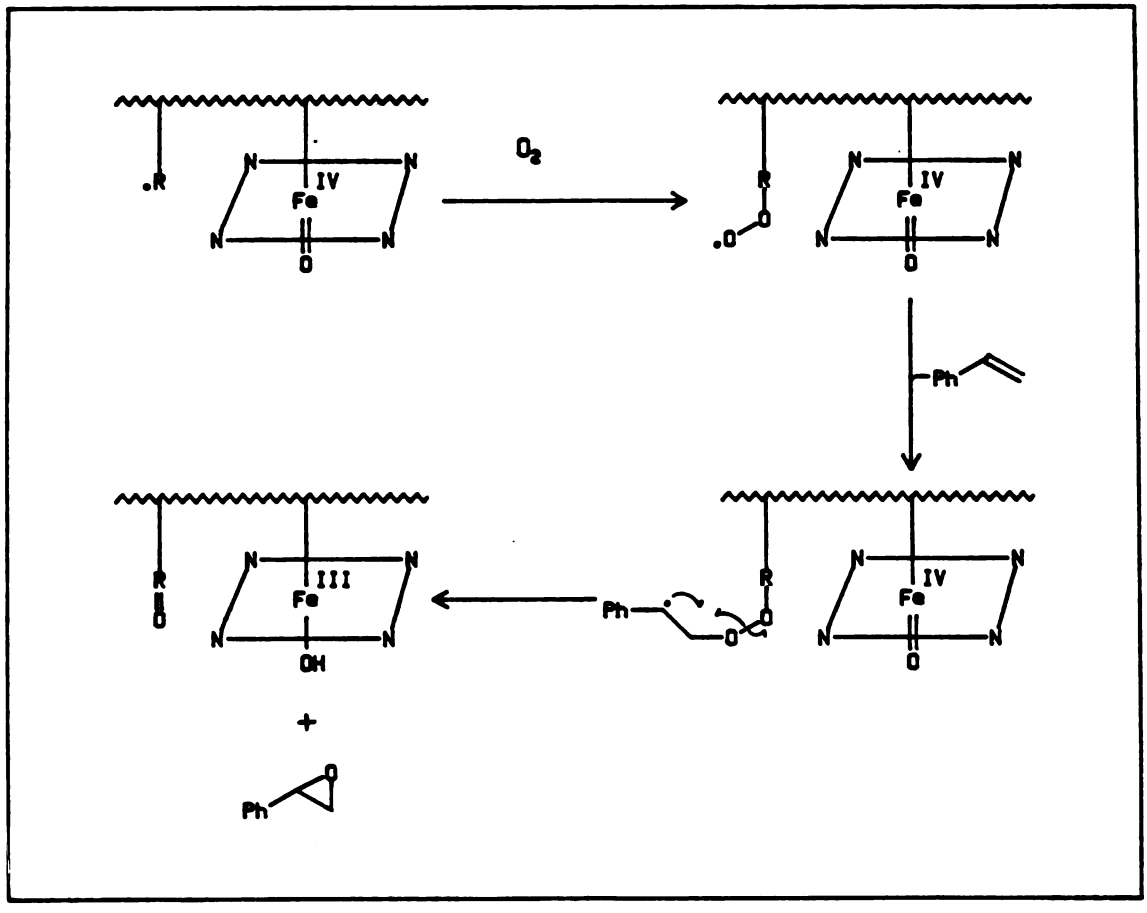

Scheme 4.2. Oxidation of Styrene by Hemoglobin and Hydrogen Peroxide: Cooxidation Mechanism.

Precedent exists in the literature for the formation of peroxy radicals by the addition of molecular oxygen to carbon centered radicals (Emanuel et al., 1984). This reaction, with reaction rates of up to 10^8 L/mol-sec being commonly reported, is very fast. The reaction of the phenyl radical with hexane or chloroform yields benzene and chlorobenzene, respectively (Russell et al., 1963), but the yields of these products are substantially reduced in the presence of oxygen due to a competing oxygen addition reaction. The ratio of k_o/k_x (Figure 4.3a) is 10^3 for the phenyl radical and 10^{10} for the benzyl radical. This difference in reaction rates was attributed to substantial ionic character in the transition state (Figure 4.3b) which places positive charge at the carbon radical site, an unfavorable situation for the phenyl radical.

The literature is replete with examples of olefin epoxidation by peroxy radical intermediates. Strong evidence exists for the cooxidation of 7,8-dihydroxy-7,8-dihydrobenzo(a)pyrene to 7,8,9,10-tetrahydroxy-7,8,9,10-tetrahydrobenzo(a)pyrene (presumably via the diol-epoxide intermediate) by lipid peroxy radicals formed during the oxidation of arachidonic acid by prostaglandin H synthase (Marnett et al., 1979; Sivarajah et al., 1979), by lipid peroxy radicals formed during the decomposition of lipid peroxides by hematin (Dix et al., 1985) and by lipid peroxy radicals formed during lipid peroxidation (Dix and Marnett, 1983). Styrene cooxidation to styrene oxide has been

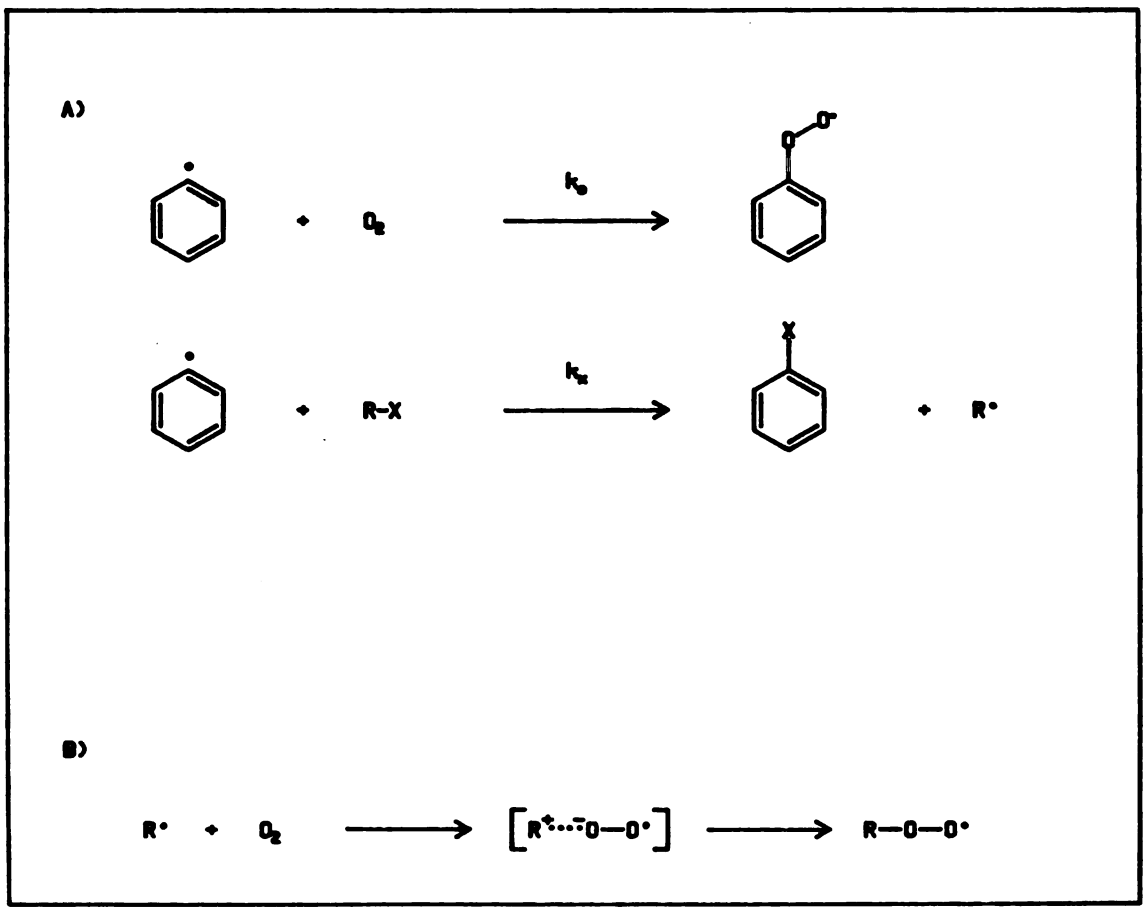

Figure 4.3. A) Reaction of the Phenyl Radical with Oxygen or Another Substrate (R-X: hexane or chloroform, see text). B) Reaction of Radicals with Oxygen Demonstrating a Polar Transition State.

reported during the lipoxygenase mediated oxidation of arachidonic acid, again presumably through the intermediacy of lipid peroxy radicals (Belvedere et al., 1983). Peroxy radicals other than those derived from lipids have also been identified as oxidizing agents. A phenylbutazone peroxy radical has been proposed as the oxidizing agent in the cooxidation of 7,8-dihydroxy-7,8-dihydrobenzo(a)pyrene by prostaglandin H synthase and phenylbutazone (Reed et al., 1984). The peroxy radical intermediate formed in the reaction of CCl_4 and superoxide (Cl_3COO°) has been invoked as the species responsible for the epoxidation of several aryl and alkyl olefins (Yamamoto et al., 1986). Finally, a glutathione peroxy radical has been proposed as the oxidizing agent in the epoxidation of styrene by glutathione, horseradish peroxidase and hydrogen peroxide (Ortiz de Montellano and Grab, 1986).

Most germane to this discussion is the peroxide dependent cooxidation of styrene to styrene oxide in a model system composed of horseradish peroxidase and cresol (Ortiz de Montellano and Grab, 1987). Data presented in this work provide strong evidence for one electron oxidation of the phenol by the peroxidase followed by interception of the carbon radical by oxygen to form a peroxy radical and subsequent oxidation of the olefin. A general scheme for phenol mediated peroxy radical epoxidation of olefins is shown in Scheme 4.3.

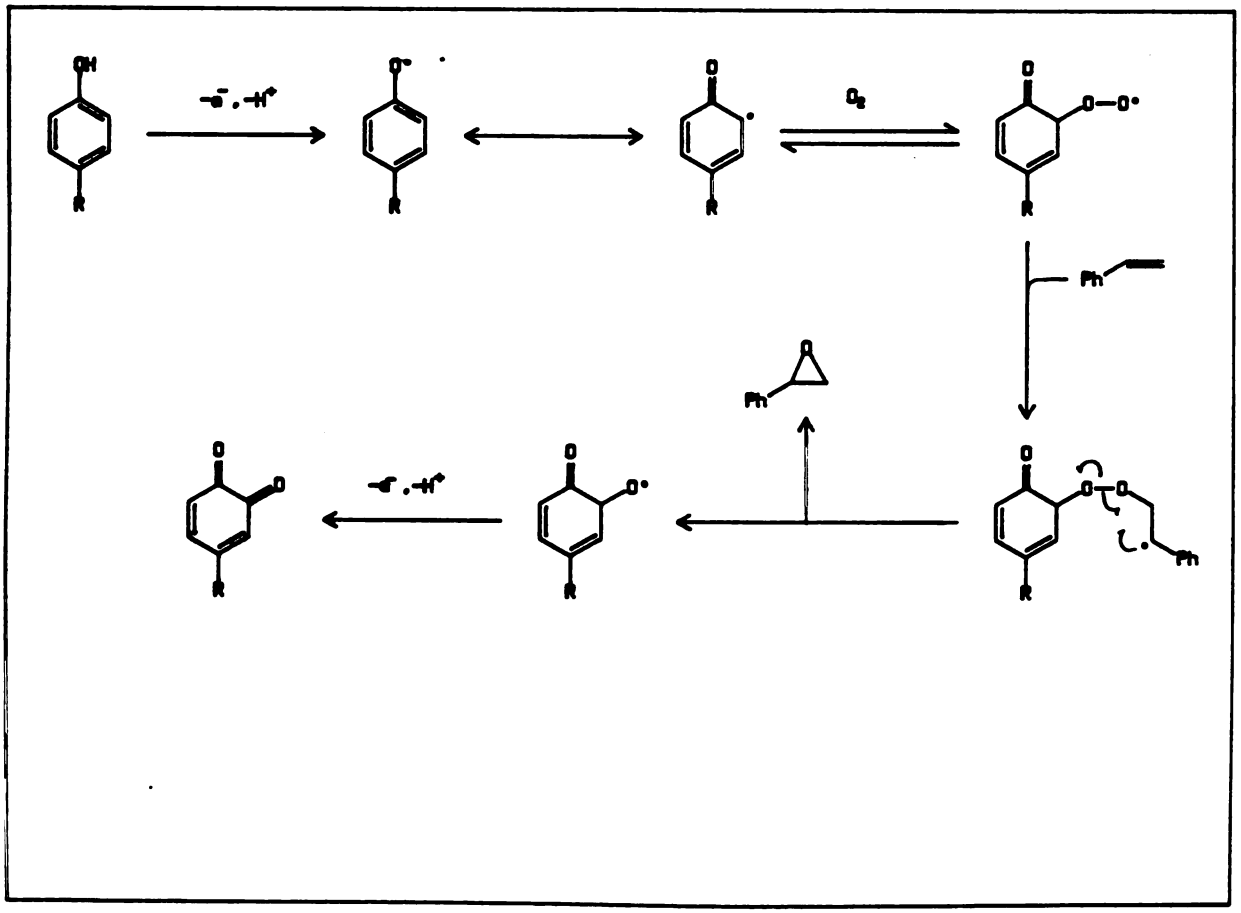

Scheme 4.3. Oxidation of Styrene by a Tyrosine Peroxy Radical Species.

The fact that only partial loss of stereochemistry is observed in the oxidation of trans-[^{2}H]-styrene (Figure 2.10), and that molecular oxygen is only partially incorporated into the oxide product, suggest that both the P450-like mechanism (vide supra) and the protein peroxy radical mechanism may be operative in the oxidation process.

Styrene oxide and benzaldehyde formation exhibit similar hemoprotein (Figure 2.5), peroxide (Figure 2.6) and styrene (Figure 2.7) dependencies. Several hemoprotein mediated mechanisms for benzaldehyde formation can be envisioned. The first is shown in Scheme 4.4. A hemoprotein-mediated one electron oxidation of the olefin yields the radical cation intermediate. Addition of molecular oxygen to the carbon radical followed by one electron reduction and ring closure then yields the dioxetane that decomposes to benzaldehyde and formaldehyde. The decomposition of dioxetanes to the corresponding aldehydes has been amply described in the literature (see Waldemar and Cilento, 1983). A similar mechanism has been invoked in the formation of adamantylideneadamantane dioxetane from the constant potential electrolysis of adamantylideneadamantane (Clennan et al., 1981), in the formation of benzaldehyde from the reaction of 1,2-dibromo-1,2-diphenylethane with superoxide (Calderwood and Sayer, 1984) and in the formation of benzaldehyde from the photosensitized oxidation of stilbene (Lopez and Calo, 1984).

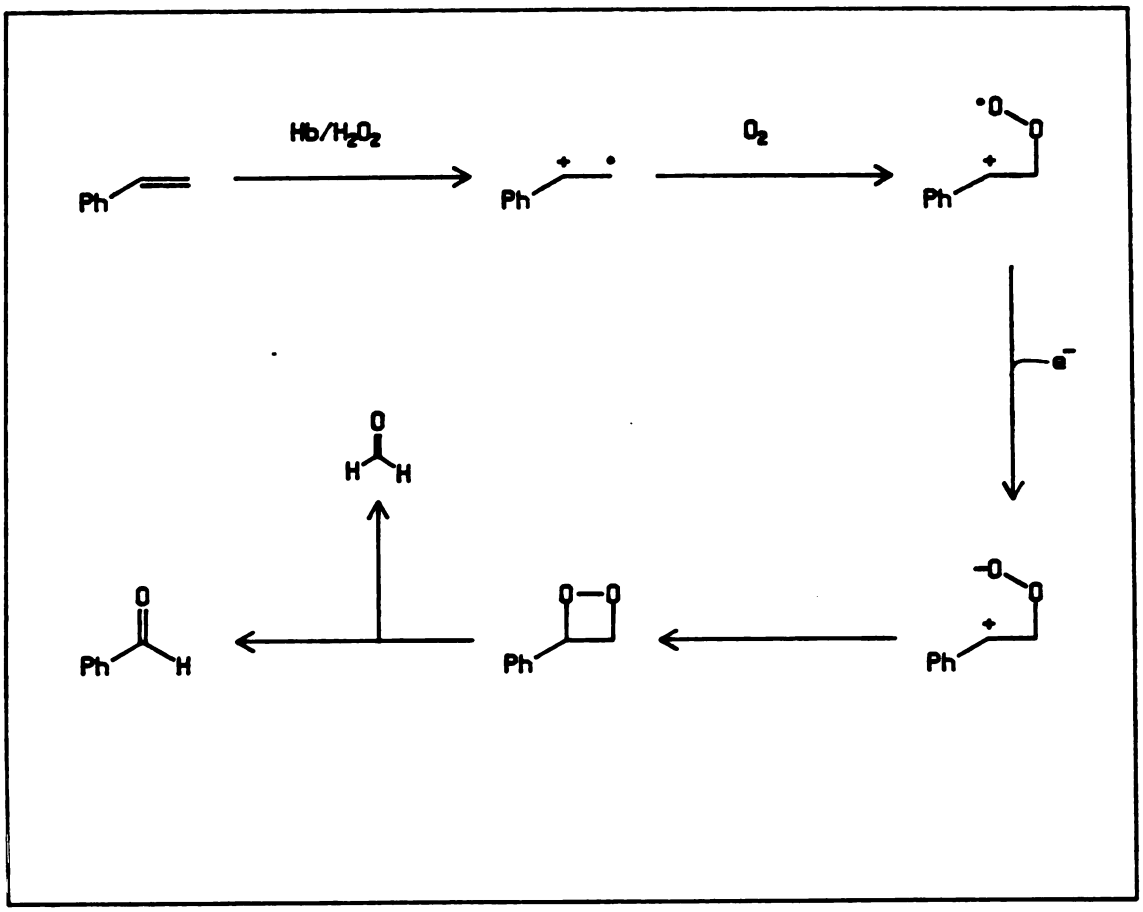

Scheme 4.4. Formation of Benzaldehyde by Hemoglobin and Hydrogen Peroxide: Radical Cation Pathway.

Another route to the aldehyde, depicted in Scheme 4.5, path a, follows closely that for oxide formation (Scheme 4.2). This route depends on radical ring closure of the peroxy-styryl radical intermediate to give the four membered dioxetane ring rather than the three membered epoxide. Decomposition of the dioxetane to the aldehydes then proceeds as above.

A third radical mechanism for the formation of benzaldehyde is shown in Scheme 4.5, path b. In this mechanism, the peroxy-styryl radical intermediate adds a second molecule of oxygen to the carbon centered radical before ring closure occurs. Reduction of the peroxy radical yields the peroxide which then dehydrates to yield the requisite benzaldehyde product. This mechanism is attractive because the addition of molecular oxygen to the styryl radical formed during the polymerization of styrene has been reported to be at a rate of 4×10^7 l/mol/sec (Miller and Mayo, 1956).

All of the mechanisms discussed above involve free radical intermediates. The latter two require a peroxy-styryl radical intermediate that partitions between epoxide and aldehyde formation. Examination of Table 2.1, however, reveals a divergence in the effects of inhibitors on the formation of styrene oxide and benzaldehyde. A decrease is observed in the yield of the oxide when POBN, a radical trap, is added to the incubation mixture, whereas the

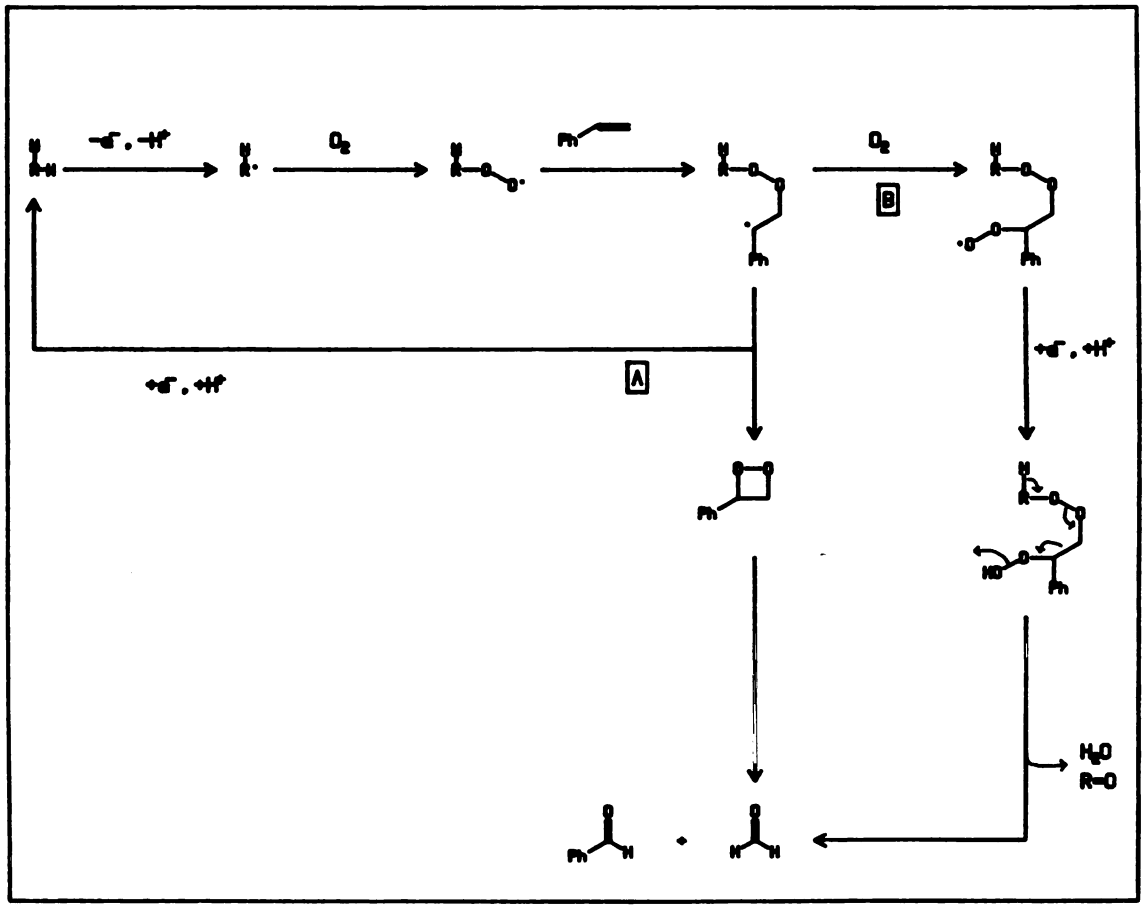

Scheme 4.5. Formation of Benzaldehyde by Hemoglobin and Hydrogen Peroxide: Peroxy Radical Pathways.

aldehyde yield is unaffected. Conversely, DABCO, a singlet oxygen scavenger, attenuates benzaldehyde formation without affecting the styrene oxide yield. These data suggest that a mechanism involving singlet oxygen rather than a radical intermediate might be responsible for the formation of benzaldehyde by hemoglobin and H_2O_2. Oxidation of styrene to benzaldehyde by singlet oxygen would proceed as depicted in Scheme 4.6. Singlet oxygen insertion into double bonds followed by decomposition of the resulting 1,2-dioxetanes to the corresponding aldehydes has been amply documented in the literature (ibid; Jefford et al., 1978).

Singlet oxygen has been observed in the reaction of hydrogen peroxide with myeloperoxidase (Khan, 1984), chloroperoxidase (Khan et al., 1983; Kanofsky, 1984a) and lactoperoxidase (Khan, 1983). The formation of singlet oxygen by these hemoproteins requires halide ions and most likely contributes to the antimicrobial activity of these enzymes (Marnett et al., 1986). Catalase, a H_2O_2 detoxification enzyme, does not generate singlet oxygen (Kanofsky, 1984b). Chemiluminesence is observed when hydrogen peroxide is added to hemoglobin (Cadenas et al., 1980) and it is enhanced by adding styrene to the incubation mixture (Cadenas, personal communication). The source for the chemilumenescence, however, has not been conclusively determined.

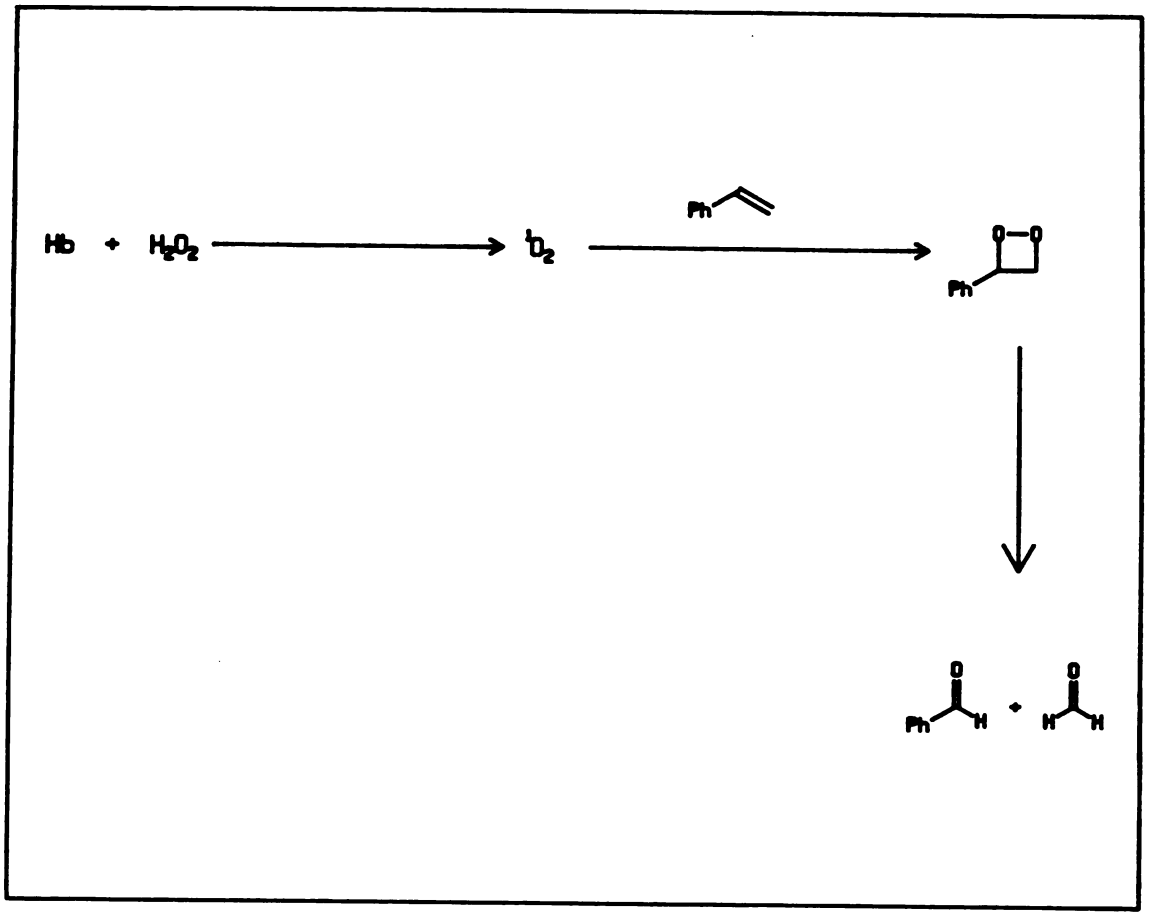

Scheme 4.6. Formation of Benzaldehyde by Hemoglobin and Hydrogen Peroxide: Singlet Oxygen Pathway.

All of the mechanisms for benzaldehyde formation discussed above result in the formation formaldehyde. All of the mechanisms, except for path b of Scheme 4.5, would also exhibit chemiluminescence from decomposition of the dioxetane intermediate, from singlet oxygen emmision, or from both. The present data are insufficient to determine which of these mechanistic pathways is responsible for benzaldehyde formation.

trans-7,8-Dihydroxy-7,8-dihydrobenzo(a)pyrene Oxidation

The products formed from trans-7,8-dihydroxy-7,8-dihyrobenzo(a)pyrene (BAPD) by hemoglobin and hydrogen peroxide are the anti-trans isomer of 7,8,9,10-tetrahydroxy-7,8,9,10-tetrahydrobenzo(a)pyrene (BAPT) and the anti-trans isomer of 10-methoxy-7,8,9-trihydroxy-7,8,9,10-tetrahydrobenzo(a)pyrene (methoxy-BAPT) (Figure 2.14). These products are the expected hydrolysis and methanolysis products, respectively, of the anti-trans isomer of 7,8-dihydroxy-9,10-oxy-7,8,9,10-tetrahydrobenzo(a)pyrene (BAP diol-epoxide). These data provide strong evidence that the anti-diol epoxide is the sole product of the oxidation of BAPD by hemoglobin.

The extent of peroxide oxygen incorporation into the tetrol product (Table 2.6) is slightly higher than that observed in the hemoglobin-mediated oxidation of styrene to styrene oxide (Table 2.3). In sharp contrast to the

oxidation of styrene, however, molecular oxygen is NOT incorporated into the BAPT product. The less than complete incorporation of peroxide oxygen, and the negligible incorporation of molecular oxygen into the tetrol, require involvement of the solvent in part of the oxidation process.

The mechanisms depicted in Scheme 4.7 for the hemoglobin catalyzed oxidation of BAPD account for the available data. Reaction of hemoglobin with hydrogen peroxide produces a ferryl-oxo species plus an amino acid radical, as already described. Attack of the iron-bound oxygen on the exocyclic double bond (path a) yields a transient intermediate that collapses to the diol-epoxide product. Alternatively, one electron oxidation of the exocyclic double bond yields a radical cation intermediate (path b). Addition of water to the cation, followed by a second one electron oxidation, yields a cationic triol that either deprotonates to yield the diol-epoxide or adds water to yield the tetrol directly.

Formation of an amino acid peroxy radical species as proposed for styrene oxidation must also occur in these incubations. Access to this radical by BAPD must be restricted, however, if the lack of incorporation of molecular oxygen into the product is to be explained.

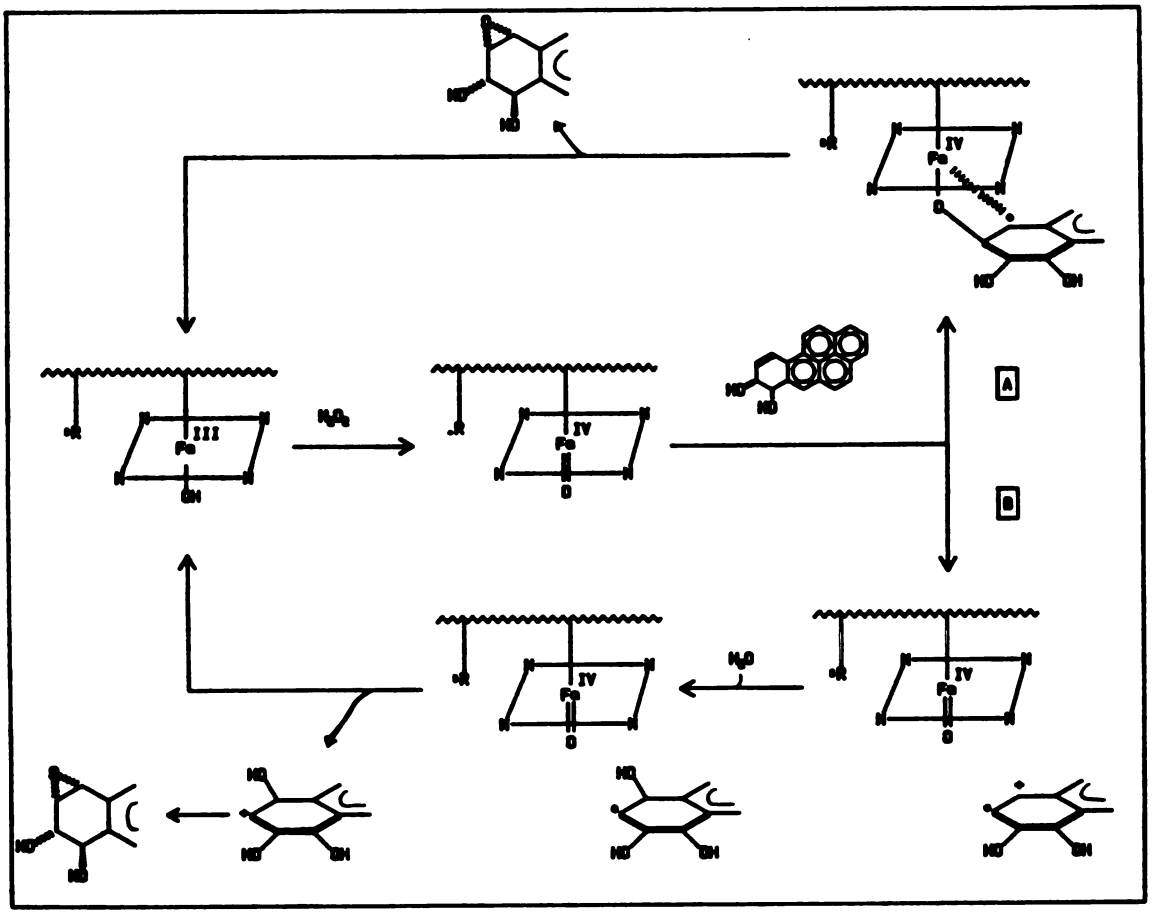

Scheme 4.7. Oxidation of 7,8-Dihydroxy-dihydrobenzo(a) pyrene by Hemoglobin and Hydrogen Peroxide.

Stilbene Oxidation

Trans-stilbene is oxidized to trans-stilbene oxide, and cis-stilbene to both of the isomeric epoxides, by hemoglobin and hydrogen peroxide (Figures 2.21 and 2.22). The quantitative incorporation of peroxide oxygen into the cis- and trans-stilbene oxides derived, respectively, from cis- and trans-stilbene (Table 2.10) suggests that both isomers of the olefin have free access to the heme-bound oxygen in the oxidized hemoprotein. These results can be rationalized by a mechanism, shown in Scheme 4.8 (path a), analogous to that postulated for the oxidation of styrene and BAPD by the hemoprotein ferryl-oxygen species (Schemes 4.1 and 4.7, path a).

Retention of stereochemistry in the oxidation of the cis isomer requires either a concerted oxygen transfer mechanism or an intermediate in which free rotation about the olefinic carbon-carbon bond is highly restrained. Two barriers to free rotation of a ferryl-oxo-stilbenyl intermediate can be envisioned. The first barrier is provided by the steric constraints imposed on the intermediate by the congested environment of the heme binding pocket (Chapter 1). Although substrates at least as large as substituted phenylhydrazines have been shown to gain access to the heme binding pocket (Kunze and Ortiz de Montellano, 1983; Ringe et al., 1984), NMR studies indicate that their motion within the heme pocket is highly

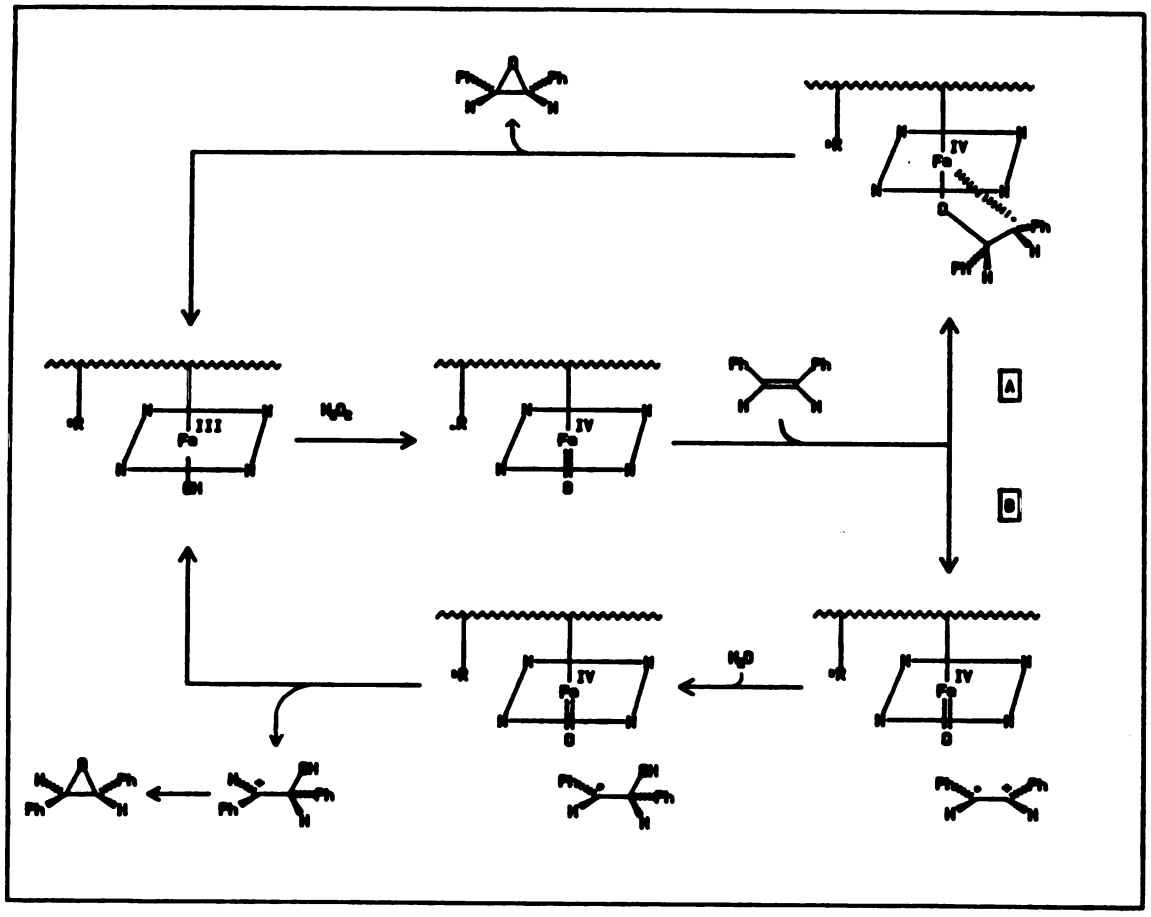

Scheme 4.8. Oxidation of Stilbenes by Hemoglobin and Hydrogen Peroxide.

restricted (Ortiz de Montellano and Kerr, 1985). The second possible barrier to rotation about the carbon-carbon bond is provided by interaction of the heme iron with the carbon to which oxygen is not bound (i.e., some degree of metallooxetane character in the the protein-bound stilbene intermediate) (Ortiz de Montellano, 1986). Such an interaction would prevent free rotation about the carbon-carbon bond and would therefore maintain stereochemical fidelity.

The inherent reactivity of the two stilbene isomers is comparable, as demonstrated by the similar rates of m-CPBA-mediated epoxidation of cis- and trans-stilbene (Groves and Nemo, 1983). Oxidation of olefins by metalloporphyrin model systems, however, always favors the cis isomer (ibid; Collman et al., 1984; Fontecave and Mansuy, 1984). This has been interpreted by Groves in terms of approach of the olefin to the iron-bound oxygen from the side, with the double bond parallel to the plane of the porphyrin, as shown in Figure 4.4. Cis olefins allow unrestrained approach of the double bond to the iron-bound oxygen whereas non-bonding interactions between the porphyrin macrocycle and the substituents of the trans olefins inhibit their oxidation.

Oxidation of stilbene by the hemoglobin iron-oxo species shows little stereoselectivity, both isomers being oxidized at approximately equal rates (Table 2.7). This suggests that both olefin isomers have equal access to the

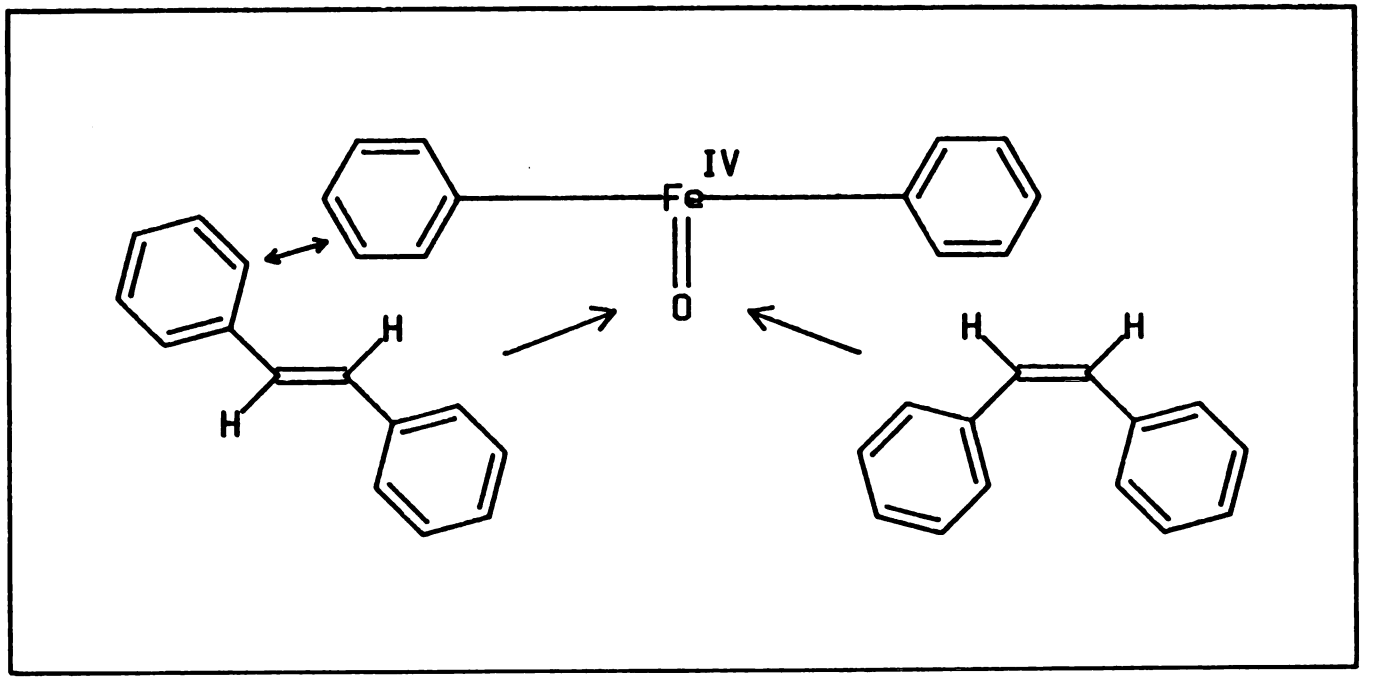

Figure 4.4. Approach of the Stilbene Isomers to a High-Valent Iron-Oxo Model Porphyrin. Non-Bonding Interactions Restrict the Approach of the <u>trans</u> isomer.

iron-bound oxygen of oxidized hemoglobin. These data, combined with the shape of the heme binding pocket (wide and flat, chapter 1) suggest that olefin approach to the iron-oxo species is end-on with the substituents parallel to the porphyrin plane, as shown in Figure 4.5.

Cis-stilbene is oxidized to trans-stilbene oxide by hemoglobin and hydrogen peroxide with less than 7% incorporation of peroxide oxygen (Table 2.10). Molecular oxygen is incorporated into approximately 32% of the oxide product. The incorporation of molecular oxygen into the trans-oxide product is proposed to occur in a mechanism analogous to that for the oxidation of styrene (Figure 4.2). The remaining oxygen in the trans-stilbene oxide product presumably derives from the solvent. Scheme 4.8 (path b) depicts mechanism for the hemoglobin-mediated oxidation of stilbene which is consistent with the incorporation of solvent oxygen. This is similar to the mechanism proposed for the oxidation of benzo(a)pyrene diol by hemoglobin (Figure 4.7, path b). Note that both the radical cation and peroxy radical oxidation pathways predict loss of stereochemistry during the oxidation process.

Linoleic Acid Oxidation

The oxidation of linoleic acid by hemoglobin and hydrogen peroxide results in the production of 13-hydroperoxy linoleic acid (Figure 2.28). Other minor

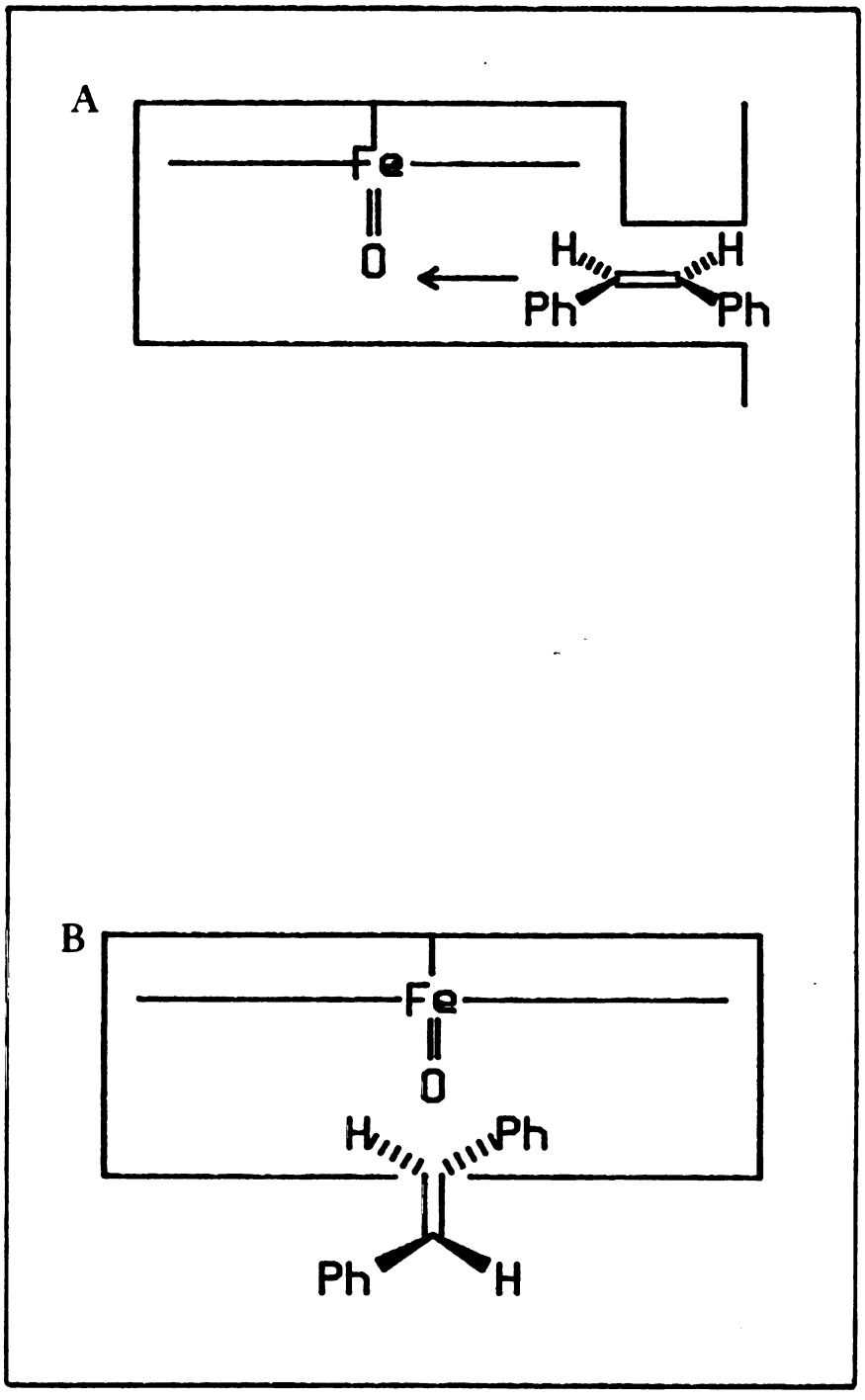

Figure 4.5. Approach of the Stilbene Isomers to the High-Valent Iron-Oxo Hemoglobin Species. Views are From the Side (A) and the Front (opening of the heme binding pocket, B).

products are observed in the incubation extracts but the peroxide is by far the major oxidation product.

It is clear from Figures 2.24 and 2.25 and Table 2.11 that oxygen is evolved in the interaction of hydrogen peroxide with hemoglobin. This oxygen evolution is clearly attenuated when linoleic acid is added to the incubation mixture, suggesting that oxygen is consumed during the oxidation of the fatty acid.

These data are consistent with the radical chain mechanism presented in Scheme 4.9 for the oxidation of linoleic acid by hemoglobin and hydrogen peroxide. This scheme is a simple lipid peroxidation mechanism with hemoglobin functioning to initiate the radical chain reaction.

A small fraction of the peroxide- and globin-dependent products have retention times similar to those of the isomeric epoxides (Figure 2.28). The amount of material was not sufficient for unambiguous structural identification, however, so the formation of linoleic acid epoxides must remain speculative.

Miscellaneous Substrate Oxidations

The hemoglobin-dependent oxidation of a variety of compounds utilizing a number of complex oxidation systems has been discussed in detail in chapter 1. The possibility

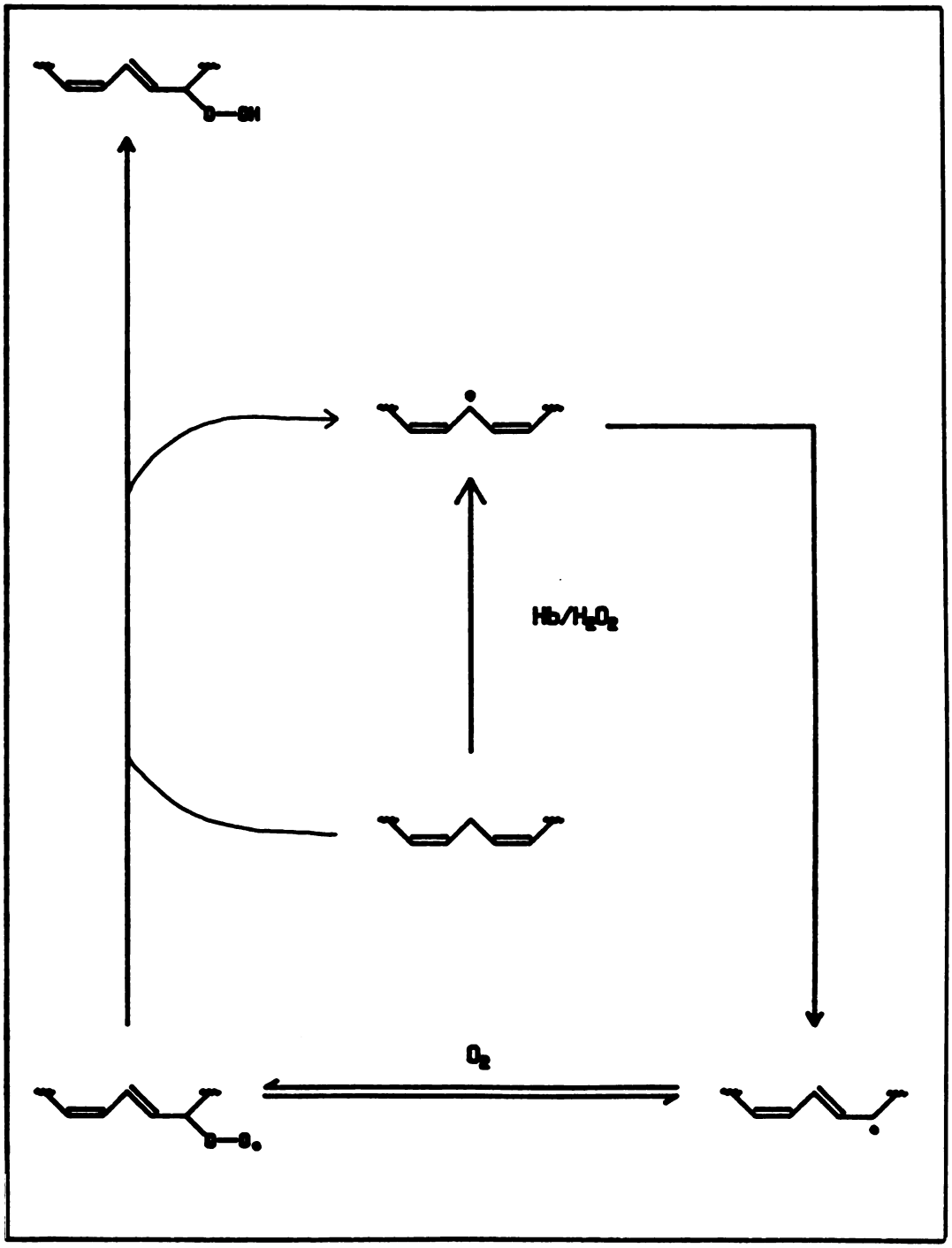

Scheme 4.9. Oxidation of Linoleic Acid by Hemoglobin and Hydrogen Peroxide.

that methemoglobin plus hydrogen peroxide formed *in situ* constitute the actual oxidizing system in the complex systems has also been discussed. The scope of the simple hemoglobin plus hydrogen peroxide system was therefore surveyed briefly by examining the representative reaction types shown in Figure 2.30.

The p-hydroxylation of aniline (Figure 2.31) and the N-dealkylation of N-methyl aniline (Figure 2.32) catalyzed by hemoglobin and hydrogen peroxide demonstrate that this simple system catalyzes the reactions attributed to the more complex systems (Starke et al., 1984). The reported O-dealkylation of p-anisidine by hemoglobin (ibid), however, was not observed under the conditions utilized in this study. It is possible that any p-aminophenol formed in the incubation mixture is further oxidized by hemoglobin to polymeric products. The formation of a highly colored, ether extractable product was observed in each of the incubations discussed above is consistent with this proposal. The oxidation of phenols and aromatic amines by horseradish peroxidase produces similar highly colored products that have been identified as oxidized dimers of the starting material (Saunders et al., 1964).

Substrate Oxidation Summary

The initial intent of this study was to evaluate the hemoglobin/hydrogen peroxide system as a model for cytochrome P450 oxidations. The data presented demonstrates that hemoglobin, like P450, oxidizes a number of olefins to the corresponding epoxides. These reactions are listed in Table 4.1 along with the product yields. Horse myoglobin also oxidizes the olefins to the same products but with attenuated yields (Table 4.1).

Table 4.1. Epoxide Yields from Met-Hemoglobin and Horse Met-Myoglobin Oxidation of Olefins

Substrate	Product	Yield[a]	
		Hemoglobin	Myoglobin[b]
Styrene	styrene oxide	35	12
trans-Stilbene	*trans*-stilbene oxide	1.0	0.13
cis-Stilbene	*cis*-stilbene oxide	0.7	0.3
	trans-stilbene oxide	0.18	0.05
BAPD[c]	BAPT[d]	0.05-0.1	0.01-0.03

[a]nmol/ml/30 min. [b]Estimated from relative yields. [c]BAPD, 7,8-dihydroxy-7,8-dihydrobenzo(a)pyrene. [d]BAPT, 7,8,9,10-tetrahydroxy-7,8,9,10-tetrahydrobenzo(a)pyrene.

The hemoglobin catalyzed oxidation of styrene to styrene oxide, the most thoroughly characterized of these reactions, is, at least in part, radical in nature. The

incorporation of molecular oxygen into the epoxide prompted the proposal that the reaction proceeds through a protein-bound peroxy radical intermediate (Scheme 4.2). These data, in conjunction with the congested environment surrounding the heme, led to the proposal that the peroxy radical was located at the surface of the protein rather than inside the crampt heme crevice. The position of an almost invariant tyrosine residue located simultaneously less than 4 Å from the heme edge and on the outer surface of the known globins supports this proposal.

The oxidation of trans-7,8-dihydroxy-7,8-dihydrobenzo (a)pyrene was examined in a search for additional support for the peroxy radical mechanism proposed for hemoglobin-catalyzed olefin oxidation. This compound was chosen with the assumption that access to the heme binding pocket would be restricted due to the steric bulk of the substrate. Additionally, oxidation of the racemic trans-diol exclusively to the anti-trans tetrol has been used as evidence that a peroxy radical mechanism is responsible for the oxidation (Dix and Marnett, 1983). The oxidation of (±) trans-BAPD to the anti-trans isomer of BAPT by hemoglobin and hydrogen peroxide thus appeared to provide prima facie evidence that the proposed radical mechanism was correct. The source of oxygen in the tetrol product, however, contradicts this conclusion. Most surprising is the incorporation of peroxide oxygen into the product (Table 4.2). This requires that there be substantial mobility in

the protein structure such that compounds as large as 7,8-dihydroxy-7,8-dihydrobenzo(a)pyrene can gain access to the heme binding pocket.

Table 4.2. Source of Oxygen in Hemoprotein Dependent Oxidations

Substrate	Percent Incorporation of ^{18}O-Oxygen			
	Bovine Hemoglobin		Horse Myoglobin	
	$^{18}O_2$	$H_2{}^{18}O_2$	$^{18}O_2$	$H_2{}^{18}O_2$
Styrene	38	46	78	16
trans-Stilbene	-	105	-	100
cis-Stilbene				
cis-oxide	1.4	101	<1	107
trans-oxide	32	<7	<1	-
BAPD	<5	66	<1	50

The lack of incorporation of molecular oxygen into the tetrol product was also unexpected (Table 4.2). The putative peroxy radical must be formed under these conditions but must be unavailable to the diol. The results are essentially the same when horse myoglobin is used in place of hemoglobin (Table 4.2).

The oxidation of *cis*- and *trans*-stilbene by hemoglobin yields results intermediate between those obtained with

styrene and BAPD. The data indicate that the oxidation of trans-stilbene occurs with complete incorporation of peroxide oxygen. Cis-stilbene oxidation occurs with retention of stereochemistry in 80% of the oxide product (see Table 4.1) and peroxide is the sole source of oxygen for this fraction of the reaction. The loss of stereochemistry observed in 20% of the oxide product itself argues that a radical mechanism is responsible for this part of the oxidation. This is supported by the fact that molecular oxygen (32% of the trans oxide, 6.4% of the total oxide product) is incorporated, presumably via the peroxy radical mechanism proposed for the oxidation of styrene (Scheme 4.2). The apparent incorporation of solvent oxygen argues, as does the analogous observation in the oxidation of BAPD, for a radical cation intermediate. The results of all the oxygen incorporation studies are summarized in Table 4.2.

The data are consistent with the three distinct olefin epoxidation mechanisms summarized in Scheme 4.10. The first mechanism (path a) involves direct oxygen transfer from the high valent iron-oxo species within the heme binding pocket. The retention of stereochemistry in the oxide product argues that either 1) the intermediate is radical in nature but cannot rotate about the carbon-carbon single bond due to steric barriers within the active site or 2) the intermediate possesses some degree of metallooxetane character which maintains stereochemical fidelity throughout

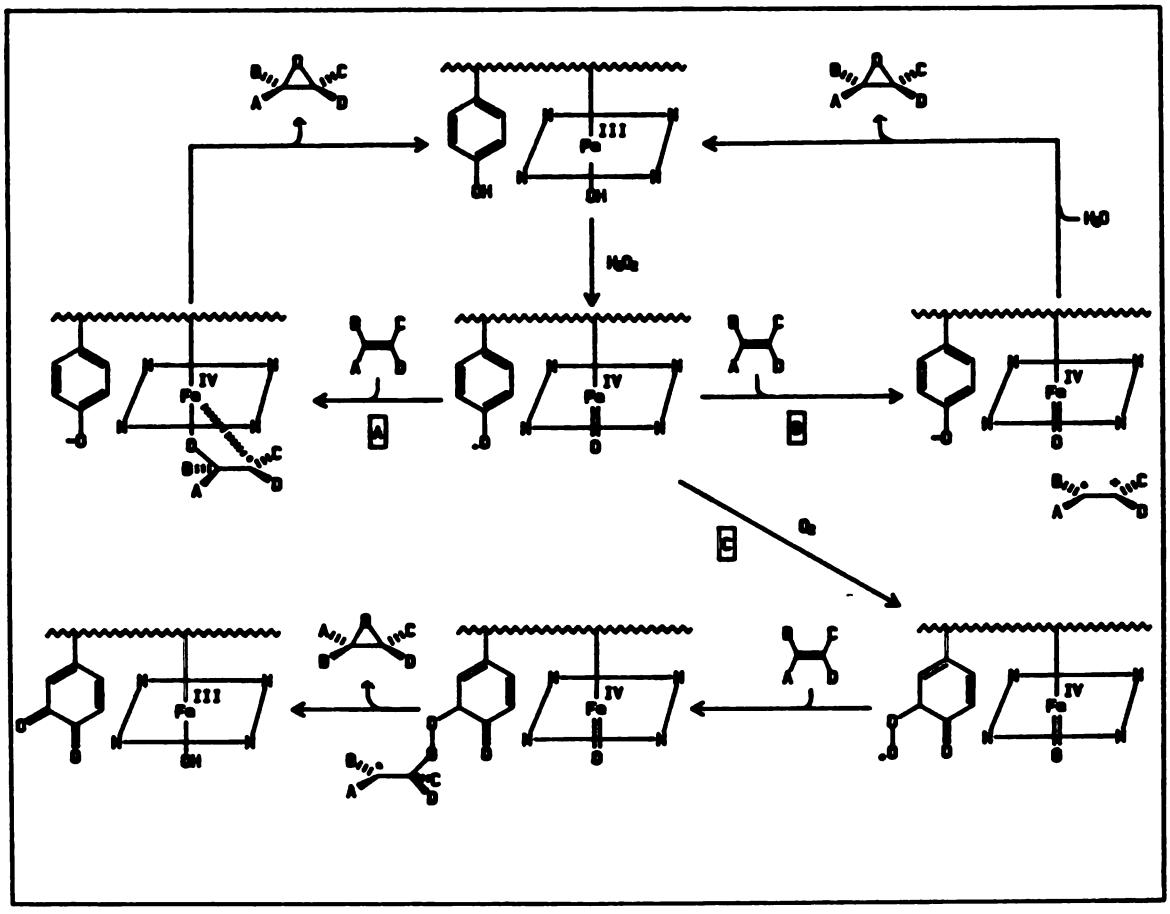

Scheme 4.10. Summary of the Mechanisms of Peroxide-Dependent Hemoglobin-Mediated Olefin Oxidation.

the reaction pathway (vide supra). This path represents a monooxygenase type mechanism and is analogous to those mediated by cytochrome P450. The details of oxygen transfer, however, necessarily differ due to differences in the electronic configuration of the two oxidized hemoproteins. The reactions of hemoglobin and myoglobin with peroxide yield a ferryl-oxo, protein radical intermediate, whereas P450 probably yields a ferryl-oxo, porphyrin radical cation similar to that of horseradish peroxidase Compound I (Chapter 1). Ferryl oxygen transfer from P450 to a substrate terminates with the protein in the ferric state (Figure 4.6, a). Similar oxygen transfer from the globins to a substrate would yield a ferrous heme, protein radical intermediate (Figure 4.6, b). Electron transfer from the heme iron to the amino acid radical returns the protein to the resting ferric state. Alternatively, electron transfer from the ferryl iron to the protein radical might occur during the oxidation process (Figure 4.6, c). A third alternative is that the reaction of peroxide with the globins produces a transient two electron oxidized intermediate, similar to that in P450, that partitions between protein and olefin oxidation. The last mechanism requires that either the olefin oxidation be very fast or that the intermediate constitute a small component in an equilibrium mixture because no species other than the ferryl-oxo, protein radical is detected. The

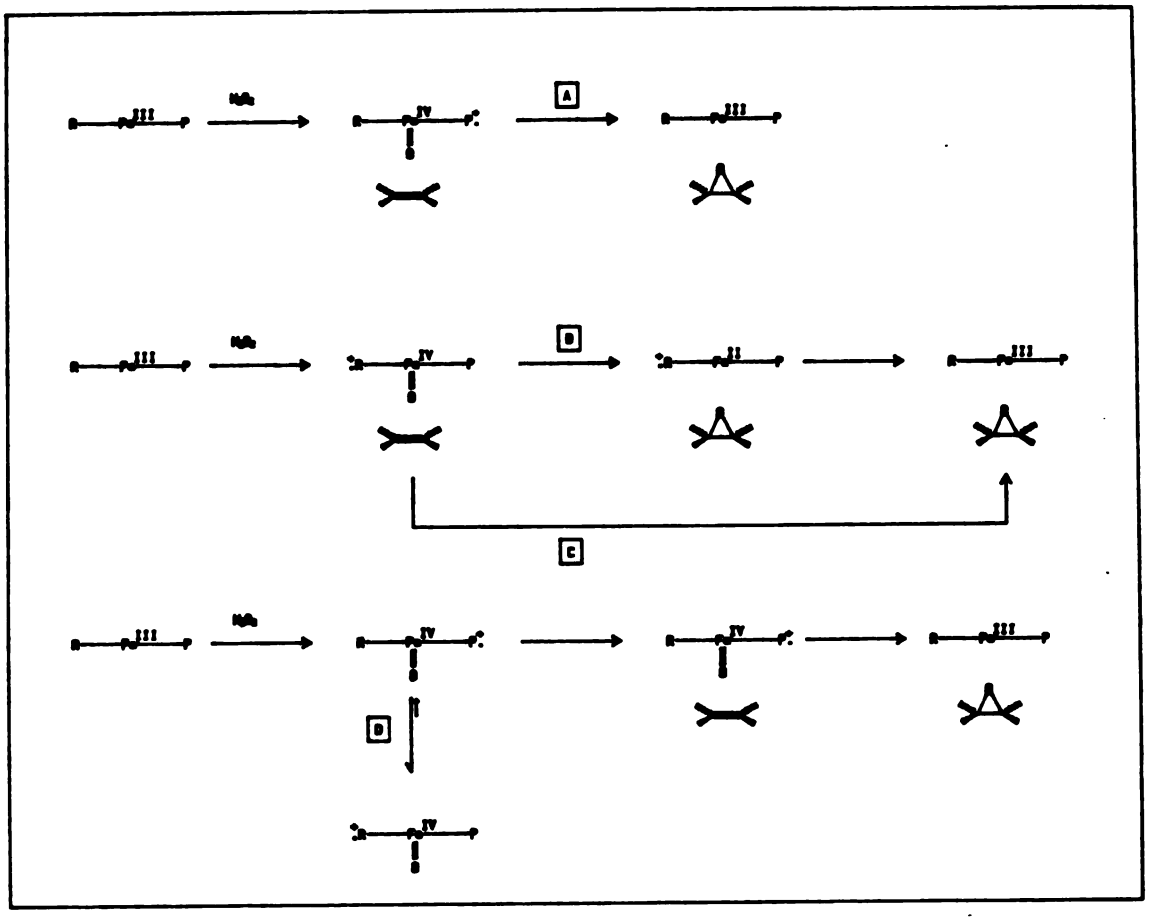

Figure 4.6. Alternate Mechainsms for Direct Oxygen Transfer From a High-Valent Iron-Oxo Protein Intermediate. $R^{+}\bullet$, a Protein Amino Acid Radical Species; $P^{+}\bullet$, a Porphyrin Radical Species. See Text for Details.

available data do not allow a distinction to be made between the ferryl oxygen transfer mechanisms.

The second epoxidation reaction (Scheme 4.10, path b) proceeds through a radical cation intermediate. This pathway begins with one electron oxidation of the substrate by the oxidized hemoprotein in a peroxidase-like mechanism similar to that proposed for the oxidation of a variety of substrates by hemoglobin (see chapter 1). The data suggest that the epoxidation of stilbene via this route occurs without dissociation of the radical cation intermediate from the protein because substantial amounts of benzaldehyde and trans-stilbene might otherwise be expected from the oxidation of cis-stilbene (Heimbrook et al., 1986). The absence of these products suggests that water adds to the radical cation and a second oxidation takes place before the substrate departs from the active site.

A third mechanism must be invoked in the hemoglobin mediated oxidation of olefins to explain the incorporation of molecular oxygen into the oxide product. A novel mechanism involving a protein-bound peroxy radical (path c) as the oxidizing species is proposed and is consistent with all of the data presented.

The significance of each of these mechanistic pathways can be estimated from the data in Tables 4.1 and 4.2 and is shown in Tables 4.3 and 4.4 for hemoglobin and myoglobin, respectively. What factors influence which pathway

Table 4.3. Significance of Each Mechanistic Pathway in the Oxidation of Olefins by Hemoglobin

Substrate	Iron-oxo[a]	Peroxy Radical[b]	Radical Cation[c]
	relative %		
Styrene	46	38	(16)
BAPD	66	<5	(29)
trans-Stilbene	100	-	-
cis-Stilbene	81[d]	6	(11)

[a]Determined from incorporation of peroxide ^{18}oxygen into the product. [b]Determined from incorporation of molecular ^{18}oxygen into the product. [c]Estimated from exclusion. [d]Determined from the relative yields of cis and trans oxides and peroxide oxygen incorporation into the trans oxide.

Table 4.4. Significance of Each Mechanistic Pathway in the Oxidation of Olefins by Horse Myoglobin

Substrate	Iron-oxo[a]	Peroxy Radical[b]	Radical Cation[c]
	relative %		
Styrene	16	78	(6)
BAPD	50	<1	(49)
trans-Stilbene	100	0	(0)
cis-Stilbene	86[d]	<1	(13)

[a]Determined from incorporation of peroxide ^{18}oxygen into the product. [b]Determined from incorporation of molecular ^{18}oxygen into the product. [c]Determined by exclusion. [d]Determined from the relative yields of cis and trans oxides and peroxide oxygen incorporation into the trans oxide.

predominates in the oxidation of a substrate? The initial hypothesis was that the putative peroxy radical was located not in the congested heme binding pocket, but at the protein surface. This suggests that the radical species is in a highly hydrophilic environment (chapter 1) and might confine hydrophobic substrates to the oxidation pathways taking place inside the hydrophobic heme binding pocket. Table 4.5 lists the octanol/water partition coefficients for each of the olefin substrates utilized in this study. Log P for styrene and BAPD are not significantly different, indicating that they should partition similarly between a hydrophobic (the heme binding pocket) and hydrophilic (hemoprotein surface) environment. Moreover, the most hydrophobic substrate (stilbene) incorporates molecular oxygen to a small degree (Table 4.2). These data suggest that hydrophobicity, in a strict sense, does not play a major role in determining which oxidative pathway a substrate takes.

Table 4.5. Hansch Octanol/Water Partition Coefficients for Compounds Used in this Study

Substrate	log P[a]
Styrene	2.95
trans-Stilbene	4.81
cis-Stilbene	-
BAPD[b]	3.24

[a]Taken from Hansch and Leo, 1979. [b]BAPD, 7,8-dihydroxy-7,8-dihydrobenzo(a)pyrene, calculated by the method of Hansch and Leo (ibid, see chapter 5)

Tables 4.3 and 4.4 show that only styrene oxide incorporates molecular oxygen to any appreciable extent. This suggest that the peroxy radical is in a highly restricted environment. One possibility is that the radical is located at the protein surface, but within a small crevice which restricts substrate access. A second possibility is that the peroxy radical is located within the hydrophobic heme pocket.

The crystal structure of hemoglobin shows that TYR 42α is located near the rear of the heme binding pocket. In order to gain access to a peroxy radical located at this site, it would be necessary for a substrate to penetrate deeply into the pocket. Steric bulk should be the most critical factor in controlling such a reaction, with large bulky substrates having the least access to the radical species. In this light, it is of interest that the

importance of peroxy radical oxidation decreases in the order styrene >> cis-stilbene = BAPD > trans-stilbene (Table 4.3 and 4.4). It can be argued that the overall steric bulk for the end-on approach of each of these olefins increases in the same order (Figure 4.7).

A second factor which probably plays a part in determining the oxidation pathway is the ease of olefin oxidation. The oxidation potentials for the olefin substrates utilized in this study are shown in Table 4.6. No direct correlation between oxidation potential and oxidation pathway can be discovered from the limited data in this table. It is interesting, however, that styrene, with an oxidation potential of 2.1, is the only substrate that proceeds significantly through the peroxy radical pathway. It is difficult to dissect the electronic effects from the steric factors, however, since styrene is also the least sterically hindered of the olefin substrates.

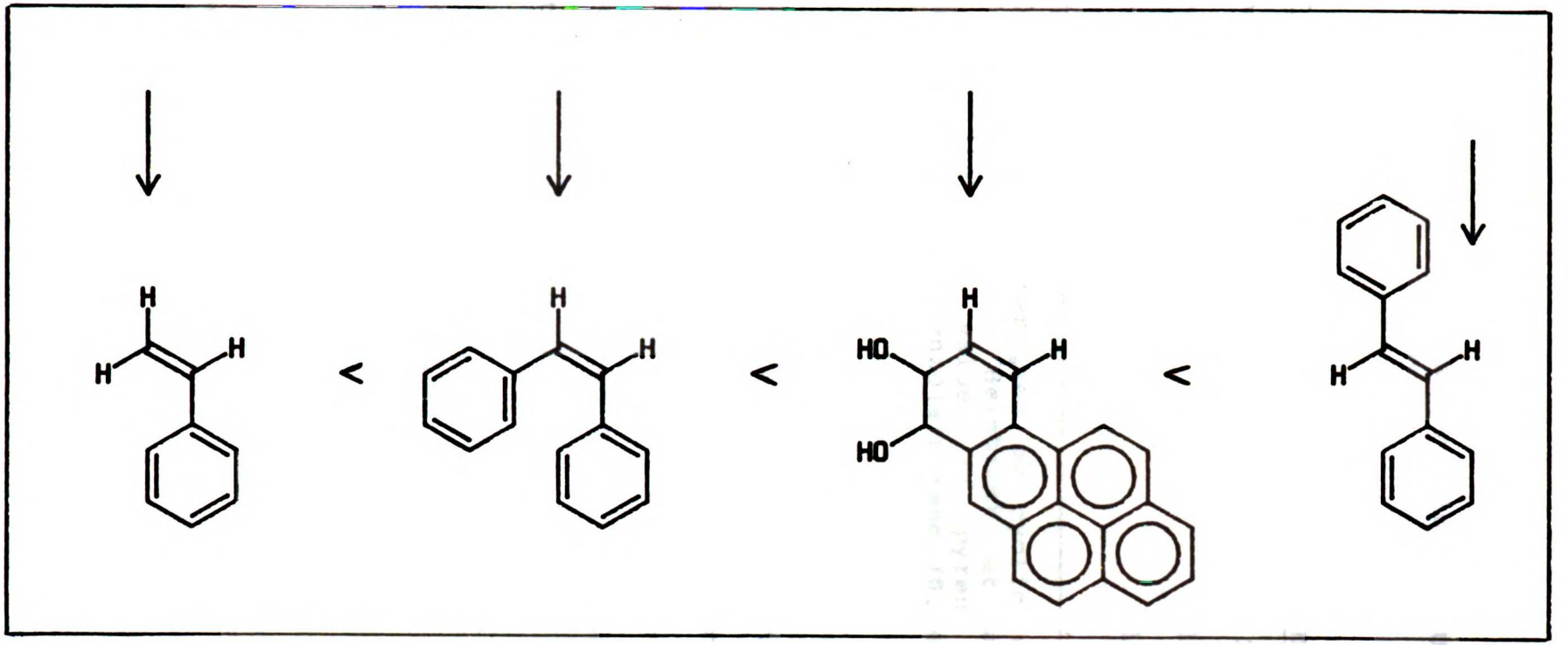

Figure 4.7. End-On Approach of an Oxidizing Species to the Olefinic Bond of the Substrates Utilized in this Study. The Substrates are Listed in Order of Increasing Steric Bulk About the End of the Olefinic Bond.

Table 4.6. Oxidation Potentials for Compounds Used in this Study

Substrate	$E_{1/2}$[a]
Styrene	2.1[b]
trans-Stilbene	1.51[c]
cis-Stilbene	1.54[d]
Benzo(a)pyrene-7,8-diol[e]	1.2-1.3

[a] $E_{1/2}$ (V) vs SCE. [b] Determined by cyclic voltammetry. [c] Taylor et al. (1984). [d] Heimbrook et al. (1986). [e] Estimated from the $E_{1/2}$ values of pyrene (1.16 V), benzo(e)pyrene (1.27 V) and benzo(a)pyrene (0.94) (Pysh and Yang, 1963)

The original purpose of this study was to validate the use of hemoglobin in P450 model systems. The results show that hemoglobin-mediated oxidations proceed, at least in part, through a ferryl oxygen transfer mechanism similar to that of cytochrome P450. Care must be taken when making mechanistic interpretations, however, because these data clearly demonstrate that hemoglobin posseses, in addition to monooxygenase activity, peroxidase and peroxy radical activities. The available data does not allow clear dissection of the factors that determine flux through a given pathway.

Horse Myoglobin Peroxide Induced Protein Damage

A protein-bound peroxy radical centered on a tyrosine residue has been proposed as an oxidant in the peroxide dependent oxidation of olefins by hemoglobin and myoglobin (vide supra). The proposed oxidation mechanism shown in Figure 4.2 predicts the modification of at least one amino acid residue. The loss of tyrosine content upon peroxide treatment of hemoglobin and myloglobin from various species has been reported (Rice et al., 1983) but the nature of the loss was not determined. Examination of the crystal structure coordinates for sperm whale myoglobin shows TYR 103 at a distance of 4 Å from the heme edge. It seems likely that the analogous tyrosine is the residue that is lost upon oxidation of horse myoglobin.

Heme extraction from peroxide treated horse myoglobin results in the unexpected observation that approximately 10% of the prosthetic heme remains covalently bound to the protein (Figure 3.6). Amino acid analysis (Table 3.2) reveals a 50% decrease in the tyrosine content with peroxide treatment. The loss of tyrosine content thus parallels that observed by Rice (ibid), although the serine and histidine losses reported in the earlier studies were not seen under the conditions used in this study. It is probable that this difference is due to the much higher (40X) peroxide concentrations utilized in the earlier study.

Peak A (Figure 3.9) derived from the tryptic digestion of both control and hydrogen peroxide treated horse myoglobin is unambiguously identified as peptide #17 (Table 3.3) by its amino acid analysis (Table 3.4), mass spectrum (Figure 3.11) and N-terminal sequence. It is of some interest that this peptide, which is not eluted from the HPLC column until a high concentration (>95%) of acetonitrile is reached, is one of the relatively insoluble "core peptides" (Lorkin, 1974).

Peroxide treatment of the hemoprotein decreases the concentration of peak A and results in concomitant appearance of a set of closely spaced peptides, collectively called the "heme-peptide" (Figure 3.9). The amino acid composition of the heme-peptide is within experimental error of that for peptide A except for the loss of serine and virtual disappearance of tyrosine. The HPLC chromatograms reveal that most of the heme chromophore (398 nm) coelutes with the heme-peptide (Figure 3.9). The electronic spectrum of the heme-peptide is consistent with the presence of an intact heme group (Figure 3.17, C: 398 (S), 498 (V), 536 (IV), 586 (III), 630 (II) and 728 nm (I)) and an aromatic amino acid (271 nm). The molecular ion of the heme-peptide is 2504 mass units, consistent with attachment of heme (616.5 mass units) to peptide A (1884 mass units). Two attempts to determine the N-terminal sequence were unsuccessful, however.

These data unambiguously identify TYR 103 as the tyrosine that is lost in peroxide-treated horse myoglobin. Peroxide treatment of the hemoprotein results, in part, in covalent attachment of the heme prosthetic group to the apoprotein. The data suggest that the heme is attached to TYR 103 but do not prove it because the acid hydrolysis required to determine the amino acid composition could release the heme from other sites on the peptide. Pronase digestion of the peptide was attempted to circumvent this problem but no heme adducts were detected by HPLC analysis. Similarly, preparative isolation of either a modified heme or a modified amino acid proved fruitless. It is of interest in this respect that meso-heme reconstituted horse myoglobin does not form covalent cross-links to the peroxide treated hemoprotein. This suggests that one of the vinyl groups exocyclic to the porphyrin macrocycle, which are replace by ethyls in meso-heme, is the site of covalent attachment to the protein.

A proposed mechanism for the covalent attachment of heme to peptide #17 consistent with all the available data is shown in Scheme 4.11. The interaction of peroxide with the hemoprotein results in the formation of a ferryl-oxo species and a tyrosine amino acid radical. The support for this intermediate has been summarized above and in chapter one of this thesis. Radical attack on the exocyclic double bond of the porphyrin macrocycle followed by oxidation to the cation by the electron transfer to the ferryl iron and

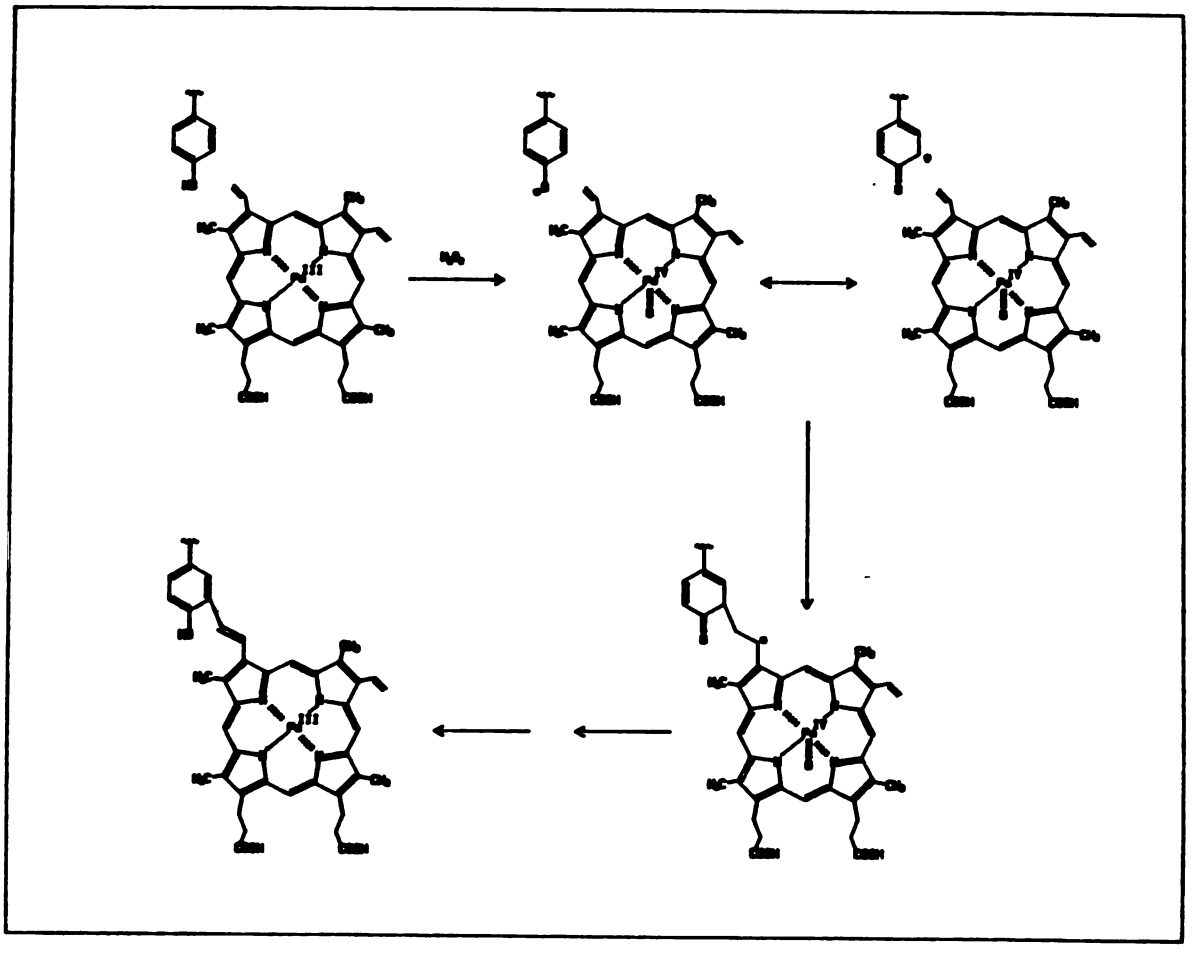

Scheme 4.11. The Mechanism for the Peroxide-Dependent Covalent Attachment of Heme to Horse Myoglobin Apoprotein.

deprotonation would yield the final structure shown in the scheme. Other possibilities exist for the attacking radical or the fate of the initial heme adduct. For example, a second possibility involves attack on the exocyclic vinyl group by the semiquinone radical expected from substrate oxidation by the postulated tyrosine peroxy radical (see Scheme 4.3). This would produce an ether linkage rather than the carbon-carbon bond shown in Scheme 4.11. However, the fact that neither styrene nor oxygen effect the degree of crosslinking (Table 3.1) suggests that substrate oxidation is not a prerequisite for covalent attachment of the heme. This data also argues against the alternative possibility that the peroxy radical is itself the species that attacks the heme. A peroxy adduct would, in any case, be quite unstable and would certainly decompose prior to analysis. It is clear, whatever the detailed mechanism, that attachment of the heme to the peptide is a logical extension of the peroxy radical mechanism for substrate oxidation (scheme 4.10, path c). The "substrate" in this case is not a xenobiotic but rather the heme prosthetic group itself.

The Big Picture

The more global question to be addressed is the mechanism by which heme proteins modulate the reactivity of the prosthetic heme group. The peroxidases utilize hydrogen peroxide as a cofactor for the one electron oxidation of

biological substrates. The cytochromes P450 bind molecular oxygen and activate it to a highly reactive oxygen species capable of oxygen insertion reactions. The hemoglobins and myoglobins reversibly bind oxygen and function in vivo as oxygen transport proteins. Some of the factors that differentiate the peroxidases, the P450's and the globins have been discussed by Poulos and Kraut (1980).

The crystal structure of cytochrome c peroxidase (see chapter 1) reveals a polar heme binding pocket with histidine and arginine ideally situated to facilitate heterolytic decomposition of the peroxide bond (Figure 4.8). This has been described as the "pull" that favors peroxide decomposition (Poulos, 1986). These residues are either absent or not properly situated in the highly hydrophobic active sites of both the P450's and the globins. In this respect, the globins resemble the P450's, although these two proteins differ in their heme iron ligands. The P450's, which are catalytic heme proteins, provide a cysteine thiolate ligand that increases the electron density at the heme iron (Figure 4.9). This has been described as the "push" towards oxygen activation in the P450's (ibid).

The globin active site is separated from those of the other hemoproteins in that it has neither "push" nor "pull" for oxygen activation. The interaction of peroxide with the globins nevertheless yields a species capable of substrate oxidation. This species consists of a ferryl-oxo complex

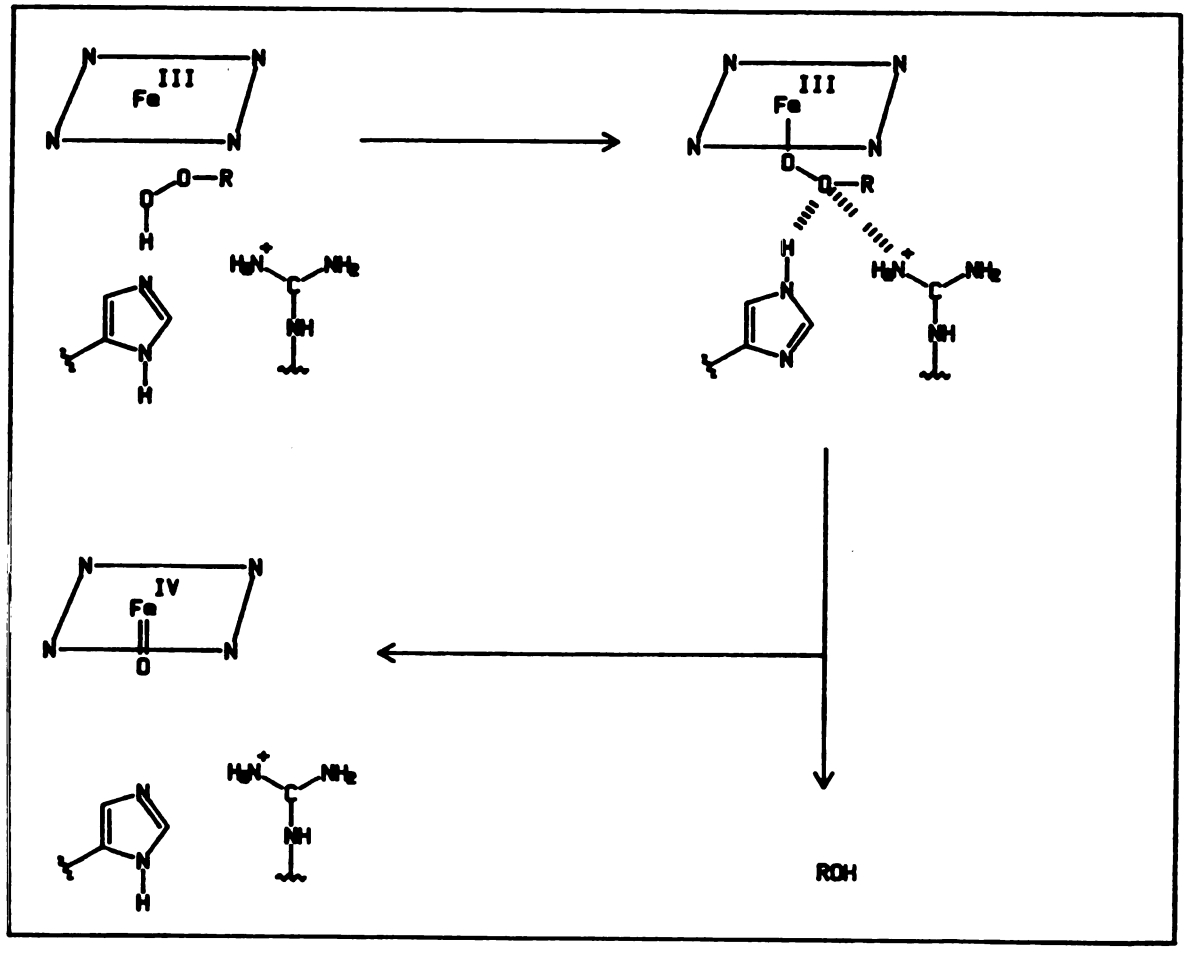

Figure 4.8. Proposed Mechanism of Peroxide Decomposition by Cytochrome C Peroxidase. Adapted from Poulous, 1986.

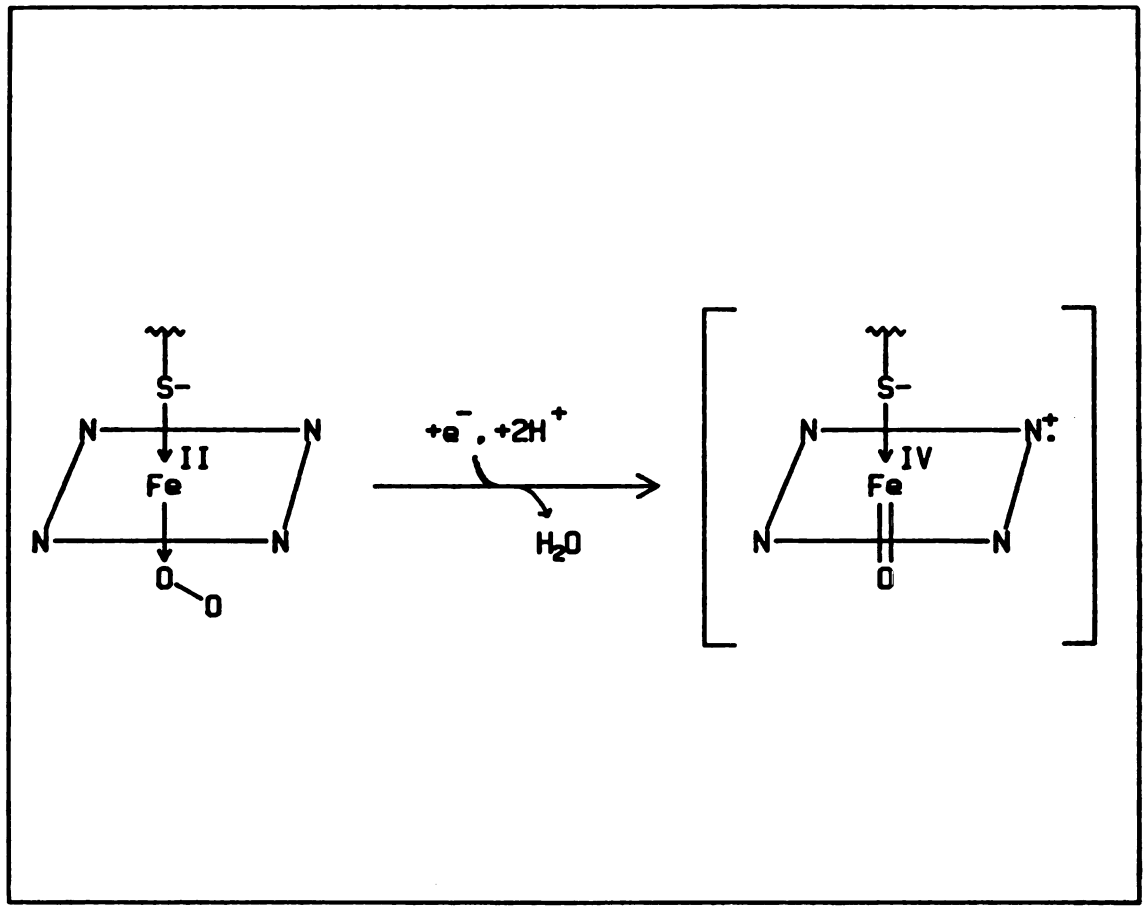

Figure 4.9. The Electronic "Push" Provided by the Cysteine Thiolate Proximal Heme Ligand in Cytochrome P450cam.

plus a protein radical not unlike those of compound ES of cytochrome c peroxidase. The hydrogen peroxide dependent peroxidation of pyrogallol by myoglobin is quite slow, however, when compared to the "classical peroxidases" (Marnett et al., 1986) and presumably reflects the slow formation of the oxidizing species (Kremer, 1981) through a polar transition state. The globins were not "designed" to support such reactive intermediates so that protein destruction ensues. Bleaching of the heme chromophore and loss of amino acid residues is observed. In this respect, it is interesting to note that peroxide-dependent loss of the heme chromophore occurs in myeloperoxidase only after loss of a single tyrosine residue (Matheson and Travis, 1985). The presence of a tyrosine residue in the active site of $P450_{cam}$ is also interesting in this light. One can speculate that aromatic amino acids near the heme prosthetic group serve to diffuse highly reactive species and thereby harness and direct the oxidative event. This proposal does not require that specific residues at the active site be involved. ESR studies with myoglobin clearly show that the first radical formed is not the most stable, so that multiple radical sites may be involved (King et al., 1967). Along similar lines, site specific mutations in the structure of cytochrome c peroxidase indicate that elimination of one site for radical formation simply results in relocation of the radical species with no loss of catalytic efficiency.

The study of hemoprotein reactivity serves to clarify the methods by which protein structure modulates chemical reactivity. It is becoming increasingly clear that reactivity is not located on a single group or residue but that the entire active site works in concert to effect the desired outcome. This concept need not be limited to hemoproteins, but has found generality among other enzyme systems. It has been demonstrated that specific mutations in amino acid residues far removed from the site of the chemical reaction affect catalysis by, for example, dihydrofolate reductase and tyrosyl-tRNA synthetase (Mayer et al., 1986; Leatherbarrow et al., 1985). Just as the lock and key model of substrate binding to a protein is now considered a simplistic description of a much more complicated event, the notion that enzymatic catalysis is centered at a single site in a protein must be considered conceptually crude. Enzyme catalysis must be envisioned as a dynamic event in which the protein superstructure is more than just a box that contains the reactants.

Chapter 5 Experimental Details

Materials and Methods

Materials. Methemoglobin (bovine, type I), myoglobins (sperm whale, type II; horse muscle, type I; horse heart, type III), catalase, superoxide dismutase, trypsin (bovine, TPCK treated, type XIII), Staphylococcus aureus, strain V8 protease (type XVII), lipoxidase (soybean, type V), hematin (bovine, type I), mesoporphyrin IX dihydrochloride, hydrogen peroxide, d_1-ethanol, sodium linoleate, Tween 20 and BSTFA were purchased from Sigma. Styrene, styrene oxide, styrene glycol, benzaldehyde, cis- and trans-stilbenes, trans-stilbene oxide, aniline, N-methyl aniline, p-aminophenol, p-anisidine, cyclohexane, n-butyllithium, mannitol, m-chloroperbenzoic acid, 2-undecanone, menadione, POBN, and Eu(hfc)III were purchased from Aldrich. The m-chloroperbenzoic acid was washed with 0.2 M phosphate buffer and dried overnight in vacuo. Mannitol was recrystallized from 10% water/ethanol. Diphenylmethane was obtained from Eastman Organic Labs. L(+)-ascorbic acid was purchased from Matheson Research Labs. Cyclohexanol was purchased from Fischer Scientific. Pronase (Streptomyces griseus protease) was purchased from Cal Biochem. $^{18}O_2$ was purchased from either MSD Isotopes (98.2% ^{18}O) or Cambridge Isotope Labs (98% ^{18}O). Racemic trans-7,8-dihydroxy-7,8-dihydrobenzo

(a)pyrene and the four isomeric tetrols were obtained from the National Cancer Carcinogenesis Research Institute. Desferrioxamine was kindly provided by CIBA Pharmaceutical Company. Distilled, deionized water was employed in the preparation of all incubation buffers. Buffers were passed through a Chelex column (2.5x30 cm) to remove free metals unless otherwise indicated.

Equipment. Electronic absorption spectra were recorded on a Hewlett-Packard Model 8450A diode array spectrophotometer. Gas liquid chromatographic analyses were performed on either a Varian 2100 gas chromatograph fitted with 6-foot packed glass columns or a Hewlett-Packard Model 5890 gas chromatograph fitted with 30-meter capillary columns. Flame ionization detection was used on both instruments. The injector and detector were maintained at 250^{o}C. High pressure liquid chromatographic analyses utilized a Beckman Model 420 gradient controller and Beckman/Altex 110A solvent metering pumps. Sample elution was monitored with either a Hitachi Model 100 variable wavelength detector, a Hewlett-Packard Model 1040A diode array detector, or a Perkin-Elmer Model 650-10S fluorescence detector. Low pressure chromatographic separations utilized an FMI Model RP1G150 lab metering pump and a Lichroprep Si-60 size B silica gel column. The Hitachi detector was used for eluent detection. Electron impact (70eV) mass spectra were obtained on a Kratos AEI-MS 25 mass spectrometer coupled to a Varian 3700 gas chromatograph fitted with 30-

meter capillary columns. Positive and negative L-SIMS mass spectra were obtained on either a Kratos MS 50 or a Wein mass spectrometer. Thioglycerol was used as the ionization matrix for positive mode and negative mode spectra, respectively. Routine NMR spectra were obtained on a Varian FT-80 instrument and high resolution spectra on either a custom built 240 MHz instrument or a General Electric GN 500 MHz NMR spectrometer. Electron spin resonance experiments were performed on a Varian Model E104A E line instrument. Oxygen concentration was measured with a YSI Model 5331 Clark oxygen electrode in a jacketed cell. A constant temperature was maintained with a Brinkmann Model RM6 circulating water bath. Calibration of the electrode was accomplished with air saturated distilled water (0.456 mM O_2) subsequently degassed by bubbling with argon (0 mM O_2). Amino acid analyses and N-terminal sequence data was obtained by the Biomolecular Resource Center of the University of California at San Francisco.

Experimental Details for Chapter 2

Styrene Oxidation

Incubations of Hemoglobin with Styrene. Unless otherwise indicated, incubations contained the hemoprotein (40 μM heme), styrene (10 mM added either as an acetonitrile solution [1% final acetonitrile concentration] or neat) and

600 μM H_2O_2 in 0.2 M phosphate buffer (pH 7.4). The hemoprotein/styrene solution was preincubated for 10-15 minutes at 0°C and the reaction initiated with the addition of similarly cooled peroxide. Duplicate 10 ml incubations were routinely used for each data point in the analytical experiments. Incubations were carried out at 0°C for 90 minutes before extraction with diethyl ether (2 x 5ml). 2-Undecanone (approximately 5 ug/ml) was added at the end of the incubation period as an internal standard when product quantification was desired. The combined ether extracts were washed with brine (5 ml), filtered or centrifuged (table top centrifuge) to remove precipitated protein, dried over K_2CO_3 and concentrated (100 μl) under a stream of N_2 for GC analysis. Incubations containing known amounts of authentic styrene oxide and benzaldehyde but no styrene were incubated and worked up in a similar manner to generate standard curves for product yield analyses. Preparative experiments were similarly performed except 100 or 500 ml volumes were used and incubation times were extended to 120 minutes.

The initial analysis of styrene oxidation by Hb/H_2O_2 was done by GC analysis: 3% OV225 on 100/120 mesh Supelcoport, 6 foot packed glass column programmed to rise from 80 to 140°C at 15° per minute (Styrene 1.9 min, benzaldehyde, 2.7 min, styrene oxide, 3.3 min, phenylacetaldehyde, 3.6 min, 2-undecanone standard, 4.4 min). Thermal rearrangement of styrene oxide to

phenylacetaldehyde during the GC analysis precluded identification of the latter as a bona fide oxidation product. HPLC was therefore also used to identify the products of styrene oxidation. The ether extract of a 100 ml incubation was concentrated to 1 ml and the styrene removed by low pressure chromatography using 15% ether/pentane at a flow rate of 7 ml/min (styrene, 20 min, styrene oxide, 31 min, benzaldehyde, 41 min). The more polar compounds were collected as a single fraction and the products then isolated by HPLC: Altech Spherisorb S-5-ODS 0.46x25cm column, 40% acetonitrile/water at 1 ml/min flow rate (benzaldehyde, 9.5 min; styrene oxide, 12 min). The Hitachi detector (258 nm) was used for product detection in both the low and high pressure chromatographic separations. The acetonitrile was removed by rotary evaporation, NaCl added to the residual aqueous phase and the products extracted with ether. The products were then identified by GC analysis: Same column, 100^{o}C isothermal.

Defined incubation atmospheres were created as follows: The hemoprotein/styrene mixtures were placed on ice in a vacuum desiccator and deoxygenated by alternately evacuating to 1-2 torr and subsequently purging with either argon (anaerobic studies) or N_2 (all other studies). After the final (seventh) evacuation, gas of known composition was allowed to enter the reaction vessel. Anaerobic incubations utilized argon as the reaction atmosphere. A 1:1 $CO:O_2$ gas mixture was used in the carbon monoxide inhibition studies.

The desiccator was placed into a glove bag before it was opened so that the incubation could be initiated with similarly deoxygenated peroxide. The remainder of the incubation conditions and work-up procedures were as above. Aerobic control incubations were treated as above except that they were purged and incubated with the ambient atmosphere.

$^{18}O_2$ Incorporation Studies. Incubations containing styrene and either hemoglobin, sperm whale myoglobin or horse myoglobin were linked by high vacuum tubing and simultaneously deoxygenated as above. An $^{18}O_2$ atmosphere was created by allowing the contents of a 100 ml $^{18}O_2$ (98%) filled glass balloon to enter the evacuated system and the pressure brought to slightly above ambient with N_2 (as judged by a balloon attached to the system). The incubations were initiated with the addition of a similarly deoxygenated peroxide solution (cannula) and then incubated and worked-up in the usual manner.

Synthesis of $H_2{}^{18}O_2$. The method of Sawaki and Foote (1979) was used for the peroxide synthesis. Hydrogen peroxide concentrations were determined by an iodometric assay (Pesez and Bartos, 1974). Measurement of ^{18}O incorporation into H_2O_2 is based on the peroxide dependent epoxidation of menadione to menadione epoxide (Fieser and Fieser, 1967, Figure 5.1) followed by mass spectrometric analysis. The peroxide solution (50 µl in 1 ml distilled-

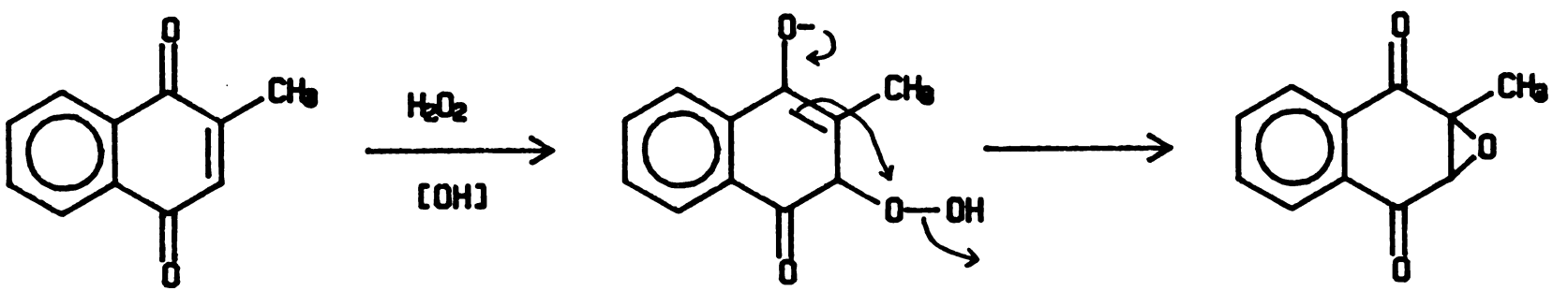

Figure 5.1. The Mechanism of Hydrogen Peroxide-Mediated Epoxidation of Menadione.

deionized water containing 35 mg Na_2CO_3) was added to 1 ml of a warm ethanolic solution of menadione (430 μg, 2.5 μmol). After 5 min the ethanol was removed by rotary evaporation and the aqueous layer extracted with ether after the addition of NaCl. The ether extract was dried over $CaCO_3$ and concentrated for GC mass spectrometric analysis. The percentage of ^{18}O-incorporation was calculated from the following equation:

$$\%^{18}O = (190 \text{ mass})/(188 \text{ mass} + 190 \text{ mass})$$

^{16}O-menadione epoxide exhibited no M+2 mass intensity. The ^{18}O content of the H_2O_2 synthesized in this manner was found to be 42%.

Synthesis of trans-[1-^{2}H]Styrene. The procedure of Baldwin and Carter (1983) was employed. All glassware was oven-dried and nitrogen-flushed while hot to ensure anhydrous reaction conditions. Triphenyltin hydride (23.8 gm, 67.9 mmol) was transferred to a 250 ml flask under a dry nitrogen atmosphere (glove bag). Freshly distilled phenylacetylene (7.55 ml, 68.7 mmol) was slowly added via cannula and the mixture stirred for 20 minutes at which point a white cake formed which precluded further stirring. The mixture was allowed to stand for an additional hour before the cake was taken up in cold pentane and 28.4 g (62.7 mmol, 92% yield) of the solid styryltriphenyltin was collected by vacuum filtration: m.p. 116-120°C; literature

119-120°C (ibid). ^{1}H NMR (80 MHz): 7.53 (m, 5.7H, Ph-), 7.28 (m, 15H, $(Ph)_3$-) and 7.08 ppm (s, 1.9H, -HC=CH-).

Tetrahydrofuran (200 ml, freshly distilled) was added to an oven-dried, nitrogen-flushed flask fitted with a 100 ml dropping funnel dried in a similar manner. The styryl tin compound (36.8 g, 81.2 mmol) was transferred to the flask and the mixture stirred continuously during the remainder of the synthesis. n-Butyllithium (54 ml 1.55 M, 83.7 mmol) was transferred to the dropping funnel via cannula and the reaction mixture cooled to -78°C to allow the dropwise addition of the lithium compound. The mixture was then allowed to warm to 0°C over 2 hours and again cooled to -78°C to allow the dropwise addition of 10 ml (170 mmol) d_1-ethanol (also transferred to the addition funnel via cannula). Pentane (200 ml, ice-cold) was added after stirring an additional 30 min and the butyltriphenyltin removed by filtration through a celite (acid-washed) pad. Butylated hydroxy toluene (35 mg, neat) was added and the filtrate concentrated by rotary evaporation. A second 100 ml portion of cold pentane was added to the residue and the mixture again filtered and concentrated. The resulting oil (30 ml) was distilled in a kugelrohr distillation apparatus (50°C, 0.5 torr, collection bulbs were kept at -78°C). The distillate was checked for styrene (80 MHz NMR) and the appropriate fractions were combined. Residual traces of pentane were removed by swirling at 0.5 torr. Product yield: 1.78 g, 17 mmol, 21%. ^{1}H NMR (80 mHz): 7.3 (m, 4.5H,

Ph-), 6.67 (d of t, 1H, J_1=1.5 Hz, J_2=17.5 Hz, Ph-CH=C-) and 5.69 ppm (d, 1H, J=17.5 Hz, cis-Ph-C=CH-). Less than 2% residual trans proton signal (5.2 ppm). ^{2}H NMR (240 MHz): 5.2 ppm (s, trans-Ph-C=CD-). No trace of cis deuterium signal (5.7 ppm). EIMS: m/e 105 (M^+), 77 (Ph^+).

Chemical Epoxidation of trans-[1-^{2}H]-Styrene. A mixture of 1 mmol each of the deuterated styrene prepared above and m-CPBA was vigorously stirred overnight in a biphasic mixture of 10 ml CH_2Cl_2 and 8 ml 0.5 M $NaHCO_3$. The alkaline aqueous layer prevents m-chlorobenzoic acid catalyzed hydrolysis of the epoxide as it is formed in the organic phase. The organic layer was removed and sequentially washed with 5 ml each of 1 N NaOH, water, and saturated NaCl, and was finally dried over anhydrous $MgSO_4$. ^{1}H NMR (80 MHz): 7.28 (m, 11H, Ph-), 3.83 (d, 1H, J=2.5 Hz, Ph-CH-C-), 3.12 (d, 0.16H, J=4.1 Hz, trans-Ph-C-CH-) and 2.77 ppm (d, 1H, J=2.5 Hz, cis-Ph-C-CH-). ^{2}H NMR (240 MHz): 3.1 (s, 1H, trans-Ph-C-CD-) and 2.7 ppm (s, 0.1H, cis-Ph-C-CD-). EIMS: m/e 121 (M^+).

Stereochemical Investigations of Styrene Oxidation. Preparative scale incubations (500 ml) were utilized when NMR spectra of the styrene oxide product were required. The ether extracts were concentrated to 1 ml and the oxide isolated by low pressure chromatography using 15% ether/pentane at a flow rate of 7 ml/min. Fractions (5 ml) were collected and examined for the presence of styrene

oxide by GC analysis: same column, 100°C isothermal. The appropriate fractions were pooled and the solvent evaporated into an NMR tube containing $CDCl_3$. Additional aliquots (2) of $CDCl_3$ were added and evaporated BUT NEVER TO DRYNESS. The near-total removal of the ether-pentane is critical since these contaminants strongly interfere with the NMR spectra of the oxide product. Extreme caution must be taken, however, since the styrene oxide is easily lost at this stage.

Absolute Chirality of Styrene Oxide. A solution of Eu(hfc)III in $CDCl_3$ (40mg/ml) was prepared and aliquots added to the styrene oxide isolated and prepared as above. An NMR spectrum (240 MHz) was recorded after each addition and the procedure continued until the enantiomeric trans protons were clearly resolved. A sample of authentic racemic styrene oxide (10mg) was treated in a similar manner.

trans-7,8-Dihydrox-7,8-dihydrobenzo(a)pyrene Oxidation

Oxidation of trans-7,8-Dihydrox-7,8-dihydrobenzo(a) pyrene (BAPD) by Hemoproteins. BAPD was dissolved in tetrahydrofuran, an appropriate aliquot transferred to a scintillation vial, and the solvent removed under a stream of N_2. The residue was re-dissolved in 1 mM Tween 20 (1 ml) by sonication. The hemoprotein (in 8 ml phosphate buffer) was then added and the mixture cooled to $0^{\circ}C$ prior to the addition of chilled H_2O_2 to initiate the reaction. Routine analytical incubations were 10 ml in volume and contained the hemoprotein (40 μM in heme), 600 μM H_2O_2 and 100 μM Tween 20 in 0.2 M phosphate buffer (pH 7.4). Early experiments employed BAPD concentrations of 210 μM. Later experiments were all 35 μM in the diol with no difference in product yield noted at the two concentrations. Incubations were carried out for 30 minutes at $0^{\circ}C$ and were then extracted with cold ethyl acetate (5 ml x 2). The anti-cis isomer of BAPT was added to the aqueous phase as an internal standard when necessary for product quantification. The combined extracts were washed with brine (5 ml), dried over either $MgSO_4$ or K_2CO_3, and taken to dryness under a stream of N_2. The residue was taken up in MeOH and filtered (5μ filter needle) for HPLC analysis. Anaerobic studies were carried out similarly but were first degassed in Schlenck tubes using the procedure described previously (see styrene oxidation). Deoxygenated H_2O_2 was added via cannula to

initiate the reaction. The extractions were done under a stream of argon using cold, argon saturated ethyl acetate. As before, aerobic control experiments utilized room air in place of argon.

Analysis of Oxidation Products by HPLC. Product identification was performed on a Whatman Partisil ODS-3 0.46x25cm column. Early experiments used a 5μ particle size column and were associated with severe back pressure problems. Solvent composition and flow rates were necessarily adjusted to minimize the back pressure and varied between 55% and 65% MeOH in water using flow rates of between 0.5 to 0.7 ml/min. A 10μ column was later used and found to be much more effective. The elution solvent used with the 10μ column was 60% MeOH in water at a flow rate of 0.7 ml/min (anti-trans-BAPT, 19 min, syn-trans-BAPT, 22 min, anti-cis-BAPT, 25 min, syn-cis-BAPT, 34 min). The HP1040A diode array detector was utilized to monitor the electronic absorption spectra of products during elution from the HPLC column. Initial product identification was made on the basis of retention time (compared to authentic standards) and the electronic spectrum of the eluted materials.

^{18}O-Incorporation into BAPD. Incubations were performed as described above except incubation volumes of 200 ml (hemoglobin) or 400 ml (myoglobin) were utilized. A BAPD concentration of 35 μM was used in all preparative

experiments. Degassing and introduction of an $^{18}O_2$ atmosphere was accomplished as previously described (vide supra). The synthesis of $H_2{}^{18}O_2$ was also previously described. The ^{18}O content of the peroxide utilized in these experiments was 76.7%. After work up the residue was taken up in MeOH, filtered (5μ filter needle) and the products isolated by HPLC as described above. The solvent was removed under reduced pressure and the residue acetylated for mass spectral analysis.

Acetylation of anti-trans-7,8,9,10-Tetrahydroxy-7,8,9,10-tetrahydrobenzo(a)pyrene. The method outlined by Marnett and Bienkowski (1980) was used. The sample to be derivatized was placed in a test tube and 1 ml 1:1 acetic acid anhydride:pyridine added. This was heated to 65°C for 120 minutes and the solvent then removed under a stream of N_2. The residue was taken up in MeOH and the product isolated by HPLC: same column, 90% MeOH in water at a flow rate of 0.7 ml/min (peracetylated BAPT, 6.5 min). The solvent was removed under reduced pressure, the residue taken up into MeOH and the compound submitted for mass spectrometric analysis (EIMS, probe).

Calculation of Octanol:Water Partition Cooefficient for Benzo(a)pyrene-diol. Log P for BAPD was calculated by the method of Hansch (Hansch and Leo, 1979) using benzo(a)pyrene (log P = 6.0, Mallon and Harrison, 1984) as the starting point:

$$\log P_{BAPD} = \log P_{BAP} + 2(f_{OH}) - f_{=}$$

$$\Rightarrow \log P_{BAPD} = 6.0 + 2(-1.64) - (-0.55)$$

$$\Rightarrow \underline{\log P_{BAPD} = 3.24}$$

where f_{OH} is the coefficient for addition of a hydroxyl group and $f_{=}$ is the factor for deletion of a site of unsaturation.

Stilbene Oxidation

Oxidation of cis-Stilbene by m-chloroperbenzoic acid. cis-Stilbene (178 µl, 1 mmol) and m-CPBA (378 mg, 2 mmol) were added to 10 ml CH_2Cl_2 and the resulting solution was stirred vigorously overnight. The organic layer was removed and sequentially washed with 1 N NaOH (5 ml x 2), water (5 ml x 1) and brine (5 ml x 1) before it was dried over K_2CO_3. GC analysis (3% OV225 on 100/120 mesh Supelcoport 6 foot glass packed column, programmed to rise from 100-200°C at 12 deg/min) showed the presence of a new peak eluting at 3.4 min which was assigned to cis-stilbene oxide. ^1H NMR (80 MHz): 7.2 (m, 6.3H, Ph-), 4.3 ppm (s, 1H, -CH=) (Contamination of the $CDCl_3$ NMR solvent with $CHCl_3$ resulted

in a large integration value for the aromatic protons); Mass spectra: EIMS m/e 196 (M^+).

Purification of cis-Stilbene. The cis-stilbene purchased from Aldrich contained approximately 2-3% trans-stilbene contamination. The cis-stilbene was freed of the majority of this contamination by low pressure chromatography using 10% ether:hexane at a flow rate of 6 ml/min (cis-stilbene, 18.1 min, trans-stilbene, 20.4 min). Fractions (5 ml) were examined by isothermal gas chromatography (DB-5 0.5mm x 30 m capillary column, 180 degrees, cis-stilbene, 9.3 min, trans-stilbene, 15.3 min). The appropriate fractions were combined and the solvent removed under reduced pressure. Gas chromatographic analysis revealed less than 0.2% residual trans-stilbene contamination in the purified cis-stilbene.

Oxidation of Stilbene by Hemoglobin. Duplicate 10 ml incubations containing the hemoprotein (bovine hemoglobin or equine myoglobin, 40 μM heme), 50 μM cis- or trans-stilbene, and 100 uM Tween 20 in 0.2 M phosphate buffer (pH 7.4) were cooled to 0°C and cold H_2O_2 was added to a final concentration of 600 μM. The solutions were kept at 0°C for 90 minutes before they were extracted with ether (5 ml x 2). The combined extracts were washed with brine, centrifuged to remove precipitated protein, dried over K_2CO_3, and concentrated for GC analysis (DB-5 0.5mm x 30m capillary column, 180°C isothermal: cis-stilbene, 9.3 min, cis-

stilbene oxide, 11.4 min, trans-stilbene, 15.3 min, trans-stilbene oxide, 15.7 min). Incubation times were shortened to 30 minutes and diphenylmethane (1 μg) was added to the incubation mixtures just prior to extraction when product quantitation was required. A series of 4 incubations containing myoglobin and peroxide but no stilbene were carried through the incubation period and authentic cis- and trans-stilbene oxides (0.1, 0.5, 1.0 and 5 μg each) were added prior to addition of the internal standard. The incubations were worked up in a similar manner and used to generate a standard curve for determination of the product yield.

The incorporation of hydrogen peroxide oxygen into the epoxide products was examined utilizing 25 ml incubation volumes. The incubations were initiated by adding $H_2{}^{18}O_2$ to the same final concentration. The synthesis of ^{18}O-labeled peroxide was performed as already described. The ^{18}O content in the peroxide utilized in the stilbene experiments was found to be 76.7% by the menadione epoxidation assay (vide supra).

Incorporation of molecular oxygen into the epoxide products was examined utilizing 100 ml incubation volumes. A mixture containing Tween 20, the olefin, and the hemoprotein was cooled on ice and was deoxygenated as described above. Introduction of an $^{18}O_2$ atmosphere and

initiation with deoxygenated peroxide was as described previously.

Linoleic Acid Oxidation

Synthesis of 9,10- and 12,13-Epoxylinoleic Acids. Linoleic acid and m-chloroperbenzoic acid (95 μmole of each) were dissolved in 5 ml of argon saturated ether and were stirred vigorously at room temperature overnight. The ether was removed under a stream of N_2 and the residue was treated with an ethereal solution of diazomethane (1 ml) for 15 minutes at room temperature. Evaporation of the solvent left a residue which was taken up in ether for gas chromatographic analysis on a DX-4 capillary column (0.5mm x 30m) programmed to rise from 200-240°C at 2° per minute (m-CPBA, 5.8 min; linoleic acid, 14.9 min). Two closely spaced peaks eluting at approximately 23.5 minutes which were not present in the linoleic acid or m-CPBA blanks were assigned to the two isomeric linoleic epoxides. GC mass spectrometric analysis was consistent with this assignment: EIMS m/e 310 (M^+), 279 ($M^+ - OCH_3$), low mass fragmentation pattern consistent with a hydrocarbon backbone. Determination of which peak corresponds to which epoxide isomer was not possible under the conditions employed.

Preparation of 13-Hydroperoxy Linoleic Acid. The method of Funk et al. (1976) was used. Na linoleate (6 mg) was dissolved in 5 ml 1 M borate buffer, pH 9 and the

mixture was cooled to 0°C. Lipoxygenase (100 µl suspension, 140,000 units) was added and the solution was stirred at 0°C for 30 minutes under a continuous stream of O_2. The solution was then acidified to pH 3 with HCl and extracted with ether (5 ml x 3). The combined extracts were washed with water (5 ml x 2), dried over $MgSO_4$, and concentrated to a volume of 5 ml. This procedure yields a 13-peroxy:9-peroxy ratio greater than 99:1 (ibid).

Derivatization of the 13-Hydroperoxy Linoleic Acid for Gas Chromatographic Analysis. The peroxide was reduced to the corresponding alcohol by treatment with $NaBH_4$ as follows. The ether solvent was removed under a stream of N_2 and the lipid peroxide residue was taken up in 1 ml of a cold (0°C) ethanolic solution of $NaBH_4$ (75 µg/ml, 2 µmole). This was left for 20 min at 0°C followed by 20 min at room temperature. Brine (1 ml) was then added and the alcohol was extracted into ethyl acetate (2 ml x 2) after acidification to pH 3 with HCl. The combined extracts were dried over $MgSO_4$ and taken to dryness under a stream of N_2. The residue was treated with 1 ml of an ethereal solution of diazomethane. After evaporation of the solvent, the sample was treated with BSTFA (55°C x 120 min) to derivatize the alcohol for GC analysis (same conditions as the epoxides). Analytical gas chromatography showed the presence of a single major peak eluting at 19.7 min not present in the linoleic acid or BSTFA blanks that was identified as the 13-hydroperoxy linoleic acid derivative, 13-O-trimethylsilyl

linoleic acid methyl ester. GC mass spectrometric analysis is consistent with this assignment (Dix and Marnett, 1985): EIMS m/e 382 (M^+), 351 ($M^+ - OCH_3$), 311 ($M^+ - C_5H_{11}$), 173 ($C_6H_{12}OTMS^+$), 73 (TMS^+), low mass fragmentation pattern consistent with a hydrocarbon backbone.

Oxidation of Linoleic Acid by Hemoglobin. Duplicate 10 ml incubations were prepared containing 10 μM hemoglobin, 400 μM linoleic acid and 100 μM Tween 20 in 0.2 M phosphate buffer (pH 7.4). Chilled H_2O_2 was added to a final concentration of 600 μM after a period of 10 minutes at 0°C and the mixture was incubated for 30 minutes at 0°C. The solutions were then acidified to pH 3 with HCl and were extracted with cold ethyl acetate (5 ml x 3). The combined extracts were centrifuged (table top centrifuge x 10 min) to remove precipitated protein, dried over $MgSO_4$, and taken to dryness. The residues were then derivatized for GC analysis as described above.

Miscellaneous Substrate Oxidations

Oxidation of Aniline, p-Anisidine, N-Methyl Aniline and Cyclohexane by Hemoglobin. Duplicate 10 ml incubations containing 10 μM bovine hemoglobin and 10 mM substrate in 0.2 M phosphate (pH 7.4) buffer containing 1 mM desferrioxamine (not chelex treated) were cooled to 0°C. The reactions were initiated by adding chilled H_2O_2 to a final concentration of 600 uM. The reactions were carried

out at 0°C for 30 min before they were extracted with two 5 ml aliquots of either pentane (N-methyl aniline) or ether (all others). The combined extracts were washed with brine (5ml), filtered or centrifuged (table top centrifuge) to remove precipitated protein, dried over K_2CO_3 and concentrated for GC analysis. The following 6 foot packed columns were utilized for chromatographic analyses: 3% OV225 on 100/120 Supelcoport, programed to rise from 80° to 200°C at 12 deg/min (aniline, 3 min; p-anisidine, 7 min; p-aminophenol, 7.4 min); same column, 90°C for 7 min then 90° to 150°C at 20 deg/min (aniline, 7.3 min; N-methyl aniline, 4.9 min); 10% Carbowax on Gaschrome Q 120/140, 130°C isothermal (cyclohexane, 0.4 min; cyclohexanol, 2.6 min).

Experimental Details for Chapter 3

Protein Assay Methods

Lowry Protein Assay. The procedure of Lowry (1951) was followed. Solution A: 1 ml 1% $CuSO_4 \cdot 5H_2O$, 1 ml 2% potassium tartrate, 20 ml 10% Na_2CO_3 in 0.5 M NaOH. Solution B: A 1:10 dilution of 2 N phenol reagent solution. Both solutions were prepared freshly immediately before use. The protein standard (bovine serum albumin or horse myoglobin holoprotein) in a total volume of 100 ul buffer was placed in a test tube and 1 ml solution A was added and mixed thoroughly. After 10 minutes at room

temperature, 3 ml of solution B was added with vigorous agitation and the mixtures were heated to 50°C for an additional 10 minutes. The samples were cooled on ice and the absorbance at 660 nm read immediately. A standard curve was generated using known amounts of the protein standard and the unknown protein concentration determined from this curve.

Biorad Protein Assay. This assay is based on the method of Bradford (1976). The assay was performed as described on the Biorad Concentrated Protein Assay Reagent bottle. The concentrated reagent was diluted with 4 volumes of glass distilled water and filtered. The protein sample (0.1 ml, 200-1400 µg/ml protein) was added to 5 ml of the diluted reagent and mixed thoroughly. The absorbance at 595 nm was read and a standard curve generated using known amounts of the protein standard (either bovine serum albumin or horse myoglobin holoprotein). The protein concentration of the unknown sample was determined from this curve.

Pyridine-Hemochromogen Heme Assay. The method as described by Riggs (1981) was used and works best with a heme concentration of 20 to 60 µM. The hemoprotein in a total volume of 500 µl buffer was added to 1.5 ml of alkaline pyridine solution (20 ml pyridine, 6 ml 1 N NaOH, 34 ml H_2O) and mixed thoroughly. After 3 minutes, excess dithionite (neat) was added to half the sample and the absorbance at 557 nm (protoheme, ϵ=34.4 mM^{-1}, Smith, 1975)

or 546 nm (mesoheme, ϵ=33.2 mM^{-1}, ibid) measured immediately.

Electronic Absorption Hemoprotein Assays. The hemoprotein concentrations were adjusted, where possible, to yield a Soret absorption of approximately 2. The millimolar extinction cooefficients are listed in Table 5.1.

Table 5.1. Horse Myoglobin Milimolar Extinction Cooefficients[a]

Protein	Derivative	ϵ 280	ϵ Soret (nm)	ϵ α-Band (nm)
Proto-Mb	aquo-met	28.9	153 (408)	- -
	cyano-met	-	111.7 (422)	11.3 (540)
Meso-Mb	aquo-met	-	102 (394)	- -
	cyano-met	-	102.8 (402)	11.3 (530)

[a]Taken from Smith and Gibson (1959)

SDS Polyacrylamide Gel Electrophoresis. Gel electrophoresis was done by the method of Lamelli (1970).

Preparation and Analysis of Peroxide Damaged Myoglobin

Hydrogen Peroxide Oxidation of Horse Myoglobin. Duplicate 100 ml incubations were prepared containing horse myoglobin (skeletal muscle, 678 mg, 40 µmol) and styrene (115 µl, 1 mmol) in 0.2 M phosphate buffer (pH 7.4)

containing 1 mM desferrioxamine, were cooled to 0°C. H_2O_2 (23 µl 30% solution, 0.2 mmol) was then added to one incubation and both mixtures kept at 0°C for 30 minutes with occasional agitation. Styrene oxide (1 µl, 8 umol) was added to control incubations without the peroxide after 15 minutes. At the end of the 30 minute incubation period, KCN (5 mmol) was added to stop the reaction and the solutions were dialyzed against glass distilled water for 48 hours. The proteins were concentrated (milipore CX-10 ultrafiltration unit) to a volume of 20 ml and were again dialyzed against water. The extent of chromophore loss due to peroxide treatment was estimated by comparing the Soret:280 nm absorbance ratio for the two hemoproteins.

Oxidation of Myoglobin Under Anaerobic Conditions. Horse myoglobin (169 mg, 10 µmol) was dissolved in 24 ml of chelex-treated 0.2 M phosphate buffer (pH 7.4) and the solution was placed in a Schlenck tube on ice. The mixture was then deoxygenated by alternately evacuating (1 to 2 torr) and flushing with argon. The incubation was left under argon at the end of the 6th cycle and similarly chilled, deoxygenated hydrogen peroxide solution (1 ml, 50 µmol) was added via a cannula. The mixture was left at 0°C for 30 minutes with occasional agitation. The reaction was stopped at the end of the incubation period by adding an anaerobic solution of KCN (1.25 mmol). An aerobic control incubation was treated in the same manner except that room air was used in place of argon in the degassing procedure

and during the incubation. The hemoproteins were dialyzed against glass distilled water for 48 hours as described above.

Preparation of Apomyoglobin: Acidic Acetone Method. The myoglobin solution was added dropwise over 10 min with rapid stirring to 200 ml of acidic acetone (16 ml of concentrated HCl per liter of HPLC grade acetone) at -20°C. The mixture was left an additional 10 min with no stirring and the precipitated protein was collected by centrifugation (3000 x g for 15 min, -20°C). The pellet was resuspended in a minimal amount of cold, glass-distilled water and the procedure repeated. The resuspended pellet was dialyzed sequentially against glass distilled water (overnight), 1.6 mM Na_2CO_3 (20 hours) and finally the buffer of choice (glass distilled water) for a minimum of 8 hours. The apoproteins were lyophylized and stored at -20°C until used.

Preparation of Apomyoglobin: 2-Butanone Method. The hemoprotein solution (30 mg/ml in glass distilled water) was cooled to 0°C and acidified to pH 1.5 (pH paper) with concentrated HCl. The mixture was then quickly extracted with 4 volumes of cold 2-butanone and the organic layer was removed after separation of the phases. The procedure was repeated twice before the aqueous layer was extensively dialyzed (at least 48 hours) against glass distilled water. NOTE: Extraction of small (1 ml) volumes results in a substantial diminution of the aqueous phase, presumably due

to saturation of the organic phase with water. Small aliquots of glass distilled water were added after each extraction to maintain an adequate aqueous volume. The apoproteins were lyophylized and stored at -20°C until used.

The amount of protein-bound heme remaining after the extraction procedure was estimated by comparing the Soret:280 nm absorbance ratio for the apoprotein to that of the holoprotein.

Proteolytic and Acidic Protein Digestion

Trypsin Digestion of Apomyoglobin. Standard analytical experiments utilized 10 mg of the apoprotein dissolved in 1 ml of glass distilled water. TPCK-treated trypsin (20 µl, 2 mg/ml water) was added followed by 100 µl of 0.5 M NH_4HCO_3. The pH was adjusted to 8.5 (pH paper) with NH_4OH. The solution was then heated to 37°C for 6 hours with additional 20 µl aliquots of trypsin being added at 2 and 4 hours (this yielded a final protease:protein ratio of 1:80). The solutions were lyophylized at the end of the incubation period, redissolved in 1 ml of 0.1% aqueous trifluoroacetic acid (TFA), filtered (5µ filter needle), and stored at -20°C until used. Preparative experiments were performed similarly except that 125 mg of the apoprotein was dissolved in 10 ml of glass distilled water and 1 ml of 0.5 M NH_4HCO_3. This was followed by 250 µl of the protease solution. The pH was adjusted and the incubation was carried out as

already described except that 250 µl aliquots of the enzyme were added at the appropriate times. The lyophylized proteins were finally dissolved in 10 ml 0.1% aqueous TFA and stored at -20°C until used.

Staphylococcal V8 Protease Digestion of Apomyoglobin. The apoprotein (10 mg) was dissolved in 1 ml of 0.1 M NH_4HCO_3 (pH 8) and 50 µl of the protease solution (2 mg/ml water) was added. The mixture was incubated for 6 hours at 37°C with additional 50 µl aliquots of protease being added at 2 and 4 hours (this yielded a final protease:protein ratio of 1:66). The solutions were lyophylized at the end of the incubation period and the residue was redissolved in 1 ml 0.1% aqueous TFA, filtered (5µ filter needle), and stored at -20°C until used.

Pronase Digestion of Myoglobin. The protein (10 mg, holoprotein may be used) was dissolved in 1 ml of 50 mM $(NH_4)_2CO_3$ (pH 7.5) buffer containing 5 mM $CaCl_2$ and 150 µl of the protease solution (10 mg/ml, same buffer) was added. The mixture was incubated at 37°C for 14 hours with an additional 150 µl aliquot of protease added after 6 hours (this yielded a final protease:protein ratio of 1:3.3). The solution was lyophylized at the end of the incubation period, redissolved in 1 ml 0.1% aqueous TFA, filtered (5µ filter needle), and stored at -20°C until used.

Preparative Acid Hydrolysis of Myoglobin. The protein sample (10mg) was dissolved in 2 ml freshly distilled HCl

(azeotropes at 6 N HCl) and transferred to a hydrolysis tube. These can either be purchased from Kontes or made by heating a 13x100 mm test tube with an oxygen torch and pulling to yield a constricted neck (hour glass shape). Thioglycolic acid, when present, was added to a final concentration of 5%. The solution was frozen in a dry ice/acetone bath and the hydrolysis tube connected to a high vacuum pump with the use of high vacuum tubing. The tube was evacuated to less than 0.1 torr and flame-sealed under vacuum. The ampules were then heated to reflux (110°C) in a heating block for 24 hours. At the end of the hydrolysis period, the ampule was opened and the solvent removed in vacuo in a desiccator containing solid NaOH. The residue was redissolved in 1 ml of either aqueous 0.1% TFA or 65:35:10 methanol:water:acetic acid and the resulting solution was filtered (5μ filter needle) and stored at -20°C until used.

Analytical Methods

HPLC Conditions for Peptide, Amino Acid and Heme Characterizations. A Whatman Partisil 5 ODS-3 0.46x25 cm column was used for peptide, amino acid and heme analyses. Elution solvents were as follows: Solvent A- 0.1% trifluoroacetic acid in water; Solvent B- 0.1% trifluoroacetic acid in acetonitrile; Solvent C- 65:35:10 methanol:water:acetic acid.

HPLC Analysis of Peptides. Analytical and semi-preparative separations utilized approximately 1 mg of protein per injection onto the HPLC column. A stepwise gradient program was used for peptide elution: 0% to 40% B over 90 minutes, 40% to 70% B over 30 minutes and finally 70% to 100% B over 5 minutes with a flow rate of 1 ml/min. Peptide detection was accomplished using the Hewlett-Packard diode array detector simultaneously recording the absorbances at 220 nm (peptide amide bonds), 280 nm (aromatic residues) and 398 nm (heme Soret). When fluorescence detection was used, excitation was at 280 nm and emission was monitored at 320 nm.

Poorly resolved Staphylococcal V8 protease peptides eluting in the 56-60 minute range were collected as a single fraction. These were rechromatographed utilizing a shallow gradient program: 10% to 30% B over 60 minutes at the same flow rate.

Preparative experiments were performed similarly except that 6-8 mg of digested protein was injected onto the HPLC column and the peptides were eluted with a shorter gradient program: 0% to 40% B over 30 minutes, 40% to 70% B over 30 minutes and 70% to 100% B over 5 minutes at a flow rate of 1 ml/minute.

HPLC Analysis of Aromatic Amino Acids and Heme. Product elution was accomplished with a stepwise gradient program: 10% B for 5 minutes, 10% to 40% B over 45 minutes

and finally 40% to 100% B over 10 minutes at a flow rate of 1 ml/min. Product elution was monitored at 280 nm (aromatic amino acids) and 398 nm (heme Soret) with the Hewlett-Packard diode array detector. L-Dopa, tyrosine and heme readily separate under these conditions with retention times of 7, 9 and 63 minutes, respectively.

HPLC Analysis of Heme: Method #2. Solvent C at 1 ml/min isocratically was used in this analysis. Product elution was monitored at 280 and 398 nm as above. Heme elutes at 11 minutes under these conditions.

Preparation of Proto- and Meso-heme Reconstituted Horse Myoglobins

Preparation of Meso Heme. The method of Morrell et al. (1961) was used. Meso porphyrin dihydrochloride (10 mg, 15.6 μmol), dissolved in 1 ml of pyridine, added to 50 ml of glacial acetic acid. A saturated aqueous solution of $FeSO_4$ (1 ml) was added and the mixture heated to 80°C for 10 minutes under a stream of N_2 and an additional 10 minutes under the ambient atmosphere. Brine was then added, and the solution was extracted with diethyl ether. The ether extracts were washed with 25% HCl to back extract the unreacted porphyrin and were dried over Na_2CO_3 before the solvent was stripped away by rotary evaporation. The electronic spectrum (ether) of the product is identical to the published spectrum of meso-hemin (Smith, 1975, p. 887):

367 (S'), 400 (S), 506 (IV), 530 (III), 580 (II) and 630 nm (I); lit. 370 (S'), 397 (S), 506-508 (IV), 534 (III), 585 (II) and 632-634 nm (I).

Reconstitution of Horse Apomyoglobin with Exogenous Hemes. The apoprotein was prepared from 500 mg of myoglobin using the acidic acetone method described above (86% yield). The lyophylized apoprotein (200 mg, 12.3 μmol) was redissolved to the extent possible in 25 ml of 0.1 M phosphate (pH 6.5) buffer and the mixture was cooled to 0°C (a substantial amount of the apoprotein remained undissolved). The heme (9 mg, 14 μmol of meso-hemin or equine hemin) was dissolved in 5 ml of 0.01 N NaOH, and the solution was added dropwise to the apoprotein at 0°C with constant (gentle) stirring. The solution was stirred for an additional 5 minutes and was then centrifuged (table top centrifuge). The supernatant was loaded onto a Sephadex G-25 column (2.5x35 cm) equilibrated and eluted with 0.01 M phosphate (pH 6.3) buffer. The colored band was collected and loaded directly onto a CM-52 cellulose column (2.5x35 cm) equilibrated with 0.01 M phosphate (pH 6.3) buffer. The column was washed with the same buffer (500 ml). The holoprotein eluted as a tight band when the buffer was changed to 0.03 M phosphate (pH 7). The hemoprotein was then dialyzed (24 hours) against 0.2 M phosphate (pH 7.4) buffer which was stirring over Chelex resin.

Characterization of the Reconstituted Hemoproteins. Four separate methods were utilized to characterize the reconstituted horse myoglobins:

1) Electronic Absorption Assay. The spectra for the aquo-met and cyano-met derivatives of the hemoproteins were obtained and are shown in Figures 5.2 and 5.3 for the proto- and meso-reconstituted myoglobins, respectively. The absorbances at the indicated wavelengths for the hemoprotein solutions are listed in Table 5.2. The micromolar protein concentrations calculated from these absorbances is also listed in the table.

Table 5.2. Hemoprotein Concentration from Spectral Data

Protein	Derivative	280 nm*	[Mb]	Soret*	[Mb]	α Band	[Mb]
Standard#	aquo-met	0.2791	97	1.513	99	-	-
	cyano-met	-	-	1.027	92	0.9590	85
Proto-Mb	aquo-met	0.3073	106	1.776	116	-	-
	cyano-met	-	-	1.235	111	1.2080	107
Meso-Mb	aquo-met	0.2088	72	1.510	148	-	-
	cyano-met	-	-	1.121	109	0.8260	73

*1:10 dilution. #Horse myoglobin, 2.06 mg/ml (121.5 μM).

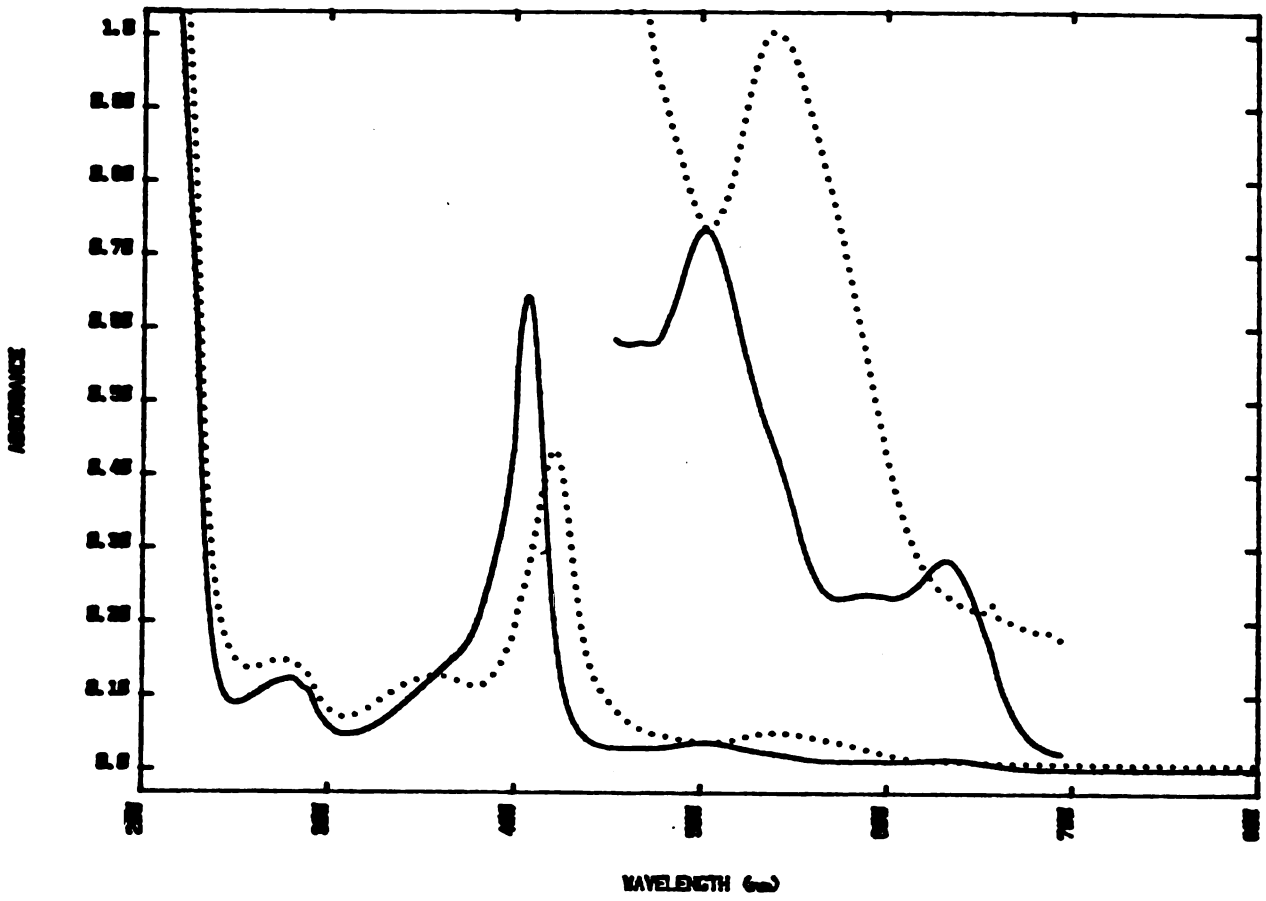

Figure 5.2. The Electronic Absorption Spectrum of Proto-Heme Reconstituted Horse Myoglobin. ——, Aquo-metmyoglobin; ····, Cyano-metmyoglobin.

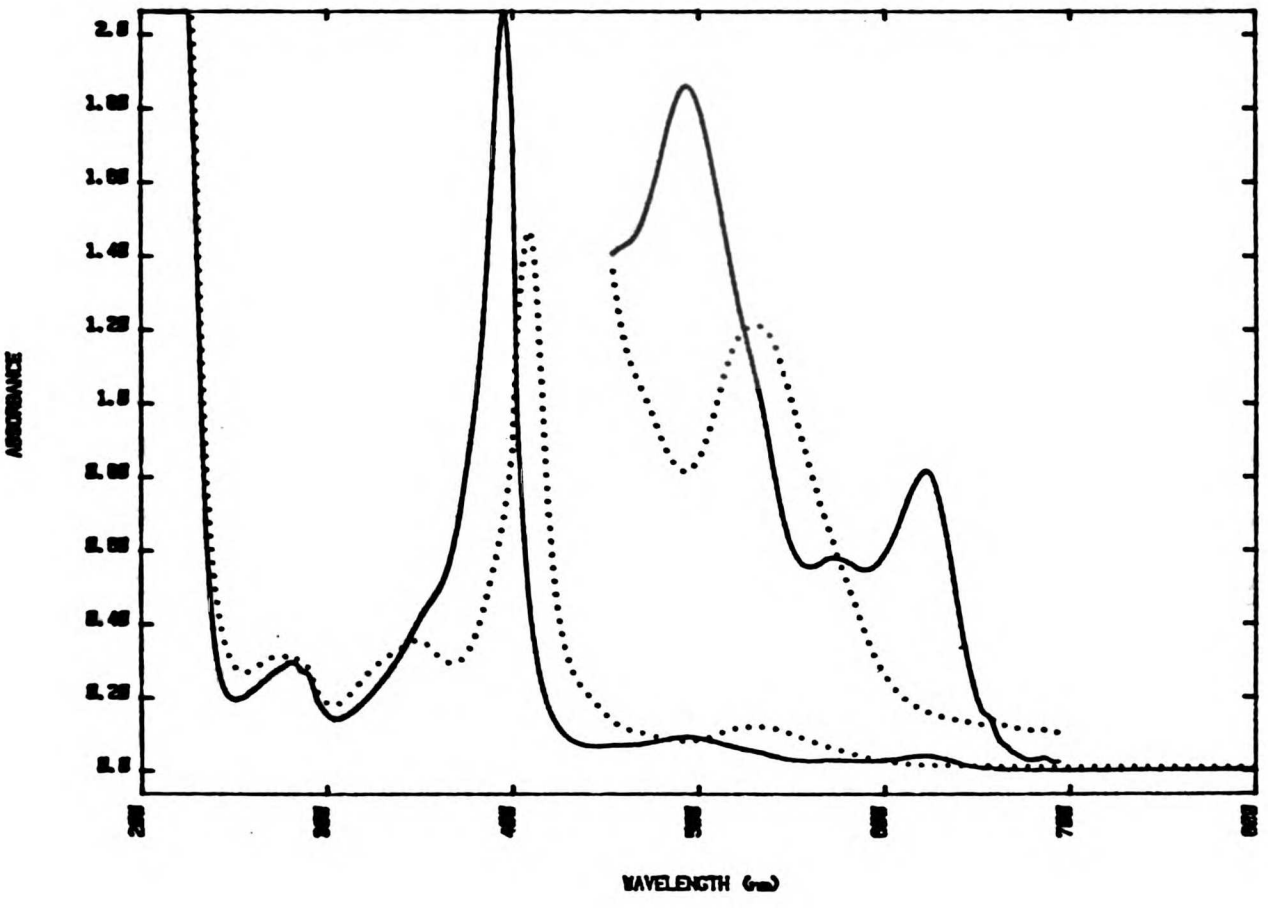

Figure 5.3. The Electronic Absorption Spectrum of Meso-Heme Reconstituted Horse Myoglobin. ———, Aquo-metmyoglobin; ····, Cyano-metmyoglobin.

2) The Pyridine Hemochromogen Assay for Heme. The extinction coefficients, absorbances and calculated hemoprotein concentrations are listed in Table 5.3.

Table 5.3. Hemoprotein concentration from Pyridine Hemochromogen Data

Protein	ϵ	(nm)	Absorbance	[Mb]
Standard*	32.0	557	0.235	73 μM
Proto-Mb	32.0	557	0.2885	90 μM
Meso-Mb	33.2	546	0.2225	67 μM

*Horse myoglobin, 2.06 mg/ml (121.5 μM). The pyridine hemochromogen spectra for meso-heme is consistent with the published spectra: 408 nm (S), 516 nm (II) and 530 nm (I). (Smith, 1975)

3) The Biorad Protein Assay. A standard curve was generated using horse myoglobin holoprotein as the protein standard (r^2=0.949). The calculated protein concentrations are shown in Table 5.4.

4) The Lowry Protein Assay. A standard curve was generated using horse myoglobin holoprotein as the protein standard (r^2=0.998). The calculated protein concentrations are shown in Table 5.5.

Table 5.4. Hemoprotein Concentration from the Biorad Protein Assay

Protein	µl	µg	Absorbance	[Mb]
Standard*	0	0	-0.011	-
	10	20.6	0.277	-
	20	41.2	0.497	-
	50	103	0.889	-
	100	206	1.150	-
Proto-Mb	50	-	0.921	160 µM
	50	-	0.927	(avg)
Meso-Mb	50	-	0.840	147 µM
	50	-	0.878	(avg)

*Horse myoglobin holoprotein, 2.06 mg/ml (121.5 uM).

Table 5.5. Protein Concentration from the Lowry Assay

Protein	µl	µg	Absorbance	[Mb]
Standard*	0	0	0	-
	20	41.2	0.179	-
	40	82.4	0.326	-
	80	164.8	1.607	-
Proto-Mb	80	-	0.683	136 µM
	80	-	0.695	(avg)
Meso-Mb	80	-	0.554	112 µM
	80	-	0.581	(avg)

*Horse myoglobin holoprotein, 2.06 mg/ml (121.5 µM).

A summary of the reconstituted myoglobin concentrations obtained by the four methods is given in Table 5.6. Note the consistently low concentration calculated for the horse myoglobin standard (actual concentration of 121.5 µM). The pyridine hemochromogen assay yields particularly low values. This may be due to incomplete heme extraction during the assay period (Riggs). Correction of the calculated values to allow for the low concentrations determined by the standard (121.5/73= 1.66) yields the concentrations listed in Table 5.7. Similar correction for the absorption of the cyano-met proto-myoglobin (121.5/92= 1.32) similarly yields the corrected hemoprotein concentrations listed in the table.

Table 5.6. Summary of Calculated Hemoprotein Concentrations. (uncorrected)

Protein		Biorad	Lowry	Pyridine Hemochrom.	Absorbance 280	Soret	α-Band
Standard	(aquo)	-	-	73	97	99	-
	(cyano)	-	-	-	-	92	85
Proto-Mb	(aquo)	160	136	90	106	116	-
	(cyano)	-	-	-	-	111	107
Meso-Mb	(aquo)	147	112	67	-	148	-
	(cyano)	-	-	-	-	109	73

Table 5.7. Corrected Values for Calculated Hemoprotein Concentrations

Protein	Biorad	Lowry	Pyridine	Soret (CN)
Standard	-	-	121.5	121.5
Proto-Mb	160 μM	136	149	147
Meso-Mb	147 μM	112	111	109*

*Not corrected.

The corrected values are much more consistent than the uncorrected values. The heme to protein ratio, as determined from the Lowry and pyridine hemochromogen assays, respectively, is approximately 1:1, as required for complete

reconstitution. Hemoprotein concentrations were subsequently determined from the electronic spectra of the cyano-met derivative using the extinction coefficient for the Soret maximum (Table 5.1).

Oxidation of the Reconstituted Myoglobins with Hydrogen Peroxide. The reconstituted hemoproteins were concentrated to a volume of 1 ml (325 and 340 μM, proto- and meso-myoglobins, respectively), using a Centricon CX-10 concentrator. A chilled solution of H_2O_2 (200 μl, 1.7 μmol) was added to each and the mixtures were left for 30 minutes at 0°C. KCN (50 mM) was added at the end of the incubation period and the solutions were dialyzed against glass distilled water for 48 hours. The heme was extracted from the holoproteins using the 2-butanone method and the apoproteins extensively dialyzed against glass distilled water (2 liters x 3 changes over 48 hours). With buffer added in place of the peroxide solution, control incubations were taken through the entire procedure. The apoproteins were concentrated to a volume of approximately 0.5 ml (Amicon 10 microconcentrator) and electronic spectra were taken.

Kangaroo Myoglobin

Purification of Kangaroo Myoglobin. The method of Wittenberg and Wittenberg (1981) was used. All procedures were carried out at 0°C unless otherwise indicated. Myoglobin from the red kangaroo (Macrofus rufus) was

isolated from 14-15 gm of a 65% saturated $(NH_4)_2SO_4$ paste kindly provided by Jack Peisach. The paste was dissolved in a minimal amount of 0.02 M TRIS-HCl (pH 8.0) buffer containing 1 mM EDTA, and applied to a Sephadex G-100 column (2.5 x 30cm) equilibrated with the same buffer. The proteins were eluted with the same buffer at a flow rate of 20 ml/hr (peristaltic pump) and 10 ml fractions collected. A plot of 408 nm absorbance (Soret) vs fraction number is shown in Figure 5.4. Peaks I and II were collected and their electronic spectra are shown in Figure 5.5. Peak I consists mainly of hemoglobin while myoglobin elutes in the the latter (ibid).

The myoglobin containing fractions were pooled and concentrated to a volume of 8 ml (millipore 10 ultrafiltration units) and the concentrate was dialyzed against 0.02 M TRIS-HCl (pH 8.5) buffer containing 1 mM EDTA, for 12 hours. The dialysate was then applied to a DEAE-Sephadex A50 column (2.5 x 35cm) equilibrated with 0.02 M TRIS-HCl (pH 8.4) buffer containing 1 mM EDTA. Application of the hemoprotein in a solution at a pH 0.1 unit higher than the column pH is reported to ensure narrow band loading. Protein elution was accomplished with the same buffer (pH 8.4) at a flow rate of 100 ml/hr (peristaltic pump) and 10 ml fractions were collected. A plot of 408 nm (Soret) and 280 nm (protein) absorbance vs. fraction number is shown in Figure 5.6. The order of

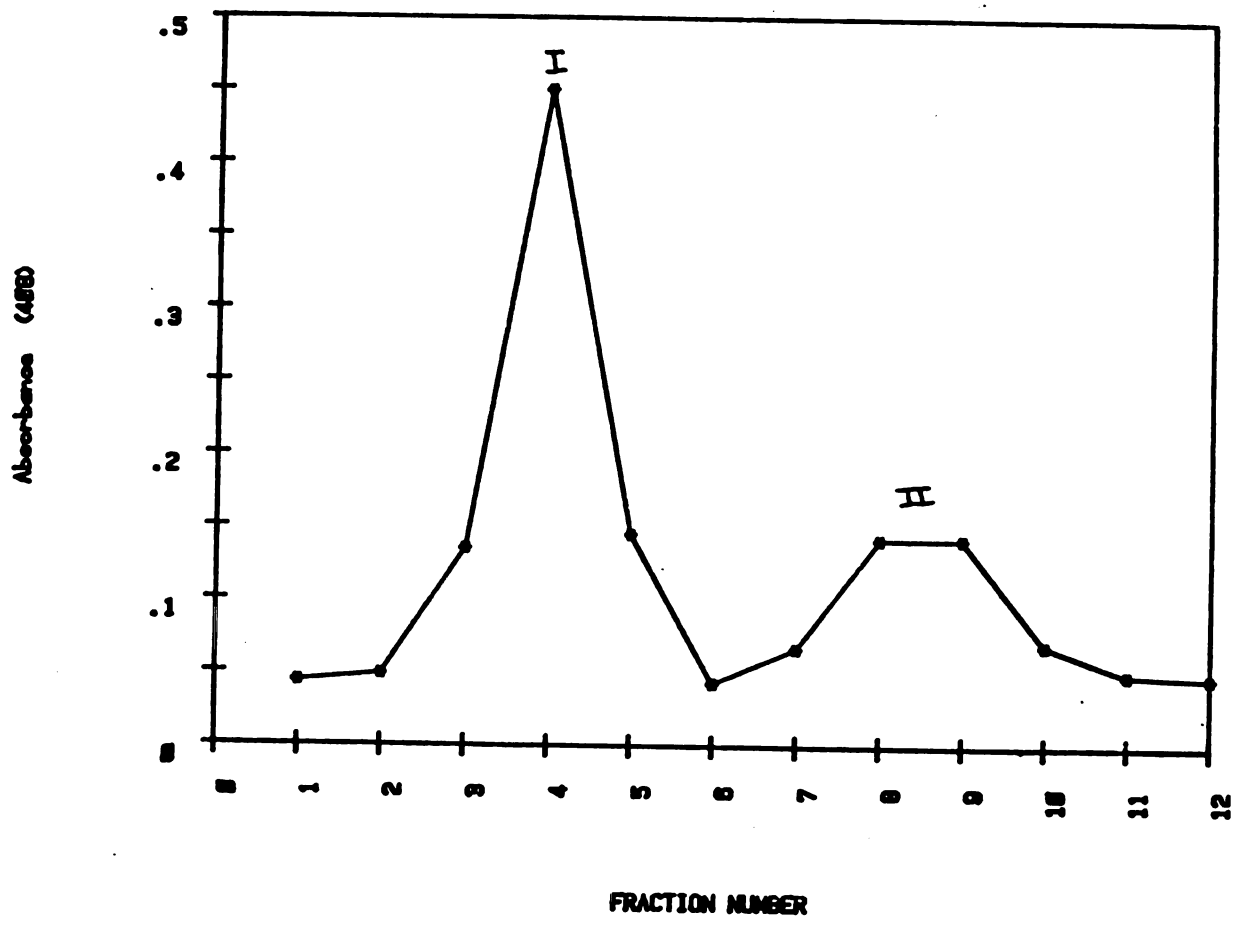

Figure 5.4. Sephadex G-100 Chromatographic Separation of Kangaroo Myoglobin and Hemoglobin. Fractions were Examined for Soret Absorption and the Appropriate Factions were Pooled.

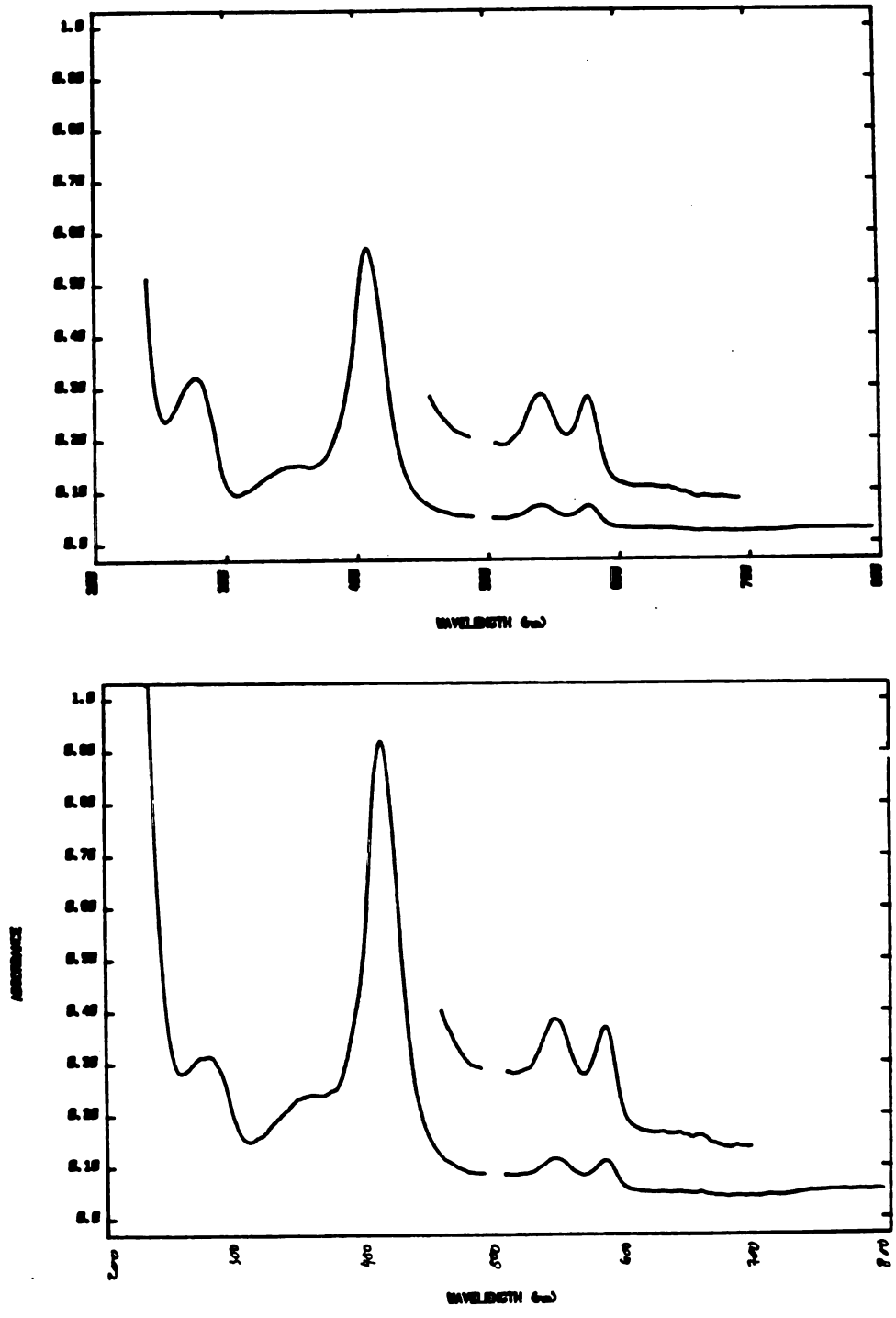

Figure 5.5. Electronic Absorption Spectra of Peak I (upper trace) and Peak II (lower trace) from the Sephadex G-100 Chromatographic Separation of Kangaroo Myoglobin and Hemoglobin (Figure 5.4).

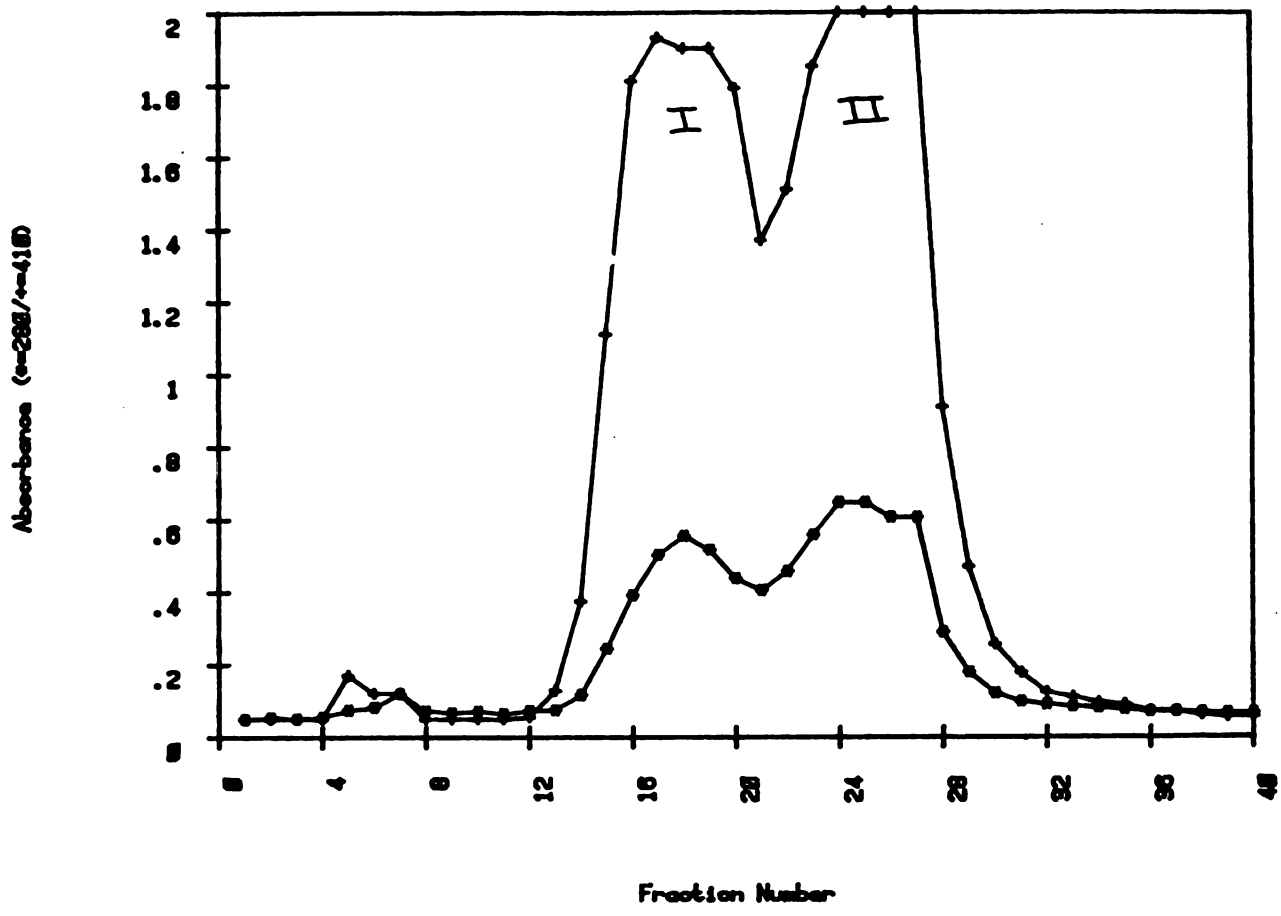

Figure 5.6. DEAE-Sephadex Chromatographic Separation of Kangaroo Myoglobins. Fractions were Examined for Soret Absorption and the Appropriate Fractions were Pooled.

elution from the DEAE-Sephadex column and their electronic spectra, shown in Figure 5.7, identifies peaks I and II as aquo-met myoglobin (Fe^{III}-OH_2) and ferrous-oxy myoglobin (Fe^{II}-O_2), respectively (ibid). The appropriate fractions were pooled and concentrated (millipore 10 ultrafiltration units). The pyridine-hemochromogen assay for heme revealed a final yield of 0.6 μmol and 1.7 μmol of metmyoglobin and oxymyoglobin, respectively.

Figure 5.8 shows a 12% SDS-PAGE gel of the myoglobin containing fractions at each step of the purification. A 12% gel of the purified myoglobins along with authentic bovine hemoglobin and sperm whale myoglobin is shown in Figure 5.9 and shows the purified myoglobins to be electrophoretically homogeneous.

Oxidation of Kangaroo Oxy-myoglobin to Met-myoglobin. $K_3Fe(CN)_6$ (62 μl of a 10 mg/ml solution, 1.88 μmol) was added to the oxy-myoglobin solution (1.7 μmol heme) with gentle swirling at 0°C. This was applied to a Sephadex G25 column equilibrated and eluted with 0.2 M phosphate (pH 7.4) buffer and the colored band was collected.

Oxidation of Styrene by Kangaroo Myoglobin and Hydrogen Peroxide. Duplicate 5 ml incubations containing 40 μM metmyoglobin and 10 mM styrene in 0.2 M phosphate (pH 7.4) buffer containing 1mM desferrioxamine were cooled to 0°C and the reaction initiated by adding chilled H_2O_2 to a final concentration of 600 μM. After 60 minutes at 0°C, 2-

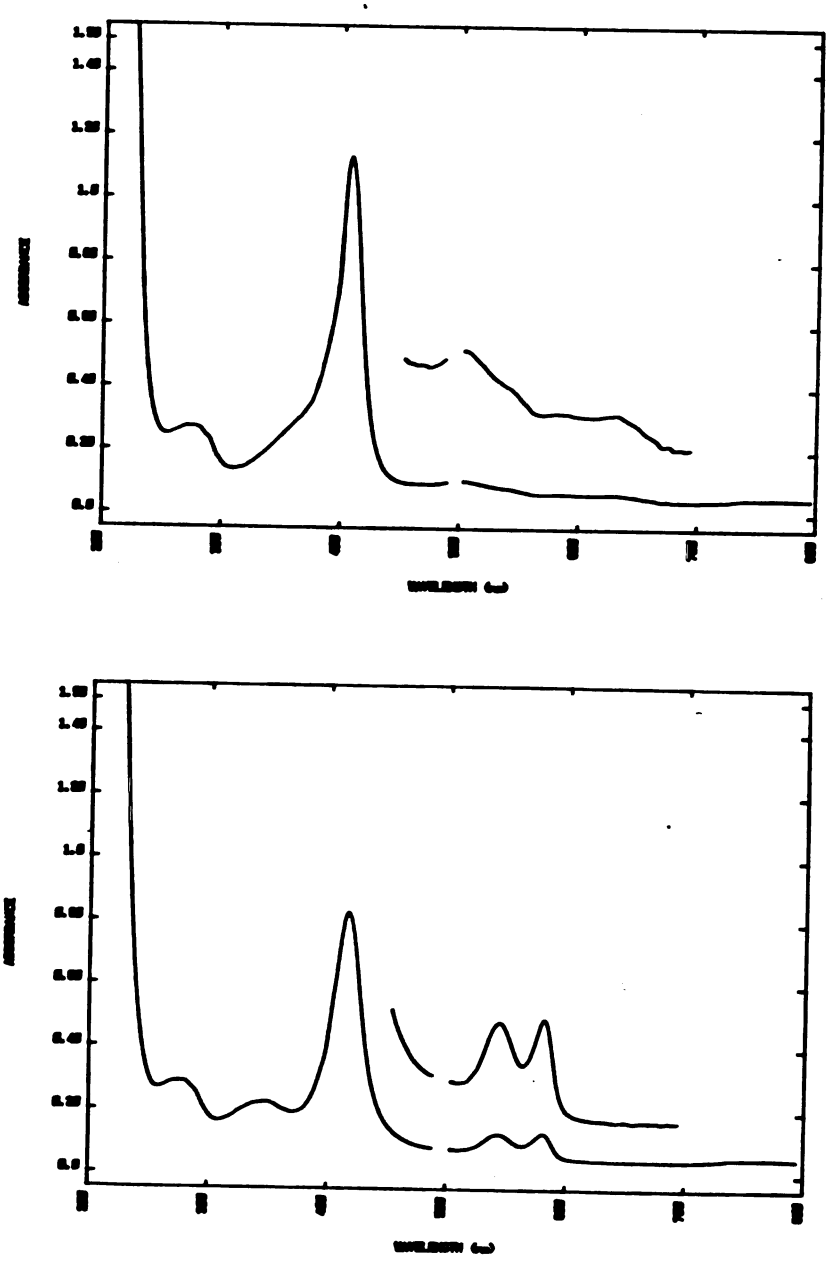

Figure 5.7. Electronic Absorption Spectra of Peak I (upper trace) and Peak II (lower trace) from the DEAE-Sephadex Chromatographic Separation of Kangaroo Myoglobins (Figure 5.6).

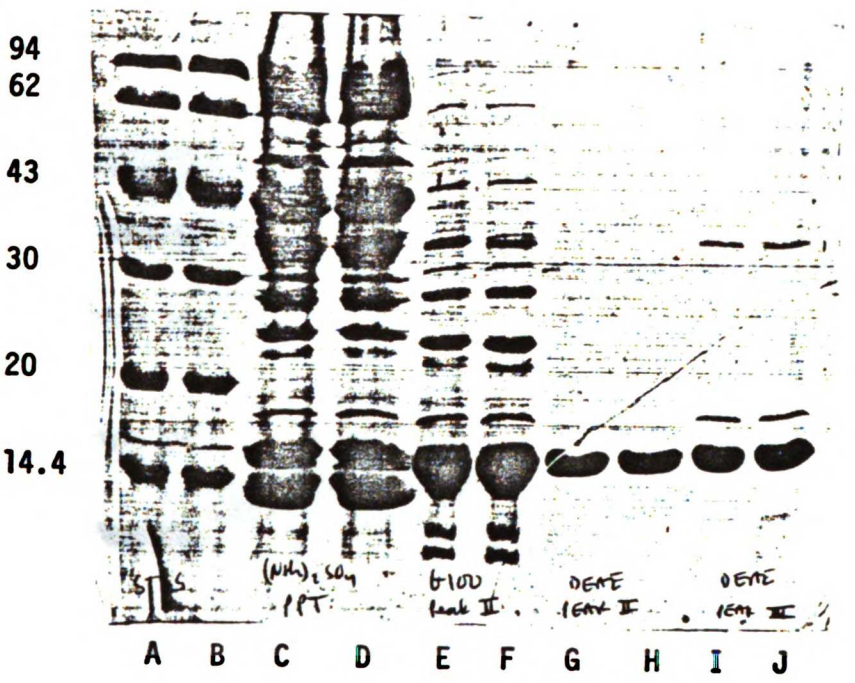

Figure 5.8. SDS-PAGE Gel of Kangaroo Myoglobin at Various Stages of Purification. Lanes A and B, Molecular Weight Standards. The Molecular Weights, in Thousands, are Listed to the Left of the Figure. Lanes C and D, $(NH_4)_2SO_4$ Paste. Lanes E and F, Sephadex G-100 Peak II. Lanes G and H, DEAE-Sephadex Peak I. Lanes I and J, DEAE-Sephadex Peak II.

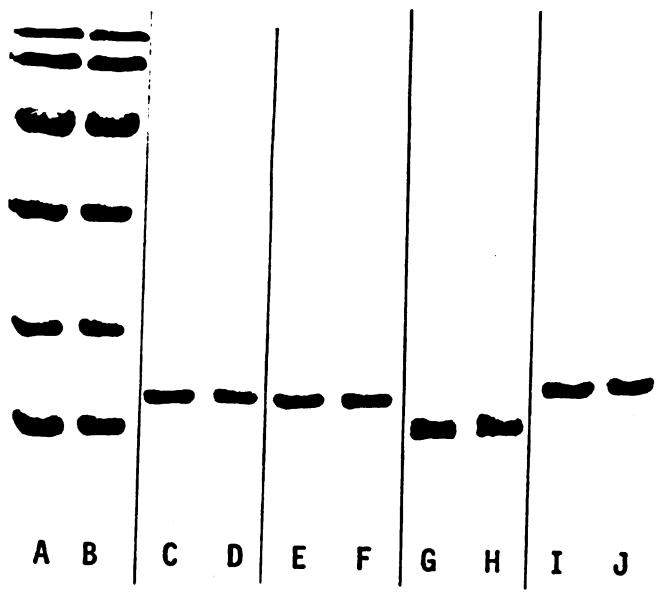

Figure 5.9. SDS-PAGE Gel of Purified Kangaroo Myoglobins. Lanes A and B, Molecular Weight Standards. Lanes C and D, DEAE-Sephadex Peak I. Lanes E and F, DEAE-Sephadex Peak II. Lanes G and H, Equine Hemoglobin. Lanes I and J, Sperm Whale Myoglobin.

undecanone was added as an internal standard and the incubations worked up as previously described (vide supra).

Cross-Linking of Peroxide Treated Kangaroo Myoglobin. A 100 µl incubation containing hemoprotein (40 µM heme) in 0.2 M phosphate buffer (pH 7.4) was cooled to 0°C and chilled H_2O_2 was added to a final concentration of 600 µM. The concentration of styrene, when present, was 10 mM. After 2 hours at 0°C, 20 µl (8 µg hemoprotein) aliquots were subjected to SDS-PAGE (12% gel) analysis.

ESR Studies

Low Temperature ESR Hardware Setup. A gas nipple on the ESR microwave guide was connected to a coil of copper tubing connected to a tank of nitrogen gas. The microwave guide and cavity were then purged with nitrogen (room temperature) for 15 minutes before the ESR Dewer was inserted into the microwave cavity. The copper coil was then immersed in liquid nitrogen and the microwave cavity cooled with a steady stream of cold nitrogen gas. This procedure stablized the temperature of the microwave cavity and minimized water condensation on the surface of the Dewar which made ESR measurements difficult. The Dewar was then filled with liquid nitrogen and capped with a piece of aluminum foil. A steady stream of cold nitrogen gas was passed through the microwave guide and cavity during the entire ESR experiment.

Low Temperature EPR Measurements. Hydrogen peroxide was added to the hemoprotein at 0°C and the sample transferred to an ESR tube. After 30 seconds, the tube was sealed with a rubber septa and the tip of the tube placed in liquid nitrogen until a fizzing sound was heard. At this point, the remainder of the tube was slowly immersed in order to freeze the entire solution. When the time course of an ESR signal examined, aliquots were removed from a large (10 ml) incubation and frozen at the indicated times. The samples were kept at -196°C until the spectrum could be recorded. ESR spectra were recorded at -196°C using an IBM PC/XT computer and a Techmar Labmaster analog to digital (12 bit resolution) converter with signal averaging performed in real time. Data was collected and manipulated using a custom data acquisition program. ESR spectral parameters are listed below in Table 5.8.

Table 5.8. Low Temperature ESR Spectral Parameters

Sample	Field Center	Mod. Freq.	Mod. Amp.	Microwave Power	Microwave Freq.	g value
Fe^{3+} Mb	1090 G	100 kHz	20 G	10 mW	9.15 GHz	6
Fe^{4+} Mb	3270 G	100 kHz	8 G	2 mW	9.15 GHz	2

References

Al-Gailany, K.A.S., Houston, J.B. and Bridges, J.W. (1978) Biochem Pharmacol. **27**, 783-788.

Allen, G. (1981) Laboratory Techniques in Biochemistry and Molecular Biology. Sequencing of Proteins and Peptides, (Work, T.S. and Burdon, R.H., eds) Elsevier Scientific Publishers, New York.

Ator, M.A. and Ortiz de Montellano, P.R. (1987) J Biol Chem. in press.

Bakes, W.L., Hogaboom, M. and Canady, W.L. (1982) J Biol Chem. **257**, 4063-4070.

Baldwin, J.E. and Carter, C.G. (1983) J Org Chem. **48**, 3912-3917.

Belvedere, G. and Tursi, F. (1981) Res Comm Chem Path and Pharmacol. **33**, 273-282.

Belvedere, G., Tursi, F., Elovaara, E. and Vainio, H. (1983) Toxicol Letters. **18**, 39-44.

Black, S.D. and Coon, M.J. (1986) in Cytochrome P-450: Structure, Mechanism and Biochemistry, (Ortiz de Montellano, P.R., ed) pp. 161-216, Plenum Press, New York.

Blisard, K.S. and Mieyal, J.J. (1979) J Biol Chem. **254**, 5104-5110.

Bradford, M. (1976) Anal Biochem. **72**, 248-254.

Cadenas, E., Boueris, A. and Chance, B. (1980) FEBS Let. **112**, 285-288.

Calderwood, T.S. and Sayer, D.T. (1984) J Am Chem Soc. **106**, 7185-7186.

Cambou, B., Guillochon, D. and Thomas, D. (1984) Enzyme Microb Technol. **6**, 11-17.

Cantoni, L., Blezza, D. and Belvedere, G. (1982) Experientia. **38**, 1192-1194.

Carrell, R.W., Winterbourn, C.C. and French, J.K. (1977) Hemoglobin. **1**, 815-827.

Chiu, D., Lubin, B. and Shohet, S.B. (1982) Peroxidative Reactions in Red Cell Biology, in Free Radicals in

Biology, vol 5. (Pryor, W.A., ed.) pp. 115-159, Academic Press, New York.

Clennan, E.L., Simmons, W. and Almgren, C.W. (1981) J Am Chem Soc. **103**, 2098-2099.

Coles, G.C. (1966) J Insect Physiol. **12**, 670-671.

Collman, J.P., Brauman, J.I., Meunier, B., Raybuck, S.A. and Kodadek, T. (1984) Proc Natl Acad Sci, USA. **81**, 3245-3248.

Coulson, A.F.W., Erman, J.E. and Yonetani, T. (1971) J Biol Chem. **246**, 917-924.

Courtin, F., Deme, D., Virion, A., Michot, J.L., Pommier, J. and Nunez, J. (1982) Eur J Biochem. **124**, 603-609.

Dayhoff, M.O. (1976) Atlas of Protein Sequence and Structure, vol 5, suppl 2. (Dayhoff, M.O., ed.) pp. 191-223, National Biomed Research Fed, Georgetown University Medical Center, Washington, D.C.

Dickerson, R.E. and Geis, I. (1983) Hemoglobin: Structure, Function, Evolution and Pathology, pp. 68-69, The Benjamin/Cummings Publishing Co, Menlo Park, Calif.

Dickinson, C. and Symons, M.C.R. (1983) Chem Soc Rev. **12**, 387-414.

Dix, T.A. and Marnett, L.J. (1981) J Am Chem Soc. **103**, 6744-6746.

Dix, T.A. and Marnett, L.J. (1983) Science. **221**, 77-79.

Dix, T.A. and Marnett, L.J. (1985) J Biol Chem. **260**, 5351-5357.

Dix, T.A., Fontana, R., Panthani, A. and Marnett, L.J. (1985) J Biol Chem. **260**, 5358-5365.

Dolphin, D. (1981) Israel J Chem. **21**, 61-71.

Doyle, M.P., Pickering, R.A. and da Conceicao, J. (1984) J Biol Chem. **259**, 80-87.

Dunford, H.B. (1982) Peroxidases, in Adv in Inorg Biochem. (Eichorn, G. and Marzilli, L.G., eds) pp. 41-68, Elsevier, Scientific Publishing Co., Amsterdam.

Emanuel, N.M., Zaikov, G.E. and Maizus, Z.K. (1984) Oxidation of Organic Compounds, Medium Effects in Radical Reactions. (Hirschler, M.M., ed.) Pergamon Press, New York.

Esclade, L., Guillochon, D. and Thomas, D. (1986) Xenobiotica. **16**, 615-624.

Fieser, L. and Fieser, M. (1967) Reagents in Organic Chemistry, pp. 466-467, John Wiley and Sons, Inc., New York.

Finzel, B.C., Poulos, T.L. and Kraut, J. (1984) J Biol Chem. **259**, 13027-13036.

Fontcave, M. and Matsuy, D. (1984) J Chem Soc, Chem Comm. 879-881.

Fuhrhop, J.H. and Smith, K.M. (1975) in Porphyrins and Metalloporphyrins, 2nd ed. (Smith, K.M., ed.) pp. 887, Elsevier Scientific Publishing Co., New York.

Funk, M.O., Isaac, R. and Porter, N.A. (1976) Lipids. **11**, 113-117.

George, P. and Irvine, D.H. (1952) Biochem J. **52**, 511-517.

George, P. and Irvine, D.H. (1956) J Colloid Sci. **11**, 327-339.

Gibson, J.F., Ingram, D.J.E. and Nichols, P. (1958) Nature. **181**, 1398-1399.

Golly, I. and Hlavica, P. (1983) Biochim Biophys ACTA. **760**, 69-76.

Goodin, D.B., Mauk, A.G. and Smith, M. (1986) Proc Natl Acad Sci, USA. **83**, 1295-1299.

Grover, T.A. and Piette, L.H. (1981) Arch Biochem Biophys. **212**, 105-114.

Groves, J.T. and Nemo, T.E. (1983) J Am Chem Soc. **105**, 5786-5791.

Hamberg, M. (1974) Lipids. **10**, 87-92.

Hansch, C. and Leo, A. (1979) Substituent Constants for Correlation Analysis in Chemistry and Biology, John Wiley and Sons, New York.

Hanson, L.K., Chang, C.K., Davis, M.S. and Fajer, J. (1981) J Am Chem Soc. **103**, 663-670.

Harel, S. and Kanner, J. (1985) J Agric Food Chem. **33**, 1188-1192.

Heimbrook, D.C., Mulholland, R.L. and Hecht, S.M. (1986) J Am Chem Soc. **108**, 7839-7840.

Ikeda-Saito, M., Prince, R.C., Argade, P.V. and Rousseau, D.L. (1984) Fed Proc. **43**, 1561-

Ito, S., Kato, T., Shinpo, K. and Fujita, K. (1984) Biochem J. **222**, 407-411.

Jefcoate, C.R. (1986) in Cytochrome P-450: Structure, Mechanism and Biochemistry, (Ortiz de Montellano, P.R., ed) pp. 387-428, Plenum Press, New York.

Jefford, C.W., Boschung, A.F. and Rimbault, C.G. (1978) in Singlet Oxygen, Reactions with Organic Compounds and Polymers, (Ranby, B. and Rabek, J.F., Eds.) pp. 182-185, John Wiley and Sons, New York.

Kanner, J. and Harel, S. (1985) Arch Biochem Biophys. **237**, 314-321.

Kanofsky, J.R. (1984a) J Biol Chem. **259**, 5596-5600.

Kanofsky, J.R. (1984b) J Am Chem Soc. **106**, 4277-4278.

Kawanishi, S. and Caughey, W.S. (1985) J Biol Chem. **260**, 4622-4631.

Keilin, D. and Hartree, E.F. (1935) Proc Roy Soc. **117**, 1-

Khan, A.U. (1983) J Am Chem Soc. **105**, 7195-7197.

Khan, A.U. (1984) Biochem Biophys Res Comm. **122**, 668-675.

Khan, A.U., Gebauer, P. and Hager, L.P. (1983) Proc Natl Acad Sci, USA. **80**, 5195-5197.

King, N.K. and Winfield, M.E. (1963) J Biol Chem. **238**, 1520-1528.

King, N.K. and Winfield, M.E. (1966) Aust J Biol Sci. **19**, 211-217.

King, N.K., Looney, F.D. and Winfield, M.E. (1964) Biochim Biophys ACTA. **88**, 235-236.

King, N.K., Looney, F.D. and Winfield, M.E. (1967) Biochim Biophys ACTA. **133**, 65-82.

Kremer, M.L. (1981) Israel J Chem. **21**, 72-75.

Kuntze, K.L. and Ortiz de Montellano, P.R. (1983) J Am Chem Soc. **105**, 1380-1381.

Kuthan, H., Tsuji, H., Graf, H., Ullrich, V., Werringloer, J. and Estabrook, R.W. (1978) FEBS Lett. **91**, 343-345.

Laemmli, U.K. (1970) Nature. **227**, 680-685.

Leatherbarrow, R.J., Fersht, A.R. and Winter, G. (1985) Proc Natl Acad Sci, USA. **82**, 7840-7844.

Lenk, W. and Sterzl, H. (1984) Xenobiotica. **14**, 581-588.

Lewis, D.F.V., Tamburini, P.P. and Gibson, G.G. (1986) Chem-Biol Interact. **58**, 289-299.

Lopez, L. and Calo, V. (1984) J Chem Soc, Chem Comm. 1266-1268.

Lorkin, P.A. (1974) in, Man's Hemoglobins, 2nd Ed. (Lehmann, H. and Huntsman, R.G., eds) pp. 431-440, North-Holland Publishing Co., Amsterdam.

Lowry, O.H., Rosebrough, N.J., Farr, A.L. and Randall, R.J. (1951) J Biol Chem. **193**, 265-275.

Mallon, B. and Harrison, F. (1984) Bull Environ Contamin Toxicol. **32**, 316-323.

Manthey, J.A., Boldt, N.J., Bocian, D.F. and Chan, S.I. (1986) J Biol Chem. **261**, 6734-6741.

Marnett, L.J. and Bienkowski, M.J. (1980) Biochem Biophys Res Comm. **96**, 639-647.

Marnett, L.J., Johnson, J.T. and Bienkowski, M.J. (1979) FEBS Letters. **106**, 13-16.

Marnett, L.J., Weller, P. and Battista, J.R. (1986) in Cytochrome P-450: Structure, Mechanism and Biochemistry, (Ortiz de Montellano, P.R., ed) pp.29-76, Plenum Press, New York.

Matheson, N.R. and Travis, J. (1985) Biochemistry. **24**, 1941-1945.

Mayer, R.J., Chen, J.T., Taira, K., Fierke, C.A. and Benkovic, S.J. (1986) Proc Natl Acad Sci, USA. **83**, 7718-7720.

Miller, A.A. and Mayo, F.R. (1956) J Am Chem Soc. **78**, 1017-1023.

Misra, H.P. and Fridovich, I. (1972) J Biol Chem. **247**, 6960-6962.

Morell, D.B., Barrett, J. and Clezy, P.S. (1961) Biochem J. **78**, 793-

Oertling, W.A. and Babcock, G.T. (1985) J Am Chem Soc. **107**, 6404-6407.

Ortiz de Montellano, P.R. (1986) in Cytochrome P-450: Structure, Mechanism and Biochemistry, (Ortiz de Montellano, P.R., ed) pp. 217-272, Plenum Press, New York.

Ortiz de Montellano, P.R. (1987) Acc Chem Res. in press.

Ortiz de Montellano, P.R. and Grab, L.A. (1986) Molecular Pharmacol. **30**, 666-669.

Ortiz de Montellano, P.R. and Grab, L.A. (1987) Submitted for Publication.

Ortiz de Montellano, P.R. and Kerr, D.E. (1985) Biochemistry. **257**, 4764-4768.

Pesez, M. and Bartos, J. (1974) Colorimetric and Fluorimetric Analysis of Organic Compounds and Drugs, (Schwartz, M. K., ed.) pp. 329-331, Marcel Dekker, Inc., New York.

Poulos, T.L. (1986) in Cytochrome P-450: Structure, Mechanism and Biochemistry, (Ortiz de Montellano, P.R., ed) pp. 505-523, Plenum Press, New York.

Poulos, T.L. and Kraut, J. (1980) J Biol Chem. **255**, 8199-8205.

Poulos, T.L., Freer, S.T., Alden, R.A., Edwards, S.L., Skogland, U., Takio, K., Eriksson, B., Xuong, N., Yonetani, T. and Kraut, J. (1980) J Biol Chem. **255**, 575-580.

Pysh, E.S. and Yang, N.C. (1963) J Am Chem Soc. **85**, 2124-2130.

Reed, G.A., Brooks, E.A. and Eling, T.E. (1984) J Biol Chem. **259**, 5591-5595.

Rice, R.H., Lee. Y.L. and Brown, W.D. (1983) Arch Biochem Biophys. **221**, 417-427.

Riggs, A. (1981) in Meth Enzymol, v76, (Antonini, E., Rossi-Bernadi, L. and Chianocone, E., eds.) pp. 20-21 Academic Press, Inc., San Francisco.

Ringe, D., Petsko, G.A., Kerr, D.E. and Ortiz de Montellano, P.R. (1984) Biochemistry. **23**, 2-4.

Roberts, J.E., Hoffman, B.M., Rutter, R. and Hager, J.H. (1981) J Am Chem Soc. **103**, 7645-7656.

Russell, G.A. and Bridger, R.F. (1963) J Am Chem Soc. **85**, 3765-3766.

Rutter, R., Hager, L.P., Dhonau, H., Hendrich, M., Valentine, M. and Debrunner, P. (1984) Biochem. **23**, 6809-6816.

Salemme, F.R. (1977) Ann Rev Biochem. **46**, 299-329.

Sannes, L.G. and Hultquist, D.E. (1978) Biochim Biophys ACTA. **544**, 547-554.

Saunders, B.C., Holmes-Siedle, A.G. and Stark, B.P. (1964) Peroxidase, pp. 10-25, Butterworth Inc., Washington, D.C.

Sawaki, Y. and Foote, C. (1979) J Am Chem Soc. **101**, 6292-6296.

Schonbaum, G.R. and Chance, B. (1976) Catalase, in The Enzymes, vol 13. (Boyer, P., ed) pp. 363-409, Academic Press, New York.

Schulz, C.E., Rutter, R., Sage, J.T., Debrunner, P.G. and Hager, L.P. (1984) Biochem. **23**, 4743-4754.

Shiga, T. and Imaizumi, K. (1973) Arch Biochem Biophys. **154**, 540-547.

Sivarajah, K., Mukhtar, H. and Eling T. (1979) FEBS Letters. **106**, 17-20.

Sligar, S.G., Gelb, M.H. and Heimbrook, D.C. (1984) Xenobiotica. **14**, 63-86.

Smith, K.M. (1975) in Porphyrins and Metalloporphyrins, 2nd ed. (Smith, K.M., ed) pp. 803-806, Elsevier Scientific Publishing Co., New York.

Smith, M.H. and Gibson, Q.H. (1959) Biochem J. **73**, 101-106.

Starke, D.W., Blisard, K.S. and Mieyal, J.J. (1984) Molecular Pharmacol. **25**, 467-475.

Tate, S.S., Orlando, J. and Meister, A. (1972) Proc Natl Acad Sci, USA. **69**, 2505-2508.

Taylor, W.I. and Battersby, A.R. (1967) Oxidative Coupling of Phenols, Marcel Dekker, Inc., New York.

Terner, J., Sitter, A.J. and Reczek, C.M. (1985) Biochim Biophys ACTA. **828**, 73-80.

Tomoda, A., Yamaguchi, J., Kojima, H., Amemiya, H. and Yoneyama, Y. (1986) Fed Eur Biochem Soc. **196**, 44-48.

Traylor, T.G., Lee, W.A. and Stynes, D.V. (1984) Tetrahedron. **40**, 553-568.

Tursi, F., Samaia, M., Salmona, M. and Belvedere, G. (1983) Experientia. **39**, 593-594.

Ushijima, Y., Nakano, M. and Goto, T. (1984) Biochem Biophys Res Comm. **125**, 916-918.

Virion, A., Courtin, F., Deme, D., Michot, J.L., Kaniewski, J. and Pommier, J. (1985) Arch Biochem Biophys. **242**, 41-47.

Waldemar, A. and Cilento, G. (1983) Angew Chem, Int Ed, Engl. **22**, 529-542.

Wallace, W.J., Houtchens, R.A., Maxwell, J.C. and Caughy, W.S. (1982) J Biol Chem. **257**, 4966-4977.

White, R.E. and Coon, M.J. (1980) Ann Rev Biochem. **49**, 315-356.

Wittenberg, J.B. and Wittenberg, B.A. (1981) in, Purification and Identification of Hemoglobins and Myoglobins, (Bonaventura, J. and Bonaventura, C., eds) Methods in Enzymology, v 76, pp. 29-37, Academic Press, New York.

Yamabe, H. and Lovenberg, W. (1972) Biochem Biophys Res Comm. **47**, 733-739.

Yamaguchi, T., Nakano, T. and Kimoto, E. (1984) Biochem Biophys Res Comm. **120**, 534-539.

Yamamoto, H., Mashino, T., Nagano, T. and Hirobe, M. (1986) J Am Chem Soc. **108**, 539-541.

Yonetani, T. (1976) Cytochrome c Peroxidase, in The Enzymes, vol 13. (Boyer, P., ed) pp. 345-362, Academic Press, New York.

Yoshio, U., Nakano, M., Takyu, C. and Inaba, H. (1985) Biochem Biophys Res Comm. **128**, 936-941.

Zbaida, S., Gilhar, D. and Silman-Greenspan, J. (1984) Pharmaceutical Res. 277-279.

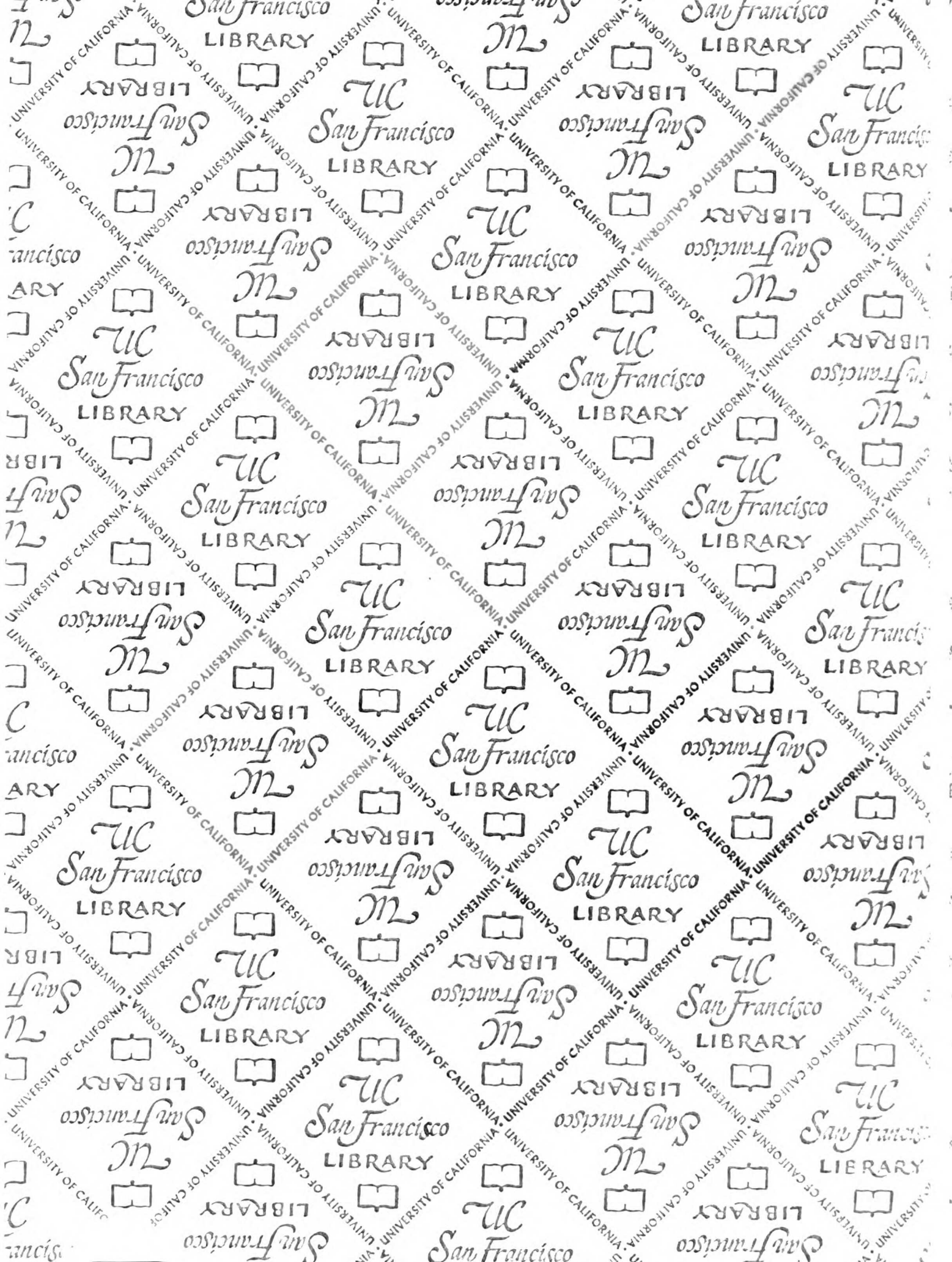
UC
San Francisco
LIBRARY
UNIVERSITY OF CALIFORNIA · UNIVERSITY OF CALIFORNIA · UNIVERSITY OF CALIFORNIA